pt. 1

This is to certify that the

dissertation entitled

Spectroscopic Studies In Low Dielectric Solvents and Molten Salts

presented by

John Warren Rovang

has been accepted towards fulfillment
of the requirements for

Ph.D. degree in Chemistry

Major professor

Date May 11, 1987

O-12771

SPECTROSCOPIC STUDIES IN LOW DIELECTRIC SOLVENTS AND MOLTEN SALTS

By

John Warren Rovang

A DISSERTATION

Submitted to
Michigan State University
in partial fulfillment of the requirements
for the degree of

DOCTOR OF PHILOSOPHY

Department of Chemistry

1986

ABSTRACT
SPECTROSCOPIC STUDIES IN LOW DIELECTRIC
SOLVENTS AND MOLTEN SALTS
By
John Warren Rovang

Several lithium salts ($LiNO_3$, LiCl, LiPi (Lithium Picrate), $LiCF_3CO_2$, LiSCN, $LiAsF_6$, $LiClO_4$, $LiBPh_4$ (Lithium Tetraphenylborate), and LiI in pyridine and 2-butanone were investigated by ^7Li NMR, electrical conductance, and infrared spectrometry. Solvation studies were confined to systems where the solubility of the salt was $\geq$0.50 M. Lithium thiocyanate, $LiNO_3$, LiPi, $LiClO_4$, and LiCl were studied in pyridine. In 2-butanone, all of the above salts were studied except $LiNO_3$ and LiCl. Ion pairing formation constants were obtained from fitting electrical conductance measurements to the Fuoss-Kraus and Justice equations. The chemical shift measurements were utilized to obtain contact ion pairing and dimerization constants.

Complexation studies with macrocyclic ligands and their linear analogs have not been carried out in the BPC-$AlCl_3$ room temperature melt. The only alkali metal salts soluble in 45 mole % $AlCl_3$ melt is lithium salts. In 67 mole % $AlCl_3$ melt all of the alkali metal cations are soluble, but the ligand is attacked by $Al_2Cl_7^-$. The stability of crown ether complexes was found to parallel the cavity size of the crown ether ligand. The formation constants were also determined in 45 mole % $AlCl_3$ melt for triglyme, tetraglyme, and pentaglyme Li^+ complexes and were found to be less stable than crown

ether complexes. Lithium complexes with lariat ethers, composed of a monoazo 15C5 ring and a ether side chain, were more stable than either 15C5 or tetraglyme complexes in basic melt. Two to one lariat complexes were also formed in basic melts.

The interaction of perchlorate, thiocyanate, and nitrate in basic melt was investigated using vibrational spectroscopy. Both thiocyanate and nitrate compete with Cl^- for coordination site on Al(III), while perchlorate does not.

To my wife, my daughter, and my parents.

ACKNOWLEDGEMENTS

The author wishes to recognize Professor A.I. Popov as his major professor and to express graditude for his guidance and encouragement throughout this course of study. Special thanks go to Dr. A. Timnick for helpful suggestions and encouragement as second reader. Also, I want to express my appreciation to Dr. D. Nocera and Dr. W. Reusch for taking time out their busy schedules to be members of my Ph.D. committee. I also want to recognize Dr. H. Eick, even though he could not be present at my oral defense, for his helpfulness and encouragement during my graduate career. I am also indebted to Dr. Atkinson for writing the IR curve fitting program.

Gratitude is also extended to the Department of Chemistry, Michigan State University and the National Science Foundation for financial aid during my graduate career. Many thanks also go to the members of Dr. Popov's research group (especially Bruce, Rick, Pam, Roger, and Ngozi) for their friendship and stimulating research ideas.

Another group of people which have meant much to me before, after, and during graduate school are the special friends that I have made at the University of North Dakota, Michigan State University, and the United States Air Force Academy. Without Dr. K. Patel's assistance and counsel I may not have come to Michigan State

University to do graduate work; he was doing postdoctoral research at the University of North Dakota when I was working there. The many discussions with Dr. Bob Schlueter, Michigan State University Engineering Professor, about Christian character kept me working on my goal of obtaining a Ph.D. degree. Special thanks to the spiritual leaders at St. Matthew Lutheran Church in Holt, Michigan for their insight and encouragement. I also want to recognize my colleagues at Frank J. Seiler Research Laboratory, United States Air Force Academy, for their encouragement and assistance in preparing this document. Special thanks go to Lt. Col. Steven Lander and Dr. John Wilkes for allowing Missy Landess use of word processor to type this document. Also, I also want to thank Dr. Roger Bunting and Major Skip Dieter for taking the time to proof read this thesis.

Deep appreciation goes to my parents, wife, and daughter during the course of the study. Through the example of my parents I am learning to be more sensitive and patient. Spending time with my wife and daughter proved very important in completing this degree objective.

I also thank Missy Landess for typing and proof reading this thesis. Her patience and command of the English language took a lot of pressure off me in preparing this document.

TABLE OF CONTENTS

TABLE OF CONTENTS, CONT'D.

LIST OF TABLES

LIST OF TABLES, CONT'D.

LIST OF FIGURES

LIST OF FIGURES, CONT'D.

CHAPTER 1

HISTORICAL BACKGROUND

I. Introduction

Numerous studies have been carried out investigating the ionic association of alkali metal salts in nonaqueous solvents. J. P. Devlin and K. Consani (1) showed by matrix isolation vibrational spectroscopy, that $LiNO_3$ forms contact ion pairs in pyridine matrices. These investigators proposed that an understanding of ion pairing interactions in solution could be obtained from studies in low temperature matrices. Earlier far-IR studies on $LiNO_3$ in substituted pyridine and pyridine solutions showed that ions exist mostly as solvent separated ion pairs or as free ions (2). These results provide a reason to re-examine the association process of lithium salts in pyridine. Ion pairing studies were also carried out in 2-butanone. Nuclear magnetic resonance spectroscopy and electrical conductance were used to measure the formation constants. Vibrational spectroscopy was utilized to identify the ion association process occurring in solution. The results of these studies are presented in Chapter III.

Until recently, solution studies were restricted to aqueous and organic solvents. The n-butylpyridinium chloride-$AlCl_3$ room temperature melts are being extensively investigated because of increased use of molten salts in the applied sciences. The n-butylpyridinium chloride-$AlCl_3$ melts dissolve metal salts when the

metal cation forms complexes with Cl^-, $AlCl_4^-$, or $Al_2Cl_7^-$. Complexation of alkali metal cations with macrocyclic ligands has not been studied in this medium. Crown ether ligands are selective complexing agents for metal cations in aqueous and nonaqueous solvents. The linear analogs of crown ethers form weaker complexes than crown ethers and do not exhibit the same degree of selectivity as crown ether ligands. The results from the complexation studies in n-butylpyridinium-$AlCl_3$ melts are discussed in Chapter IV.

II. Theory

In 1926, Bjerrum introduced the concept of ion pairing into the calculation of interionic forces in electrolyte solutions (3). Bjerrum proposed that two ions form an ion pair where the interionic distance ranges between a minimum distance of closest approach, a, and a limiting distance, q. The limiting distance corresponds to the separation at which the coulombic attraction is balanced by the energy of the random thermal motion of ions (4). A relationship was derived by Bjerrum for the ion pairing constant which is given by:

$$K_a = \frac{4\pi N}{1000} \left(\frac{|Z_+ Z_-|e^2}{\epsilon kT}\right)^3 \int_2^b \exp(y) y^{-4} dy \qquad (1\text{-}1)$$

$$y = 2q/r \qquad (1\text{-}2)$$

$$b = (|Z_+ Z_-|e^2)/ a\epsilon kT \qquad (1\text{-}3)$$

$$Q(b) = \int_2^b \exp(y) y^{-4}\, dy \qquad (1\text{-}4)$$

$$K_a = \left(\frac{4\pi N}{1000}\right) \int_a^q \exp\left(\frac{2q}{r}\right) r^2\, dr \qquad (1\text{-}5)$$

where N is Avogadro's number, ϵ is the dielectric constant of the solvent, e is the unit of electrical charge, and r is the radius of the spherical shell around the reference ion. Values for Q(b) have been computed by Bjerrum (3,4) for b from 1 to 15 and by Fuoss and Kraus for values from 15 to 30 (5). For the calculation of the contact ion pairing constant, the a parameter is the sum of the ionic radii of the ions of the ion pair. The formation constant for solvent separated ion pairs can be calculated using Bjerrum's theory by taking a+d as the closest distance of approach, where d is the diameter of a solvent molecule. The expression represented by equation (1-5) is another form of the Bjerrum equation where the limits of the integral extend from the closest distance of approach, a, to the Bjerrum distance, q.

Some years later Fuoss questioned the Bjerrum approach to ion pairing because it failed to describe physical reality at distances greater than q. Fuoss presented an alternate model of ion pairs and derived an equation for the ion association constant (6). This model counted ion pairs as those that are in physical contact. The equation, derived in 1958 by Fuoss, is (7):

$$K_a = \frac{4\pi N a^3}{3000} \exp\left|\frac{|Z_+ Z_-|e^2}{a\epsilon kT}\right| \qquad (1\text{-}6)$$

where a is the distance of separation between the cation and anion in the ion pair. As the a parameter increases the $4\pi Na^3/3000$ term increases while the $\exp(|Z_+Z_-|e^2/a\epsilon kT)$ term decreases, which leads to a minimum of K_a. The distance, a, which yields a minimum of K_a is determined by (8):

$$a_{min} = \frac{|Z_+ Z_-|e^2}{3\epsilon kT} = 2/3q \qquad (1\text{-}7)$$

Jagodzinski and Petrucci (9) introduced a multiplier, $\exp(-\Delta U/RT)$, into the Fuoss equation (1-6) where ΔU is the change in internal energy on the formation of an ion pair. The ΔU term was calculated to be (1/2)RT, a gain of (1/2)RT of internal energy per mole of ion pairs formed.

There are four predictions based on the Bjerrum and Fuoss models that are contradicted by experimental results (10-17): (a) since K_a is a function of the a parameter and ϵ, then for a given electrolyte having the same a parameter, the ion pairing should be the same in different solvents of the same dielectric constant. (b) the K_a decreases as ϵ increases. (c) both models require the consistency of the Walden product for a given electrolyte in different solvents. (d) the distances of the closest approach, a, of two ions should not vary with the solvent if ions are in contact. The Bjerrum and Fuoss models take into consideration only the electrostatic forces between ions,

and there are no terms to account for specific solvent effects (18-22). D'Aprano and coworkers (17,23) explained the dependence of the Walden product on the dielectric constant of the solution using the Eyring equation for transport in liquids, which accounts for solvent structural differences. Gilkerson was the first to derive an expression for the ion pairing constant, (K_a), taking into consideration solvation effects (16).

$$K_a = \left|\frac{2\pi\mu kT}{h^2}\right|^{3/2} (g\nu\bar{\sigma}) \exp\left|\frac{-E_s}{RT}\right| \exp\left|\frac{-Ne^2}{\epsilon aRT}\right| \qquad (1\text{-}8)$$

This equation was derived by use of the Kirkwood zeroth-order partition function for a particle in solution. Equation (1-8) contains several unknown parameters: a is the distance of closest approach of the ions, E_s is the difference in the solvation energy of the free ions and ion pair, ($g\nu\bar{\sigma}$) term which is a function of the free volumes available to the free ions and ion pairs. The ($g\nu\bar{\sigma}$) term contains ν which is the free volume available to the free ions and the ion pair, g which corresponds to the internal rotational and vibrational contribution to the molecular partition function, and $\bar{\sigma}$ which is a factor between unity and e for solids and gases, respectively. This approach was successful in explaining the differences in the ion association constants for tetraalkylammonium salts in solvents with the same dielectric constant. In 1970, Gilkerson reconsidered the problem of ion solvation from the standpoint of specific solvation interactions. He substituted for

the energy term, E_s, the change in molar free energy of the specific solvation, $\Delta G_s = \Delta H_s - T\Delta S_s$ (24).

Gilkerson introduced a correction factor to the Bjerrum equation to account for specific solvent effects (25). The modification was introduced by considering a square mound potential of fixed extent and variable magnitude (26). The potential energy of the ion pair interaction becomes

$$U_{+-} = U^*_{+-} - \frac{|Z_+ Z_-| e^2}{\epsilon r} \qquad (1\text{-}9)$$

where U^*_{+-} is $+\infty$ for $r \leq a$, $U^*_{+-} = h_{+-}$ for $a < r < a+d$ (d is the average solvent molecular diameter), and $U^*_{+-} = 0$ for $r > a+d$. The h_{+-} is a perturbation energy term related to the energy of the interaction of the free ion and ion pairs with surrounding solvent molecules. The observed value of the association constant, $K_a(obs)$, is given by:

$$K_a(obs) = \frac{4\pi N}{1000}\left[e^{-h_{+-}/kT} \int_a^{a+d} \exp\left|\frac{2q}{r}\right| r^2 dr + \int_{a+d}^{q} \exp\left|\frac{2q}{r}\right| r^2 dr \right] \qquad (1\text{-}10)$$

Using the measured $K_a(obs)$, the h_{+-}/kT term can be determined; a positive h_{+-}/kT term means that specific solvent effects make the solvated ions more stable than the contact ion pair. A negative h_{+-}/kT value implies that the solvent favors contact ion pairs instead of the free ions.

Fuoss (27) proposed that a real solution consists of solvated free ions, solvent separated ions, and contact ion pairs. The relationship between solvated free ions, solvent separated ions, and contact ion pairs can be summarized by the following equation:

$$M^+S_n + N^-S_n \overset{K_1}{\rightleftharpoons} M^+SN^- \overset{K_2}{\rightleftharpoons} M^+N^- \qquad (1\text{-}11)$$

where S is a solvent molecule, and n corresponds to the number of solvating molecules. The formation constant, K_1, for the formation of solvent separated ion pairs is diffusion controlled and is given by (10):

$$K_1 = \frac{4\pi N(a+d)^3}{3000} \exp\left|\frac{|Z_+ Z_-|e^2}{\epsilon(a+d)kT}\right| \qquad (1\text{-}12)$$

The equilibrium constant between solvent separated ion pairs and contact ion pairs is described by (10):

$$K_2 = \exp(-E_s/kT) \qquad (1\text{-}13)$$

in which E_s is the difference in energy between the contact and solvent separated ion pair. The overall association constant is given by:

$$K_{TOTAL} = K_1(1 + K_2/C_s) \qquad (1\text{-}14)$$

where C_s is the molar concentration of the solvent.

Fuoss (27) proposed that a real solution consists of solvated free ions, solvent separated ions, and contact ion pairs. The relationship between solvated free ions, solvent separated ions, and contact ion pairs can be summarized by the following equation:

$$M^+S_n + N^-S_n \overset{K_1}{\rightleftharpoons} M^+SN^- \overset{K_2}{\rightleftharpoons} M^+N^- \qquad (1\text{-}11)$$

where S is a solvent molecule, and n corresponds to the number of solvating molecules. The formation constant, K_1, for the formation of solvent separated ion pairs is diffusion controlled and is given by (10):

$$K_1 = \frac{4\pi N(a+d)^3}{3000} \exp\left|\frac{|Z_+ Z_-|e^2}{\epsilon(a+d)kT}\right| \qquad (1\text{-}12)$$

The equilibrium constant between solvent separated ion pairs and contact ion pairs is described by (10):

$$K_2 = \exp(-E_s/kT) \qquad (1\text{-}13)$$

in which E_s is the difference in energy between the contact and solvent separated ion pair. The overall association constant is given by:

$$K_{TOTAL} = K_1 (1 + K_2/C_s) \qquad (1\text{-}14)$$

where C_s is the molar concentration of the solvent.

According to the Fuoss-Kraus conductance theory (28), when the concentration of a univalent salt is equal or greater than $C_o = (1.19 \times 10^{-14})(\epsilon T)^3$ where ϵ is the dielectric constant of the medium and T is the absolute temperature, the formation of triple ions becomes important. The triple ion formation constant of a univalent electrolyte is given by the expression:

$$K_T = \left|\frac{N\pi a^3}{1000}\right| e^{-3/2} \exp\left\{\frac{e^2}{2a\epsilon kT}\right\} \qquad (1\text{-}15)$$

where πa^3 is the volume of the contact ion pair assumed to be a cylinder having a radius of a/2 and a height of 4a (9). The factor, $e^{-3/2}$, which accounts for the change of internal energy upon the formation of a mole of triple ions. This model envisions triple ions as composed of three spheres in contact in an aligned configuration (corresponding to a minimum in the potential energy). Fuoss and Kraus derived an equation for the formation of triple ions which is based on the Bjerrum model (29). This derivation led to an integral which was difficult to solve. Petrucci and coworkers obtained a theoretical expression for the triple ion association constant based on the interaction between an ion and an ion pair having a permanent dipole moment, μ (30). The derivation was much simplier than the expression obtained previously by Fuoss and Kraus. This approach eliminated the restriction that the complexing ion must be in contact with the ion pair to be a triple ion. The expression obtained for K_T is:

$$K_T = \left|\frac{N2\pi a^3}{1000}\right| b^{3/2} \quad Q(b) \qquad (1\text{-}16)$$

The a term corresponds to the minimum distance between the ion and the dipole, and $b = e\mu/\epsilon a^2 kT$. The Q(b) term is a converging series which is limited to nine terms:

$$Q(b) = -\frac{b^{-3/2}}{1.5} + \frac{b^{1/2}}{(0.5)(3!)} + \frac{b^{5/2}}{(2.5)(5!)} + \frac{b^{9/2}}{(4.5)(7!)} + \frac{b^{7}}{(7)(9!)}$$

$$+ \frac{b^{17/2}}{(8.5)(11!)} + \frac{b^{21/2}}{(10.5)(13!)} + \frac{b^{25/2}}{(12.5)(15!)} - 0.2556 \qquad (1\text{-}17)$$

In solvents having a low dielectric constant and medium basicity or low donicity, the formation of dimers becomes important. In solvents which contain steric groups around the donor group higher aggregates than dimers exist (31). The Fuoss expression, equation (1-6), can be adapted to the association of two ion pairs into a dimer (32):

$$K_D = \left|\frac{4\pi N r^3}{3000}\right| \quad \exp \quad \left| \frac{\mu^2}{\epsilon r^3 kT} \right| \qquad (1\text{-}18)$$

where r is the separation between the center of two dipoles, μ the dipole moment, and ϵ is the dielectric constant of the medium. The orientation of the dimer corresponds to the two dipoles locked into an antiparallel configuration. In this model, the ion pairs and dimers are considered immersed in a continuum with a dielectric constant ϵ.

The change in the number of degrees of freedom in going from two ion pairs to a dimer should be considered. Equation (1-18) is multiplied by e^{-2} to account for the change in nonelectrostatic internal energy upon the formation of a dimer. The position of minimum approach can be found by maximizing equation (1-18). The result of this operation gives the distance as the minimum of K_F at:

$$r_M = \left| \frac{\mu^2}{\epsilon kT} \right|^{1/3} \qquad (1\text{-}19)$$

Many researchers (33-35) prefer to use the Bjerrum approach. Therefore, it is important to develop a Bjerrum-like theory for dimer formation. The expression derived for the association constant which follows a procedure similar to that of Bjerrum is:

$$K_D = \frac{N4\pi a^3}{3000} b \int_{3/2}^{b} \left| \frac{\sinh Y}{Y^3} \right| dY = \frac{N4\pi a^3}{3000} bQ \qquad (1\text{-}20)$$

where $b = \mu^2/\epsilon a^3 kT$, and $Y = \mu^2/\epsilon r^3 kT$. The integral can be evaluated by expanding the factor $\sinh Y$ into a converging power series and integrating term by term. The result is:

$$Q = 0.6667 - 1/b + \sum_{1}^{\infty} \frac{1}{(n+2)!n} [b^n - (1.5)^n] \qquad (1\text{-}21)$$

with odd n's from 1 to ∞. For the Bjerrum model, the two dipoles may not be in contact, and by definition can vibrate as two independent entities at any distance $q \geq r \geq a$. This approach has been criticized because it reduces a finite ion pair to a point

dipole. Fuoss (36-38) and Fuoss and Kraus (39,40) treated the problem of a dipole-dipole interaction with a model more sophisticated than the previous models. They assumed the dipole to be an ellipsoid with axes a (major axis) and λa ($\lambda < 1/2^{1/2}$, minor axis). Contained at the center of the ellipsoid is a point dipole (with its axis parallel to the major axis of the ellipsoid). An expression was obtained for the dimer formation constant assuming a dimer with an antiparallel configuration which is:

$$K_D = \frac{N}{2000} \left|\frac{\pi}{3}\right|^{3/2} \left|\frac{\mu^2}{\epsilon kT}\right| \frac{e^y}{y^{7/2}} (1/2\lambda^2 - 1)^{-1/2} \qquad (1\text{-}22)$$

where $y = \mu^2/(\lambda a)^3\ \epsilon kT$. This equation contains two adjustable parameters, a and λ. For example, the λ term is assumed to be 1/2 for triisoamylammonium picrate in benzene, where the charge separation in the ion pair is small with respect to the physical dimensions of the ion pair. Another model was examined by Fuoss and Kraus, where the dipole distance is comparable with the dimension of the ion pair, and the expression for the dimer formation constant is:

$$K_D = \frac{14.68N}{4000} \left|\frac{e^2}{\epsilon kT}\right|^3 \frac{\exp\left[(2-2^{1/2})\beta\right]}{\beta^{11/2}} \qquad (1\text{-}23)$$

where $\beta = e^2/a\epsilon kT$. Here the ion pair was envisioned as formed by two spheres in contact.

III. Electrical Conductance

Electrical conductance measurements in aqueous and nonaqueous

solvents have been used to obtain information concerning the transport of ions in solution and ion pairing formation constants. Numerous models have been proposed for the interpretation of conductance data. The key equations are: (1) the Fuoss-Onsager equation, (2) the Pitts equation, (3) the Fuoss-Hsia equation, (4) the Justice equation (5), and the revised Fuoss equation (41).

A computer program is used to obtain values for the limiting conductance (Λ_o), the ion pairing formation constant (K_a), and the center-to-center distance of the ions (41). The meaning of the distance parameter depends upon the model. For the first three equations listed above, the distance parameter, a, is the contact distance, and when obtained from curve fitting, is not necessarily equal to the sum of the ionic radii of contact ion pairs except when the ionic volumes are large compared to the volume of the solvent molecules (e.g. tetrabutylammonium tetraphenylborate in acetonitrile) (42). For the Justice and the revised Fuoss equations, the distance term has a different meaning; these distance terms will be discussed in the following pages.

The use of any of the conductance equations requires initial estimates of these parameters. Extrapolation of the Fuoss plots has been used to obtain values of Λ_o, the limiting equivalent conductance at infinite dilution. However, for ion pairing constants $\gtrsim 10^5$ $\underline{M}^{-1}$, the extrapolation procedure does not provide accurate estimates for Λ_o (43). The Kohlrausch rule of additivity of limiting conductances or the Walden product have been used to

obtain approximate values of Λ_o (32). Conductance studies using the equations listed in the first paragraph in this section of the thesis have been carried out at low concentrations ($\sim 10^{-4}$ M) in nonaqueous solvents to obtain values for Λ_o, K_a, and a, but in some cases, the resistances are too low to be measured accurately (9). At higher molar concentrations, $\geq (1.19 \times 10^{-14})(\epsilon T)^3$, a different equation must be used to account for the formation of triple ions.

Different equations give various results for ion pairing constants. When the ion pairing association constant is small, it is very sensitive to the equation used. The Fuoss–Onsager equation is the most popular one and is applicable at electrolyte concentrations lower than C_o . According to the Fuoss–Kraus conductance theory, the concentration at which triple ion formation becomes important is given by: $C_o = (1.19 \times 10^{-14})(\epsilon T)^3$ where ϵ is the dielectric constant and T is the absolute temperature (28). The Fuoss–Onsager equation used for 1:1 electrolytes that are associated in solution is (41,44):

$$\Lambda = \Lambda_o - S(\alpha C)^{1/2} + E\alpha C \log \alpha C + J_1 \alpha C - K_a \alpha C f_{\pm}^2 \Lambda - J_2 (C\alpha)^{3/2} \pm F\Lambda_o \alpha C$$

in which

$$E = E_1 \Lambda_o - E_2$$

$$E_1 = 2.303\kappa^2 a^2 b^2 / 24C$$

$$E_2 = 2.303\kappa a b \beta / 16C^{1/2}$$

$$b = e^2 / a\epsilon kT$$

$$ab = (16.708 \times 10^{-4})/\epsilon T$$

$$\kappa^2 = 8\pi Ne^2C/1000\epsilon kT$$

$$B = 82.501/\eta(\epsilon T)^{1/2}$$

$$\kappa/C^{1/2} = (0.50294 \times 10^{10})/(\epsilon T)^{1/2}$$

$$\kappa = \left| \frac{8\pi e^2 NC}{1000\epsilon kT} \right|^{1/2}$$

where C is the concentration of the electrolyte, N is Avogadro's number, e is the charge on the electron, ϵ is the dielectric constant of the medium, η is the viscosity, and k is the Boltzmann constant. The S term is the coefficient of the limiting law. The E term depends on the physical properties of the solvent and on the charges on the ions. The coefficients J_1 and J_2 depend on the same parameters as E, but also the distance of the closest approach of the ions (28,41). Included in equation (1-24) is the $F\Lambda_o\alpha C$ term, which corrects for viscosity changes; however, for small ions, this term is unnecessary. For small association constants, it is important to include the $J_2(C\alpha)^{3/2}$ term in the conductance equation, otherwise the ion pairing formation constant will be masked by the fitting procedure (45,46).

The Fuoss-Onsager equation has been used for fitting conductance data of a 1:1 electrolyte with 10 $\underline{M}^{-1} < K_a < 1000\ \underline{M}^{-1}$ for a wide range of dielectric constants (47). For $K_a \geq 1000\ \underline{M}^{-1}$, the $E\alpha C\text{Log } C\alpha + J_1C\alpha - J_2(C\alpha)^{3/2}$ terms are small in respect to $K_a\alpha Cf_{\pm}^2\Lambda$ and can be disregarded (45).

Other models have been used to obtain more accurate fits to the conductance data. The conductance at infinite dilution can be determined with better accuracy using either the Fuoss-Hsia or the Pitts equation (48-50). The Fuoss-Hsia equation better accounts for all unassociated electrolytes than the Fuoss-Onsager equation, except for HCl and NaOH in water (48). The Pitts equation is more successful than either the Fuoss-Onsager or Fuoss-Hsia equations for electrolytes in water and DMF solution (48). Justice (51,52) proposed a modification to the Fuoss-Onsager equation by replacing the ion size parameter, a, with the Bjerrum distance, q, in several of the terms in the conductance equation. This change describes ions as charged spheres of diameter, a, surrounded by an impenetrable shell of thickness equal to (q-a)/2 (53). This equation does not always produce a distance parameter, R, equal to the Bjerrum distance. In solvents with high dielectric constants, $R > q$; in low dielectric solvents, $R < q$, and in the intermediate range, $R = q$. These three conductance equations have the same linearized form as the Fuoss-Onsager equation (1-24), but the J_1 and J_2 terms are different.

In 1974, a new model was proposed to replace the above models which had been derived on the basis of a classical charge sphere model in a continuum (54,55). The new model represented the solution as a continuum containing a Gurney sphere centered on ions with the diameter R. The Gurney sphere defines the region surrounding an anion where an ion of the opposite charge must exist

to constitute an ion pair. This model separated the long range and short range interactions; the relaxation and electrophoretic terms are defined in terms of long range interactions. Earlier models incorporated short range distances into these terms incorrectly. Also, the macroscopic ϵ and η were legitimately used in the calculation of the relaxation and electrophoretic terms. The equation derived in 1975 generated a function $\Lambda(c)$ which reproduced observed equivalent conductances as a function of concentration within experimental error for concentrations up to approximately $2x10^{-7}\epsilon^3$ eql^{-1}, where ϵ is the dielectric constant. Using this conductance equation, the value for R calculated from the conductance data in a series of mixed solvents is found to increase as ϵ decreases. The ion pairing formation constants obtained for these systems show no consistent pattern, which may imply that K_a is separated into the product of two terms, one depending on the ion-solvent interaction and the other on the ion-ion interaction (56).

The ions diffuse in solution until they form ion pairs. Ion pairs can exist when ions are in contact or when the Gurney spheres overlap. Two ions of opposite charge with overlapping Gurney spheres are referred to as solvent separated ion pairs, and those in contact are called contact ion pairs. Fuoss, in 1978, derived a conductance equation which accounts for these two types of ion pairs (27). It contains three parameters, Λ_o, R, and E_s, where E_s is the difference in energy between the contact and solvent separated ion pair.

The appearance of a minimum in the conductance curve has been taken to indicate the formation of triple ions. A triple ion is a three ion charged cluster, two cations interacting with an anion or two anions interacting with a cation. Triple ion formation constants have been obtained from conductance measurements for electrolyte molar concentrations $\geq(1.19 \times 10^{-14})(\epsilon T)^3$ using the Fuoss–Kraus equation (57, 58):

$$C^{1/2}\Lambda\, g(c) = \Lambda_o K_a^{-1/2} + \Lambda_o^T K_T K_a^{-1/2}(1-\Lambda/\Lambda_o)C \qquad (1\text{-}25)$$

$$g(c) = \frac{\exp\left(\frac{-2.303\beta'}{(\Lambda_o)^{1/2}}(\Lambda C)^{1/2}\right)}{(1 - S/\Lambda_o^{3/2}(\Lambda C)^{1/2})(1 - \Lambda/\Lambda_o)^{1/2}} \qquad (1\text{-}26)$$

$$\beta' = 1.8247 \times 10^6/(\epsilon T)^{3/2} \qquad (1\text{-}27)$$

$$S = \left(\frac{0.8204 \times 10^6}{(\epsilon T)^{3/2}}\right)\Lambda_o + \frac{82.501}{\eta(\epsilon T)^{1/2}} \qquad (1\text{-}28)$$

where β' is the Debye–Hückel activity coefficient term, S is the Onsager conductance term, ϵ is the dielectric constant of the medium, η is the viscosity, and T is the absolute temperature. The Λ_o and Λ_o^T are the limiting equivalent conductances of the ions and the two types of triple ions, respectively. The K_a and K_T terms are the ion pairing and triple ion formation constants, respectively. The product $\Lambda_o^T K_T$ can be obtained by fitting the conductance data. The Λ_o^T term is set arbitrarily at either $2/3\Lambda_o$ or $1/3\Lambda_o$ to obtain the triple ion formation constant (28,58,59). Two types of triple ions

are possible; the theory assumes that the two formation constants are equal (28). For solutions having low dielectric constants (ϵ < 3.0), the g(c) term in equation (1-25) becomes equal to unity since very few ions exist in these media (60). Beronius and Lindback (61) offered an alternate approach to obtain the triple ion formation constant by using the K_a obtained at lower concentrations (~10^{-4} M). At higher concentrations, >0.01 M, equation (1-25) can be used as long as no aggregates are formed and the dielectric constant of the solution and the solution viscosity are used (57).

Sukhotin and Timofeeva (62) found that transference data are not consistent with the formation of triple ions. Their explanation for the minimum in the conductance curve was not the formation of triple ions but the redissociation of ion pairs which were formed at lower concentrations. Using a mean sphere approximations-mass action law theory, a conductance equation was derived to account for conductance data without the consideration of the triple ions (63). The redissociation of ion pairs causes the conductance curve to rise after the minimum. This behavior has been understood from the determination of the solution dielectric constant, which comes from dielectric relaxation measurements using collision diffusion theory and the rotation of ion pairs. These measurements indicate that the solution dielectric constant is no longer equal to the solvent dielectric constant and becomes concentration dependent. Therefore, the ion pairing formation constant is no longer a thermodynamic

constant (64-66).

As the concentration of the electrolyte increases, the free ion concentration increases after going through the minimum in the conductance curve. However, this model does not take into account the formations of species more complex than triple ions (43). Infrared spectral results for alkali metal thiocyanates in dimethoxymethane (ϵ = 2.7) indicate that at concentrations >0.1 M, the ions are associated, and IR bands assigned to freely solvated anions are not present (32). Therefore, these dielectric measurements have been reinterpreted as reflecting the relaxation of the rotation of dipolar species and not the redissociation of ion pairs caused by collisional diffusion. Conductance measurements based on the existence of aggregates have been understood based on the ion hopping model; the cation hops from one cluster to the next (67). The larger the cluster, the more the distance gained by each step; hence a higher conductivity. To fit conductance data when dimers are present, the Fuoss-Kraus equation can be used. The viscosity, the dielectric constant of the solution, and a correction term which accounts for the formation of dimers must be utilized (57). This equation is identical to equation (1-25) except that C is replaced with C_p, the ion-paired concentration.

IV. Nuclear Magnetic Resonance Spectroscopy

Nuclear magnetic resonance spectroscopy has been widely used to study ionic interactions in solution. In the earlier studies,

proton NMR was used to observe solvent protons of solvated molecules neat or in inert solvents (68). In most cases, the protons are several atoms removed from the interaction site, and consequently the chemical shifts are not very sensitive to the solvent interactions. Better information has been obtained by observing directly the resonance of the solvated ion. Numerous studies have been published in which alkali metal NMR was used as a probe to study ionic interactions in nonaqueous and aqueous solutions of alkali metal salts (69-71). Halogen NMR and relaxation measurements, especially for chlorine, have also been utilized to investigate ion interactions between alkali metal cations and halogens or halogen polyatomic anions in solution.

For all alkali metal cations except lithium, the paramagnetic screening term is dominant. For lithium, the diamagnetic and paramagnetic terms are approximately equal and tend to cancel one another, thus the ring currents and neighbor anisotropy effects have a strong influence on the magnitude and direction of the chemical shift (72). For nuclei that exhibit paramagnetic behavior, an increase in the electron intensity at the nucleus causes a downfield shift (73). This behavior is reflected by the correlation between chemical shifts and the Gutmann donor number of the solvent which is observed for ^{23}Na chemical shifts (74). Correlation with the Gutmann donor number is less obvious with ^{39}K and ^{133}Cs chemical shifts and fails completely with ^{7}Li (74,75).

Chemical shift behavior in NMR spectroscopy is dependent on the

kinetics of exchange. In slow exchange processes, separate NMR signals are observed for each species, and an equilibrium constant for a given reaction can be obtained from the areas of the bands. When the exchange kinetics are faster than the time scale of the measurements, a fast exchange condition exists. For all ion pairing studies of alkali metal salts, the exchange processes are fast at room temperature, and the measured chemical shift is given by (73,76):

$$\delta_{obs} = \sum_i x_i \delta_i \qquad (1\text{-}29)$$

where δ_i is the chemical shift characteristic of species i, and X_i is the mole fraction of the i^{th} species. Under these conditions, a single NMR band is observed. From the measurements of chemical shifts at numerous concentrations, equilibrium constants can be obtained by fitting the chemical shift measurements using a nonlinear least square fit program. For example, ion pairing formation constants obtained from ^{133}Cs NMR measurements for cesium picrate in 2-butanone solutions were within experimental error of those obtained by UV-visible spectrometry and electrical conductance measurements (77). In methylamine, the ion pairing constants determined by ^{133}Cs are significantly different from those obtained by electrical conductance because the concentration range extended into the triple ion region, and the conductance equations did not take this into account (78). For cesium tetraphenylborate in

2-butanone, the ion pairing formation constant is dependent on the concentration range used in the measurement. This behavior is attributed to the formation of triple ions (77).

In aqueous solutions, the chemical shifts of alkali metal salts are usually linear with activity and anion dependent. The order of increasing nuclear shielding is I^- < Br^- < Cl^- < F^- < H_2O < NO_3^-, which is related to the basicity of the anion (79). The chemical shift behavior has been interpreted as resulting from collisions of ions in solution. The electronic distribution around the ions is modified by the electrostatic field generated when ions collide or by changes in the water structure around the ions due to the colliding ions (79,80). Evidence to support ionic collisions was obtained by adding different amounts of other alkali metal salts to aqueous cesium salt solutions. This produces linear chemical shift changes which depend both on the cation and anion (81). Collisions between two cations have been shown to occur in aqueous solutions of LiCl and $NiCl_2$, and $Al(ClO_4)_3$ and $Ni(ClO_4)_2$ (82,83). Lithium-7 and ^{27}Al relaxation measurements indicate that two hydrated cations collide and the aqueous shell around the NMR sensitive nucleus is disrupted. The ^{133}Cs chemical shifts measured in water were reproduced using an interionic collisional model. The theory used a concentration dependent shielding constant which was determined from collisional probabilities calculated from a form of the Debye-Hückel model which accurately represents ^{133}Cs chemical shifts from the lowest up to a very high concentration in H_2O. (84,85). Later, the

theory was used to obtain chemical shifts in low dielectric solvents; however, the agreement was not good.

Linewidth measurements have also been used to obtain information about ion interactions in solution. The lineshape of the nuclear magnetic resonance band is Lorentzian, and the spin-spin relaxation, T_2, is related to the lineshape by (86):

$$\Delta\nu_{1/2} = \frac{1}{\pi T_2} \qquad (1\text{-}30)$$

where $\Delta\nu_{1/2}$ is the full width of the NMR band at half height. All alkali metal cations and chlorides in solution relax by only a quadrupolar mechanism except for lithium. In aqueous and methanol solutions, the lithium ion relaxes by a magnetic dipole-dipole and quadrupolar mechanism (87). For other nonaqueous solvents, the quadrupolar mechanism is predominant. If the molecular rotation is much faster than the Larmor frequency, the relaxation rate is given by (88):

$$1/T_1 = 1/T_2 = \left(\frac{3\pi^2}{10}\right)\left(\frac{2I+3}{I^2(2I-1)}\right)\left(\frac{e^2qQ}{h}\right)^2 (1+\eta^2/3)\tau_c \qquad (1\text{-}31)$$

where I is the nuclear spin, Q is the nuclear quadrupole moment, q is the electric field gradient at the nucleus, and τ_c is the correlation time characterized by the reorientation of the field gradient tensor. The asymmetry parameter, η, expresses the symmetry of the principal components of the electric field gradient tensor.

In the extreme narrowing condition where $T_1=T_2$, measurements of T_1 relaxation times using the Meiboom-Gill modification of the Carr-Purcell sequence is a more sensitive method for studying weak ion-ion interactions (89). This approach is more sensitive than measuring the linewidth of the NMR resonance band at half height.

The quadrupolar coupling constant, (e^2qQ/h), depends largely on the ionic character of bonds formed with the quadrupolar nucleus; the coupling constant increases as the ionic character decreases (90). The quadrupolar coupling constants of alkali metal cryptate and aluminum, gallium, and indium acetylacetonate complexes in solution have been measured using multinuclear NMR and ^{13}C NMR (91,92). The authors assumed that the corrrelation time for the carbons of the ligands is the same as that of the enclosed metal cation. Assuming Debye-Stokes-Einstein behavior, the correlation time, τ_c, of spherical molecules is given by:

$$\tau_c = \frac{4\pi\eta a^3}{3kT} \qquad (1\text{-}32)$$

where a is the molecular radius and η is the macroscopic viscosity. This relationship is applicable to simple systems; however, for high concentration solutions and solutions containing macromolecules, this is not a realistic model (86). Other models have been proposed to account for the discrepancies. Gierer and Wirtz (93) introduces the microviscosity correction factor in equation (1-32). Hill (94,95) proposed another model for the correlation time where he

used the mutual viscosity instead of the macroscopic viscosity.

The relaxation rates are very sensitive to the electric field gradient. However, changes in τ_c resulting from viscosity changes can also affect the linewidths. Changes in τ_c can be removed by correcting the linewidths for the macroscopic viscosity, which is done by dividing by the viscosity; however, this is only valid for systems that obey the Debye-Stokes-Einstein equation. The viscosity correction allows for comparing the linewidths of NMR bands between different solutions (86).

Nuclear magnetic resonance relaxation times of the ^{35}Cl nucleus have been used to study interactions of perchlorate and chloride ions in solution. The free ClO_4^- has a T_d symmetry with a zero field gradient which gives a ^{35}Cl linewidth of a few hertz in solution (86). The ^{35}Cl viscosity corrected linewidth for the chloride ion in water is also relatively narrow, about 12 hertz over a wide concentration range from 3 mM to 10 M (96). However, when ion pairing occurs, the chloride ion loses its solvent sphere symmetry, and a large field gradient is created at the nucleus, which produces broad lines. For fast exchange processes, the observed linewidth of the ^{35}Cl resonance is represented by:

$$\Delta\nu_{1/2}^{obs} = \sum_i x_i(\Delta\nu_{1/2})_i \qquad (1\text{-}33)$$

where X_i and $(\Delta\nu_{1/2})_i$ are the mole fraction and linewidth of the i^{th} species, respectively (96). It has been reported that the ^{35}Cl

linewidths for perchlorate salts are narrower in solvents with high dielectric constants and high basic strength, but they broaden and become concentration dependent as the dielectric constant and basic strength decrease (86). The higher the charge on the cation, the larger amount of ion pairing. In water, the amount of ion pairing with perchlorate ions decreases in the following order Fe^{3+} › Ba^{2+} › Ca^{2+} › Mg^{2+} › Li^{+} › Na^{+} › NH_4^{+} › H^{+} (89). The ^{35}Cl linewidths for $NaClO_4$ in water are very small even in concentrated solutions. Therefore, ion pairing in $NaClO_4$ aqueous solutions does not lead to a significant reduction in the symmetry of the electric field gradient at the ^{35}Cl nucleus (97). The formation of solvent separated ion pairs leads to smaller linewidths than observed for contact ion pairs, and the formation of ion and neutral aggregates leads to larger linewidths than observed for contact ion pairs. (86). Chlorine-35 linewidths have been used to measure the ion pairing constant of 18C6 complexed with K^{+} with Cl^{-} in water (96). The formation constant and linewidth of the ion pair are log K_a = 0.7(±0.3) and 90(±20) hertz, respectively. Chlorine-35 linewidths of the ion paired KCl-18C6 complex were reported in other solvents. In acetonitrile, the linewidth is narrow and has only a slight concentration dependence, which is taken as evidence for the lack of ion pairing in dilute solutions. In other nonaqueous solvents, the ^{35}Cl linewidths of Cl^{-} are much narrower than that of tetraethylammonium chloride, which indicates a smaller degree of ion pairing for the complex than for tetraethylammonium chloride.

Chlorine-35 NMR has also been used to study the interaction of chloride ions with bicyclic and tricyclic macrocycles that contain amino units which are protonated in aqueous solutions (98).

V. Vibrational Spectroscopy

Vibrational spectroscopy has been a valuable tool for investigating ion pairing is solution. Numerous studies have used the vibrational bands of perchlorate, nitrate, and thiocyanate ions as spectroscopic probes to investigate ionic interactions in solution. Information concerning the makeup of the solvation coordination sphere around the cation can be obtained from far-IR measurements.

A. Vibrational Modes of the Nitrate Ion

The unperturbed NO_3^- (D_{3h}) has four fundamental vibrational frequencies of which three are Raman active and three are infrared active. In aqueous solutions, the frequencies and symmetries for NO_3^- are as follows: $\nu_1(A_1')$, symmetrical stretch vibration, about 1049 cm^{-1}, Raman active only; $\nu_2(A_2'')$, out-of-plane deformation, about 830 cm^{-1}, infrared active only; $\nu_3(E')$, anti-symmetrical stretching vibration, about 1380 cm^{-1}, Raman and infrared active; $\nu_4(E')$, anti-symmetrical bending vibration, about 719 cm^{-1}, Raman and infrared active (99,100). When an ion pair is formed with NO_3^-, the symmetry of the free nitrate ion is reduced to C_{2v}, C_s, or C_1. Studies earlier than 1978 proposed that nitrate binds to a cation

through a single oxygen; however, recent molecular orbital calculations predicted that the structure with the minimum energy was the bidentate species (101). The $\nu_3(E')$ mode has been used to probe the distortion of the nitrate ion. In aqueous solutions, the $\nu_3(E')$ band is split by the formation of a hydrogen-bonded complex (100,102-104). In aprotic solvents, when contact ion pairs are formed with the nitrate ion, the $\nu_3(E')$ band is split, and the magnitude of the splitting is related to the solvent's ability to transfer charge to the cation (1,101). Also, steric forces between the solvent and nitrate ion of the ion pair increase the $\nu_3(E')$ band splitting (1). The relationship between the band splitting and the existence of contact ion pairs is supported by the observation of a single $\nu_3(E')$ band in Me_2SO, a dissociating solvent (105).

Three new bands appear in the IR spectrum in addition to the two bands, due to the loss of degeneracy of the $\nu_3(E')$ band as a result of contact ion pairing (102,106,107). The splitting of the $\nu_4(E')$ band is not observed because deformation vibrations are not very sensitive to variations in the symmetry of the ion (108). In concentrated $AgNO_3$ acetonitrile solutions ($C > 4$ M), additional bands appear in the $\nu_1(A_1')$, $\nu_2(A_2'')$, and $\nu_4(E')$ regions, which indicate the existence of multiple ion aggregates (106).

Quantitative Raman spectroscopy has been carried out. The bands in the $\nu_1(A_1')$, $\nu_2(A_2'')$, or $\nu_4(E')$ region were used, depending on how free the regions were of interference (107,109). Silver nitrate ion pairing constants in water were determined from the intensities

of the bands appearing in the $\nu_1(A_1')$ and $\nu_4(E')$ regions. The association constants are within experimental error of each other, 0.08 $\underline{M}^{-1}$ and 0.11 $\underline{M}^{-1}$, respectively (107). Frost and James (110) reported four bands in the $\nu_1(A_1')$ region in aqueous alkali metal nitrate solutions, which were assigned to solvated ions, solvent separated ion pairs, contact ion pairs, and aggregates. For lithium nitrate, all of the above bands are observed; however, only the aggregate band is observed at molar concentrations ≥ 4 $\underline{M}$. In the case of sodium nitrate, all four bands are observed. For potassium and rubidium nitrates, bands assigned to the solvated ion, ion pair, and aggregates are observed. The difference in frequency between the contact ion pair band and the solvent separated ion pair band is approximately 3 cm^{-1}. The interpretation of these results is rather questionable. Further studies were carried out with $AgNO_3$, $TlNO_3$, $Zn(NO_3)_2$, $Cd(NO_3)_2$, $La(NO_3)_3$, and $Th(NO_3)_4$ salts in aqueous solutions. Bands due to solvated ion pairs, solvent separated ion pairs, and contact ion pairs were observed (111).

B. Vibrational Modes of the Perchlorate Ion

The perchlorate ion is tetrahedral (T_d) and has nine fundamental vibrational modes. Figure 1 shows the splitting of these bands when ion-ion interactions occur through a single oxygen (C_{3v}) or through two oxygens (C_{2v}) of the perchlorate ion (112). Since the non-degenerate band of the free perchlorate ion is not IR active, more information about the structure of the perchlorate ion in solution

Figure 1: Vibration of the ClO_4^- as a function of symmetry.

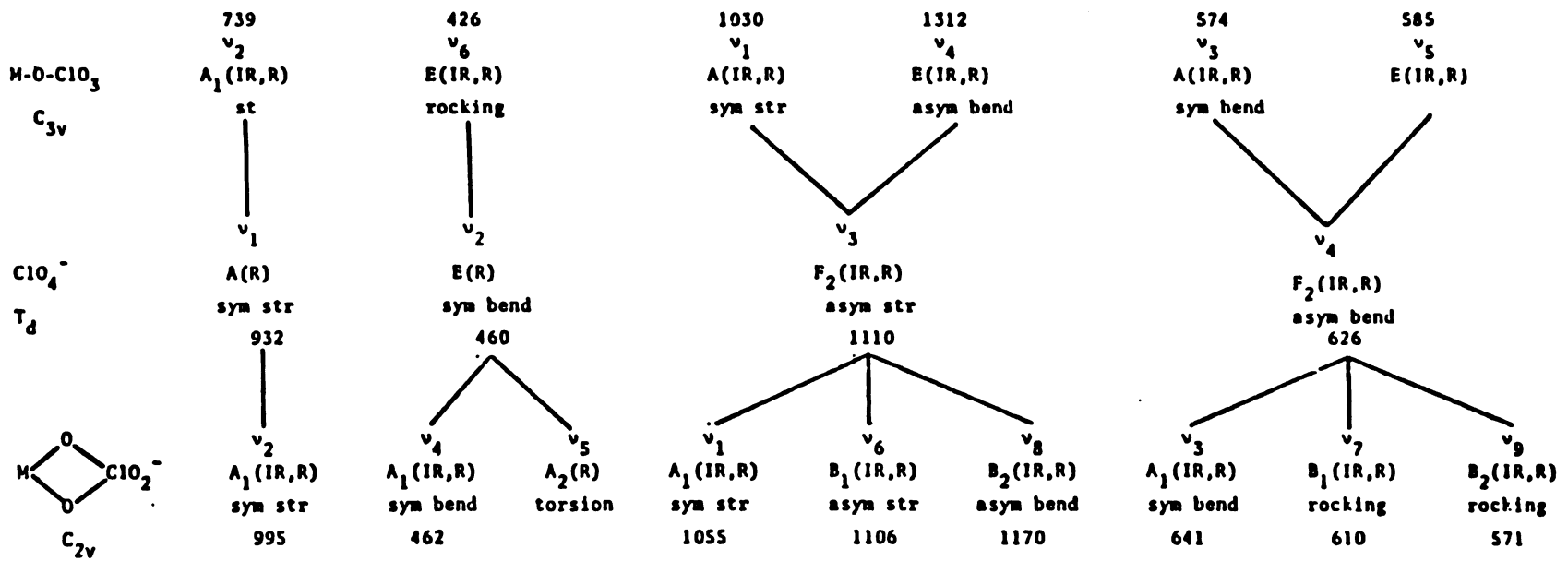
739
ν_2
A_1(IR,R)
st
426
ν_6
E(IR,R)
rocking
1030
ν_1
A(IR,R)
sym str
1312
ν_4
E(IR,R)
asym bend
574
ν_3
A(IR,R)
sym bend
585
ν_5
E(IR,R)
H-O-ClO$_3$
C_{3v}
ν_1
A(R)
sym str
932
ν_2
E(R)
sym bend
460
ν_4
ν_5
ν_3
F_2(IR,R)
asym str
1110
ν_1
ν_6
ν_8
ν_4
F_2(IR,R)
asym bend
626
ν_3
ν_7
ν_9
ClO_4^-
T_d
O
H
ClO_2^-
O
C_{2v}
ν_2
A_1(IR,R)
sym str
995
A_1(IR,R)
sym bend
462
A_2(R)
torsion
A_1(IR,R)
sym str
1055
B_1(IR,R)
asym str
1106
B_2(IR,R)
asym bend
1170
A_1(IR,R)
sym bend
641
B_1(IR,R)
rocking
610
B_2(IR,R)
rocking
571

can be obtained by Raman spectrometry. The triply degenerate stretching vibration, $\nu_3(F_2)$, has been used to probe the perturbation of the perchlorate ion resulting from an interaction with the cation. Infrared spectra of alkali metal perchlorates in an argon matrix indicate the existence of two types of species, an ion pair and a dimer (113). Six bands are observed in the $\nu_3(F_2)$ region, three for the ion pair and three for the dimer. The splitting of the $\nu_3(F_2)$ band of the ion pair is approximately 200 cm^{-1}. The extent of splitting is very sensitive to the type of matrix; for water and ammonia matrices, the band collapsed to a third of the value obtained in argon. This has been understood in terms of the reducing power of the solvated cation together with the transfer of electrons via the cation to the π bonding MO's of the anion (114). Using Raman spectroscopy, Greenberg and coworkers (115) studied $NaClO_4$ in nonaqueous solvents. They monitored the $\nu_1(A)$, $\nu_2(E)$, and $\nu_4(F_2)$ regions and observed new bands or changes in the shape of bands. These were attributed to contact ion pairing. Cahen (116) examined the $\nu_1(A)$ region using Raman spectroscopy for $LiClO_4$ in nitromethane, methanol, acetonitrile, and tetramethylguanidine solutions and also observed changes in the spectra resulting from contact ion pairing. In methanol solutions, the appearance of new Raman bands attributed to contact ion pairs occurred at concentrations >4 M.

The band intensities of the Raman active $\nu_1(A)$ bands have been used to calculate association constants, since each band is

associated with a single oscillator. Four bands were identified for $NaClO_4$ in water; three of the bands are assigned to the ion pair, the solvent separated ion pair, and the solvated ion. A difference of ~2 cm^{-1} occurs between the solvated free ion and the solvent separated ion pair (117,118). It should be noted that the interpretation of these data is questionable, and the distinction between solvent separated ion pairs and solvated free ions is not possible with vibrational spectroscopy. Similar studies were also carried out with $LiClO_4$ in acetone and diethyl ether (119). Bands for the solvated ion, solvent separated ion pairs, contact ion pairs, and aggregates were identified.

C. Vibrational Modes of the Thiocyanate Ion

Infrared spectra of the thiocyanate ion have been used to identify its mode of coordination. In aqueous solutions, the linear thiocyanate ion shows three bands: $\nu_1(A)$, an out-of-phase C-N stretch around 2066 cm^{-1}, $\nu_2(A)$, a SCN bend (double degenerate) at 470 cm^{-1}, and $\nu_3(A)$, an in-phase C-S stretch at 747 cm^{-1} (120). The thiocyanate ion can coordinate to the metal cation through either the nitrogen or sulfur atoms, or both. Nitrogen coordination causes the $\nu_2(A)$ and $\nu_3(A)$ bands to increase in frequency, while the $\nu_1(A)$ band either decreases or increases in frequency depending on the complexing metal cation. The sulfur bonded complexes show a large increase in the frequency of the $\nu_1(A)$ band and a decrease in the frequency of both the $\nu_2(A)$ and $\nu_3(A)$ bands (121,122). Solvent

bands often obscure the $\nu_2(A)$ and $\nu_3(A)$ spectral regions.

In solvents with low dielectric constants and basic strength, lithium, sodium, and potassium thiocyanates often form dimers identified by the appearance of bands around 2040 cm^{-1} in the IR spectra (all bands appear around 2051 cm^{-1} in the Raman), which are at lower frequencies than the free thiocyanate band (122,123). A tetramer, $(LiSCN)_4$, has been postulated as forming in tertiary amines and ether solutions (1993 cm^{-1} in the IR) (31). Dimerization of LiSCN, KSCN, and NaSCN in THF was found to be an entropy controlled process due to the desolvation of ion pairs, and the dimerization constant is concentration dependent due to the existence of solvent separated dimers which are spectroscopically indistinguishable from the contact ion pairs (121,122).

D. Vibrational Studies in the Far-IR

Far-IR spectra of alkali metal salts and tetraalkylammonium salt solutions contain broad bands as a result of solute-solvent interactions. In solvents with high dielectric constants, only one band is observed and is attributed to the vibrating cation in a solvent cage. The bands observed in these solutions are dependent on the cation and are independent of the anion. In solvents with low dielectric constants or low basic strength, the frequencies of the bands are cation and anion dependent, which indicates the existence of contact ion pairs. Evans and Lo (124) observed anion dependent bands in the 70-120 cm^{-1} region for tetraalkylammonium

salts in benzene solutions. Edgell and coworkers (125,126) also observed anion dependent bands in THF solutions of lithium, sodium, and potassium tetracarbonyl cobaltate and pentacarbonyl manganate. In DMSO solutions, far-IR bands were observed for the free alkali metal solvated cation which were only cation dependent (127-129). Solvents with low Gutmann donor numbers and/or low dielectric constants, such as 1-methyl-2-pyrrolidone, propylene carbonate, 2-chloropyridine, nitromethane, and acetone are favorable solvents for ion pairs, which is evident from the anion dependent bands for the far-IR spectra of alkali metal salt solutions (130). Glacial acetic acid, with a dielectric constant of 6.2, is a good solvent for ion pairs and has only a single band, at 390(±4) cm^{-1}, for a series of lithium salts. This indicates the existence of solvent separated ion pairs. The bands exist at the same frequency as the solvated lithium cation in glacial acetic acid (131). Chang and coworkers (132) found that the far-IR band for the contact ion pair splits when the temperature of the solution is lowered. One band is due to an ion pair oscillation while the other is due to the oscillation of the cation against neighboring solvent molecules.

The bands observed in the far-IR spectra are broad. Thus, it is difficult to observe all the bands for all the species in solution. In acetone solutions containing $LiClO_4$, a single band was observed whose absorbance was linear up to 0.4 M. At high concentrations, the absorbance plot was also linear, but the slope was considerably different. The frequency of the band did not change. The band

broadened at concentrations greater than 0.4 M (133). Low temperature matrix isolation techniques have been used to obtain sharp bands. Matrix isolation IR measurements were obtained for lithium halide molecular species using isotopic substitution (134).

Solutions prepared from solvents which have solvent bands in the far-IR produce two new bands in the IR spectrum on solvation, one attributed to the ion cage vibration and the other due to solvating molecules. For pyridine and acetone, the displaced solvent bands are observed at higher frequencies than the solvent cage bands (2,135). A solvent band may overlap the ion cage band and the displaced solvent band to such a degree that it is difficult to obtain an accurate measurement of the band frequencies (136).

VI. Electronic Spectrometry

Electronic spectrometry has been used to study the ion pairing of carbanion and of iodide salts in solution. The formation of ion pairing with carbanions perturbs the energy levels of the solvated anion, and as a result, new absorption bands occur. For iodide, the absorption bands correspond to charge transfer transitions which are very sensitive to environmental changes around the anion (137-145).

The carbanion absorption bands that are independent of the cation are attributed to the anions being surrounded by solvent molecules; those that are cation dependent are due to contact ion pairs. The contact ion pair bands are typically at lower wavelengths than the solvated anion band. The position of the

contact ion pairing band is sensitive to the size of the cation; for large cations, the band appears at a greater wavelength (146,147).

The dependency of the electronic spectrum on the solvent is the result of the formation of specific solvent complexes and/or a general solvation phenomena (147-149). General solvent effects depend on the ability of the solvent to solvate the excited state and/or raise the ground state to higher energies relative to the electronic excited state (150). The solvation of the electronic excited state depends on the polarization and the dipole orientation of the solvent molecules. When specific solvent complexes are formed with contact ion pairs, the complexing solvent molecule disperses the charge on the carbanion, thereby weakening the coulombic interaction and increasing the average interionic distance in the contact ion pair. This changes the degree of perturbation and shifts the band to greater wavelengths. Specific solvation is distinguished from general solvation effects because distinct spectral changes occur in the presence of a small amount of complexing molecules. A general solvation effect is characterized by a progressive shift in proportion to the average solvating ability of the solvent. When two bands are observed and their relative heights are concentration independent (solvent in large excess) and unaffected by addition of a common ion salt, the anion solvated band is assigned to the solvent separated ion pair (149,151-153). The solvent separated ion pair absorption maximum is nearly independent of the solvent if the solvating ability of the

solvent is poor. Changes in solvent polarity and structure can change the equilibrium between contact and solvent separated ion pairs.

The iodide ion UV spectrum is relatively simple; two well resolved charge transfer transitions ($^2P_{3/2}$, $^2P_{1/2}$) are observed, and no bands resulting from intermolecular transitions exist in the spectrum, thus making it easy to identify the absorbance bands (137,154). The band positions are very sensitive to the type of cation because a different degree of stabilization in the ground state occurs with different cations. Also, the degree of stabilization is dependent on the distance between the cation and anion.

The absorbance behavior of a series of NaI solutions prepared from solvents with dielectric constants ranging from <5 to 78 indicates the existence of three different types of species. When the dielectric constant is low ($\epsilon < 5$), contact ion pairs are present. When the dielectric constant of solvent is between 5 and 11, solvent separated ion pairs are the predominant species. With solvents having higher dielectric constants, $23 > \epsilon > 11$, both solvent separated ion pairs and ion pairs separated by more than one solvent molecule are present. And when the dielectric constant of the solvent is $\epsilon > 23$, only ion pairs separated by more than one solvent molecule are present (155).

VII. Macrocyclic Ligands

Pedersen's (156,157) discovery that crown ethers form stable complexes with alkali, alkaline earth, and several transition metal cations has generated considerable interest in these ligands. Typical examples of these crown ether ligands are given in Figure 2. Crown ether ligands exhibit considerable selectivity toward metal cations (158-169) and neutral molecules (170,171). Their selectivity and stability depend on several factors: (a) the relative size of the cation and ligand cavity, (b) the type and number of donor atoms in the ring that are participating in the bonding, (c) the substituents on the macrocyclic ring, (d) the nature of the cation and its charge, (e) the solvating ability and the dielectric constant of the solvent, and (f) the conformation of the bound and unbound ligand (158,172-182). In general, the stability constant is largest when the metal cavity is equal to the diameter of the metal cation. When the cavity size is larger than the diameter of the metal cation, the stability of the crown ether complex may be larger than expected based on the cavity and cation diameters because of the formation of a three dimensional wrap around complex (156,157,183-185). The cavity size is an especially important criterion when the ligands are relatively inflexible (186). When the metal cation is larger than the crown ether cavity, 2:1 sandwich complexes can form (185,187-189). When the crown ether ligand is larger than the metal cation, more than one metal cation can fit into the crown ether cavity (190-192). These complexed metal cations can interact with solvent molecules, anions, or both,

Figure 2: Synthetically prepared macrocylic ligands.

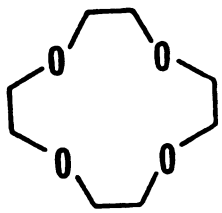

12C4

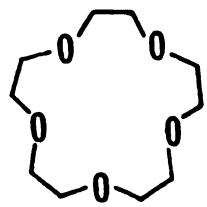

15C5

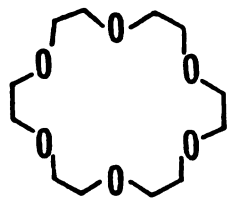

18C6

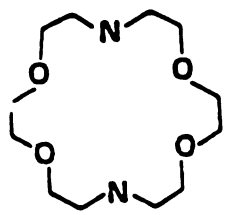

DA18C6

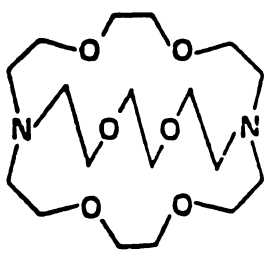

C222

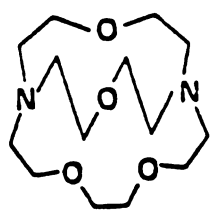

C211

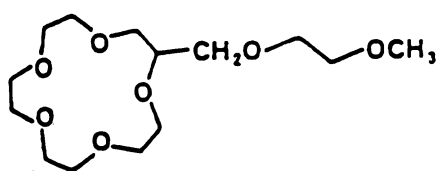

Methoxyethoxymethylmonoazo 15C5

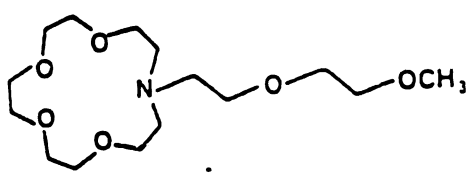

Methoxyethoxyethylmonoazo 15C5

unless they are fully coordinated by the ligand (96).

The bonding between the alkali metal cation and the ligand occurs through an ion-dipole interaction. Substitution of nitrogen or sulfur for oxygen decreases the stability of the alkali metal complexes, while it increases the stability of the complexes with softer metal cations such as Ag^+ and Tl^+ (167,193-199). The bonding in these complexes is more covalent than in the oxygen containing crown ether ligands (158).

Ligands containing three-dimensional cavities formed by three ether chains attached to nitrogen atoms are called cryptands (Figure 2) (200). Inclusive complexes contain the metal cation inside the ligand cavity, isolated from any interaction with solvent molecules, and exclusive complexes are those in which the metal cation is partially inside the cavity so the complexed metal cation can still interact with solvent molecules. Inclusive complexes are obtained when the cavity size is approximately equal to the diameter of the cation. When the metal cation is larger than the cavity, an exclusive complex is formed, and in some cases the ligand may be flexible enough to accommodate both an exclusive and inclusive interaction (201,202). When both types of complexes exist in solution, substituting a benzene ring on the ether chains of the cryptand reduces the flexibility of the ligand, and as a result, only exclusive complexes are formed (203).

The noncyclic analogs of oxygen containing crown ethers have not been extensively investigated. They form complexes whose formation

constants are three to four orders of magnitude smaller than those of the cyclic analogs. They also exhibit very little selectivity (204-206). The difference in the stability between the noncyclic and macrocyclic ligands is denoted as the macrocyclic effect (205-207). At this time, the exact nature of the macrocyclic effect is somewhat controversial.

Gokel and coworkers (208-210) have synthesized a series of macrocyclic polyethers with one or two side chains, with electron donating groups. These chains are attached to either the carbon (carbon pivot lariats) or nitrogen atoms (nitrogen pivot lariats) of the ring (Figure 2). In the complexes, the cation is inside the ring, and the flexible side chain orients its donor group axially (if the site is sterically accessible) to interact with the complexed cation (211). In some cases, the addition of side chains increases the stability and selectivity of crown ether complexes relative to the parent crown ether (212,213). The nitrogen pivot lariats are more flexible and form more stable complexes than the carbon pivot lariats when the side arm participates in the complexing process (214,215). The lariat ethers have a smaller stability constant with alkali or alkaline earth metal cations than the cryptands; however, the lariat ethers are easier to prepare than the cryptands (216).

VIII. Molten Salt Chemistry

The chemistry in molten salts has been extensively investigated

in the last twenty years (217,218). Applications in the areas of batteries, nuclear reactors, extraction of metal ores, electrorefining, etc. have motivated studies of fundamental properties of these systems. Molten salts have several advantages over conventional solvents: (a) the capacity to dissolve inorganic and organic species which are insoluble in ordinary solvents, (b) a wide range of redox potentials, and (c) the wide temperature range of the liquid state. However, one of the main disadvantages of their use in technical applications is that the majority of molten salt systems can only be used at high temperatures (218).

Molten chloroaluminates have received considerable attention because they exist as liquids below 200 °C. Two types of chloroaluminate melts have been studied, those prepared with alkali metal chlorides and those prepared with organic chlorides. The two organochloroaluminates that have received the most attention are the n-butylpyridinium chloride-$AlCl_3$ (BPC-$AlCl_3$) and the 1-methyl-3-ethylimidazolium chloride-$AlCl_3$ (MEIC-$AlCl_3$) melts (219-223). The working temperature range of the alkali metal chloroaluminates is between 100 and 400 °C, allowing an accessible composition range from slightly basic to greater than 66.7 mole % $AlCl_3$. Both the BPC-$AlCl_3$ and the MEIC-$AlCl_3$ melts are liquid at or near room temperature, and the composition ranges are 45-67 mole % $AlCl_3$ and 33-67 mole % $AlCl_3$, respectively. These room temperature melts are very convenient for studying the behavior of organic species that have low boiling points or decompose at high temperatures.

Organic solvents such as benzene, toluene, etc. are miscible to some degree in these room temperature melts (224,225). Addition of benzene to melt solutions reduces the viscosity and the dielectric constant but does not affect the solution equilibrium. The organic cations in the organic chloroaluminates absorb in the UV region of the spectrum. Therefore, the spectral window is smaller than those obtained for the alkali metal chloroaluminates (226). The electrochemical window of basic BPC-$AlCl_3$ melt is smaller than the basic MEIC-$AlCl_3$ melt because the BP^+ is easier to reduce than MEI^+ (227,228). Substituting a dimethylamino substituent for a proton in the para position of the pyridinium ring produces a cathodic window 700 mv's more negative than the cathodic limit of the BPC-$AlCl_3$ basic melt. Chloroaluminate melts are good media for stabilizing the low oxidation states of various cations (229-236). Likewise, these media have been shown to stabilize radical cations of certain aromatic amines, sulfur heterocycles, and polyatomic sulfur species (237-240). Metal cations, which are good Lewis acids and have a strong affinity for chloride, exist as chlorocomplexes in the melt (241-257). The formation of inorganic and organic complexes with $AlCl_4^-$, $AlCl_3$, and $Al_2Cl_7^-$ have also been reported (257-262). Sulfide, telluride, oxide, and selenide act as strong bases that compete with chloride ions for coordination sites around the aluminum(III) cation (263-267). Several oxide anions have been shown to be unstable in the chloroaluminate melts and decompose to provide a source of oxide anions (268,269).

The most important equilibrium in these melts is:

$$2AlCl_4^- \rightleftharpoons Al_2Cl_7^- + Cl^- \qquad (1\text{-}34)$$

where $Al_2Cl_7^-$ and Cl^- ions are the dominant Lewis acid and base, respectively. In mixtures with more than 50 mole % $AlCl_3$, the melt is acidic due to the presence of $Al_2Cl_7^-$, and at less than 50 mole % $AlCl_3$, the melt is basic due to the presence of Cl^-. At 50 mole %, the melt is neutral due to the presence of a large concentration of $AlCl_4^-$. In alkali chloroaluminate melts, $AlCl_3$ and Al_2Cl_6 have been identified in acidic melts (270,271). Raman spectra of acidic NaCl-$AlCl_3$ melts (73 mole % $AlCl_3$) indicate the existence of a new species that has been proposed to be $Al_3Cl_{10}^-$ (272). The appearance of a band at 390 cm^{-1} was attributed to the formation of $Al_3Cl_{10}^-$ at this melt composition. Raman spectra of other aluminum halide-alkali halide melt systems do not exhibit this band (273). At >80 mole % $AlCl_3$, the alkali chloroaluminate melts exist as two phases, which makes it difficult to characterize the species present and the equilibria. In PCl_5-$AlCl_3$ melts at 80-90 mole % $AlCl_3$, which remain homogeneous, three Raman bands observed at 100, 297, and 395 cm^{-1} have been assigned to $Al_3Cl_{10}^-$; no evidence has been obtained for higher polynuclear aluminum chloride species (274). In acidic alkali metal chloroaluminate melts between ~250-300 °C, vapor pressure measurements above the melts could not be explained without including $Al_3Cl_{10}^-$ (275,276). To obtain the equilibrium constants

for equation (1-34) from potentiometric measurements in alkali chloroaluminate melts, it was necessary to include an activity correction or to assume the formation of $Al_3Cl_{10}^-$ to obtain a good fit to the data (270,271). Evidence for the presence of $Al_3Cl_{10}^-$ in the organic chloroaluminate melts was obtained from potentiometric, IR reflectance, and vapor pressure measurements (277-279).

The value of the equilibrium constant represented by equation (1-34) is dependent on the type of chloride salt. For example, for alkali chloroaluminate melts, the presence of large cations reduces the value of the equilibrium constant ($pK(Li^+)$ = 3.8, $pK(Na^+)$ = 5.0, $pK(K^+)$ = 5.8, and $pK(Cs^+)$ = 7.4 at 400 °C) (280). The variation in the equilibrium constants can be attributed to the cation-anion interactions:

$$M^+ + Cl^- \leftrightharpoons M^+Cl^- \qquad (1\text{-}35)$$

$$M^+ + AlCl_4^- \leftrightharpoons M^+AlCl_4^- \qquad (1\text{-}36)$$

$$M^+ + Al_2Cl_7^- \leftrightharpoons M^+Al_2Cl_7^- \qquad (1\text{-}37)$$

which depend on the nature of the metal cation (245). Ionic interactions between the cation and $AlCl_4^-$ in the melt were first observed by Rytter (281) in the Raman spectra of a 50 mole % $AlCl_3$ LiCl-$AlCl_3$ melt at 175 and 200 °C, where the $\nu_3(F_2)$ $AlCl_4^-$ band (~500 cm^{-1}) splits into two bands. The authors proposed that the lithium ion interacts with two of the chlorine atoms of $AlCl_4^-$.

Carbon-13 NMR and IR studies of the BPC-$AlCl_3$ and MEIC-$AlCl_3$

melts indicate an interaction between the organic cation and all the anion species (245,282,283). Evidence of the interaction with $AlCl_4^-$ and Cl^- was supplied using fast atom bombardment (FAB) mass spectrometry. The mass spectra indicate the existence of clusters, BP_2Cl^+ and $BP_2AlCl_4^+$ (284). In MEIC-$AlCl_3$ melt mixtures, the MEIC has a higher degree of ionic association than BPC in BPC-$AlCl_3$ melts. Wilkes and coworkers (283,285) suggested on the basis of NMR studies, that ion-ion interactions in this room temperature melt occur in the form of oligomeric chains held together by electrostatic forces. Infrared studies indicate that in basic MEIC-$AlCl_3$ and BPC-$AlCl_3$, the Cl^- hydrogen bonds to a hydrogen in the MEI^+ and BP^+ cations. For the BPC-$AlCl_3$ melts, changes in band shape and peak frequencies as the melt acidity is varied indicate an ion pairing reaction taking place in both acidic and basic melt (286). These same spectral changes occur in MEIC-$AlCl_3$ melts, but they are more pronounced. These IR results indicate that there is some loss of aromaticity in the pyridine and imidazolium rings resulting from the interaction with Cl^- in basic melts.

CHAPTER 2

EXPERIMENTATION

I. Materials

A. Lithium Salts

Lithium nitrate ($LiNO_3$, Mallinckrodt), lithium chloride (LiCl, Fisher), and lithium perchlorate ($LiClO_4$, G. F. Smith Chemical Company) were dried at 190 °C for several days. Lithium iodide (LiI, Aldrich) was dissolved in purified acetone and precipitated as the acetonate on cooling with a dry ice bath (116). The acetonate was heated at 35 °C for one day, and then the temperature was gradually increased to 85 °C, after which the acetonate was dried for an additional three days. All drying steps were carried out under vacuum. Lithium thiocyanate (LiSCN, Alfa) was dried under vacuum while the temperature was gradually increased to 110 °C over a five day period (287). Lithium tetraphenylborate ($LiBPh_4$) was prepared by metathesis from sodium tetraphenylborate (Aldrich) and lithium chloride in THF solution. The product was dissolved in ethylene dichloride, precipitated from solution with cyclohexane, and dried at 80 °C under vacuum for several days (288). It was found to be chloride free (289). Lithium picrate (LiPi) was prepared by the reaction of equimolar amounts of lithium carbonate (Mallinckrodt) and picric acid (MCB) in ethanol (290). It was recrystallized from a benzene-acetone mixture and dried at 100 °C for two days, followed by drying at 132 °C under vacuum for several

days (291). Both lithium trifloroacetate ($LiCF_3CO_2$, Alfa) and lithium hexafluoroarsenate ($LiAsF_6$, Agri Chemical Company, Atlanta, GA) were dried under vacuum at 70 °C for three days (57).

B. Sodium Salts

Sodium chloride (NaCl, CCL) was used after drying at 190 °C for several days. Sodium oxide (Na_2O, Alfa) was used directly without drying. Sodium thiocyanate (NaSCN, Fisher) was recrystallized once from methanol and dried under vacuum for three days at 70 °C. Sodium tetraphenylborate ($NaBPh_4$, Aldrich) was used after drying at 55 °C under vacuum for two days.

C. Cesium Salts

Cesium bromide (CsBr, Alfa) and cesium chloride (CsCl, Alfa) were dried at 190 °C for several days. Cesium thiocyanate (CsSCN, Pfaltz and Bauer) was recrystallized from methanol and dried at 45 °C under vacuum for two days (47). Cesium tetraphenylborate ($CsBPh_4$) was prepared by the reaction between sodium tetraphenylborate and cesium chloride in THF solution. The precipitated cesium tetraphenylborate was washed with distilled water and dried for two days at 70 °C under vacuum (292). Cesium picrate (CsPi) was synthesized from picric acid and cesium hydroxide in ethanol, recyrstallized from ethanol, and dried at 70 °C under vacuum for several days (73). Cesium acetate (CsAc, Kawecki Chemical Company) was recrystallized from ethanol and dried for

several days under vacuum at 70 °C. Cesium floride (CsF, Alfa) was recrystallized from methanol and then dried under vacuum at 40 °C for several days. Cesium sulfate (Cs_2SO_4) was prepared from H_2SO_4 and cesium carbonate (Alfa) in ethanol solution; it was then dried at 70 °C under vacuum for several days. Cesium nitrate ($CsNO_3$, Alfa), cesium carbonate (Cs_2CO_3, Alfa), and cesium perchlorate ($CsClO_4$, Alfa) were used after drying at 70 °C under vacuum for several days. Cesium iodide (CsI, Alfa) was used after drying at 40 °C under vacuum for several days.

D. Tetraalkylammonium Salts

Tetrabutylammonium perchlorate (NBu_4ClO_4, Eastman), tetrabutylammonium nitrate (NBu_4NO_3, Pfaltz and Bauer), and tetraisoamylammonium thiocyanate ($N(i\text{-}am)_4SCN$, RSA Corporation) were dried under vacuum for several days at 60 °C, then under high vacuum ($<10^{-5}$ torr) for another three days using a specially designed container which can be connected to a glass manifold (Figure 3). Tetramethylammonium chloride (NMe_4Cl, Aldrich) was recrystallized twice from ethanol, washed with chloroform, and dried under vacuum for several days (293).

E. Crown Ether Ligands

Polyether 18-crown-6 (18C6, Aldrich) was purified by converting it to the acetonitrile complex, filtering, and then removing acetonitrile under vacuum (294). Twelve-crown-four (12C4, Aldrich)

Figure 3: Vacuum drying flask.

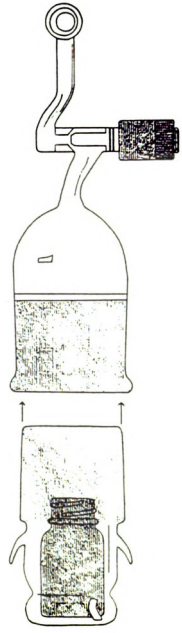

and 15-crown-5 (15C5, Aldrich) were fractionally distilled under reduced pressure and dried under vacuum for three days.

Benzo-15-crown-5 (B15C5, Parish) was recrystallized twice from spectrograde n-heptane and then dried under vacuum for several days. Dibenzo-18-crown-6 (DB18C6, Parish) was recrystallized twice from benzene and dried under vacuum for several days.

F. Lariat Ethers

Both methoxyethoxyethylmonoazo 15C5 ($CH_3OCH_2CH_2OCH_2CH_2N15C5$) and methoxyethylmonoazo 15C5 ($CH_3OCH_2CH_2N15C5$) were synthesized at the University of Miami by G.W. Gokel researh group. They were used as received.

G. Linear Ethers

Triglyme (Aldrich) and tetraglyme (Aldrich) were fractionally distilled under reduced pressure and dried under vacuum for three days. Pentaglyme was synthesized by N. Okorofor following the procedure of Izatt and coworkers (295), and then was dried under vacuum for three days before use.

H. Cryptands

Cryptand C211 (MCB) was used as received. Cryptand C222 (MCB) was recrystallized from n-hexane and dried under vacuum for three days.

I. Solvents

Acetonitrile (Baker) was refluxed for a week over calcium hydride and then fractionally distilled under dry nitrogen. Methyl ethyl ketone or 2-butanone (Fisher) was refluxed over calcium carbonate for three days and then fractionally distilled. Pyridine (Fisher) was refluxed over barium oxide for five days, then fractionally distilled. Ethyl acetate (EM) was refluxed over calcium hydride for several days and then fractionally distilled over dry nitrogen. The 1-chlorobutane (Eastman) was extracted with H_2SO_4, H_2O, dilute Na_2CO_3, and H_2O, dried over $CaCl_2$, and then refluxed over P_2O_5, and finally fractionally distilled under dry nitrogen (293). Benzene (Fisher) was extracted several times with H_2SO_4 to remove thiophene. It was then washed with water to remove H_2SO_4, refluxed over P_2O_5 for three days, and then fractionally distilled. Nitromethane (Aldrich, Gold Label) was refluxed over calcium hydride under reduced pressure for two days, and then fractionally distilled at reduced pressure. Since there is some decomposition of nitroalkanes above 90 °C, care was taken to keep the pot temperature under 90 °C (296). Chloroform-d (Cambridge Isotope Laboratory) and pyridine-d_5 (Aldrich, Gold Label) were used as received. All nonaqueous solvents except the deuterated solvents and nitromethane were stored over freshly activated Linde 3 Å or 4 Å molecular sieves in brown bottles in a dry box containing dry nitrogen. The water content of the nondeuterated nonaqueous solvents, except 1-chlorobutane, nitromethane, and ethyl acetate,

was determined by gas chromatography and was found to be under 100 ppm (296). The water content of nitromethane was checked by ^1H NMR since it decomposes in the GC. Since no resonance due to water was detected in the ^1H NMR, the water content of nitromethane was judged to be below 100 ppm. A water band was observed in CCl_4 saturated with water. The concentration of water in this solution is 100 ppm (296).

J. Distillation of Aluminum Chloride

Aluminum(III) chloride (Fluka AG, > 99% as $AlCl_3$) was distilled in a sealed pyrex ampule containing aluminum wire (Alfa, n5N purity), with an extra coarse (150-250 microns) pyrex fritted glass disk, to remove boron, iron, and aluminum oxide contaminates. A diagram of the ampule is shown in Figure 4. The ampule was rinsed with acetone, dried in an oven, and then stored in the dry box containing dry helium until used.

The aluminum wire was cut into 3-4 cm lengths and soaked in a 30:30:40 H_2SO_4-HNO_3-H_3PO_4 (v/v/v) concentrated acid solution for thirty seconds to remove oxide coating. The wire then was rinsed with deionized water and acetone, briefly air dried, and stored in a dry box.

Three pieces of clean aluminum wire were placed in the ampule with approximately 30 grams of $AlCl_3$. The ampule was capped, removed from the dry box and placed on a high vacuum line ($<10^{-5}$

Figure 4: Pyrex ampule used for $AlCl_3$ distillation.

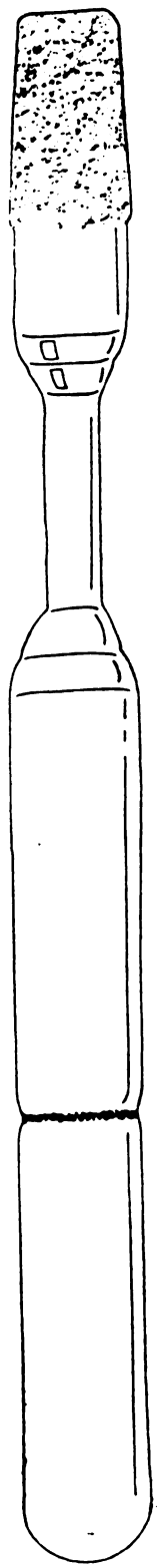

torr). After 24 hours, it was flame sealed.

The ampule was vertically suspended, empty chamber up, in a tube furnace with a small mica window. The temperature was controlled with a Love Control Corporation model 149 proportional controller and measured with a chromel-alumel thermocouple which was attached to the ampule. During the first three hours, the temperature was raised slowly (5 °C per 5 minutes) to between 190-205 °C where the solid melted to produce a clear liquid. The ampule was raised out of the tube furnace with extreme care (1 cm per hour) exposing the empty chamber to room temperature. The $AlCl_3$ vapors passed through the frit and crystallized in the upper chamber. The ampule was opened in the dry box under dry helium, and the $AlCl_3$ was ground up and stored in a sealed ampule or a vacuum flask having a glass cap held together with a Fisher Porter joint.

K. Synthesis of n-Butylpyridinium Chloride

The n-butylpyridinium chloride salt (BPC) was synthesized from pyridine and 1-chlorobutane. The purification of the starting materials is described under solvents in the material section.

Since n-butylpyridinium chloride is hygroscopic, the entire synthesis was carried out under dry nitrogen. To a three-necked round-bottomed flask containing pyridine (800 ml), 1-chlorobutane (1000 ml) was added dropwise (2 ml per minute). The reaction mixture was maintained at a temperature of 70-80 °C until the reaction was complete, then the flask was transferred to a dry box

containing nitrogen. The mother liquor was decanted, and the crude product was rinsed with acetonitrile to remove trace amounts of mother liquor. A minimal amount of acetonitrile (750-1500 ml) heated to approximately 60-70 °C was used to dissolve the crude product; one gram of activated carbon (Alfa, 28 mesh) was then added to the warm solution. The solution was filtered through a large buchner funnel with a porous glass frit (350 ml, 10-15 microns) which was wrapped with heat tape to maintain the temperature between 60-70 °C. After cooling to room temperature, 5 ml portions of ethyl acetate were added to the filtrate to promote precipitation of the product. The liquid was decanted, and the product was dried under vacuum ($\sim 10^{-3}$ torr) for 12 hours until the n-butylpyridinium chloride salt was slightly damp. The product was ground up and dried at 60 °C under vacuum ($< 10^{-5}$ torr) for at least four days. The melting point of the synthesized n-butylpyridinium chloride salt was determined to be 131°(±2) °C.

II. Procedure

A. Dry Box Manipulation

Two vacuum atmosphere dry boxes were available, one with dry helium atmosphere (DRI-TRAINHE-493, combined H_2O and O_2 estimated to be less than 10 ppm) and the other with dry nitrogen atmosphere (DRI-TRAINHE-493). In the dry box containing helium, the amount of oxygen was continually checked by monitoring the lifetime of a light bulb whose filament was exposed (297). The helium dry box contained

a Mettler balance. In this box, solutes were weighed and molten salt work was carried out. In the nitrogen dry box, all the purified nonaqueous solvents were stored over molecular sieves. All work requiring use of nonaqueous solvents was carried out in this box.

B. Preparation of Molten Salt Mixtures

Melt batch mixtures were prepared by weighing appropriate amounts of $AlCl_3$ and BPC in a pyrex weighing bottle containing a teflon stirring bar. Since the reaction between BPC and $AlCl_3$ is exothermic, initially small amounts (0.1 grams) of each component were added to avoid thermal decomposition. Once 1-2 ml of melt was prepared, larger amounts (0.5 grams) of each component were added until the desired mole fraction and batch size were obtained. After stirring for two days, the batch was vacuum filtered through a buchner funnel with a medium pyrex glass frit (5-15 microns) and stored in a pyrex weighing bottle in the dry box containing helium. The basic melt was pale yellow. As the melt became more acidic, the yellow color became more intense.

The buchner funnel and pyrex weighing bottles were soaked in concentrated HNO_3, rinsed with distilled water and acetone, and then dried in the oven before use. If the pyrex glass frits of the buchner funnels were still stained after following the above cleaning procedure, they were then soaked in hot concentrated HNO_3 which proved effective in removing the stains. Only buchner funnels

with unstained glass frits were used to filter the melt.

C. Sample Preparation

Molten salt solutions were prepared in three different ways, depending on the experiment. For individual samples, the amounts of solute and melt were weighed in a 5 mm pyrex NMR tube. For mole ratio studies, two stock solutions were prepared in pyrex weighing bottles, each containing a teflon stirring bar and both having the same concentration of lithium chloride. One of these contained the ligand. These stock solutions were stirred at approximately 50 ^{o}C for one week before use. Weighed amounts of each solution were transferred to a 5 mm pyrex NMR tube. For concentration studies, a stock solution was used containing a weighed amount of salt and melt. Weighed amounts of the stock melt solution and of the melt whose composition is the same as that of the stock were transferred to a 5 mm pyrex NMR tube. All sample tubes were flame sealed after being evacuated to $<10^{-5}$ torr. All NMR samples were conditioned at 70 ^{o}C for an additional three weeks before making measurements. For IR measurements, solutions were weighed out in pyrex weighing bottles and stirred at 50 ^{o}C for at least a week before use.

Aluminum chloride stock solutions were prepared by sublimation procedurs at pressures $<10^{-5}$ torr. Figure 5 shows the pyrex flask used for this operation. This flask is equipped with Kontes valves and Fisher Porter joints which allow for work at pressures of 10^{-7} torr. The solvent was sublimed into the flask which contained a

Figure 5: $AlCl_3$ sublimation flask.

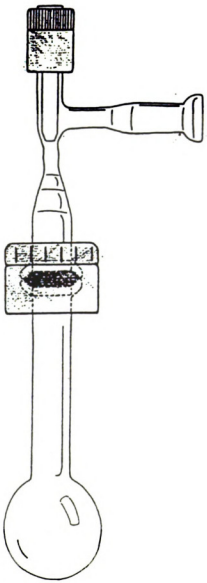

weighed amount of $AlCl_3$. The $AlCl_3$ dissolved in the solvent as the flask cooled to room temperature. Next, the flask was taken into the dry box containing nitrogen, and disassembled. The contents were quantitatively transferred to a volumetric flask, and then the flask was filled to the mark with the solvent. Aliquots of this solution were taken by using an Eppendorf automatic pipet.

Since lithium salts and nonaqueous solvents are very hygroscopic, the solutions were prepared in a dry box containing helium or nitrogen. Dilute solutions of salt were prepared by appropriate dilutions of a stock solution. Aliquots of the stock solutions were taken with an Eppendorf automatic pipet. Single samples were prepared by weighing out the desired quantities of salt and/or ligand into a volumetric flask. Initially, only enough solvent was added to the volumetric flask to dissolve the contents. The volumetric flask was not filled completely until just before use, to prevent concentration errors due to solvent evaporation.

All glassware used to prepare melt and nonaqueous solutions was cleaned according to the procedure described in the procedure section, Part II-B.

D. Viscosity Measurements.

Viscosity measurements were made with a Canon-Fenske viscometer in a water bath equilibrated at 25.00(±0.02) ^{o}C. The viscometer used was recommended for solutions having a viscosity between 0.5 and 2.0 centistokes. The viscometer was rinsed with concentrated

HNO_3, distilled water, and acetone, and then placed in the oven to dry before measurements were made.

Measurements were obtained at several different concentrations, and the relative viscosities were fitted to the following equation using KINFIT (298,299) on a CDC Cyber 750 computer.

$$\eta_r = \eta/\eta o = 1 + A_\eta C^{\frac{1}{2}} + B_\eta C + D_\eta C^2 \qquad (2\text{-}1)$$

The following constants determined are A_η, B_η, and D_η. The η and η_o terms are the viscosities of the solution and solvent, respectively. The A_η term is a constant dependent on long range coulombic forces, B_η is related to the size of the ion and different ion-solvent interactions, and D_η is part of an extra term which accounts for solvent-solute or solute-solute interactions not accounted for by the other terms. Once the three constants have been determined, the viscosity at any particular concentration can be obtained. The three constants determined from fitting the relative viscosities ($\eta/\eta o$) at different molar concentrations are found in the same table as the ^{35}Cl linewidth measurements in Appendix 1.

To transform time measurements into viscosities the following relationship was used:

$$\eta/\rho = Bt \qquad (2\text{-}2)$$

where η is the viscosity, ρ is the density, and t is the time required for the upper meniscus to fall from the upper to lower fiducial mark. To obtain B, the apparatus constant water was used as the calibrating solvent. The viscosity and density of water at 25 °C is 0.89025 centapoise and 0.9970 g/cm^3, respectively (300). The apparatus constant B determined for this viscometer is 0.0164(±0.0003). It was assumed in the calculation that the solvent density is equal to the solution density.

III. Instrumentation

A. Multinuclear Nuclear Magnetic Resonance Spectroscopy

Multinuclear magnetic resonance measurements were made on a Bruker WH-180 spectrometer with a field strength of 42.3 kG. At this field, ^{133}Cs, ^{7}Li, ^{35}Cl, ^{27}Al, and ^{23}Na resonate at 23.61, 69.95, 17.64, 46.90, and 47.61 Mhz, respectively. Chemical shifts that are downfield (paramagnetic) from the reference are positive. Tubes used for NMR measurements were cleaned with concentrated HNO_3, rinsed with distilled water and acetone, and then dried in the oven before use.

For ^{7}Li chemical shift measurements in nonaqueous solvents, a 5 mm tube or a 4 mm od insert was placed inside a 10 mm pyrex NMR tube. A 0.10 M LiCl/D_2O solution was used as the external reference.

Chemical shift and linewidth measurements were made with ^{35}Cl NMR. A 0.10 M LiCl/D_2O solution was used as the external reference.

Chemical shift measurements were made with ^{27}Al NMR. The

chemical shift of the $AlCl_4^-$ band was measured by use of a 0.6 M $Al(H_2O)_6^{3+}$ reference. The chemical shifts of the other bands in the ^{27}Al spectrum were determined from the chemical shift of the $AlCl_4^-$ band. The $Al(H_2O)_6^{3+}$ species exists in a 0.6 M $Al(NO_3)_3$ solution when the HNO_3 concentration is 1 M.

For molten salt solutions, a 5 mm pyrex NMR tube was mounted with teflon spacers within a 10 mm pyrex NMR tube. The outer tube contained the reference solution. The references were 0.01 M LiCl/D_2O solution, 0.01 M CsBr 20 % D_2O/H_2O solution, and 0.01 M NaCl/D_2O solution. All molten salt samples were run at high temperatures ($\geq$40 °C). To reduce the conditioning time in the NMR probe, samples were heated before measurements were taken.

Linewidths were obtained either by fitting a Lorentzian function to the data by use of NTCCAP or by directly using the cursor in the peak print routine. The second procedure was used for all spectra taken on the WH-180 prior to the installation of the operating system which utilized the program NTCFTB.

For the Fourier transform spectrometer which utilizes a superconducting magnet, the observed chemical shifts were corrected for the magnetic susceptibility of the solvent with an equation derived from the equation of Martin, et al. (301)

$$\delta cor = \delta obs + \frac{4\pi}{3} (\chi_v^{ref} - \chi_v^{sample}) \times 10^6 \qquad (2\text{-}3)$$

where χ_v^{ref} and χ_v^{sample} are the unitless volumetric magnetic

susceptibilities of the reference and sample, respectively, and δcor and δobs are the corrected and observed chemical shifts. The volume susceptibility for pyridine, 2-butanone, benzene, and nitromethane are -0.611×10^{-6}, -0.509×10^{-6}, -0.611×10^{-6}, and -0.391×10^{-6}, respectively (302). The magnetic susceptibility corrections for pyridine, 2-butanone, benzene, and nitromethane are -0.45, -0.87, -0.45, and -1.37, respectively, determined versus a water reference. Magnetic susceptibility corrections were calculated at 32 °C, 25 °C, 20 °C, and 20 °C for benzene, nitromethane, pyridine, and 2-butanone, respectively. It is assumed that these corrections are accurate enough to correct NMR measurements made at ambient temperature (~25 °C). Chemical shifts listed on tables or in figures are corrected for the magnetic susceptibility of the solvent unless otherwise specified.

The complexation and association constants were obtained by fitting chemical shift and linewidth measurements to the appropriate mechanism using KINFIT on a VAX-11/780 or a CDC Cyber 750 computer (299). The crown ether complexation constant in 45 mole % $AlCl_3$ melt were obtained in mole fraction units. The formation constants were converted to molarity using the density and the average molecular weight of the melt. The density and molecular weight of 45 mole % $AlCl_3$ melt are 1.2007 g/cm^3 and 154.977 g/mole, respectively. The density of the melt was obtained from a linear equation obtained from fitting known melt densities at different compositions.

$$\rho = (6.66 \times 10^{-3})(\text{Mole \% } AlCl_3) + 0.901 \qquad (2\text{-}4)$$

B. Carbon-13 and Proton Nuclear Magnetic Resonance Spectrometry

Carbon-13 and proton NMR measurements were obtained on a Bruker WH-250 spectrometer operating at a field strength of 58.7kG at frequencies of 250 and 62.9 Mhz, respectively. In ^{13}C studies, downfield shifts are taken as positive. The NMR tubes used for NMR measurements were cleaned as described in the instrumental section, Part III-A. A 10 mm probe was used for ^{1}H measurements. Two different probes were used for ^{13}C measurements, a 5 mm and a 10 mm probe. Using the 10 mm probe, a 5 mm pyrex NMR tube containing the sample was placed inside a 10 mm pyrex NMR tube containing the reference. For molten salt solutions, an 8% DMSO/D_2O solution or one of the lines from the BP^+ contained in the melt was used as a reference. The chemical shift of the BP^+ and the DMSO bands were determined from a 5% TMS chloroform-d reference at 45 ^{o}C. When using the 5 mm probe, a 5 mm tube containing the sample was used, and the spectra were obtained without lock. The position of the solute band was determined by use of one of the BP^+ bands as a reference. For ^{1}H measurements, a 5% TMS chloroform-d reference was used. All ^{1}H measurements were made at room temperature.

C. Infrared Spectrometry

Infrared spectral measurements were carried out on a Bomen DA3 FT-IR spectrometer. Data were collected at 32K range memory and

treated with a Hammon apodizing function to minimize fringe patterns in the spectra. For all measurements, the sample port was purged with nitrogen.

Samples were placed in an Aries model 20500 vacuum tight liquid cell or in a standard dismountable Barnes liquid cell. For molten salts and 2-butanone solutions, the Aries cell was used with 6mm NaCl windows. The Aries 20500 liquid cell was advertized as a vacuum tight cell; however, when the cell was evacuated in the sample port of the IR, melt solution leaked out from between the cell plates. For pyridine solutions, the Barnes mount was also used. The windows used in the mid-IR range with the Barnes mount were 3 mm CaF_2, 2 mm itran, and 3 mm KBr plates. Teflon spacers were placed between the IR plates. For nonaqueous solutions, after the IR spectrum was obtained, the cell was flushed with absolute ethanol. For molten salt solutions, after the IR spectrum was obtained, the cell was flushed with CCl_4 (Fisher, spectroanalyzed grade), acetone (Baker, 'Photrex' Reagent for UV Spectrometry), and again with CCl_4. The flushing solvents were removed by drawing air through the cell using a vacuum produced from a water aspirator.

To obtain areas for the IR bands, the lineshape was described with a Gaussian-Lorentzian product function:

$$I = I_o \exp \left| \frac{-(\nu-\nu o)^2}{2\sigma^2} \right| \left| 1 + \frac{(\nu-\nu o)^2}{\sigma^2} \right|^{-1} \qquad (2\text{-}5)$$

where I is the intensity (absorbance units) at frequency ν, νo is

the frequency of the maximum intensity, σ is the variance (σ = $1.46\Delta\nu_{1/2}$ and $\Delta\nu_{1/2}$ is the band half width) (303). Using the program MULDAT, specific segments of a large data file were rewritten in MULPLT format. Each IR band was fitted to the Gaussian-Lorentzian product function by use of CRVFIT written by T. Atkinson. This program was written to be used on a PDP-11 computer.

D. Electrical Conductance

Solution resistances were measured at these frequencies in hertz, 398(±2), 629(±2), 971(±6), 1942(±11), and 3876(±18). The bridge used was initially designed by Thompson and Rogers (304) and rebuilt with minor improvements by Smith (305). The cell was connected in parallel to a capacitor. When the cell's resistance became greater than 90,000 ohms, it was shunted in parallel with a 90,000 ohm standard resistor. A Heath company laboratory oscilloscope was used as a null point detector. The conductance flasks were of the volumetric type with platinum electrodes (Figure 6). Each conductance flask was equipped with a glass cover which was attached to the volumetric flask by a Fisher Porter connection. The conductance flasks were soaked with concentrated HNO_3, rinsed with distilled water, and then steamed. After steaming, the conductance flasks and the glass covers were dried in an oven before use.

The resistance of the sample with highest salt concentration was

Figure 6: The electrical conductance flask.

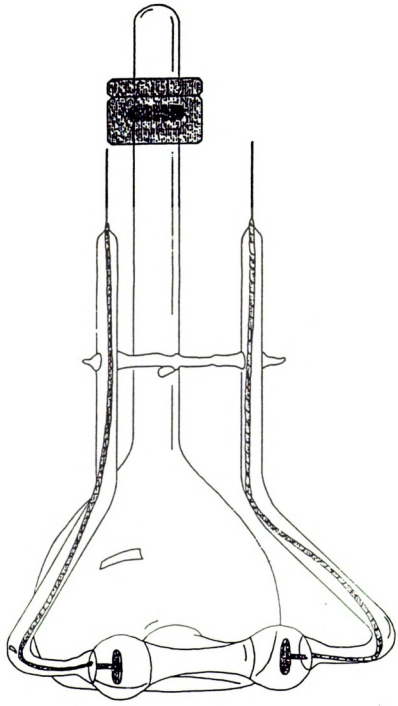

obtained first. To this solution contained in the conductance flask, a series of solvent additions were made to reduce the solution concentration. Resistance measurements were made after every addition. A buret was used for this operation. Solutions were prepared in a dry box containing dry nitrogen. An oil bath thermostated at 25.00(±0.05) °C was used.

All measured resistances were corrected for both irreversibility at the electrodes and the capacitance bypass effect by using:

$$R_m = R_o + af^2 + b/\sqrt{f} \qquad (2\text{-}6)$$

in which R_m and R_o are the measured and corrected resistance, f is the frequency in hertz, and a and b are adjustable parameters. The best value of R_o for each concentration was obtained by using the least square KINFIT program on a CDC Cyber 750 computer (299). The R_o's were used to obtain the equivalent conductances from the following equation:

$$\Lambda = \frac{1000K}{C}\left(\frac{1}{R_o^{SOL}} - \frac{1}{R_o^{SOLV}}\right) \qquad (2\text{-}7)$$

where R_o^{SOL} and R_o^{SOLV} are the resistances of the solution and the solvent, respectively, and K and C are the cell constant and the molar concentration of the salt, respectively. When the standard resistor was used, the actual resistance (R_o^{SOL}) was computed using this equation:

$$\frac{1}{R_o^{SOL}} = \frac{1}{R_{o,m}^{SOL}} - \frac{1}{R_o^{ST}} \qquad (2\text{-}8)$$

where R_o^{ST} is the resistance of the standard resistor and $R_{o,m}^{SOL}$ is the measured resistance using the standard resistor. The standard resistance (R_o^{ST}) was measured when the electrical connections were disconnected from the cell.

The cell constant was determined by resistance measurements taken on an aqueous potassium chloride solution of known composition. the equation of Barthill et al. (306) was used to determine the equivalent conductance.

$$\Lambda = 149.873 - 95.01C^{1/2} + 38.48C\log C + 183.1C - 176.4C^{3/2} \qquad (2\text{-}9)$$

Two cells were used, a 25 ml and 30 ml cell. The cell constant determined for the 25 ml cell was 2.601(±0.009), and for the 30 ml, cell it was 1.376(±0.003).

The association constants were obtained by fitting the equivalent conductances measurements to the Fuoss-Kraus and Justice equations using KINFIT on a CDC Cyber 750 computer (299).

E. Electron Spin Resonance Spectrometry

The ESR experiments were carried out on an X-band spectrometer (Bruker ER200D) instrument. Samples were prepared in 5 mm NMR tubes and sealed under vacuum ($<10^{-5}$ torr). These NMR tubes were cleaned following the procedure described in the instrumental section, Part

Part III-A. The samples were frozen with temperature-regulated nitrogen gas before measurements were obtained.

F. Magnetic Susceptibility Measurements

Magnetic susceptibility measurements were made on an S.H.E. Corporation computer variable temperature susceptometer equipped with a superconducting quantum interference device (SQUID) at a field strength of 5000 G. Samples were weighed out in a KelF bucker in the dry box. The bucket was a cylindrical with a diameter of 7 mm and height of 9 mm with a screw on cover to prevent spilling (Figure 7). The bucket was rinsed tith concentrated HNO_3 before use. This bucket was removed from the dry box, placed in the air lock of the susceptometer, evacuated to ~500 millitorr and flushed with helium gas three times before being lowered into the SQUID. The readings were taken at 40 ^{o}C.

To obtain the weight susceptibility of the sample, the following equation was used:

$$X_g = \frac{\bar{M}}{(SENS)\ (DM)\ (FIELD)\ (WT)} \qquad (2\text{-}10)$$

where $\bar{M}$ is the difference in the magnetic moment of the empty bucket and the bucket containing the melt solution, SENS is the sensitivity of the instrument, FIELD is the magnetic field in guass, DM is the susceptibility multiplier, and WT is the weight in grams of the melt sample. To convert from weight susceptibility to volume susceptibility, the

Figure 7: Sample bucket for magnetic susceptibility measurements.

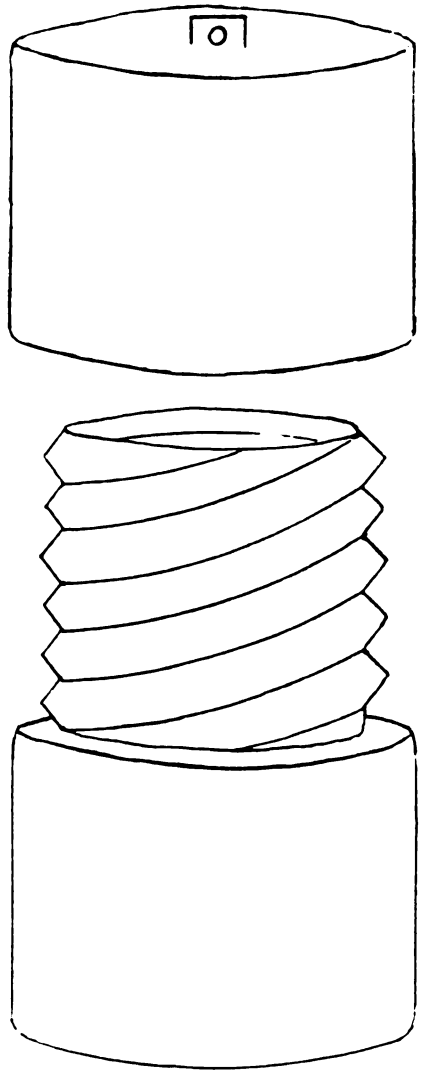

weight susceptibility was multiplied by the density (ρ = 1.2007 g/cm^3).

For 45 mole % melt, the value obtained from this technique was X_v = -.71(±0.08) X 10^{-6}. Therefore the correction term, $4\pi/3(X_v^{ref} - X_v^{sol})$ X 10^{-6}, in equation (2-1) was determined to be -0.037(±0.335) versus water (reference solvent). Measurements on acidic melts were not attempted because these melt solutions are very corrosive, and spilling would have caused severe damage to the SQUID.

CHAPTER 3

SOLVATION STUDIES OF LITHIUM SALTS IN 2-BUTANONE AND PYRIDINE

I. Introduction

Solvation studies of a series of lithium salts in 2-butanone and pyridine were carried out to investigate the ionic interactions occurring in these solutions. Infrared spectrometry was used to identify the chemical processes occurring in these solutions. Electrical conductance and ^{7}Li NMR measurements were made to obtain the ion association constants.

II. Electrical Conductance

Electrical conductance measurements for a series of lithium salts in pyridine and 2-butanone solutions were used to determine ion association constants. The lithium salt concentrations ranged from ~1.0 mM to ~0.01 M for these measurements.

The Fuoss-Kraus theory considers ion pairing the only process occurring in solution if the molar concentration of the salt is lower than C_o given by $C_o=(1.19 \times 10^{-14})(\epsilon T)^3$ where ϵ is the dielectric constant of the solvent and T is the absolute temperature (28). The values for the dielectric constant of 2-butanone and pyridine are given in Table 1.

According to the Fuoss-Kraus theory, at molar concentrations $\geq C_o$, the conductance equation must account for the formation of triple

Table 1

Important Physical Properties of Different Solvents[a]

	2-Butanone	Pyridine	Propylene Carbonate	Acetone
Molecular Weight (M, g/mole)	72.108	79.102		
Density at 25 °C (ρ, g/cm^3)	0.7997	0.9782		
Viscosity at 25 °C (η, centapoise)	0.384	0.884	2.513	0.3040
Dielectric constant (ϵ)	18.51	12.4		
Molecular diameter (Å)	6.58	6.35		
Limiting Conductance (Λ_o, cm^2/ohm mole)			$LiCF_3CO_2$ 25.9[b]	LiCl 214[c]

[a] ref. 300
[b] ref. 307
[c] ref. 308

ions. At 25 °C in 2-butanone and pyridine solutions, the concentrations at which triple ion formation becomes important are 2.0 mM and 0.6 mM, respectively. The introduction of triple ions to explain the poor fits of the conductance data to numerous theoretical equations has been debated. The concentration range of the conductance measurements obtained in our laboratory overlapped with the triple ion region as defined by the Fuoss-Kraus theory.

Two models were used to fit the electrical conductance measurements obtained in our laboratory. Both models have been used by other investigators to obtain ion pairing formation constants in other low dielectric solvents at these concentrations (57,309). The Justice equation used to fit the electrical conductance data is (33,34):

$$\Lambda=\Lambda_o - S(\alpha C)^{1/2} + E\alpha C \ln \alpha C + J_1\alpha C - J_2(\alpha C)^{3/2} - K_a\alpha C f_{\pm}^2\Lambda \qquad (3\text{-}1)$$

The constants J_1 and J_2 were determined from the equations derived by Fernandez-Prini (310), and the $E\alpha C \ln \alpha C$ term was obtained from the equation derived by Chen (47,311). The other terms have been defined in the historical section, Chapter I. The ion pairing formation constant and the mean activity coefficient are defined as:

$$K_a = \frac{(1 - \alpha)}{\alpha^2 C f_{\pm}^2} \qquad (3\text{-}2)$$

$$\ln f_{\pm} = \frac{-A(\alpha C)^{1/2}}{1+Ba(\alpha C)^{1/2}} \qquad (3\text{-}3)$$

The J_1, J_2, mean activity coefficient, and EαCln αC terms are dependent on the interatomic distance. The interatomic distance parameter in the J_1 term and the mean activity coefficient equation were set equal to the Bjerrum distance (q). The Bjerrum distance was calculated using:

$$q = \frac{e^2}{2\epsilon kT} \qquad (3\text{-}4)$$

The dielectric constant (ϵ) and the viscosity (η) of the solution were assumed to be equal to those of the solvent and are given in Table 1. Using the viscosities measured in our laboratory for 2-butanone and pyridine, given in Appendix 2, instead of those given in Table 1 does not significantly change the values of the ion pairing constants. The equation was fitted to the electrical conductance measurements using KINFIT to obtain the value of the limiting conductance, Λ_o, the ion pairing constant, K_a, and the distance parameter in the equations for the EαCln αC and J_2 terms (299). The only exception to this procedure was for $LiCF_3CO_2$ and LiCl where K_a was determined by setting the Λ_o values constant in the fitting program. The ion pairing constants for these salts in these solvents are $\gtrsim 10^5$ M^{-1}; therefore, it is impossible to obtain accurate values for both Λ_o and K_a from fitting the Justice equation to the electrical conductance measurements (43). For LiCl in pyridine, Λ_o = 73.59 $\Omega^{-1}cm^2mol^{-1}$ was determined based on Λ_o obtained from electrical

conductance measurements in LiCl acetone solutions at 25 °C (308). The Walden product was used to obtain Λ_o for LiCl pyridine solutions. For $LiCF_3CO_2$ in 2-butanone, Λ_o = 169.5 $\Omega^{-1}cm^2mol^{-1}$ was obtained from the sum of ionic limiting conductances at 25 °C in propylene carbonate and the Walden product (307). The Λ_o and the viscosities used in the Walden product calculation are found in Table 1. The Walden product is the product of the Λ_o and the η, which should be constant for a particular salt in solvents that exhibit the same solvation properties. Therefore, an estimate for the limiting conductance can be calculated for any salt in a particular solvent if the limiting conductance for that salt has been measured in another solvent where the viscosity at that temperature is known. The accuracy of the ion pairing formation constant using the Λ_o obtained from the Walden product is unknown. The results of fitting the conductance data obtained from the 2-butanone and pyridine solutions to the Justice equation are listed in Table 2. Values in parentheses are the standard deviations obtained from the fits.

The Justice equation does not take into account the formation of triple ions. According to the Justice theory, the distance parameters in the equations for J_2 and EαCln αC obtained from the fit should be equal to the Bjerrum distance (q = 15.1 Å in 2-butanone, q = 22.6 Å in pyridine) (53). The distance parameters obtained from the fits do not equal the Bjerrum distance (Table 1), which could be attributed to missing terms to account for triple ion formation in the Justice equation (3-1). Therefore, these results indicate that the distance

Table 2

Ion Pairing Constants, Limiting Conductances, and the Interatomic Distances for Several Lithium Salts Determined in Pyridine and 2-Butanone Using the Justice Equation at 25 °C

Salt	Solvent	$K_a(\underline{M}^{-1})$	$\Lambda_o(cm^2/ohm\ mole)$	a(Å)
LiPi	2-butanone	5000(±1080)	117(±10)	7(±1)
$LiAsF_6$	2-butanone	310(±12)	149(±1)	19.5(±0.6)
LiSCN	2-butanone	13000(±3840)	87(±13.)	30(±9)
LiI	2-butanone	336(±65)	136(±7)	22.6(±0.5)
$LiBPh_4$	2-butanone	283(±35)	104(±3)	17.8(±0.2)
$LiClO_4$	2-butanone	503(±32)	137(±2)	21.8(±0.1)
$LiCF_3CO_2$	2-butanone	$2.2(\pm0.1) \times 10^5$	169.5*	69.(±166.)
LiCl	pyridine	$2.6(\pm0.3) \times 10^6$	73.59*	14.(±1.)
$LiClO_4$	pyridine	1900(±168)	76(±3)	2.7(±0.2)
$LiNO_3$	pyridine	3200(±658)	12(±1)	23.(±2.)
LiPi	pyridine	2900(±120)	30.8(±0.6)	32.1(±0.5)
LiSCN	pyridine	8600(±924)	20.4(±0.4)	0.7(±0.8)

Values in parentheses are the standard deviations obtained from the fit.

parameters obtained from the fits using the Justice equation represent simply a fitting parameter, and they may have no physical significance.

To determine the accuracy of the ion pairing constants obtained from the Justice equation, another conductance equation was used to fit the electrical conductance data. The Fuoss–Kraus equation, which accounts for triple ion formation, was the second equation used (58). The Fuoss–Kraus equation is:

$$\Lambda g(C)C^{1/2} = \frac{\Lambda_o}{K_a^{1/2}} + \frac{K_T\Lambda_o^T}{K_a^{1/2}}(1 - \Lambda/\Lambda_o)C \qquad (3\text{-}5)$$

with

$$g(C) = \frac{\exp\left((-2.303\beta'/(\Lambda_o^{1/2}))(\Lambda C)^{1/2}\right)}{(1-S/\Lambda o^{3/2}\ (\Lambda C)^{1/2})(1 - \Lambda/\Lambda_o)^{1/2}} \qquad (3\text{-}6)$$

where β' and S are the Debye–Hückel activity coefficient and the Onsager term, respectively. These terms are defined in the historical section of the thesis, Chapter I. The limiting conductance, Λ_o, is set to a constant, and fitting the conductance data produces the K_a and $\Lambda_o^T K_T$ terms. The values of the Λ_o, η, and ϵ terms used in fitting the electrical conductance data to the Fuoss–Kraus equation are the same as the values used in fitting the Justice equation. To obtain the K_T and $\Lambda_o^T K_T$, one assumes that $\Lambda_o^T = 2/3\Lambda_o$. This relationship is not necessarily always correct; therefore, the accuracy of K_T is undetermined although the choice of Λ_o^T does not affect the values obtained for the ion pairing formation constants.

Equivalent conductances and concentrations must be transformed to $\Lambda g(C)C^{1/2}$ and $(1 - \Lambda/\Lambda_o)C$ to utilize KINFIT in the curve fitting mode (299). Utilizing the equations for the variance of $\Lambda g(C)C^{1/2}$ and $(1 - \Lambda/\Lambda_o)C$ derived from error propagation methods, the variance of K_a and K_T were determined by the fitting program (Appendix 4-C).

The ion pairing and triple ion formation constants obtained from fitting the Fuoss-Kraus equation to the electrical conductance measurements are listed in Table 3. As expected, the triple ion pairing constants are smaller than the ion pairing formation constants. For LiI in 2-butanone, the triple ion formation constant obtained from the fit is negative, which indicates that the extent of triple ion formation is very small. All the formation constants obtained from fitting the electrical conductance data to the Fuoss-Kraus equation are in reasonable agreement to the ion pairing formation constants obtained from fitting the Justice equation. The fitting errors for the ion pairing constants obtained from the Fuoss-Kraus equation are less than those obtained from the Justice equation. The fitting errors which are standard deviations obtained from the fit are listed in the parentheses following the K_a values. The differences in the experimental errors of the ion pairing formation constants obtained from fitting these two equations to the electrical conductance data may also be attributed to the fact that the Justice equation does not take into account the formation of triple ions (61).

The ion pairing constants obtained from fitting the conductance

Table 3

Ion Pairing and Triple Ion Constants for Several Lithium Salts in Pyridine and 2-Butanone Using the Fuoss-Kraus Equation at 25 °C

Salt	Solvents	$K_a(\underline{M}^{-1})$	$K_T^a(\underline{M}^{-1})$
LiPi	2-butanone	5790(±66)	9(±1)
LiSCN	2-butanone	14300(±224)	25(±2)
$LiClO_4$	2-butanone	486(±7)	6(±3)
$LiBPh_4$	2-butanone	240(±12)	120(±17)
LiI	2-butanone	334(±9)	-35(±5)
$LiCF_3CO_2$	2-butanone	3.1(±0.4) X 10^5	89(±19)
$LiAsF_6$	2-butanone	273(±7)	57(±8)
LiCl	pyridine	4.5(±0.2) X 10^6	65(±7)
LiPi	pyridine	3520(±36)	11(±1)
$LiClO_4$	pyridine	1990(±25)	9(±2)
$LiNO_3$	pyridine	1600(±168)	43(±16)
LiSCN	pyridine	7627(±97)	15(±1)

[a]Triple ion formation constant.

Values in parentheses are the standard deviations obtained from the fits.

data are dependent upon the ability of the solvents to solvate the anions. In 2-butanone solutions, $LiBPh_4$, LiI, $LiClO_4$, and $LiAsF_6$ have ion pairing formation constants <600 $\underline{M}^{-1}$; the other salts have ion pairing formation constants >1000 $\underline{M}^{-1}$ in these solutions. The ion pairing constants obtained from conductance measurements indicate that salts having large symmetrical anions are solvated better in 2-butanone than salts containing small unsymmetrical anions. A list of the ion pairing formation constants determined for a series of alkali metal salts in these solvents at other laboratories is given in Table 4. The ion pairing formation constants measured for LiI and LiPi in 2-butanone in our laboratory are comparable to these values. However, the ion pairing constants for LiPi in pyridine measured in our laboratory were significantly smaller than the value reported in the literature.

By comparing the measured ion pairing formation constants to the theoretical calculated contact ion pairing and the solvent separated ion pairing constants, it is possible to determine whether ion pairs exist as contact or solvent separated. In Table 5, the interatomic distances and the ion pairing formation constants calculated from the Bjerrum equation are listed (312). The radii used to calculate the interatomic distances were determined from the crystal ionic radii except for Pi^- (r = 1.41 Å) and BPh_4^- (r = 3.8 Å) (77). The crystal ionic radii were obtained from the Handbook of Chemistry and Physics (302). The radii of the polyatomic atoms were calculated from the center of the molecular ion with the use of the crystal ionic radii of

Table 4

Ion Pairing Constants, Limiting Conductances, and the Interatomic Distances Obtained from Conductance Measurements at 25 °C

Salt	Solvents	Eq	$K_a(\underline{M}^{-1})$	$\Lambda_o(cm^2/ohm\ mole)$	a(Å)	Ref
LiI	2-butanone	F	362	147.2	--	314
LiPi	2-butanone	FK	6140	123.92	2.64	316
LiPi	2-butanone	LW,P	6765, 6646	131.43, 130.85	7.8, 7.1	77
		F,J	6688, 6557	131.00, 130.17	7.4, 13.0	
NaI	2-butanone	F	405	147.7	--	314
KI	2-butanone	F	469	150.8	--	314
LiPi	pyridine	--	1.2×10^4	--	3.61	315
NaI	pyridine	FA	2.22×10^3	75.05	7.1	313
KI	pyridine	FA	3.98×10^3	80.0	7.9	313

Abbreviation	Equation
F	Fuoss Equation
FK	Fuoss-Kraus Equation
FA	Fuoss-Accascina
LW	Lee-Wheaton
P	Pitts Equation
J	Justice Equation

Table 5

Calculated Ion Pairing Constants for Contact and Solvent Separated Ion Pairs Using the Bjerrum Equation at 25 °C

Salt	Solvent	a(Å)	$^{a}K_a^{c}(\underline{M}^{-1})$	$^{b}K_a^{ss}(\underline{M}^{-1})$
LiCl	pyridine	2.49	6.6×10^5	561
$LiNO_3$	pyridine	3.45	4.2×10^4	480
$LiClO_4$	pyridine	3.59	3.5×10^4	470
LiPi	pyridine	2.09	1.0×10^7	607
LiSCN	pyridine	4.39	6.9×10^3	417
$LiClO_4$	2-butanone	3.59	679	67
LiI	2-butanone	2.88	2.9×10^3	78
LiPi	2-butanone	2.09	1.8×10^4	93
$LiAsF_6$	2-butanone	4.44	374	55
$LiCF_3CO_2$	2-butanone	4.01	512	61
$LiBPh_4$	2-butanone	4.48	363	54
LiSCN	2-butanone	4.39	389	55

In the third column are the interatomic distances calculated for the contact ion pairs.

[a]Contact ion pairing constants

[b]Solvent separated ion pairing constants

the atoms, except for those of $CF_3CO_2^-$ and AsF_6^- (307,309). The calculation of the ion pairing formation constants for solvent separated ion pairs using the Bjerrum model was identical to the calculation used to obtain contact ion pairing constants, but the interatomic distance was taken as the sum of the radii of the cation and anion plus the diameter of the solvent molecule. The mean molecular diameter of the solvent molecule was calculated from the equation $d = 2(3M/4\pi N\rho)^{1/3}$, where M is the molar mass and ρ is the density of the solvent (317). The numerical values used in this calculation and the molecular diameters for 2-butanone and pyridine are listed in Table 1. All the lithium salts studied in 2-butanone and pyridine are primarily contact ion paired in these solutions, based on the Bjerrum theory. The measured ion pairing constants are much larger than the calculated solvent separated ion pairing formation constants. For $LiCF_3CO_2$ and LiSCN in 2-butanone and LiCl in pyridine, the measured ion pairing formation constants are larger than the calculated contact ion pair formation constants.

Since the dielectric constant for pyridine (ϵ = 12.4) is lower than that of 2-butanone (ϵ = 18.51), it is expected that the ion pairing formation constants should be larger in pyridine than in 2-butanone. This is true for $LiClO_4$ in these solvents. The ion pairing formation constant is ~4 times larger in pyridine than in 2-butanone. However, the ion pairing formation constants for LiPi and LiSCN are larger in 2-butanone than in pyridine. Such behavior may be accounted for by considering specific solvent effects. Justice and

Justice (318) redefined the Bjerrum theory of ion pairing by introducing an additional term, $\exp(-h_{+-}/T)$, which accounts for specific solvent effects. The h_{+-}/kT term is referred to as the square mound potential (SMP). The h_{+-} is the energy related to the interaction of free ions and ion pairs with surrounding solvent molecules. When SMP is positive, the solvent interactions make the solvated ions more stable than contact ion pairs, and when this term is negative, contact ion pairs are solvated better than free ions. When SMP has a large positive value, this implies that ion pairs in solution behave as solvent separated ion pairs. The SMP term was calculated from the following equation:

$$\exp(-h_{+-}/kT) = \frac{K_a(obs) - K_a(b')}{K_a(b) - K_a(b')} \qquad (3\text{-}7)$$

where $K_a(b)$ and $K_a(b')$ are the Bjerrum ion pairing constants for contact and solvent separated ion pairs, and $K_a(obs)$ is the measured ion pairing constant. Other terms include the $b=2q/a$, and $b'=2q/(a+d)$, where d and a are the mean solvent diameter and interatomic distance of the contact ion pair, respectively. The SMP was calculated for each salt solution and are listed in Table 6. The $K_a(obs)$ was taken as the ion pairing constant determined from electrical conductance by use of the Justice equation. These ion pairing formation constants are listed in Table 2.

For LiSCN and $LiCF_3CO_2$ in 2-butanone and LiSCN and LiCl in pyridine, the SMP is negative, which implies that the ion pairs in

Table 6

Square Mound Potentials of Various Lithium Salts in 2-Butanone and Pyridine at 25 °C

Salt	2-Butanone	Pyridine
LiCl		-1.37
$LiNO_3$		+2.72
$LiClO_4$	+0.34	+3.18
LiSCN	-3.66	-0.23
LiPi	+1.29	+8.38
LiI	+2.39	
$LiAsF_6$	+0.21	
$LiCF_3CO_2$	-6.19	
$LiBPh_4$	+0.31	

these solutions exist as contact ion pairs. For LiPi, $LiClO_4$, and $LiNO_3$ pyridine solutions and LiI 2-butanone solutions, the large positive SMP indicates that ion pairs behave as solvent separated ion pairs. For $LiBPh_4$, LiPi, $LiClO_4$, and $LiAsF_6$ in 2-butanone, the SMP is intermediate, which indicates that both solvent separated and contact ion pairs coexist. It must be kept in mind that the interpretation of the results of the square mound potentials depends on whether the interatomic distance determined from the crystal ionic radii and the calculated average solvent diameter is a good approximation to the actual interatomic distance of the contact and solvent separated ion pairs in solution. Also, the amount of water in these lithium salt solutions may affect the electrical conductance data because these measurements are made at such low salt concentrations, ~1.0 mM to ~0.01 M. Since most organic solvents cannot be obtained in a completely anhydrous state, it is obvious that meaningful measurements can be obtained only if the water concentration is much lower than the concentration of the salt.

III. Nuclear Magnetic Resonance Spectroscopy

Lithium-7 chemical shifts and ^{35}Cl linewidths were measured for a series of lithium salts in 2-butanone and pyridine at concentrations greater than ~1.0 mM. Since lithium salts are hygroscopic, it is essential that the amount of water in these solvents be as low as possible. The water contamination in these solvents was kept below

100 ppm, but the water concentration was still too high to obtain meaningful ^{7}Li NMR measurements below 0.01 M. Chemical shifts for concentrations below 0.01 M are obtainable with our instrument, but the chemical shift measurements do not exhibit predictable behavior based on measurements at higher concentrations. Below 0.01 M $LiNO_3$ and LiCl in pyridine solutions, the chemical shifts were expected to move toward the chemical shift of the solvated Li^+ as the concentration was decreased. Instead the chemical shifts remained essentially constant from 1.0 mM to 0.01 M (Appendix 1). The chemical shift behavior at these low concentrations indicates the formation of solvent separated ion pairs. If the water concentration is large, water molecules will strongly solvate the ions to produce ion pairs that are solvent separated.

Petrucci and coworkers (30,32,319-322), using vibrational spectroscopy, conductance, and relaxation techniques studied ionic association processes of lithium salts in low dielectric solvents. Lithium perchlorate, $LiBF_4$, LiSCN in dimethoxymethane, and $LiAsF_6$, LiBr, LiSCN in dimethyl carbonate, and $LiClO_4$ in 1,2 dimethoxyethane, and $LiAsF_6$, $LiBF_4$, and $LiClO_4$ in 2-methyltetrahydrofuran are heavily associated in ion pairs and triple ions. At higher concentrations (>0.10 M), these salts associate into dimers. In 2-methyltetrahydrofuran, the extent of dimerization for the three electrolytes seems to follow this order: $LiAsF_6 \approx LiBF_4 < LiClO_4$ (322). Lithium hexafluoroarsenate in 1,2 dimethoxyethane and $LiClO_4$ in dimethyl carbonate exists as solvent and contact ion pairs. The

formation of dimers was not detected in these systems.

Electrical conductance measurements do not allow a distinction between the formation of contact and solvent separated ion pairs. Nuclear magnetic resonance measurements are sensitive only to the formation of contact ion pairs (323). Therefore, for ion pairing processes in solution, only contact ion pairing shows a concentration dependence, and from NMR measurements, the contact ion pairing formation constant can be obtained. Chemical shifts and linewidth measurements are also sensitive to the formation of dimers and larger aggregates, and from these measurements, formation constants for these processes can also be determined.

In pyridine and 2-butanone solutions, the ^{7}Li chemical shifts are concentration dependent (Figures 8,9). The error of the ^{7}Li chemical shift measurements in these experiments was found to be ±0.01 ppm. No error bars are included in these figures because they are too small to be observable. For all solution studies except LiPi in pyridine, the variation in the ^{7}Li resonance with concentration is nonlinear. The behavior indicates that the Li^{+} exists in different environments in these solutions. The linear change in the chemical shifts observed in LiPi pyridine solutions is caused by collisions (79). Collisional ion pairs are transient species that are formed in solution by the collision of ions, ion pairs, or aggregates. Ion formation constants cannot be measured by NMR when collisional ion pairs are the only ion pairs in solution. Further discussions about collision ion pairs can be found in the historical section, Chapter I.

Figure 8: Lithium-7 NMR chemical shifts of a series of lithium salts in pyridine at different molar concentrations. Measurements were made at ambient temperature.

a. LiCl (+)

b. $LiClO_4$ (∘)

c. $LiNO_3$ (×)

d. LiPi (□)

e. LiSCN (▷)

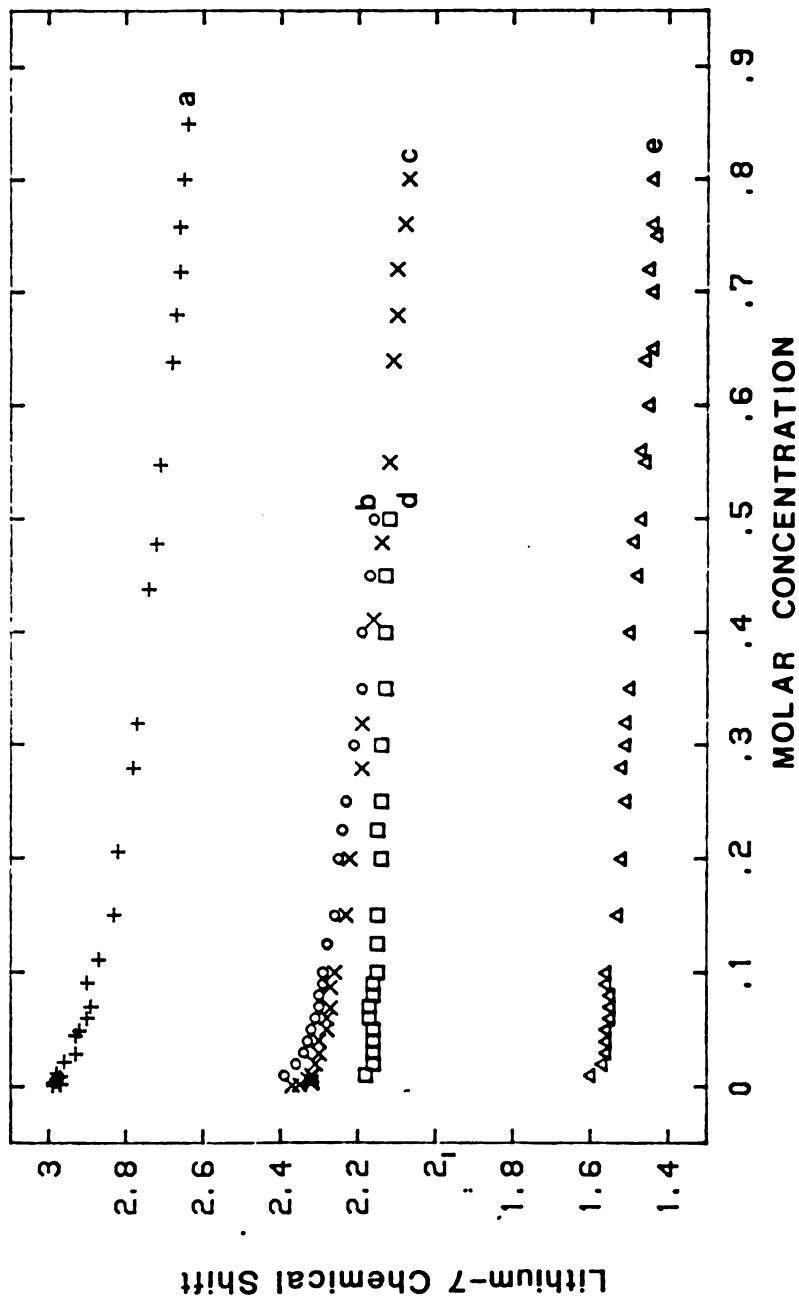
Lithium-7 Chemical Shift
MOLAR CONCENTRATION
3
2.8
2.6
2.4
2.2
2
1.8
1.6
1.4
0
.1
.2
.3
.4
.5
.6
.7
.8
.9
a
b
c
d
e

Figure 9: Lithium-7 NMR chemical shifts of a series of lithium salts in 2-butanone at different molar concentrations. Measurements were made at ambient temperature.

a. $LiAsF_6$ (▷)

b. LiI (□)

c. $LiBPh_4$ (x)

d. LiPi (○)

e. $LiClO_4$ (◇)

f. $LiCF_3CO_2$ (+)

g. LiSCN (x)

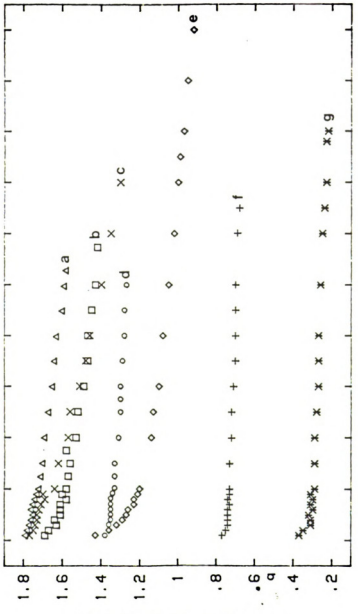
Lithium-7 Chemical Shift
1.8
1.6
1.4
1.2
1
.8
.6
.4
.2
0
.1
.2
.3
.4
.5
.6
.7
.8
.9
1
MOLAR CONCENTRATION
a
b
c
d
e
f
g

The ^{7}Li chemical shifts were fitted to either a two site or three site exchange mechanism. The three site exchange model was used only when the two site exchange mechanism did not fit the chemical shift data. When the concentration of free ions, calculated by using the ion pairing formation constants obtained from electrical conductance measurements, is >30% of the total lithium salt concentration at 0.01 M, an activity correction is included in the fitting program. The mean activity coefficient was calculated using the familiar Debye-Hückel equation:

$$\ln f_{\pm} = - \frac{A(\alpha C)^{1/2}}{1+aB(\alpha C)^{1/2}} \qquad (3\text{-}8)$$

The mean activity coefficient is a function of the interatomic distance, a, and in the fitting program, this parameter is held constant. Using the interatomic distance determined from the crystal ionic radii in equation 3-8, values for the fitting parameters were not accurately determined; however, when the Bjerrum distance was used, the errors for the values obtained from the fit were much less (299). The mean activity coefficient was included in fitting the chemical shifts for $LiClO_4$, $LiAsF_6$, LiI, and $LiBPh_4$ in 2-butanone. For $LiClO_4$ solutions, ^{35}Cl linewidths and ^{7}Li chemical shift measurements were fitted simultaneously.

The two site exchange model for ion pairing was used to fit the NMR measurements for $LiBPh_4$, $LiClO_4$, $LiAsF_6$, and LiI in 2-butanone, and $LiClO_4$ in pyridine (Table 7). The fitting program calculated

Table 7

Contact Ion Pairing Constants of Several Lithium Salts and the Chemical Shifts of the Solvated Cation and the Ion Pair in 2-Butanone and Pyridine at Ambient Temperature

Salts	Solvent	$K_a(\underline{M}^{-1})$	$^{a}\delta_L$ (PPM)	$^{b}\delta_{IP}$ (PPM)
$LiAsF_6$	2-butanone	4(±1)	1.799(±0.005)	0.8(±0.2)
$LiBPh_4$	2-butanone	2.6(±0.7)	1.796(±0.008)	-0.7(±0.4)
LiI	2-butanone	9(±3)	1.69(±0.01)	0.9(±0.1)
LiI	2-butanone	49(±7)	1.80[a]	1.25(±0.03)
$LiClO_4$	2-butanone	38(±13)	1.49(±0.05)	0.72(±0.04)
$LiClO_4$	2-butanone	156(±15)	1.80[a]	0.81(±0.02)
$LiClO_4$	pyridine	4(±2)	2.39(±0.01)	1.95(±0.06)

Values in parentheses are standard deviations for the respective quantities. The second set of values for LiI and $LiClO_4$ in 2-butanone are determined by holding the $^{a}\delta_L$ constant. This value was taken as the chemical shift of the solvated cation.

$^{a}\delta_L$ is chemical shift at C = 0 which corresponds to the chemical shift of the solvated cation.

$^{b}\delta_{IP}$ is the chemical shift of the ion pair.

[a] Value held constant in the fitting program

simultaneously the ion pairing constant and the ^{7}Li chemical shifts of the solvated cation and the contact ion pair (Appendix 4-A). The chemical shifts for LiI and $LiClO_4$ in 2-butanone were also fitted to an ion pairing mechanism where the limiting chemical shift was held constant. This value was set to the limiting chemical shift determined from the measured chemical shifts obtained from $LiAsF_6$ and $LiBPh_4$ 2-butanone solutions. These limiting chemical shifts were the same, and were assigned to the chemical shift of the solvated cation. Similar approaches could not be applied to pyridine solutions since the chemical shift of the solvated cation could not be accurately determined, because the limiting chemical shifts of any two salts were not the same. These ion pairing constants are also found in Table 7. The values in parentheses correspond to the standard deviations obtained from the fits.

For $LiClO_4$ solutions, ^{35}Cl linewidths were also available; the fitting program then also calculated the ^{35}Cl linewidths of solvated anion and the contact ion pair. The infrared studies presented in Section IV of this chapter show that at concentrations $\geq$0.01 $\underline{M}$ $LiClO_4$, solvated ions exist in 2-butanone and pyridine. The large ion pairing constant (K_a = ~1900 $\underline{M}^{-1}$) determined from conductance data at concentrations <0.01 $\underline{M}$, indicates that the majority of solvated ions exist as solvent separated ion pairs in pyridine solutions. Therefore, no mean activity correction was used when fitting the ^{7}Li NMR chemical shifts obtained from $LiClO_4$ pyridine solutions. In the two site exchange model at higher concentrations, the fits were poor

(Figures 10,11). For $LiClO_4$ solutions of pyridine and 2-butanone, the best fit was obtained using a three site exchange model which included dimerization.

For $LiClO_4$ 2-butanone solutions, the fitting program utilized to fit a three site exchange mechanism calculated the chemical shifts for the ion pair and the dimer, the linewidth for the solvated anion, ion pair, and the dimer, and the ion pairing and dimerization constant (Appendix 4-A). The chemical shift of the solvated cation was held constant in this program. Two fits were generated, one where the chemical shift of the solvated cation was taken as the limiting chemical shift determined from chemical shift measurements obtained from $LiClO_4$ 2-butanone solutions, and the other was where the chemical shift of the solvated cation was set equal to the limiting chemical shift determined from chemical shift measurements obtained from $LiAsF_6$ or $LiBPh_4$ 2-butanone solutions. The fit obtained using the limiting chemical shift determined for $LiBPh_4$ or $LiAsF_6$ was much better than using the limiting chemical shift determined from $LiClO_4$ measurements. The fitting program used to fit chemical shifts from $LiClO_4$ pyridine solutions was the same program that was used to fit 2-butanone solution data except that the chemical shift of the solvated cation was also calculated by the program instead of being set to a constant (Appendix 4-A). Using these programs, accurate values for the ion pairing and the dimerization formation constants could not be obtained because there was too much correlation between the variables. The improvement in the fits using the three site

Figure 10 KINFIT output resulting from fitting ^{7}Li chemical shift measurements at different molar concentrations of $LiClO_4$ in pyridine. Measurements were made at ambient temperature.

a. Three site exchange (solvent separated ion pairs, contact ion pairs, dimers)

b. Two site exchange (solvent separated ion pairs, contact ion pairs)

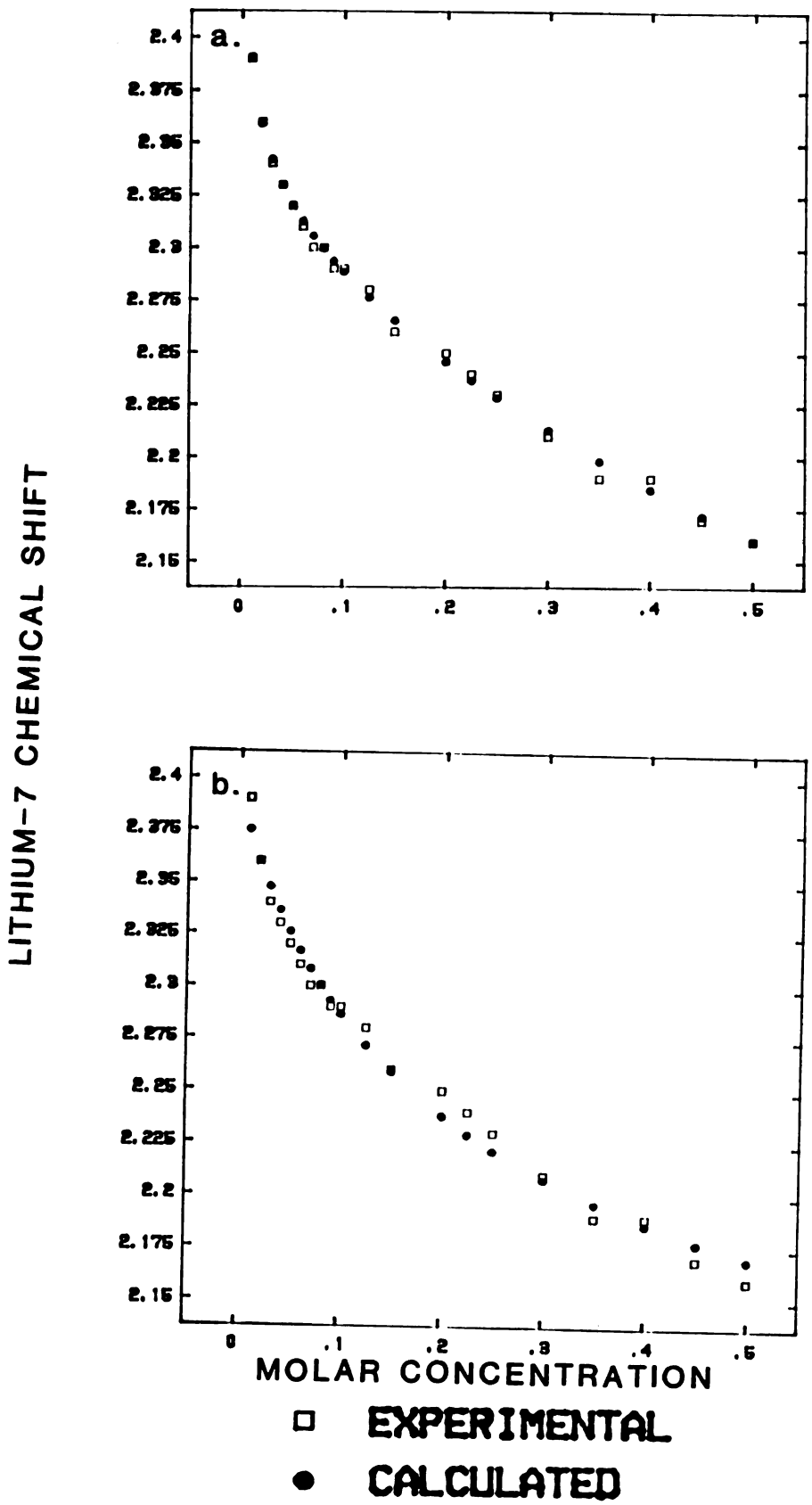
a.
b.
2.4
2.375
2.35
2.325
2.3
2.275
2.25
2.225
2.2
2.175
2.15
0
.1
.2
.3
.4
.5
LITHIUM-7 CHEMICAL SHIFT
MOLAR CONCENTRATION
EXPERIMENTAL
CALCULATED

Figure 11 KINFIT output resulting from fitting ^{7}Li chemical shift measurements at different molar concentrations of $LiClO_4$ in 2-butanone. The limiting chemical shift was set equal to 1.80 ppm. Measurements were made at ambient temperature.

a. Three site exchange (solvated ions, contact ion pairs, dimers)

b. Two site exchange (solvated ions, contact ion pairs)

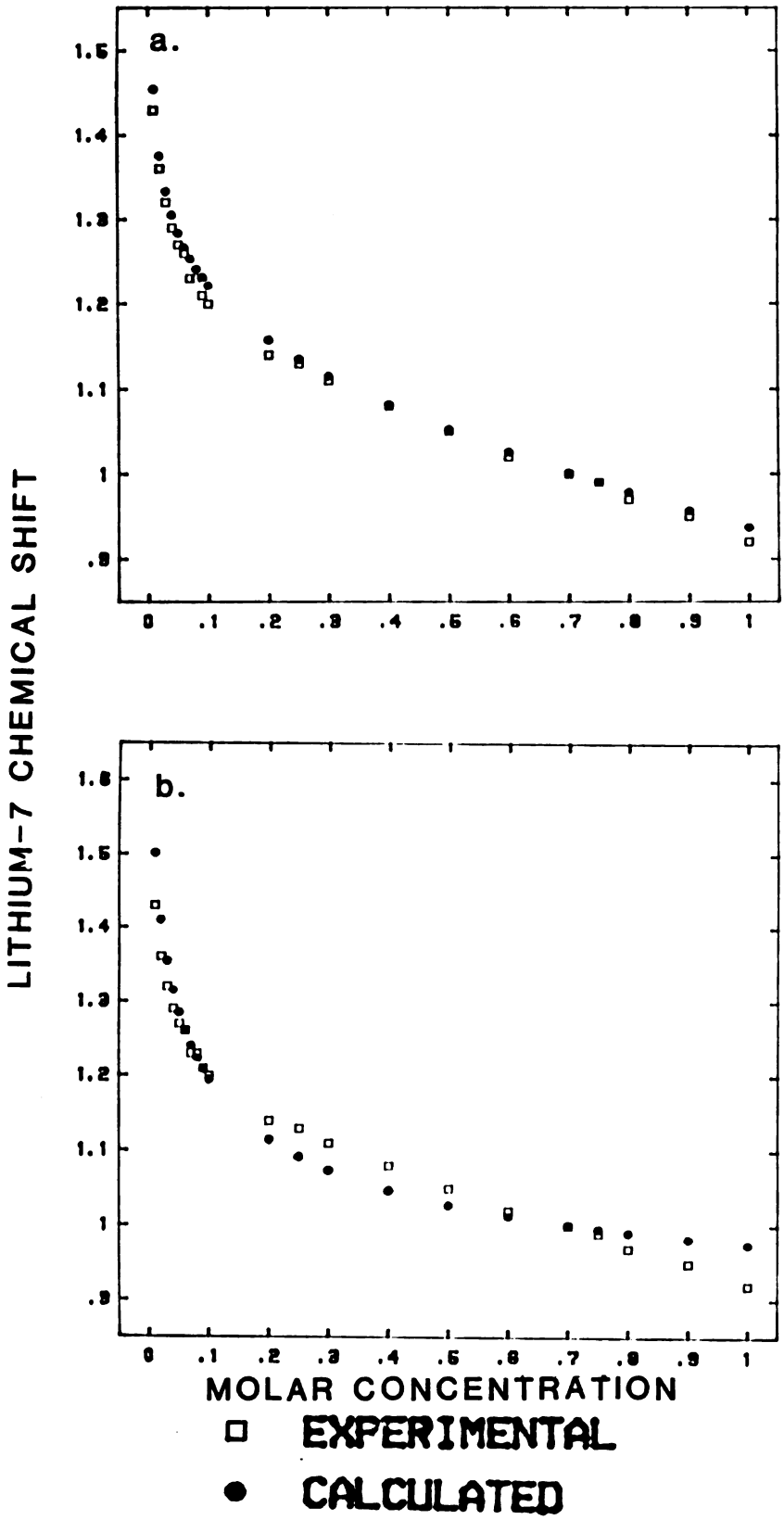
a.
b.
LITHIUM-7 CHEMICAL SHIFT
MOLAR CONCENTRATION
EXPERIMENTAL
CALCULATED

exchange model indicates not only the existence of contact and solvent separated ion pairs but also dimers.

The contact ion pairing formation constants determined by fitting ^{7}Li NMR measurements for $LiClO_4$ are larger in 2-butanone than in pyridine (Table 7). Values are considered indistinguishable when their confidence limits ($\bar{X}\pm 2s$) overlap. The contact ion pairing formation constant for $LiClO_4$ in 2-butanone, obtained using the fitting program where the chemical shift of the solvated cation is set equal to the limiting chemical shift obtained from chemical shift measurements from $LiAsF_6$ or $LiBPh_4$ solutions, is larger than the one obtained from the fitting program which calculated the limiting chemical shift. Therefore, the ClO_4^- is solvated better in pyridine than in 2-butanone. The contact ion pairing constants determined by ^{7}Li NMR for $LiClO_4$ in 2-butanone and pyridine solutions are smaller than the ion pairing constants determined by electrical conductance. Therefore, a large fraction of ion pairs in these solutions are solvent separated.

Listed in Table 8 are the ^{35}Cl linewidths at zero concentration and infinite obtained from fitting NMR measurements obtained from $LiClO_4$ solutions to a two site ion pairing mechanism. A detailed explanation of the fitting procedures used to calculate these numbers have been previously described. Two sets of linewidths are listed for $LiClO_4$ in 2-butanone solutions. The linewidths at zero concentration and at infinite correspond to the solvated anion and the anion

Table 8

Chlorine-35 Linewidth Measurements at Ambient Temperature

Salt	Solvents	$C = 0$ $\Delta\nu_{1/2}$ (hz)	$C = \infty$ $\Delta\nu_{1/2}$ (hz)
$LiClO_4$	2-butanone	21(±3)	60(±3)
LiClO4	2-butanone	8(±3)[a]	54(±2)[a]
$LiClO_4$	pyridine	30(±2)	66(±5)
LiCl	pyridine	354(±15)	1418(±63)

Values in parentheses are standard deviations as determined from the fits. The superscripts on the $\Delta\nu_{1/2}$ in columns three and four correspond to the concentrations where the linewidths were obtained. For $LiClO_4$, the linewidths correspond to the solvated anion and the contact ion pair; for LiCl, the linewidths correspond to the ion pair and the dimer.

[a] Obtained from the fit where the limiting chemical shift was held constant at 1.80 ppm. This chemical shift was taken as the chemical shift of the solvated cation.

existing as a contact ion pair, respectively. The linewidths, determined at zero concentration and infinite by fitting NMR measurements obtained from $LiClO_4$ pyridine and 2-butanone solutions where the limiting chemical shift is calculated by the program, are not significantly different. The statistical criterion for determining whether values are distinguishable has been presented in the previous paragraph. The linewidth at zero concentration obtained from fitting the NMR measurements from $LiClO_4$ 2-butanone solutions is reduced utilizing the fitting program where the limiting chemical shift is set equal to the limiting chemical shift determined from the chemical shift measurements from $LiAsF_6$ or $LiBPh_4$ 2-butanone solutions. The ^{35}Cl linewidths broadened as the concentration of $LiClO_4$ in 2-butanone and pyridine increased indicating contact ion pairing. The measured ^{35}Cl linewidths at different concentrations in 2-butanone and pyridine were not significantly different (Appendix 1). Therefore, the difference between the ion pairing constants obtained for $LiClO_4$ in 2-butanone and pyridine is not large enough to cause significant differences in the measured linewidths. For fast exchange processes on the NMR time scale, the measured linewidth is a function of the linewidth and mole fraction of each species formed in solution. When ClO_4^- molecules exist as ion pairs, the ^{35}Cl linewidth is larger than that of the solvated ClO_4^-. As the concentration of contact ion pairs increases, the linewidth of the ^{35}Cl resonance broadens.

The reason for the ^7Li chemical shift changes can be understood in part by comparing the limiting chemical shift obtained from the

measured chemical shift data. The limiting chemical shifts obtained from the lithium salts in 2-butanone are not equal except for those of $LiBPh_4$ and $LiAsF_6$. Therefore, the limiting chemical shifts for these salts correspond to the chemical shift of the solvated Li^+ (~1.8 ppm). The chemical shifts for the other salts curve toward the chemical shift assigned to the solvated Li^+. Infrared measurements presented in Section IV of this chapter show that the $LiClO_4$ chemical shift behavior in 2-butanone solutions can be attributed to contact ion pairing at concentrations $\geq$0.01 M. The limiting chemical shift obtained from NMR measurements of $LiClO_4$ solutions is significantly different than what is identified as the chemical shift of the solvated Li^+. The difference in the limiting chemical shifts between both LiI and $LiClO_4$ and the solvated Li^+ in 2-butanone exists because the chemical shifts measurements below 0.01 M does not adequately describe the curvature in the chemical shifts versus concentration plots (Figures 8,9). Consequently, the ion pairing formation constants measured by NMR for LiI and $LiClO_4$ may not be very accurately determined, because the limiting chemical shift is identified as the chemical shift of the solvated Li^+ which is important in the calculation of the ion pairing formation constants. To overcome this difficulty, the chemical shifts corresponding to the solvated cation (δ_L for $LiBPh_4$ and $LiAsF_6$) were entered into the fitting program as a constant and the chemical shifts obtained for LiI and $LiClO_4$ at different concentrations in 2-butanone were refitted (Table 7). The fitting program calculated the ion pairing constant

and the ^7Li chemical shift for the ion pair (Appendix 4-A). In pyridine solutions, the limiting chemical shifts obtained for $LiClO_4$ should be close to the chemical shift of the solvated Li^+(~2.5 ppm) in pyridine, since the chemical shift behavior is due to contact ion pairing. Again, the accuracy of the ion pairing formation constant for $LiClO_4$ in pyridine depends on how close the limiting chemical shift is to the chemical shift of the solvate Li^+ in pyridine. Similar fitting procedures done for LiI and $LiClO_4$ in 2-butanone could not be applied to $LiClO_4$ in pyridine because all the limiting chemical shifts for each salt were significantly different in pyridine; therefore, the chemical shift of the solvated cation can not be accurately determined. It is expected that the chemical shifts for the other salt should curve in the direction of the chemical shift of the solvated Li^+. This is the case for LiSCN and $LiNO_3$ but not for LiCl. The solution chemistry of LiCl pyridine solutions at concentrations $\geq$0.10 M cannot be attributed to contact ion pairing. Therefore, the chemical shift measurements for the lithium salts studied can be interpreted as being due either to contact ion pairing, dimerization, or both.

Infrared and NMR measurements for LiSCN, LiCl, and $LiNO_3$ in pyridine and LiSCN in 2-butanone indicate that these salts exist as ion pairs or aggregates at concentrations $\geq$0.01 M. For LiSCN in 2-butanone and pyridine, the IR spectrum contains several bands, one for the ion pair and the others due to the dimer and higher aggregates. For $LiNO_3$ in pyridine solutions, two $\nu_3(E')$ doubly

degenerate bands are split due to the formation of contact ion pairs and dimers. More detailed discussions of these IR results can be found in Section IV of this chapter.

Since the Li^+ vibration in a solvent cage shows an anion dependency for lithium halide salts in substituted pyridine and pyridine solutions, these salts exist as contact ion pairs in these solutions (2). Also, ^{35}Cl NMR measurements should provide additional support to the formation of LiCl contact ion pairs in pyridine solutions. Figure 12 shows the ^{35}Cl NMR spectra of a LiCl pyridine solution containing C211 and LiCl in pyridine alone. A single line is observed in each spectrum. The band identified by the letter R corresponds to the reference in Figure 12. The C211 ligand complexes Li^+ and isolates the metal cation from any interaction with solvent molecules and the counter ion. Band F in Figure 12 corresponds to the spectrum of the free Cl^- produced when adding C211 to a LiCl pyridine solution. The free Cl^- band appears downfield from the ^{35}Cl band, labeled IP, obtained from LiCl in pyridine. The Cl^- is deshielded by the formation of contact ion pairs; therefore, the band appearing upfield from the free Cl^- band is attributed to the contact ion pair. Also, the linewidth of the ^{35}Cl band is larger for the LiCl pyridine solution than for that of the LiCl-C211 pyridine solution, which indicates that the Cl^- is in an asymmetrical environment caused by the presence of Li^+ in the primary solvation sphere of the Cl^- (Figure 12). The ^{35}Cl linewidths obtained from LiCl solutions are $\geq$376 hz at concentrations $\geq$0.02 M. (Appendix 1). The ^{35}Cl linewidths are related

Figure 12: Chlorine-35 NMR spectra of LiCl pyridine solutions (MR = mole ratio). The chemical shifts have not been corrected for magnetic susceptibility of the solvent. The NMR spectra were obtained at ambient temperature.

a. 0.10 M LiCl, C211 = 0.10 M, MR = 1.0

b. 0.10 M LiCl

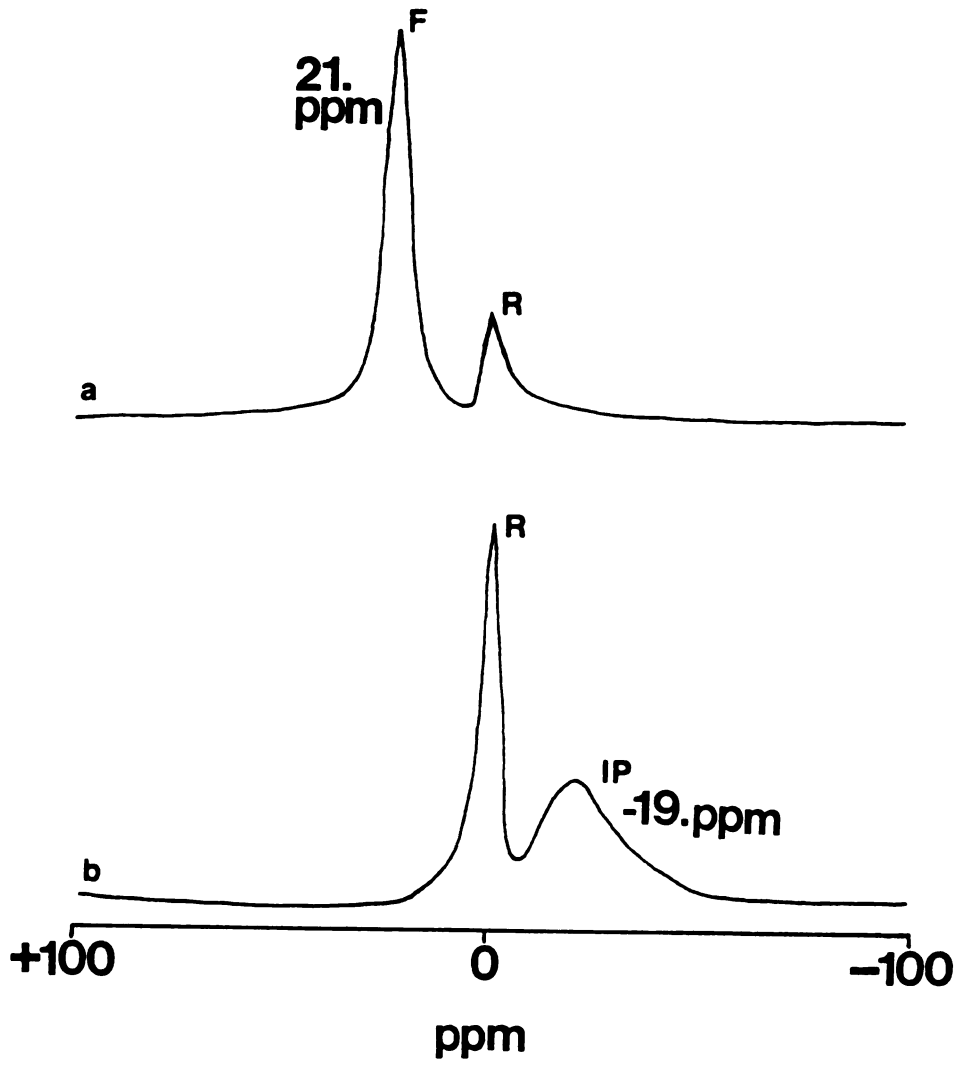
F
21.
ppm
R
a
R
IP
-19.ppm
b
+100
0
-100
ppm

to the symmetry of the environment in which the Cl^- resides. Small linewidths indicate that Cl^- exists in a symmetrical environment.

The ion pairing formation constants obtained from electrical conductance meausrements for $LiCF_3CO_2$ and LiPi in 2-butanone indicate that at concentrations $\geq$0.01 M these salts exist primarily as contact ion pairs in solution. These measured ion pairing formation constants are much larger than the calculated solvent separated ion pairing formation constant for these salts using the Bjerrum equation (Tables 2,3,5). For $LiCF_3CO_2$ solutions, the measured ion pairing formation constant is even larger than the calculated contact ion pairing constant.

In $LiNO_3$, LiCl, and LiSCN in pyridine, and $LiCF_3CO_2$, LiPi, and LiSCN in 2-butanone, the chemical shift changes are attributed to the formation of dimers. Table 9 lists the dimerization constants determined from the ^7Li chemical shifts. The values in parentheses correspond to the standard deviations obtained from the fits. The fitting program calculated the dimerization constant, and the chemical shifts of the Li^+ cations that exist as the ion pair and dimer. For LiCl in pyridine, ^{35}Cl linewidths were available so the linewidths of the anion existing as an ion pair and a dimer were also obtained. The linewidths calculated by the fitting program for the ion pair and dimer are listed in Table 8. The linewidth at zero concentration corresponds to the ion pair and the linewidth at infinite corresponds to the dimer. This two site exchange model which describes dimerization is very similar to the two site exchange model for ion

Table 9

Dimerization Constants of Lithium Salts in

Pyridine and 2-Butanone at Ambient Temperature

Salts	Solvent	$K_a(\underline{M}^{-1})$	δ_L[a] (PPM)	δ_D[b] (PPM)
LiPi	2-butanone	1.7(±0.5)	1.386(±0.005)	1.15(±0.03)
$LiCF_3CO_2$	2-butanone	1.4(±0.8)	0.759(±0.005)	0.62(±0.03)
LiSCN	2-butanone	5.(±3.)	0.37(±0.02)	0.18(±0.02)
$LiNO_3$	pyridine	0.46(±0.08)	2.319(±0.004)	1.60(±0.06)
LiSCN	pyridine	0.20(±0.09)	1.576(±0.004)	0.9(±0.2)
LiCl	pyridine	1.2(±0.2)	2.988(±0.007)	2.33(±0.03)

[a] δ_L is chemical shift at C = 0.

[b] δ_D is chemical shift of the dimer.

pairing, except the existence of two Li^+ cations per dimer must be taken into consideration. It was also assumed that the chemical shifts of the two Li^+ of the dimer were the same; therefore, both Li^+ cations exist in the same environments. For LiSCN in 2-butanone, the fit to the two site exchange model was poor (Figure 13). Introducing the formation of tetramers to the model drastically improves the fit (Figure 13). The fitting program utilized calculated values for five parameters simultaneously (Appendix 4-A). These five parameters are the ^7Li chemical shift of the ion pair, dimer and tetramer, and the dimerization and tetramer formation constants. The numerical values for the formation constants for these parameters highly correlate, so accurate values cannot be obtained from the fit.

IV. Infrared Spectrometry

A. Pyridine Solutions

A strong ν_{CN} band is observed at 2067 cm^{-1} for concentrations $\geq$0.01 M LiSCN, which is 11 cm^{-1} higher than that of the freely solvated anion at 2056 cm^{-1} (Figure 14). The ν_{CN} band frequency for the freely solvated thiocyanate ion in pyridine was identified by adding a greater than equimolar amount of C211 to 0.10 M LiSCN solution, which breaks up the ion pairs which produces free anions and a complexed cation (Figure 15). The band positions of the free anion and ion pair are the same as those reported earlier by Chabanel and coworkers (324). The observed difference in frequency between the

Figure 13: KINFIT output resulting from fitting ^{7}Li chemical shift measurements at different molar concentrations of LiSCN in 2-butanone. Measurments were made at ambient temperature.

a. Three site exchange (ion pair, dimer, tetramer)

b. Two site exchange (ion pairs, dimer)

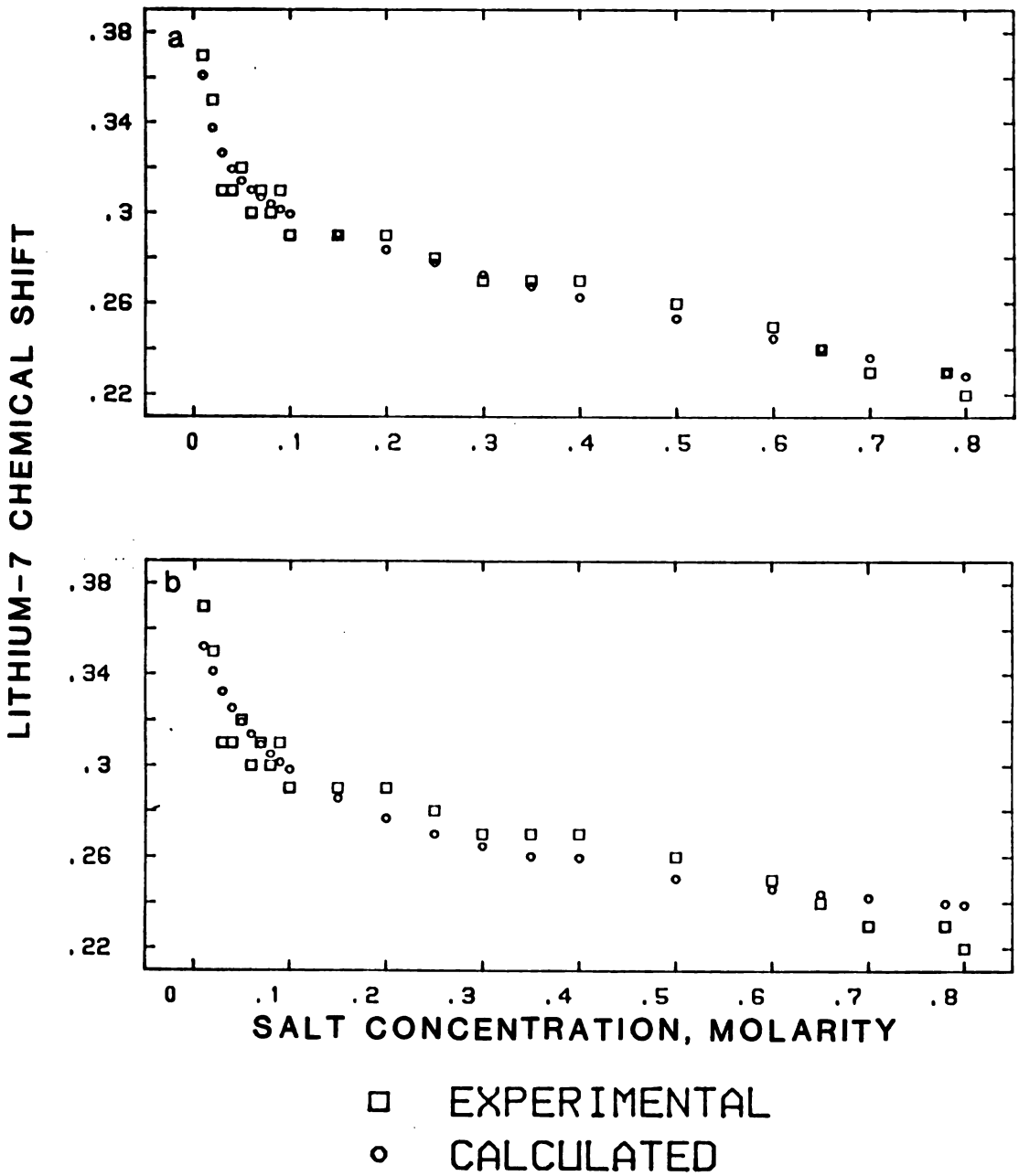
a
b
.38
.34
.3
.26
.22
0
.1
.2
.3
.4
.5
.6
.7
.8
LITHIUM-7 CHEMICAL SHIFT
SALT CONCENTRATION, MOLARITY
EXPERIMENTAL
CALCULATED

Figure 14: The ν_{CN} absorption bands observed for a series of LiSCN concentrations in pyridine. The symbol x indicates the band assigned to the dimer. Spectra were obtained at ambient temperature.

a. 0.60 M

b. 0.40 M

c. 0.20 M

d. 0.08 M

e. 0.04 M

f. 0.02 M

g. 0.01 M

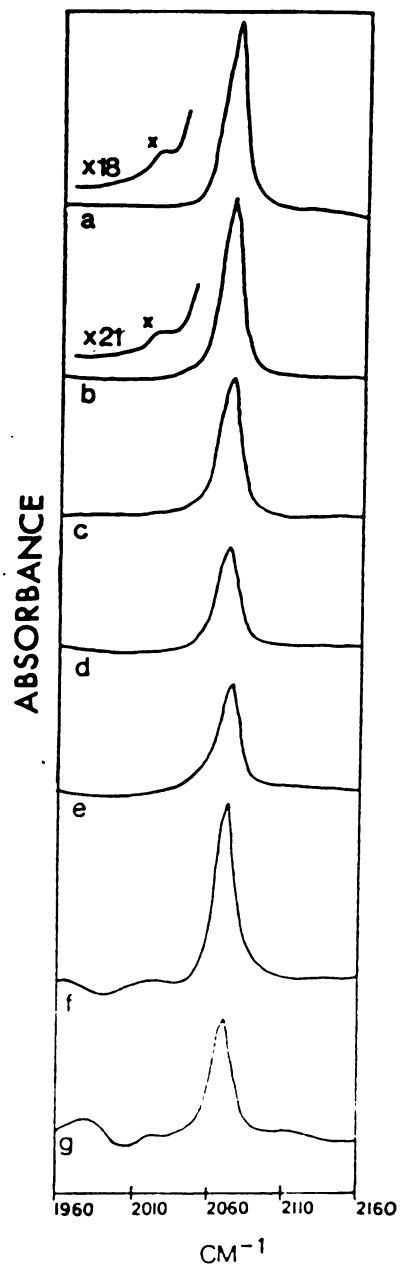
x18
x
a
x21
x
b
c
d
e
f
g
ABSORBANCE
1960
2010
2060
2110
2160
CM⁻¹

Figure 15: Identification of ν_{CN} absorption maximum for the free SCN^- ion in pyridine (MR = mole ratio). Spectra were obtained at ambient temperature.

a. 0.04 M LiSCN with C211 (MR = 1.25)

b. 0.04 M LiSCN

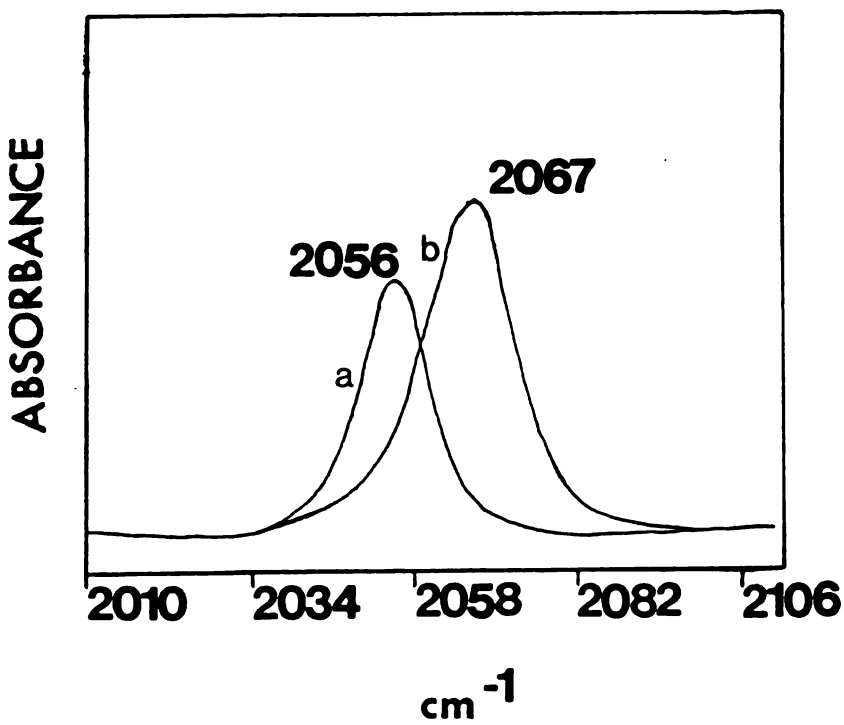
ABSORBANCE
2067
2056
b
a
2010
2034
2058
2082
2106
cm -1

freely solvated anion and the ion pair is characteristic of a nitrogen bonded complex. Larger frequency differences (~50 cm^{-1}) are expected for the sulfur bonded complexes (325). Bands appearing in the far-IR at 268 cm^{-1} and around ~480 cm^{-1} are also indicative of N-bonding (Figure 16). The 268 cm^{-1} band is observed only in concentrated solutions of LiSCN; this band corresponds to the Li-N stretch (326). The band around 480 cm^{-1} corresponds to the δ(SCN) bend for the LiSCN contact ion pair (122). The 406 cm^{-1} band is a pyridine solvent band. Other bands appearing in the far-IR spectra are attributed to solvation, an ion cage vibration (~370 cm^{-1}), and a pyridine band displaced by solvation (~428 cm^{-1}). In the mid-IR spectra for concentrations above 0.20 M LiSCN, another weak ν_{CN} band appears at 2020 cm^{-1} indicating the association of ion pairs into aggregates. This band is identified in Figure 14 by x. This band is easily observed when the pyridine bands are removed from the spectrum. From the Gaussian-Lorentzian fitting program, the area of the 2067 cm^{-1} band was obtained for a series of solutions from 0.01 M to 0.60 M LiSCN. The program does not calculate the errors in the areas that result from the fit. The areas are linear for concentrations up to 0.20 M; at higher concentrations, there is an obvious deviation (Figure 17). The nonlinear behavior occurs at the same concentration where the 2020 cm^{-1} band is observed. Chabanel and coworkers (123) reported low frequency bands around 2030 cm^{-1} in LiSCN ether solutions which they attribute to the formation of centrosymmetric dimers.

Figure 16: Far-IR absorption curves of LiSCN in pyridine. Spectra were obtained at ambient temperature.

a. 0.67 M LiSCN

b. 0.20 M LiSCN

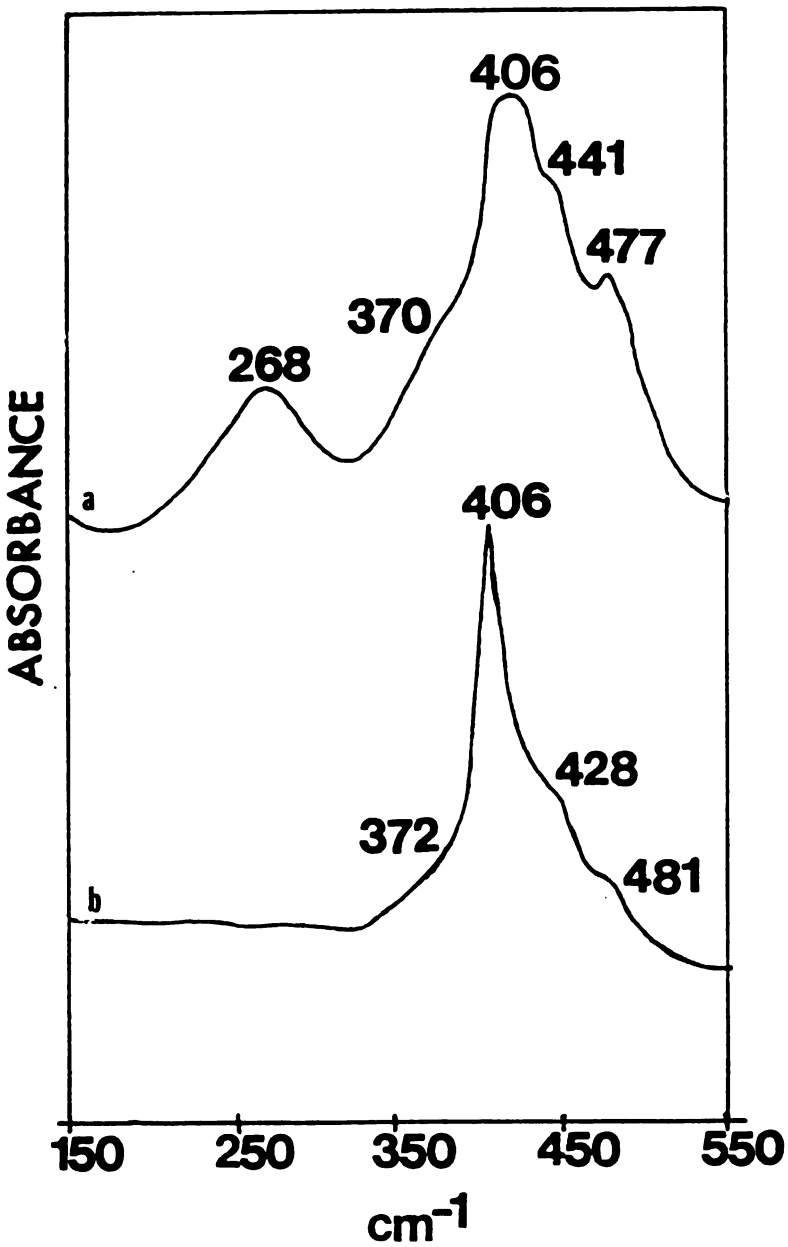
406
441
477
370
268
a
406
428
372
481
b
ABSORBANCE
150
250
350
450
550
cm-1

Figure 17: Plot of the 2067 cm $^{-1}$ ν_{CN} absolute band areas vs. molar concentration of LiSCN. Measurements were obtained at ambient temperature.

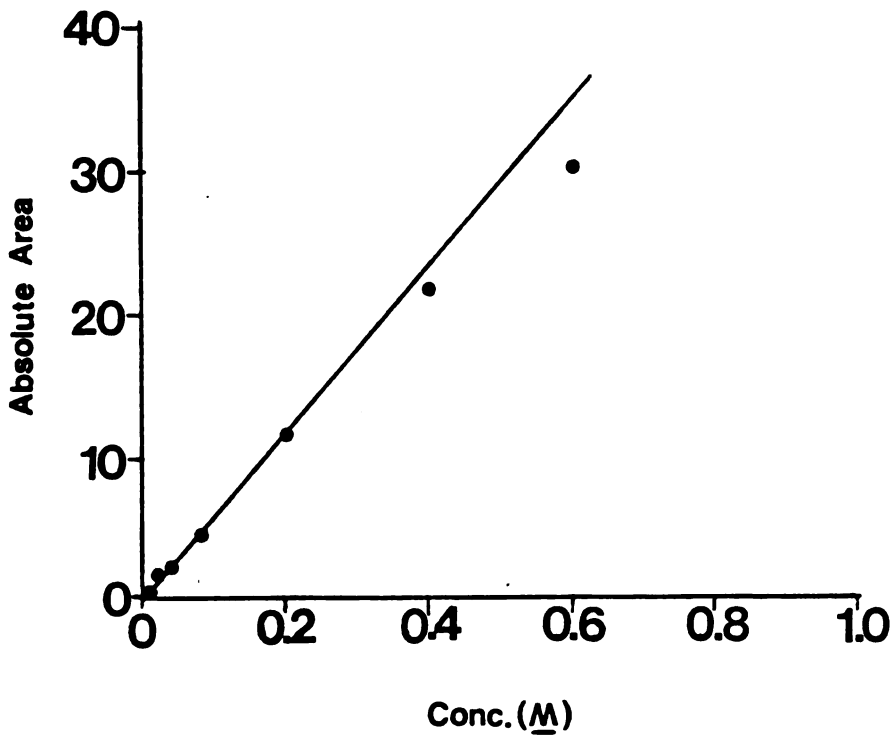
40
30
20
10
0
Absolute Area
0
0.2
0.4
0.6
0.8
1.0
Conc. (M)

Based on these results, the 2020 cm^{-1} band observed in LiSCN pyridine solutions could be assigned to the dimer. Bands which correspond to the dimer species at 503 and 489 cm^{-1} are not present in the far-IR spectrum (122). This is possibly true because the concentration of the dimer is below the detection limits of the instrument.

The state of the NO_3^- anion in solution was determined by examining changes in the $\nu_3(E')$ doubly degenerate vibrational band corresponding to the anti-symmetrical stretch. When contact ion pairing occurs in solution, this band loses it degeneracy and splits into two bands. The frequency difference between these two bands is related to the type of coordination. Nitrate can either act as a monodentate or bidentate ligand. A larger splitting usually occurs for the bidentate interaction than for the monodentate interaction (327). Two bands at 1327 and 1420 cm^{-1} are observed in $LiNO_3$ pyridine solutions at concentrations $\geq$0.04 M (Figure 18). The 1420 cm^{-1} band is easily observed when the pyridine bands are removed from the spectra (Figure 18). The dashed regions in Figure 18 correspond to pyridine bands that could not be completely removed by spectral subtraction. Neither of these bands appears at the frequency corresponding to the freely solvated NO_3^- (1351 cm^{-1}) (Figure 19). The existence of a single band for the solvated NO_3^- indicates that the solvation of NO_3^- in pyridine does not cause this band to lose its degeneracy. The freely solvated NO_3^- band was identified in tetrabutylammonium nitrate and was also identified by adding C211 to a $LiNO_3$ solution to break up ion pairs (Figures 19,20). With C211, it

Figure 18: The ν_3 (E') absorption bands of NO_3^- for a series of $LiNO_3$ pyridine solutions. The dashed lines indicate where pyridine bands exist but have been removed from the spectra. Spectra were obtained at ambient temperature.

a. 0.41 M

b. 0.10 M

c. 0.04 M

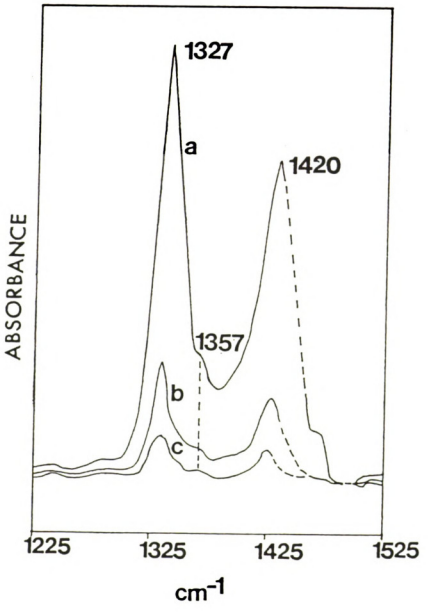
1327
a
1420
ABSORBANCE
1357
b
c
1225
1325
1425
1525
cm-1

Figure 19: Infrared absorption curve of a 0.10 M tetrabutylammonium nitrate pyridine solution. The intense bands that are cut off are due to pyridine. Spectrum was obtained at ambient temperature.

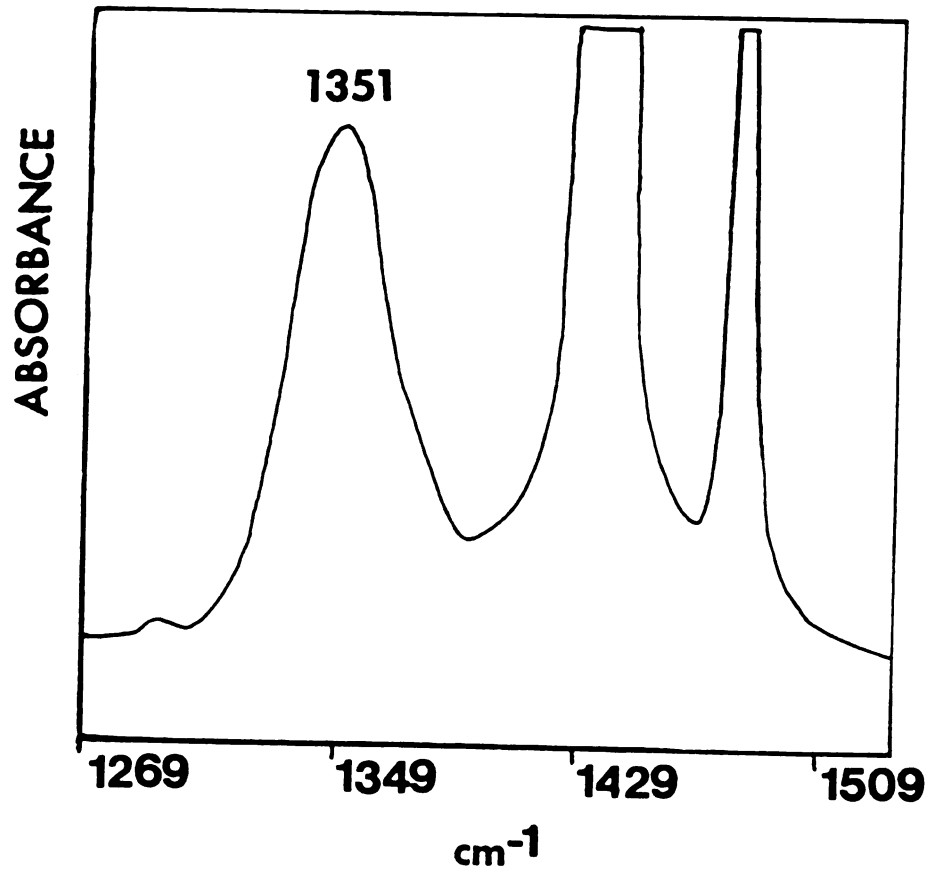
1351
ABSORBANCE
1269
1349
1429
1509
cm-1

Figure 20: Identification of the ν_3 (E') band for the free NO_3^- using C211 (MR = mole ratio). Spectra were obtained at ambient temperature.

a. 0.10 M $LiNO_3$

b. 0.10 M $LiNO_3$, C211 (MR = 0.22)

c. 0.10 M $LiNO_3$, C211 (MR = 1.22)

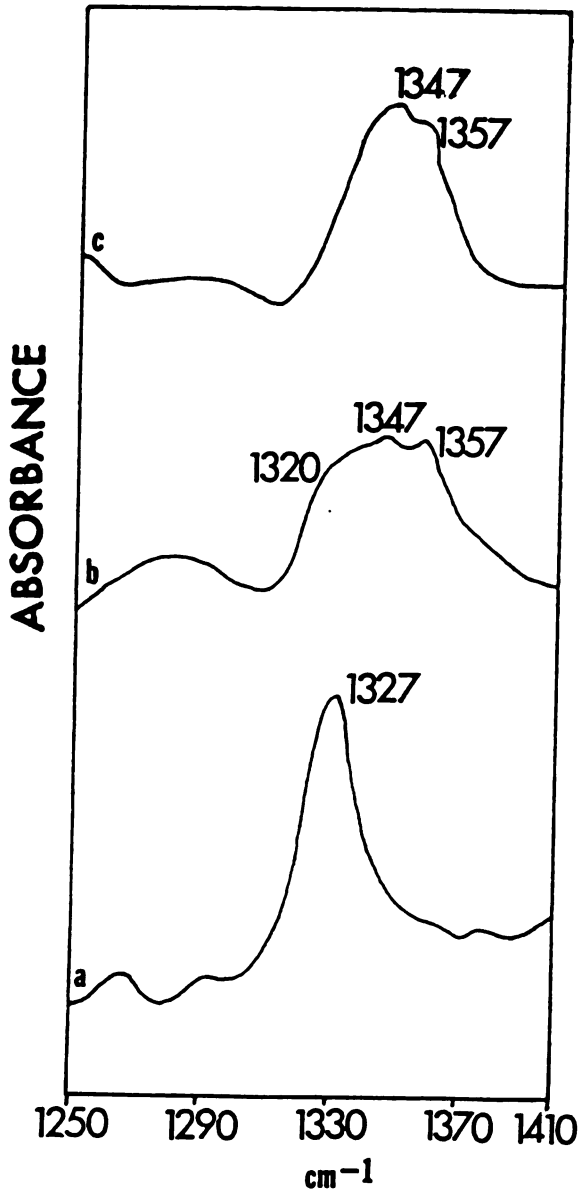
1347
1357
c
1347
1320
1357
b
1327
a
ABSORBANCE
1250
1290
1330
1370
1410
cm−1

was found that another band appeared at 1357 cm^{-1}, attributed to the complex, making it difficult to determine accurately the position of the free NO_3^- band (Figure 20). The band associated with the freely solvated NO_3^- in solution containing C211 is observed at 1347 cm^{-1}.

Another method utilized for obtaining the frequency of the freely solvated NO_3^- band was by adding 12C4 to a $LiNO_3$ solution. Using 12C4, a new band appears at 1362 cm^{-1} which grows as the ligand concentration is increased and while the intensity of the 1327 cm^{-1} band remains essentially constant (Figure 21). Because of the difficulty of observing the 1420 cm^{-1} band in the IR spectra of pyridine solutions, only the behavior of the 1327 cm^{-1} band was monitored. This new band was assigned to the ligand because the same band was observed in the IR spectrum of 0.30 M 12C4 pyridine solution. This suggests either that the contact interaction between NO_3^- and Li^+ is so strong that the Li^+ cannot be complexed by 12C4, or that NO_3^- is ion paired to the complexed Li^+.

When the pyridine solvent bands are subtracted from the spectra of the $LiNO_3$ solutions, a weak band is observed at 1357 cm^{-1} which appears at the foot of the 1327 cm^{-1} band (Figure 18). Irregularities in the shoulders of the $\nu_3(E')$ bands, similar to what was observed in pyridine, have been reported in $LiNO_3$-glassy DMSO matrices (1429 cm^{-1}), and $LiNO_3$-THF solutions (1459 cm^{-1}) (328). Perelygin, Klimchuk, and Belaborodova (329) previously observed these bands and another band in $LiNO_3$ pyridine solutions at 1440 cm^{-1}. The high frequency band was not observed in our spectra because it overlaps

Figure 21: The IR spectra of a 0.30 M $LiNO_3$ solution containing different amounts of 12C4 (MR = mole ratio). The * corresponds to the 12C4 band. Spectra were obtained at ambient temperature.

a. MR = 2.0

b. MR = 1.0

c. MR = 0.0

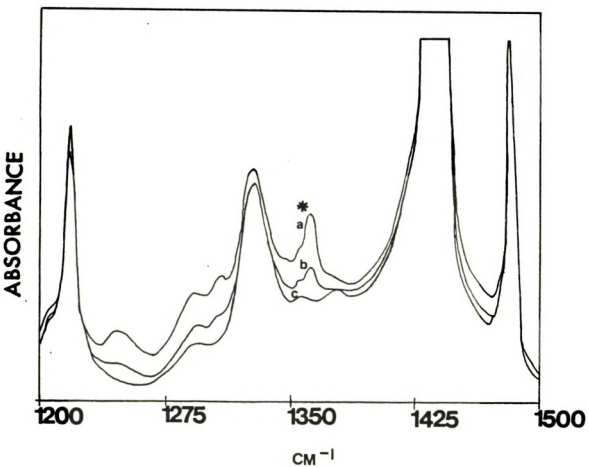
ABSORBANCE
*
a
b
c
1200
1275
1350
1425
1500
CM⁻¹

with the pyridine solvent band. In pyridine-d_5 solutions, the pyridine bands do not appear in the $\nu_3(E')$ region; therefore, it was possible to identify the high frequency band at 1457 cm^{-1} (Figure 22). Two sets of $\nu_3(E')$ bands (1328 and 1423 cm^{-1}; 1345 and 1457 cm^{-1}) for pyridine-d_5 and three bands for pyridine indicate the existence of species in solution where the NO_3^- ion pairs to the Li^+ as a monodentate and a bidentate anion. The bands at 1328 cm^{-1} and 1423 cm^{-1} (Δ = 95 cm^{-1}) indicate a monodentate interaction, and the 1345 and 1457 cm^{-1} (Δ = 112 cm^{-1}) bands indicate a bidentate interaction.

The state of ClO_4^- in pyridine solutions was obtained from the behavior of the 624 cm^{-1} triply degenerate band, $\nu_4(F_2)$, corresponding to the anti-symmetrical stretch. Three bands are observed at 614, 624, and 638 cm^{-1} above 0.08 M. Below 0.28 M, only the 624 cm^{-1} band is observed (Figure 23). The x's in Figure 23 indicate the $\nu_4(F)$ ClO_4^- bands. Increasing the spacer size did not reveal any new bands at 0.01 and 0.02 M. The spectra in Figure 23 at concentrations below 0.04 M were obtained using the larger spacer. The freely solvated ClO_4^- band appears at 624 cm^{-1} (Figure 24). At higher concentrations, the loss of degeneracy of the $\nu_4(F_2)$ band indicates the existence of contact ion pairs. The 624 cm^{-1} band observed at all concentrations is due either to solvated anions or solvent separated ion pairs. Similar chemistry has been reported for $LiClO_4$ in nitromethane, methanol, acetonitrile, and tetramethylguanidine as observed from the behavior of the 935 cm^{-1} Raman active bands (116).

Figure 22: Infrared absorption curve of 0.04 M $LiNO_3$ in pyridine-d_5. The dashed lines indicate where solvent bands have been removed. Spectrum was obtained at ambient temperature.

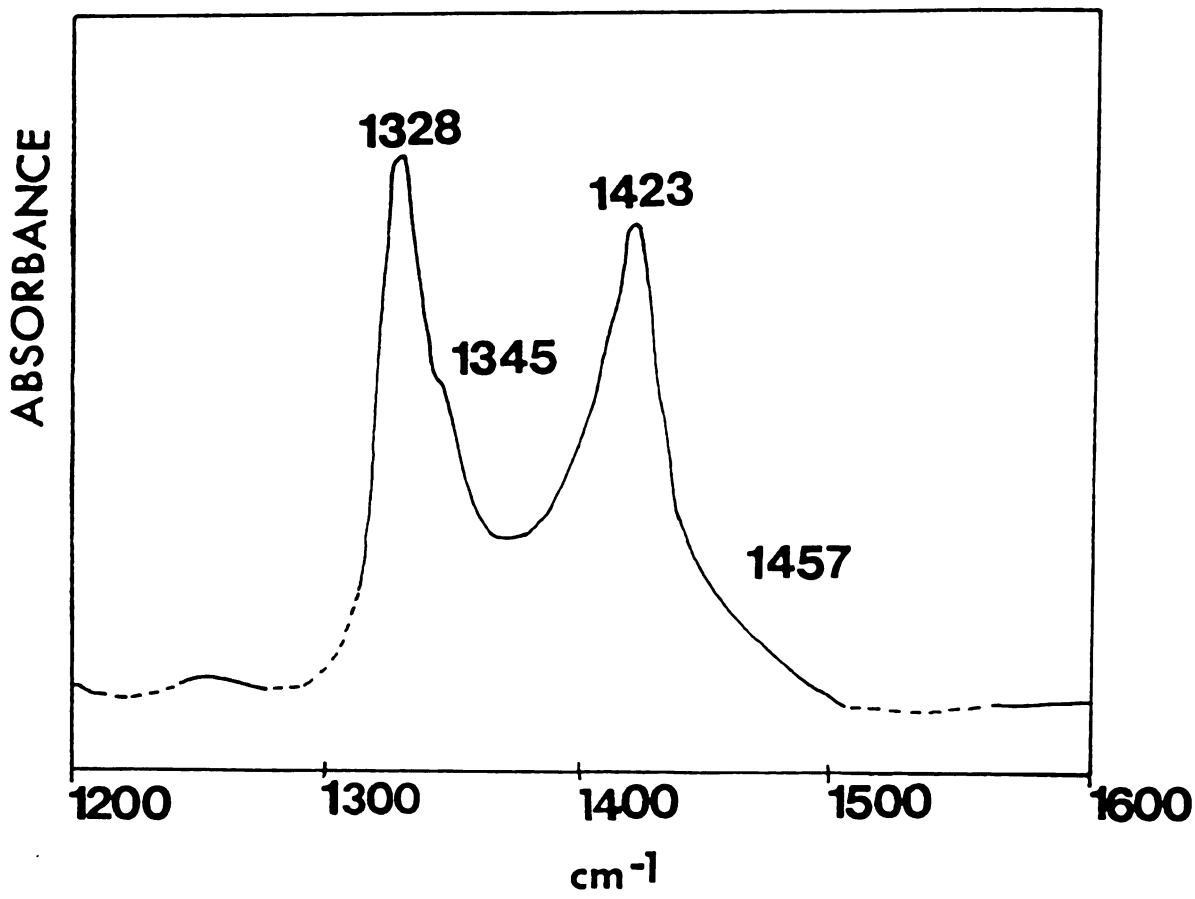
ABSORBANCE
1328
1423
1345
1457
1200
1300
1400
1500
1600
cm-1

Figure 23: The $\nu_4(F_2)$ absorption bands of ClO_4^- anion for a series of $LiClO_4$ pyridine solutions at different molar concentrations. The x points out the ClO_4^- bands. The other band in the spectra corresponds to a pyridine band. Spectra were obtained at ambient temperature.

a. 0.01 M

b. 0.02 M

c. 0.04 M

d. 0.08 M

e. 0.28 M

f. 0.48 M

g. 0.64 M

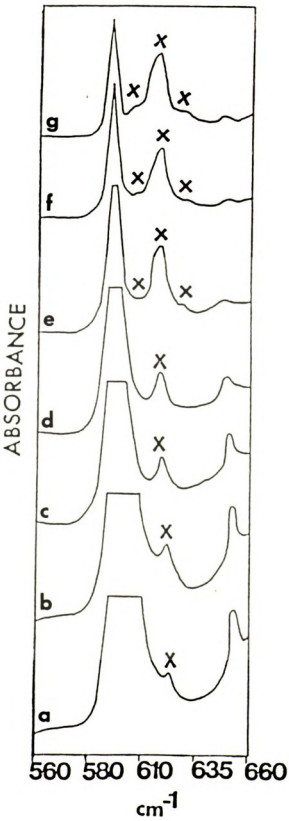
ABSORBANCE
g
f
e
d
c
b
a
560 580 610 635 660
cm-1

Figure 24: The IR absorption curve of a 0.10 M tetrabutylammonium perchlorate pyridine solution. Spectrum was obtained at ambient temperature.

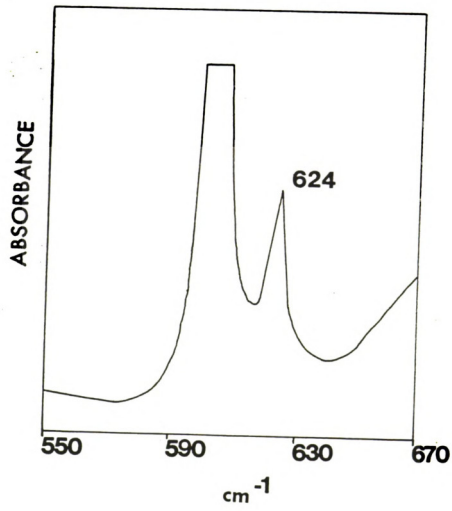
ABSORBANCE
624
550
590
630
670
cm -1

B. 2-Butanone Solutions

For LiSCN solutions in 2-butanone at concentrations of 0.01-0.60 M, a total of three IR bands were observed in the CN stretching region (Figure 25). Below 0.20 M, only a single band is observed at 2073 cm^{-1}. This band is 18 cm^{-1} higher in frequency than the solvated SCN^- band which is observed at 2055 cm^{-1} (Figure 26). This difference corresponds to an N bonded complex with the Li^+ (325). In the IR spectra, a band was observed at ~480 cm^{-1} corresponding to the δ(SCN) band for the ion pair where the interaction is at the nitrogen end of the SCN^- anion (Figure 27) (122). Numerous 2-butanone bands occur in the far-IR spectra at 260, 407, 517, and 586 cm^{-1}. The 268 cm^{-1} band due to the Li-N stretch observed in pyridine is absent from the far-IR spectra because it overlaps with the 260 cm^{-1} band assigned to 2-butanone (326). The other bands that appear in the far-IR are due to the solvation of LiSCN, the ion cage band (~377 cm^{-1}) and the displaced 2-butanone band (~433 cm^{-1}). The ion pairing band at 2073 cm^{-1}, which was present at all concentrations, was fit to a Gaussian-Lorentzian product function to determine the band areas. The uncertainty of the areas of the IR bands were not obtainable from the program. The areas calculated from the fits show a linear relationship for concentrations up to 0.08 M, and at higher concentrations, an obvious deviation is observed (Figure 28). At concentrations of 0.20 M, two new IR bands were observed at 2024 and 2040 cm^{-1} (Figure 25). These observations indicate that at higher concentrations ion pairs are associated into larger aggregates. The

Figure 25: Infrared absorption curves of LiSCN in 2-butanone at different molar concentrations. The x identifies the bands due to the aggregates. Spectra were obtained at ambient temperature.

a. 0.60 M

b. 0.40 M

c. 0.20 M

d. 0.08 M

e. 0.04 M

f. 0.02 M

g. 0.01 M

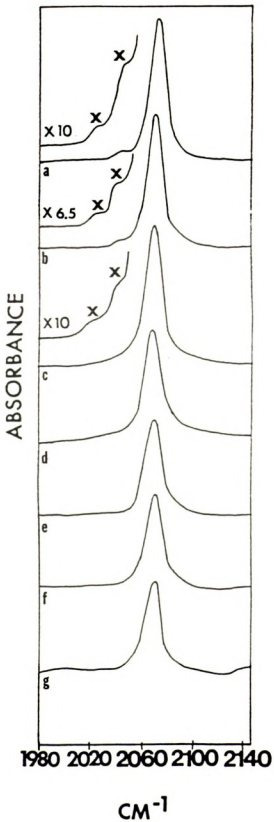
X 10
a
X 6.5
b
X 10
c
d
e
f
g
ABSORBANCE
1980 2020 2060 2100 2140
CM-1

Figure 26: Infrared absorption curves of the SCN^- anion in the presence of different cations in 2-butanone. Spectra were obtained at ambient temperature.

a. 0.40 M tetraisoamylammonium thiocyanate ($N(i\text{-amy})_4SCN$)

b. 0.40 M LiSCN

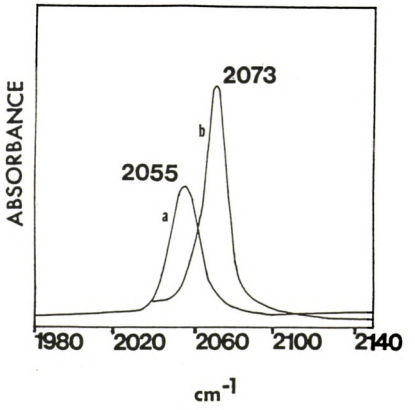
ABSORBANCE
2073
b
2055
a
1980
2020
2060
2100
2140
cm-1

Figure 27: Far-IR absorption spectra at different molar concentrations of LiSCN in 2-butanone. Spectra were obtained at ambient temperature.

a. 0.20 M

b. 0.53 M

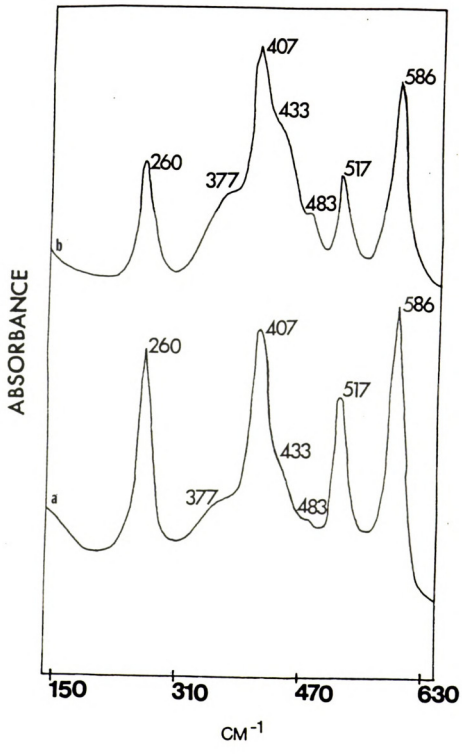
407
586
433
260
377
517
483
b
ABSORBANCE
586
260
407
517
433
a
377
483
150
310
470
630
CM-1

Figure 28: Plot of the 2073 cm^{-1} ν_{CN} absolute band areas vs. molar concentration of LiSCN in 2-butanone. Measurements were obtained at ambient temperature.

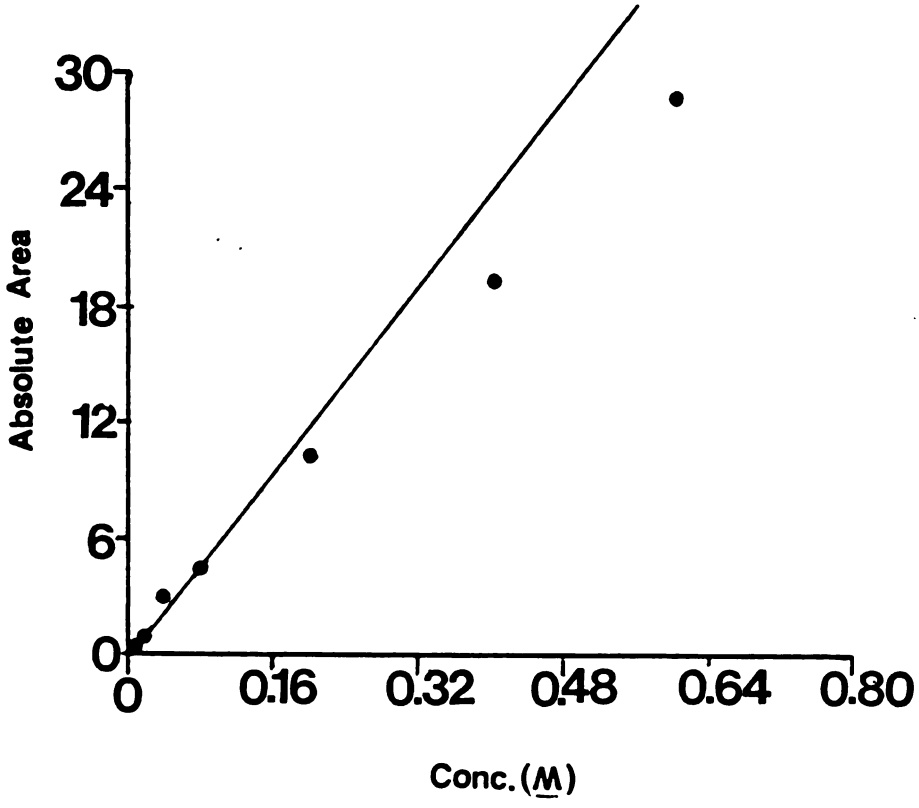
30
24
18
12
6
0
Absolute Area
0
0.16
0.32
0.48
0.64
0.80
Conc. (M)

2040 cm^{-1} band appears in the region where bands have been observed for the centrosymmetric dimer in ether solutions (122,123). The next higher aggregate formed is the tetramer, which is favored over the trimer for steric reasons (31). The tetramer has a cubane like structure with T_d symmetry (Figure 29). The IR bands assigned to the tetramer have been observed at 1993 cm^{-1} in tertiary amines and alkyl ethers. In nitromethane, the $\nu_{CN}(T_2)$ tetramer band was identified at 2040 cm^{-1} (330). It is, therefore, likely that the 2024 cm^{-1} band can be assigned to the tetramer. No far-IR bands were observed for the dimer or tetramer, which indicates that the concentration of these species is below the detection limits of the instrument.

The $\nu_4(F_2)$ triply degenerate perchlorate bands were used as a probe to study the behavior of $LiClO_4$ in 2-butanone. In all the spectra, a strong band was observed at 624 cm^{-1} (Figure 30). This band appears at the same frequency as the freely solvated ClO_4^- band or the solvent separated ion pair band which was identified from a NBu_4ClO_4 solution (Figure 31). In addition, a shoulder appears at 633 cm^{-1} which indicates the existence of contact ion pairs. The shoulder is indentified by X in Figure 30. This shoulder was difficult to observe at $\leq$0.08 M, so the spacer size was increased. The shoulder then became observable at 0.04 and 0.08 M. These results indicate that at concentrations $\geq$0.01 M, the ClO_4^- in 2-butanone associates with Li^+ to form contact and solvent separated ion pairs.

The behavior of $LiAsF_6$ in 2-butanone solutions was investigated by monitoring the changes in the $\nu_3(F_{1u})$ triply degenerate vibrations

Figure 29: Structures of the LiSCN dimers and tetramers that exist in nonaqueous solutions.

a. Dimers

b. Tetramers

A.

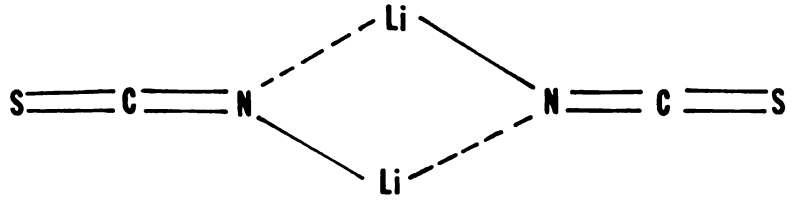

B.

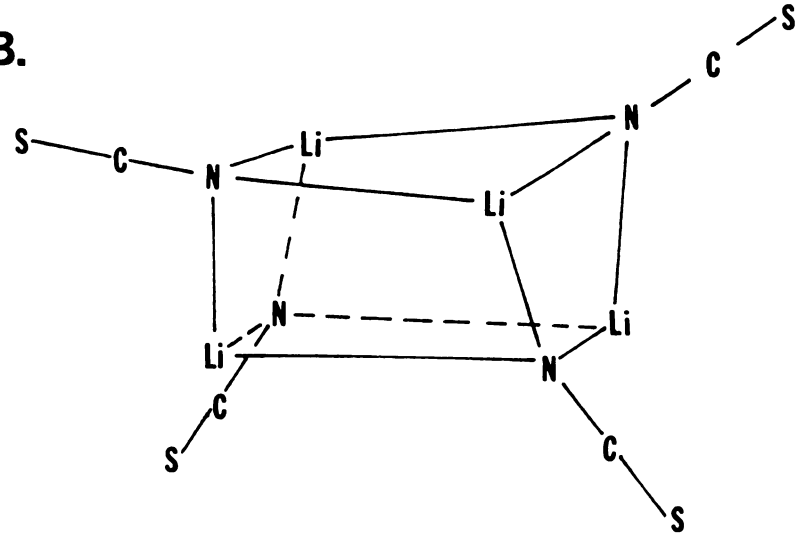

Figure 30: Infrared absorption curves for $LiClO_4$ in 2-butanone at different molar concentrations. The x indicates the band assigned to the contact ion pair. Spectra were obtained at ambient temperature.

a. 0.01 M

b. 0.02 M

c. 0.04 M

d. 0.08 M

e. 0.40 M

f. 0.60 M

g. 1.00 M

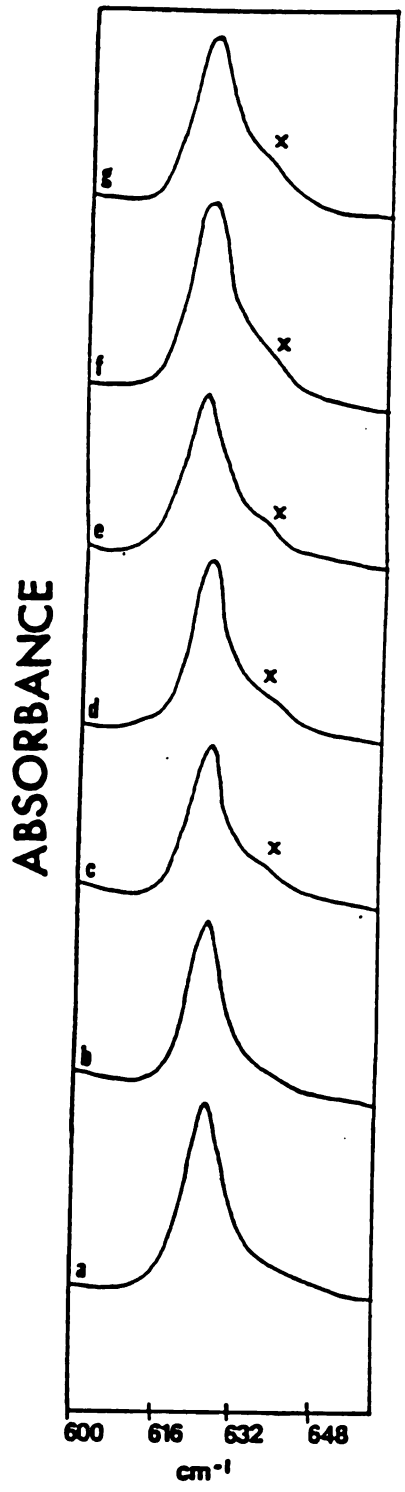
ABSORBANCE
g
f
e
d
c
b
a
x
600
616
632
648
cm⁻¹

Figure 31: Infrared absorption curves for ClO_4^- anions in the presence of different cations in 2-butanone. Spectra were obtained at ambient temperature.

a. 0.41 M tetrabutylammonium perchlorate (NBu_4ClO_4)

b. 0.41 M $LiClO_4$

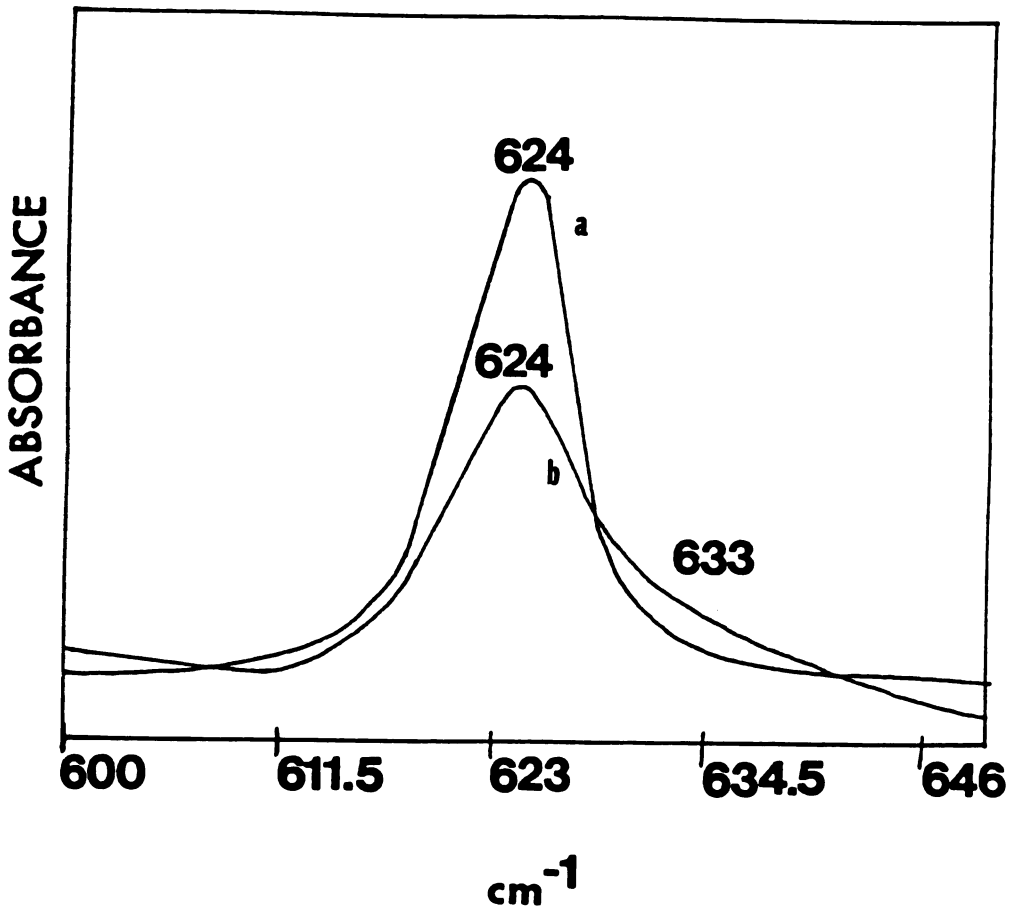
624
a
624
b
633
ABSORBANCE
600
611.5
623
634.5
646
cm-1

(331). For the freely solvated AsF_6^- or the solvent separated ion pair, a single band is expected; the existence of contact ion pairs would produce new bands in the spectra resulting from the loss of degeneracy of this vibration. At 0.04 M $LiAsF_6$ in 2-butanone, a single band was observed at 701 cm^{-1} indicating that the AsF_6^- is either freely solvated or exists as solvent separated ion pairs (Figure 32).

V. Conclusions

In 2-butanone and pyridine solutions, lithium salts form ion pairs and higher aggregates. The process occurring in solution depends upon the solvent's ability to solvate the ions, ion pairs, and aggregates. Salts having large symmetrical anions are solvated better in these low dielectric solvents than salts containing small unsymmetrical anions. For $LiClO_4$, $LiAsF_6$, $LiBPh_4$, and LiI in 2-butanone, the ion pairing formation constants determined by electrical conductance are <600 M^{-1}. For those salt solutions, a significant number of solvated free ions (>30%) exists at 0.01 M; therefore, contact ion pairing is important at a higher concentration. Infrared spectra obtained from $LiClO_4$ solutions indicate the existence of both solvated ions and contact ion pairs. For $LiClO_4$ in pyridine at concentrations ≥ 0.01 M, the majority of the solvated ions in solution exist as solvent separated ion pairs.

Electrical conductance measurements are sensitive to both the formation of solvent separated ion pairs and contact ion pairs, while

Figure 32: Infrared absorption curve for a 0.04 M $LiAsF_6$ in 2-butanone. The band corresponds to a triply degenerate $\nu_3(F_{1u})$ band. Spectrum was obtained at ambient temperature.

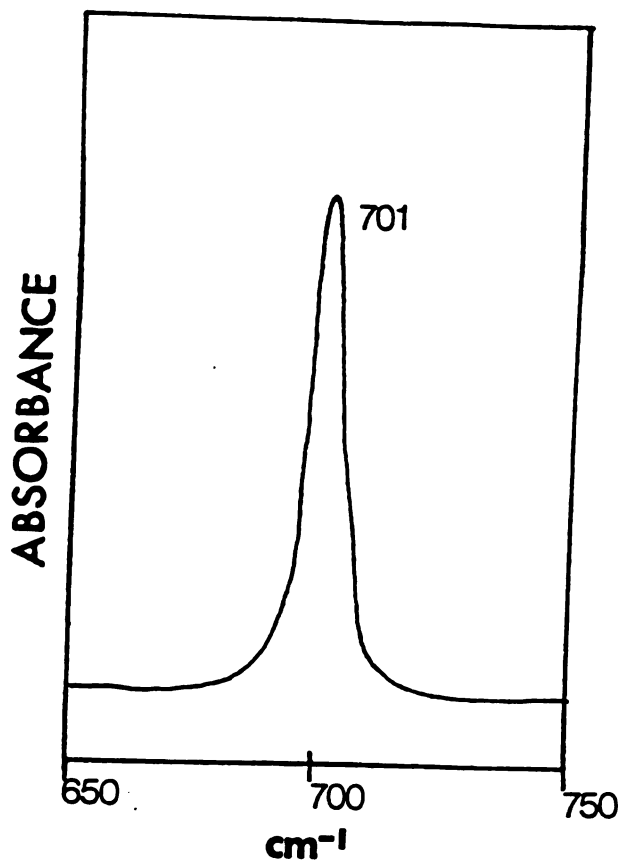
ABSORBANCE
701
650
700
750
cm⁻¹

NMR is sensitive to interactions in solution where the ions associate to form both contact ion pairs and aggregates. Therefore, the ^{7}Li chemical shift behavior at $\geq$0.01 M for these lithium salt solutions, except LiPi in pyridine, can be attributed to the formation of contact ion pairs and/or dimers in 2-butanone and pyridine solutions. For $LiClO_4$ in pyridine and 2-butanone, the two site ion pairing mechanism did not fit the ^{7}Li chemical shifts at higher $LiClO_4$ concentrations, but incorporating dimer formation into the fitting program improved the fit.

The other salts (LiSCN, LiCl, $LiNO_3$, $LiCF_3CO_2$, LiPi) in these solvents are totally contact ion paired at $\geq$0.01 M. The ^{7}Li chemical shift changes, except for LiPi in pyridine, can be attributed to dimerization. The chemical shift behavior obtained from LiPi solutions at these concentrations were attributed to collisional effects. For LiSCN in 2-butanone at concentrations $\geq$0.01 M, a two site dimerization mechanism fit the data poorly. Refitting the data to include the formation of tetramers drastically improved the fit. Bands are observed in the CN stretching region in the IR spectrum of LiSCN 2-butanone solutions which have been assigned to the dimer and tetramer species.

CHAPTER FOUR

SPECTROSCOPIC STUDIES IN BPC-$AlCl_3$ MELTS

I. Introduction

Studies were carried out with alkali metal salts to determine their solution chemistry in BPC-$AlCl_3$ melts. The complexing ability of ether ligands with alkali metal cations was also investigated in the BPC-$AlCl_3$ melts between 45-67 mole % $AlCl_3$. Multinuclear NMR was the primary technique used; these measurements are sensitive to changes in the environment around NMR sensitive nuclei.

II. Solvation of Alkali Metal Salts in BPC-$AlCl_3$ Melts

Numerous studies have reported that in basic, Cl^- rich melts, metal cations form chloroanionic complexes (248,252,255,262,332,333). In acidic, $AlCl_3$ rich melts, metal cations form complexes with $AlCl_4^-$ and $Al_2Cl_7^-$ (262,253,334,254,247). For metal cations with charges greater than one, positively charged chlorocomplexes can also exist in acidic melt solutions (247,253,255,332,335). The majority of the studies have been carried out with transition metal salts. Except for LiCl, the behavior of alkali metal salts in these melts has not been investigated. Solution studies in nonaqueous solvents have shown that alkali metal NMR is a sensitive probe for investigating solvent interactions with NMR sensitive nuclei (69,323,336).

A. Lithium Salts in Melt Solutions

Taulelle and Popov (245) observed a ^7Li NMR signal at 25 °C in a 1.0 mole % LiCl mixture of 45-47 mole % $AlCl_3$ melt; the solubility of LiCl in the 47 mole % $AlCl_3$ is less than 1.0 mole %. (Figure 33). Since basic melts contain an excess of Cl^-, dissolving LiCl results in the formation of anionic chlorocomplexes. Potentiometric measurements showed that two Cl^-'s are bound to each lithium cation (337). Therefore, it has been proposed that the lithium species that exists in basic melt is $LiCl_2^-$. The ^7Li chemical shifts of the 45 mole % $AlCl_3$ containing LiCl are concentration dependent (Figure 34). The error bars in Figure 34 correspond to ±2s, where s is the estimate of the error of the chemical shift measurements. The value of s was assumed to be ±0.02 ppm. As the concentration of LiCl increases, the ^7Li chemical shift moves upfield. A dimerization mechanism was found to fit the chemical shift data.

$$2LiCl_2^- \leftrightarrow Li_2Cl_4^{2-} \qquad (4\text{-}1)$$

The dimerization formation constant and the chemical shifts of the dimer and monomer were determined with the aid of the KINFIT program (Figure 35). The fitting program calculated the dimerization constant and the ^7Li chemical shift of the $LiCl_2^-$ and $Li_2Cl_4^{2-}$ species simultaneously (Appendix 4-B). The log K_D and the chemical shift of the monomer and dimer obtained are 2.8(±0.4), 4(±1.), and 1.11(±0.01), respectively. Earlier studies with WCl_3 showed that these molecules

Figure 33: Variation in the ^{7}Li chemical shift with composition of BPC-$AlCl_3$ melts at 25 °C. Mole fraction of LiCl is 0.01. These chemical shifts were not corrected for the magnetic susceptibility of the melt.

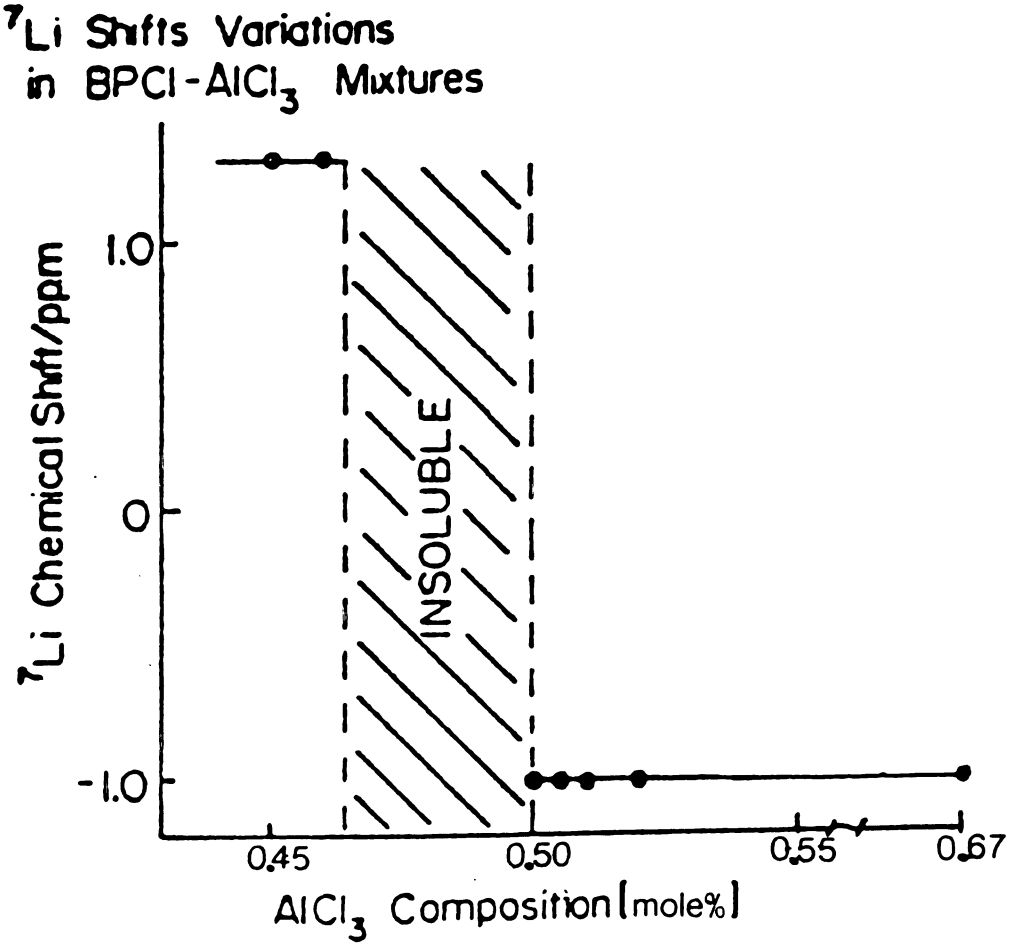
^{7}Li Shifts Variations
in BPCl-AlCl$_3$ Mixtures
^{7}Li Chemical Shift/ppm
1.0
0
-1.0
INSOLUBLE
0.45
0.50
0.55
0.67
AlCl$_3$ Composition [mole%]

Figure 34: Lithium-7 chemical shifts as a function of the LiCl concentration in 45 mole % $AlCl_3$ BPC-$AlCl_3$ melts at 40 °C. The error bars correspond to ±2s, where s is the estimate of the error of the chemical shift measurements. The value of s was assumed to be ±0.02 ppm.

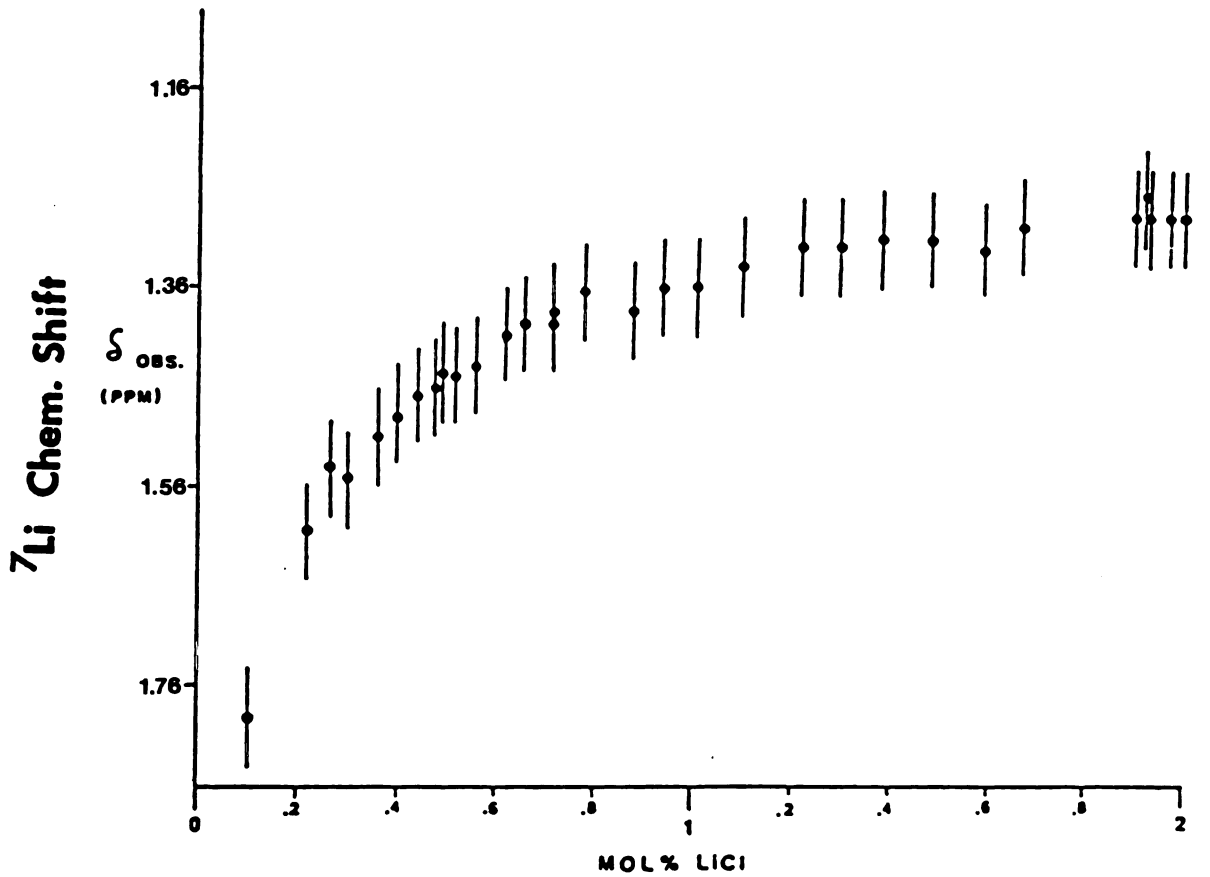
^{7}Li Chem. Shift
δ OBS. (PPM)
1.16
1.36
1.56
1.76
0
.2
.4
.6
.8
1
.2
.4
.6
.8
2
MOL% LICl

Figure 35: KINFIT output of the ^{7}Li chemical shifts fitted to a dimerization mechanism.

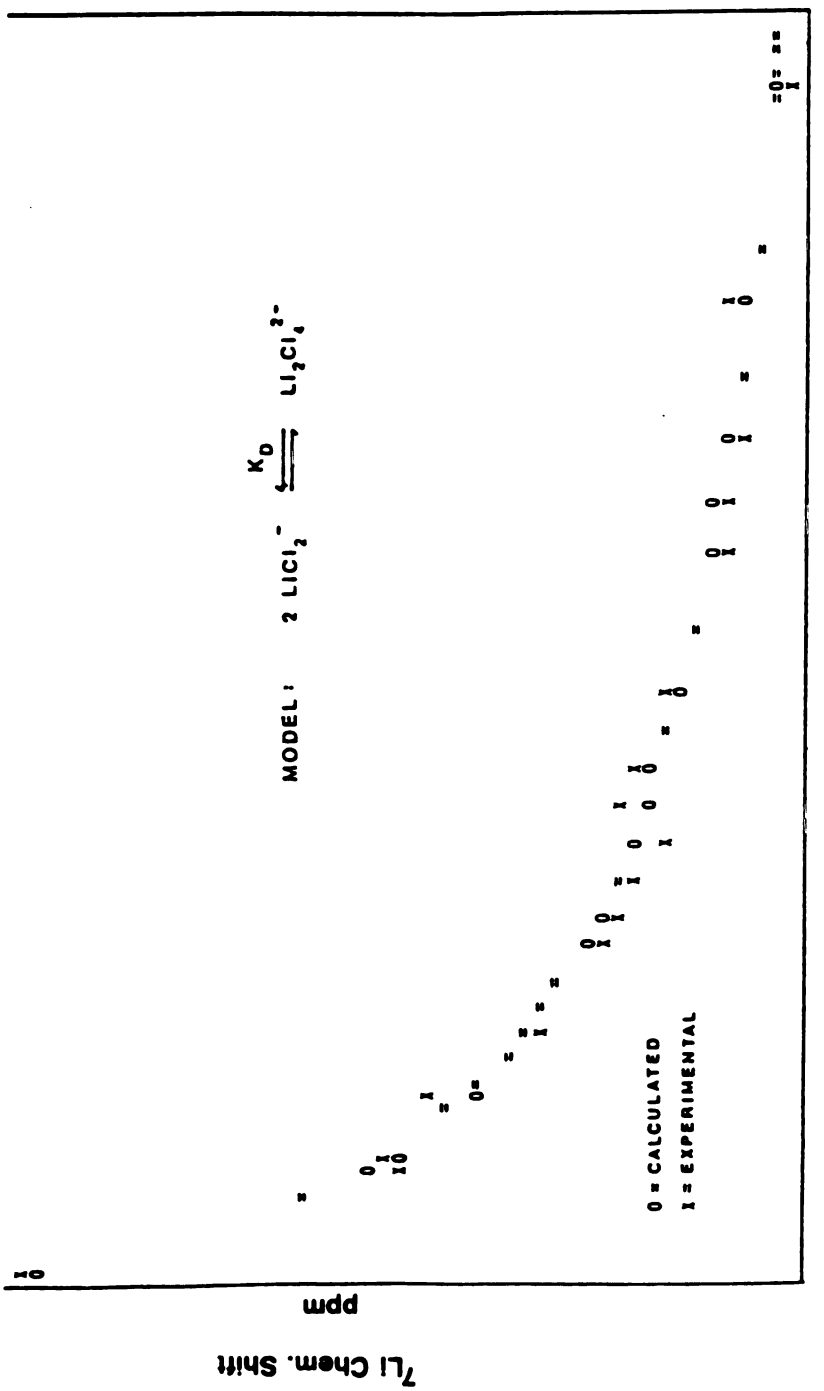
^{7}Li Chem. Shift
ppm
Conc.(mole %)
MODEL : 2 $LiCl_2^-$ $\underset{}{\overset{K_D}{\rightleftharpoons}}$ $Li_2Cl_4^{2-}$
O = CALCULATED
I = EXPERIMENTAL

form dimers ($W_2Cl_9^{3-}$) in basic melt solutions (252,255,338). In solvents with low dielectric constants, LiSCN ion pairs form dimers and tetramers (31,123). Assuming that the lithium cation forms four coordinate complexes, possible structures for the $Li_2Cl_4^{2-}$ and $LiCl_2^-$ are shown in Figure 36. The coordination sites around the Li^+ not occupied by free Cl^-'s are occupied by two chlorides from the $AlCl_4^-$ ligand.

In acidic melts, the chemical shift at 25 °C of a 1.0 mole % LiCl solution is 2.4 ppm upfield from the signal obtained from a 1.0 mole % LiCl solution in basic melt (Figure 33). The addition of LiCl to acidic melts titrates the melt in the basic direction according to the following equation: (m=1,2)

$$LiCl + Al_2Cl_7^- \leftrightarrow Li^+ + 2AlCl_4^- \qquad (4\text{-}2)$$

The chemical shift was reported to be constant for a 1.0 mole % LiCl between 50-67 mole % $AlCl_3$ (Figure 33) (245,337). The 1.0 mole % LiCl melt solution prepared with neutral melt was not completely homogeneous. The lithium cations generated by the reaction with $Al_2Cl_7^-$ form complexes with $AlCl_4^-$ and unreacted $Al_2Cl_7^-$. Infrared studies indicate that the Li^+ can form a complex, described as a cage complex, with one $Al_2Cl_7^-$ (339). The Li^+ is large enough to accommodate two $Al_2Cl_7^-$ ligands, which results in a six coordinate complex as shown in Figure 37. Rytter and coworkers (281) proposed a C_{2v} model where the lithium cation is interacting with two $AlCl_4^-$

Figure 36: Possible structure for lithium chlorocomplexes in 45 mole % $AlCl_3$ melt. The coordination sites around the Li^+ not occupied by free Cl^-'s are occupied by two chlorides from the $AlCl_4^-$ ligand.

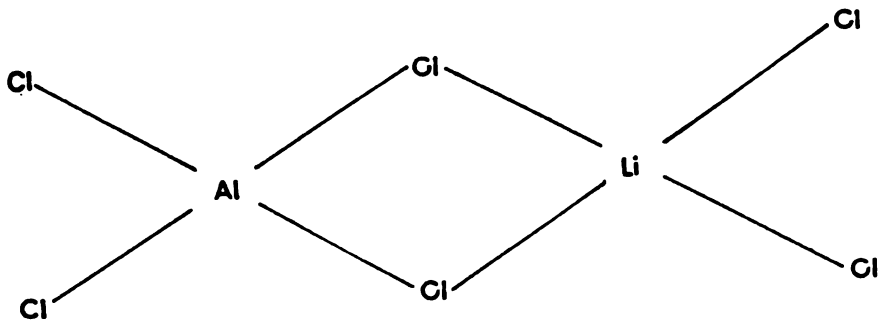

Monomer

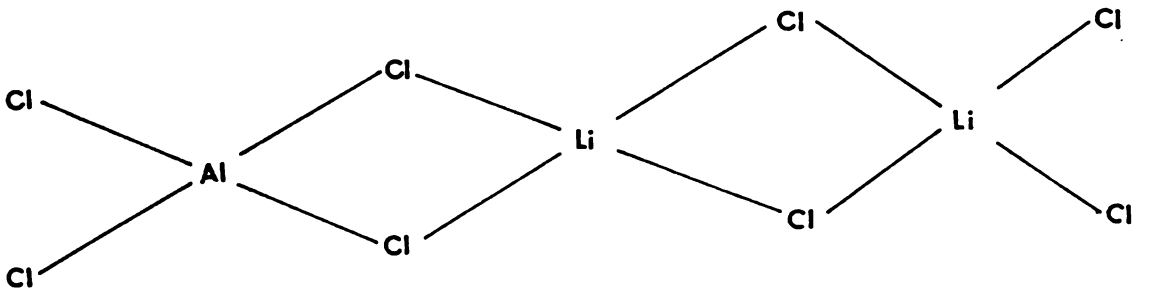

Dimer

Figure 37: Possible environment for the Li^+ cation in acidic melt (50-67 mole % $AlCl_3$).

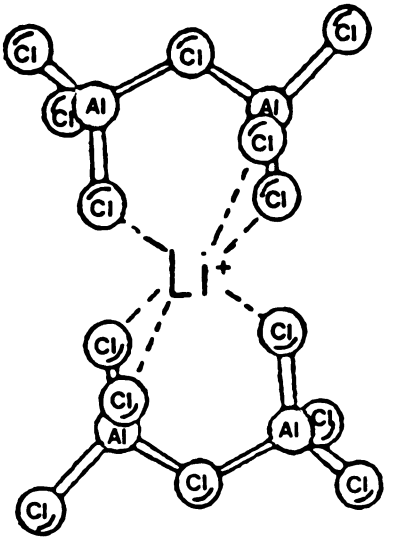
Cl
Cl
Cl
Al
Al
Cl
Cl
Cl
Li+
Cl
Cl
Cl
Al
Al
Cl
Cl
Cl
Cl

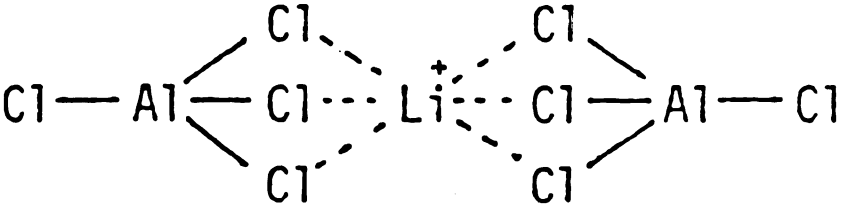
Cl
Cl
Cl—Al—Cl
Li+
Cl—Al—Cl
Cl
Cl

molecules, which would be possible in acidic melts, especially near neutrality. Two Cl^- ions from each $AlCl_4^-$ are coordinated to the Li^+, which produces a four coordinate complex. The ^7Li chemical shifts obtained from acidic melt solutions indicate that at acidic compositions, the environment around the Li^+ is independent of the composition of the melt. This suggests either that a single Li^+ complex exists with $AlCl_4^-$ ligands, or a mixture of complexes having $AlCl_4^-$ and $Al_2Cl_7^-$ ligands where the coordination and the geometry around the Li^+ is not significantly different when interacting with either aluminum chloride ligands. The concentration of $Al_2Cl_7^-$ at melt compositions around 50 mole % $AlCl_3$ is very low; therefore, complexes with $AlCl_4^-$ are more likely to occur. The C_{2v} structure and the cage structure have different number of atoms coordinated to Li^+. These two complexes will have different chemical shifts. An equally probable structure is the C_{3v} structure where the Li^+ interacts with three Cl^- from two $AlCl_4^-$ producing an environment around the Li^+ very similar to that produced with two $Al_2Cl_7^-$ (Figure 37). Mixed complexes may exist if $AlCl_4^-$ and $Al_2Cl_7^-$ coordinate in the same fashion as in the C_{3v} and cage structure, respectively.

B. Sodium and Cesium Salts in Melt Solutions

The solution behavior of both sodium and cesium salts in BPC–$AlCl_3$ melts is similar but different in basic melts from that observed for lithium salts. In basic melts, neither ^{133}Cs nor ^{23}Na resonances were observed for a series of sodium (Na_2O, $NaBPh_4$,

NaCl) and cesium salts (CsCl, CsSCN, $CsBPh_4$, CsF, CsBr, CsI, CsPi, $CsNO_3$, Cs_2CO_3, $CsClO_4$, CsAc, and Cs_2SO_4). Figure 38 shows the ^{133}Cs NMR's of cesium chloride melt solutions at 45 °C at different melt compositions. These solutions are all inhomogeneous. The composition ranges from 0.66-1.10 mole % CsCl. These melt solutions are considered to be saturated, which assumed that the condition time of three weeks at 70 °C is long enough to allow for saturation. The ^{133}Cs chemical shifts are essentially the same if the samples are conditioned for an additional week. One mole % NaCl acidic melt solution is homogeneous in 55-67 mole % $AlCl_3$. In 67 mole % melts, ^{23}Na and ^{133}Cs resonances were observed at 45 °C for all the cesium and sodium salts. The solubility of CsCl is below 0.66 mole % CsCl in 67 mole % $AlCl_3$ melts; the NaCl solubility exceeds 1.0 mole % NaCl at this melt composition.

Absence of ^{23}Na and ^{133}Cs resonances in basic melts indicates that neither cesium nor sodium cations form chloroanionic complexes, or the solubility kinetics are very slow (Figures 38,39). Slow solubility was eliminated as a possible explanation when a ^{23}Na resonance was not observed in a 45 mole % $AlCl_3$ melt solution prepared by titrating a 0.98 mole % NaCl solution prepared with 67 mole % $AlCl_3$ melt.

The solubility behavior of alkali metal thiocyanates was examined by IR spectrometry. Since NaCl is insoluble in basic melts, NaCl windows were used for solution IR studies using the ν_{CN} bands to detect the existence of thiocyanate ions in basic melt solutions. Infrared spectra of a 0.99 mole % LiSCN solution, a filtered 1.05 mole

Figure 38: Cesium-133 NMR spectra of saturated CsCl solutions for different BPC-$AlCl_3$ compositions at 45 °C. The R corresponds to the reference (0.01 M CsBr 20% D_2O/H_2O) solution. To the left of each spectrum is the melt composition in mole %. Chemical shifts have not been corrected for the magnetic susceptibility of the melt.

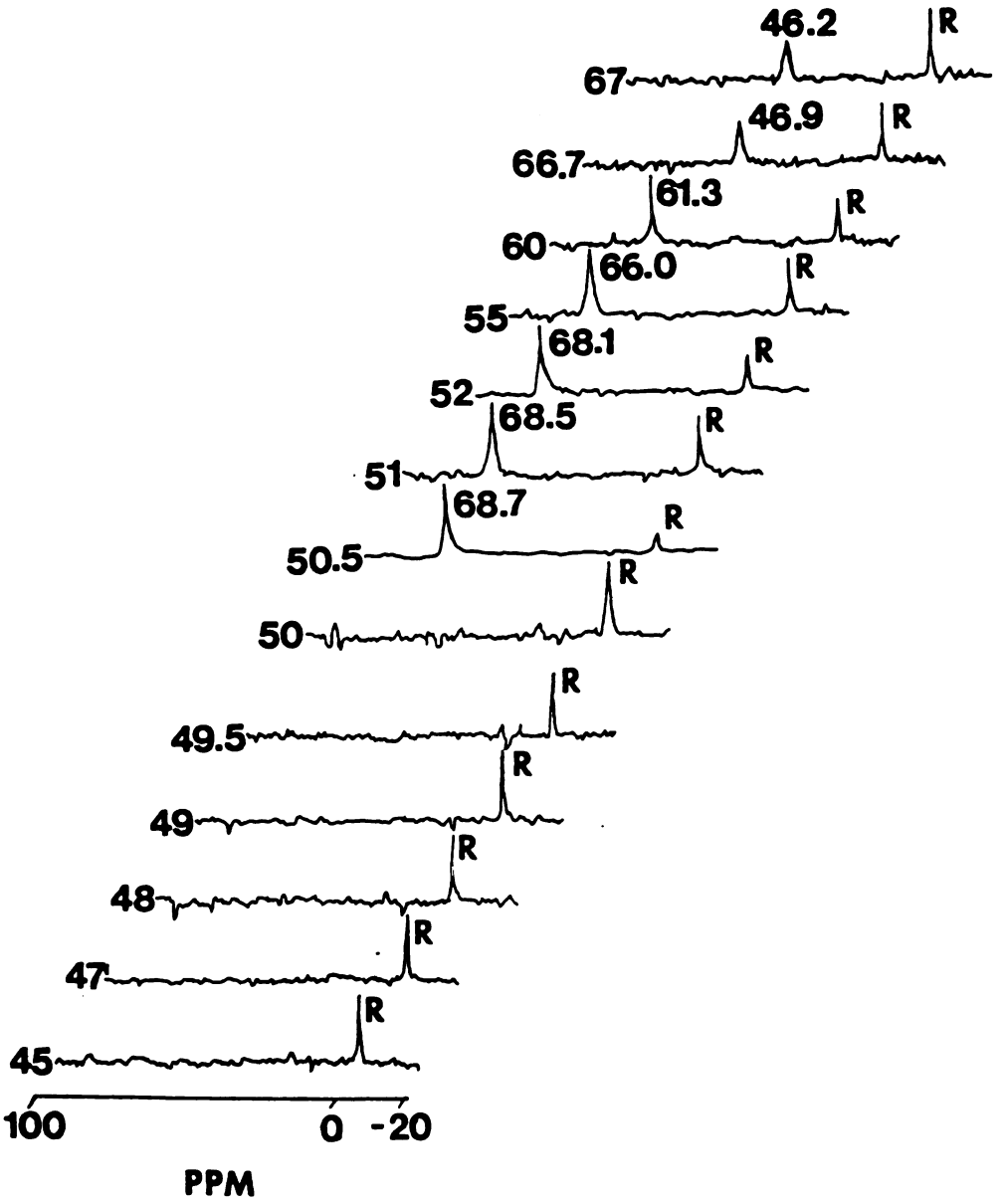
46.2
R
67
46.9
R
66.7
61.3
R
60
66.0
R
55
68.1
R
52
68.5
R
51
68.7
R
50.5
R
50
R
49.5
R
49
R
48
R
47
R
45
100
0
-20
PPM

Figure 39: Sodium-23 NMR spectra of 1.00(±.12) mole % NaCl solutions for different BPC-$AlCl_3$ compositions at 45 °C. The band identified by R is the reference (0.01 M NaCl 100% D_2O solution). The number at the left of each spectra is the composition of the melt in mole %. All samples below 55 mole % were inhomogeneous. The chemical shifts have not been corrected for the magnetic susceptibility of the melt.

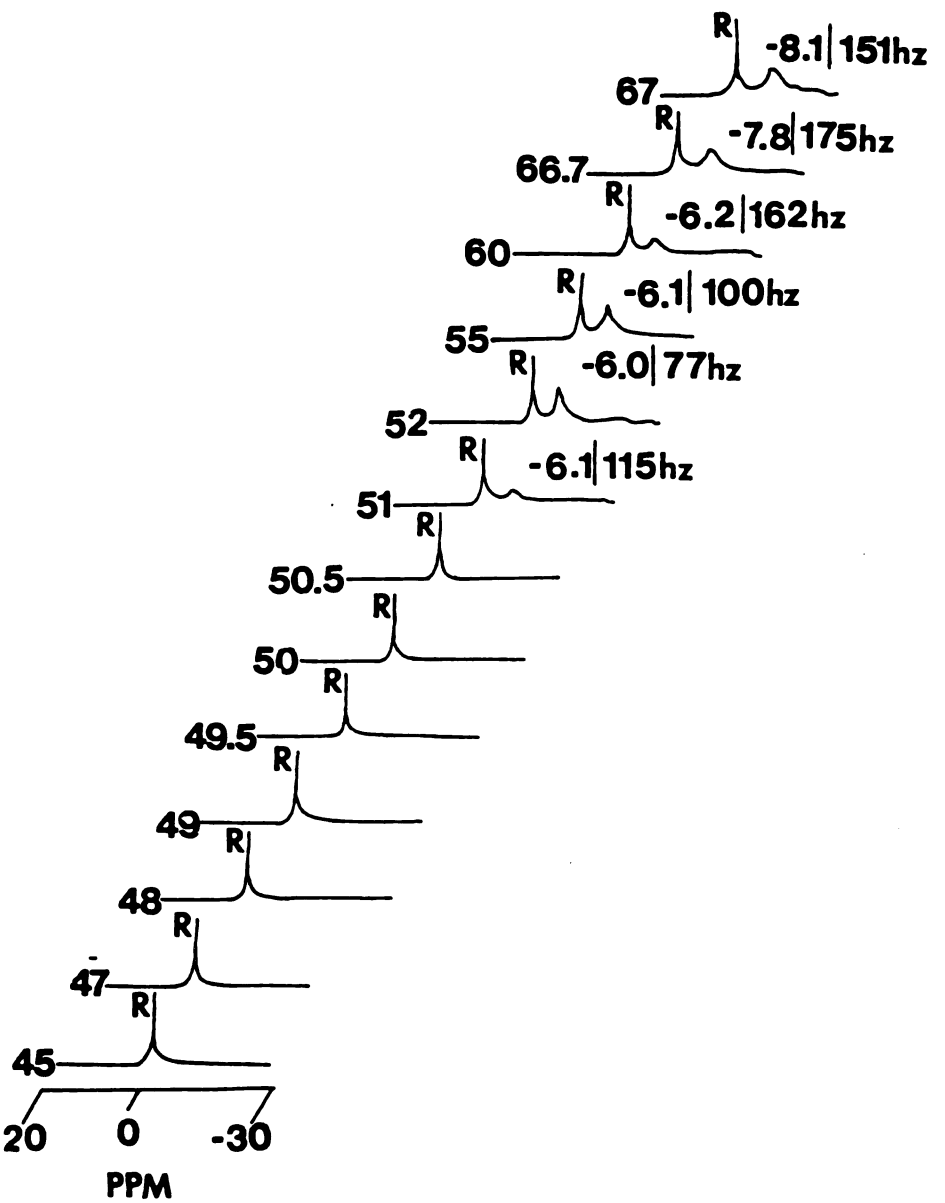
R
-8.1|151hz
67
R
-7.8|175hz
66.7
R
-6.2|162hz
60
R
-6.1|100hz
55
R
-6.0|77hz
52
R
-6.1|115hz
51
R
50.5
R
50
R
49.5
R
49
R
48
R
47
R
45
20
0
-30
PPM

% NaSCN melt solution, and a filtered 0.98 mole % CsSCN basic melt solution consisted of two bands in each spectrum; the band positions were independent of the alkali cation (Figure 40). Also, addition of an equimolar amount of C211 to a 1.0 mole % LiSCN did not affect the ν_{CN} bands of the IR spectrum. The C211 ligand encapsulates the cation in a cavity, isolating the cation from any interaction with anions found in the melt solution. These results indicate that cesium and sodium thiocyanate salts are soluble in 45 mole % $AlCl_3$ melt; however, since ^{133}Cs and ^{23}Na resonances were not observed, the cesium and sodium cations fail to form soluble chloroanionic complexes. They precipitate out of the melt as chloride salts, and the SCN^- coordinates to Al(III) according to the following equation:

$$AlCl_4^- + MSCN \leftrightarrow AlCl_3NCS^- + MCl\downarrow \qquad (4\text{-}3)$$

Further discussion of the IR spectra of thiocyanate salts is found in Section II-C.

In acidic melts, ^{133}Cs and ^{23}Na resonances at 45 °C were observed for a series of cesium salts (CsSCN, $CsBPh_4$, CsF, CsCl, CsBr, CsI, $CsNO_3$, Cs_2CO_2, $CsClO_4$, CsAc, and Cs_2SO_4) and sodium salts (NaCl and $NaBPh_4$). The ^{133}Cs bands of CsCl are observed from melt composition 50.5-67 mole % $AlCl_3$; the ^{23}Na bands of sodium salts are observed from 51-67 mole % $AlCl_3$ (Figure 38,39). The ^{23}Na and ^{133}Cs chemical shifts in acidic melts remain constant up to 55 mole % $AlCl_3$ and then begin to shift upfield. From 60 to 66.7 mole % $AlCl_3$, a large change

Figure 40: Infrared absorption curves of alkali thiocyanate mixtures in 45 mole % $AlCl_3$ BPC-$AlCl_3$ melt. The NaSCN and CsSCN mixtures were inhomogeneous and were filtered before the infrared spectra were obtained. Spectra was obtained at ambient temperatures.

a. 0.98 mole % CsSCN

b. 1.05 mole % NaSCN

c. 0.99 mole % LiSCN

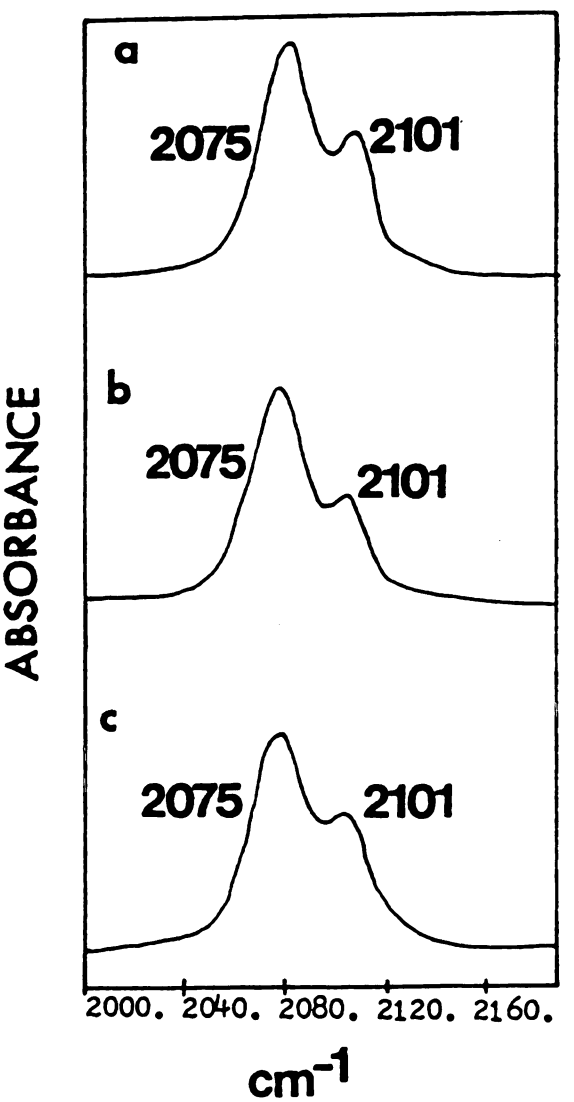
a
2075
2101
b
2075
2101
c
2075
2101
ABSORBANCE
2000. 2040. 2080. 2120. 2160.
cm-1

in the chemical shift is observed. Potentiometric measurements indicate that at ~60 mole % $AlCl_3$ and higher, the concentration of $Al_2Cl_7^-$ becomes higher than that of $AlCl_4^-$ (222). Hvistendahl and coworkers (339) have suggested that both Cs^+ and Na^+ form complexes with $Al_2Cl_7^-$. The metal cation interacts with the three terminal Cl^-'s of $Al_2Cl_7^-$, to produce a three-coordinate complex with an $Al_2Cl_7^-$ ligand. The environments of Na^+ and Cs^+ are taken to be six-coordinate; therefore, two $Al_2Cl_7^-$ molecules can coordinate in this fashion to the cation. When ligand exchange occurs with an NMR sensitive nuclei, the chemical shift changes are dependent on the electron-donating ability of the ligands. The overlap of the outer orbitals of the $AlCl_4^-$ and $Al_2Cl_7^-$ with the orbitals of the sodium or cesium ion induces orbital angular momentum in the electrons of metal ion which produces changes in the chemical shifts (73). For both Na^+ and Cs^+ complexes increasing the donicity of the ligands causes the sodium and cesium resonances to shift downfield. In acidic melt solutions both $AlCl_4^-$ and $Al_2Cl_7^-$ coexist; $AlCl_4^-$ is a better electron donor than $Al_2Cl_7^-$. Therefore, substituting a $AlCl_4^-$ ligand for an $Al_2Cl_7^-$ should shift the sodium and cesium resonances downfield, which is what is observed from alkali metal NMR measurements obtained from NaCl or CsCl acidic melt solutions at different acidities. The C_{2v} structure proposed by Rytter and coworkers (281) for $AlCl_4^-$ complexes does not explain the observed chemical shift behavior. When an acidic melt is titrated basic, $Al_2Cl_7^-$ ligands are being exchanged for $AlCl_4^-$. The formation of a C_{2v} structure reduces the coordination to

the me

ligand

(281) i

and 13

coordina

move do

titrated

from two

coordina

$AlCl_4^-$ w

Na^+ and

Sodi

at three

from 55 a

chemical

42,43).

spectral

position

change in

quadrupol

viscosity

(340,341).

increases

of the 23

made more

the metal cation by one for each $AlCl_4^-$ that replaces an $Al_2Cl_7^-$ ligand assuming the structure proposed by Hvistendahl and coworkers (281) is correct for Na^+ and Cs^+ complexes with $Al_2Cl_7^-$. Both ^{23}Na and ^{133}Cs chemical shift measurements move upfield when the coordinations number decreases. The ^{23}Na and ^{133}Cs chemical shifts move downfield instead of upfield as an acidic melt solution is titrated basic. Therefore, the C_{3v} structure where three chlorides from two $AlCl_4^-$ are coordinated to the metal cation producing a six coordinate complex is a better description of the interaction of $AlCl_4^-$ with Na^+ and Cs^+. Figure 41 shows the possible complexes with Na^+ and Cs^+ in acidic melt solutions.

Sodium-23 linewidth measurements for melt mixtures were obtained at three different temperatures for two NaCl melt mixtures prepared from 55 and 66.7 mole % $AlCl_3$ melts. The linewidths decrease and the chemical shift remains constant as the temperature increases (Figures 42,43). The chemical shifts were measured from the edge of the spectral window because the change in temperature also affects the position of the reference. This linewidth behavior reflects both a change in viscosity and chemical exchange. The ^{23}Na nuclei relax by a quadrupolar mechanism. The rate of relaxation is dependent upon the viscosity, which affects the molecular reorientation correlation time (340,341). The viscosity of the melt decreases as the $AlCl_3$ content increases (341). Therefore, in the absence of exchange, the linewidth of the ^{23}Na band should decrease as the composition of the melt is made more acidic. The measurement of the ^{23}Na linewidths from the

Figure 41: Possible environments for the Na^+ and Cs^+ cations in acidic melts (50-67 mole % $AlCl_3$).

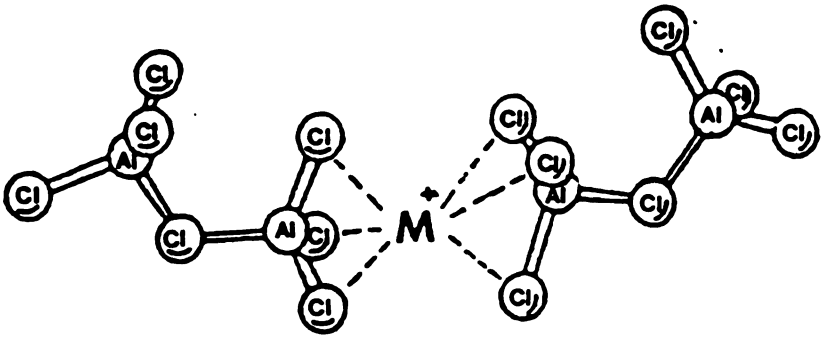
Cl
Al
M

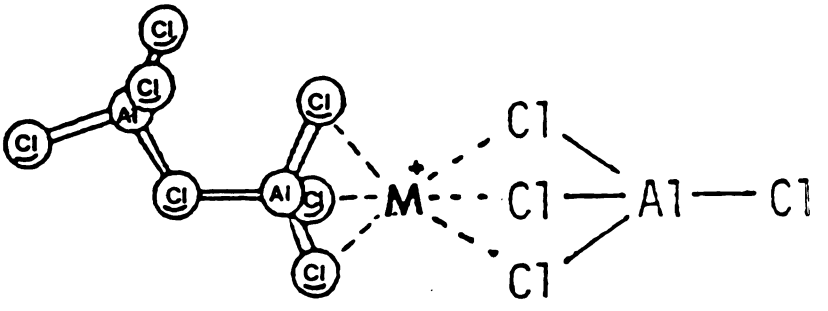
Cl
Al
M
Cl
Cl
Al
Cl

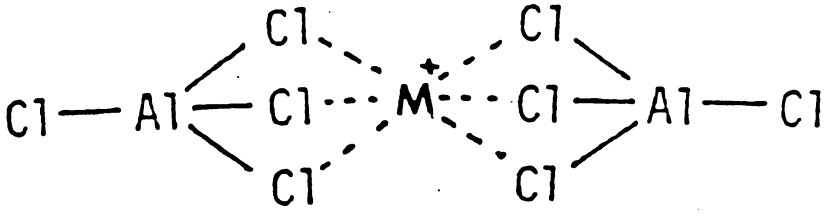
Cl
Cl
Al
Cl
M
Cl
Cl
Al
Cl

Figure 42: Sodium-23 NMR spectra of 0.99 mole % NaCl 66.7 mole % $AlCl_3$ BPC-$AlCl_3$ mixture showing the variation of linewidth (hz) as a function of temperature.

a. 45 °C

b. 60 °C

c. 80 °C

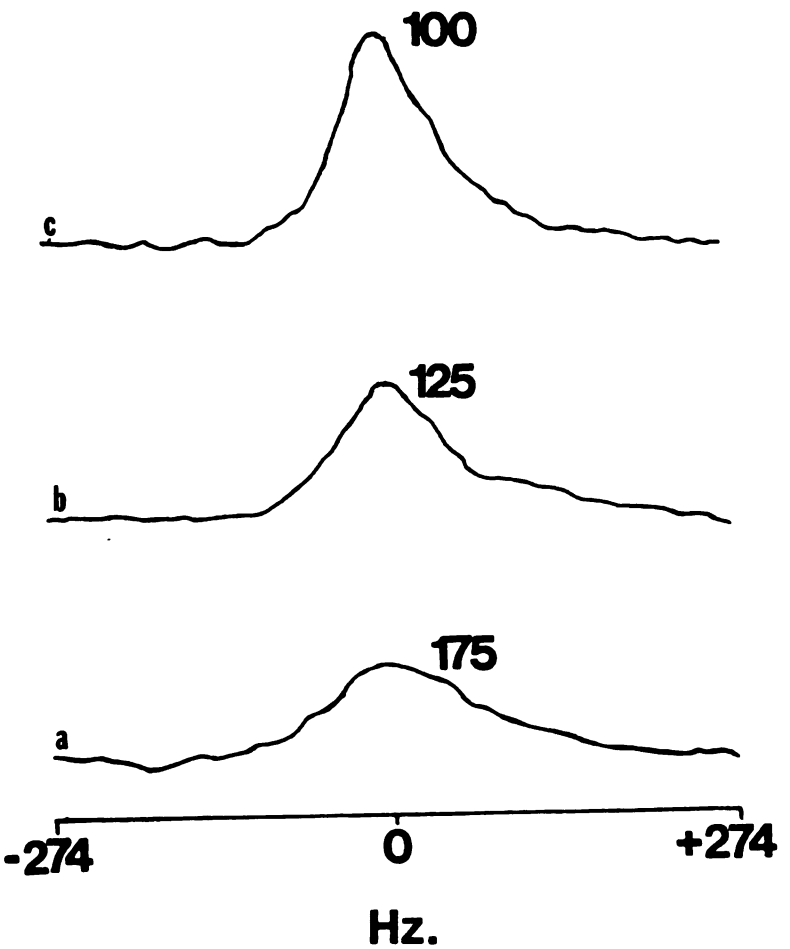
100
c
125
b
175
a
-274
0
+274
Hz.

Figure 43: Sodium-23 NMR spectra of a 0.95 mole % NaCl 55 mole % $AlCl_3$ BPC-$AlCl_3$ mixture showing the variation of linewidth (h_3) as a function of temperature.

a. 45 °C

b. 60 °C

c. 80 °C

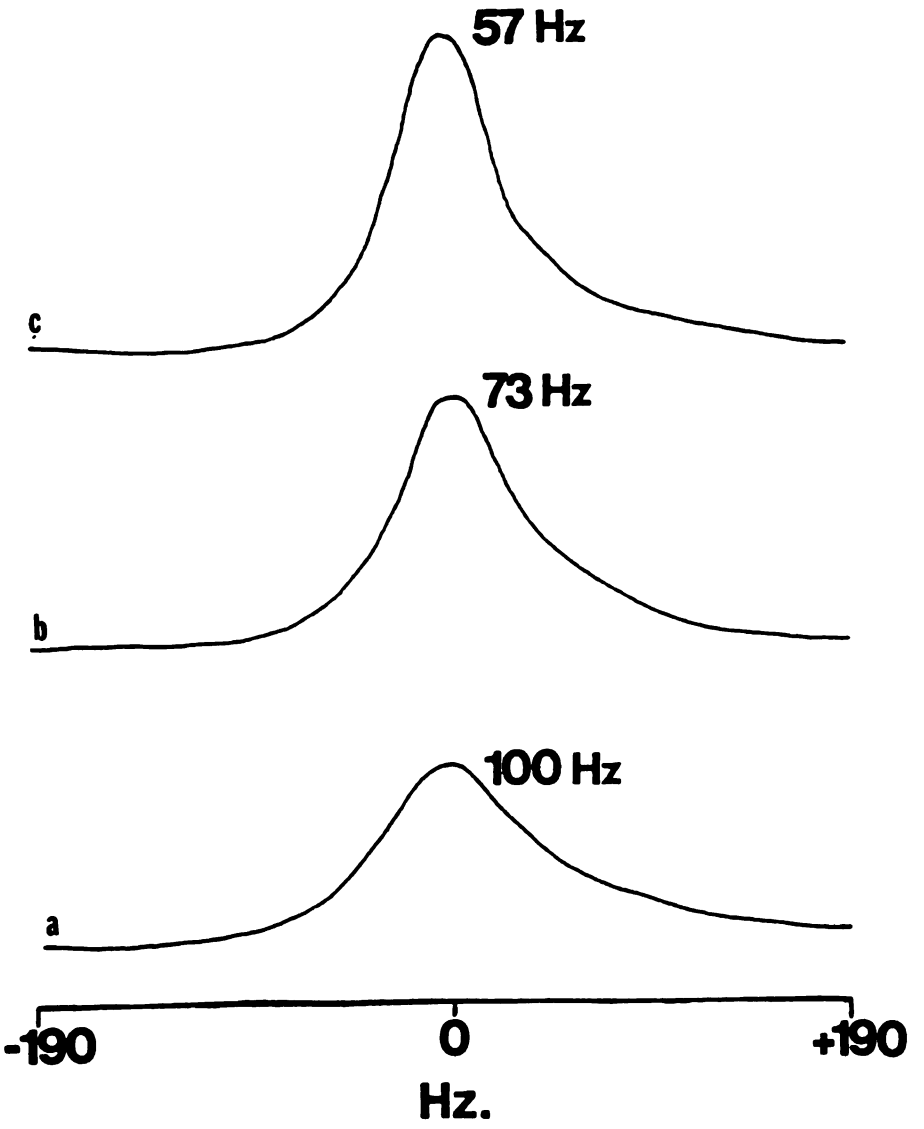
57 Hz
c
73 Hz
b
100 Hz
a
-190
0
+190
Hz.

51-67 mole % $AlCl_3$ does not totally reflect a viscosity effect (Figure 39). From 51-52 mole % $AlCl_3$, the linewidth decreases, which reflects the decrease in viscosity. At compositions from 55-66.7 mole % $AlCl_3$, the linewidth increases and then decreases again at 67 mole % $AlCl_3$ melt solution. The broadening that occurs between 55-66.7 mole % $AlCl_3$ is probably due to the exchange of $AlCl_4^-$ and $Al_2Cl_7^-$ ligands between Na^+ complexes in the melt.

Other sodium and cesium salts were added to a 67 mole % $AlCl_3$ melt. The ^{23}Na chemical shift at 45 °C does not change for melt solutions containing other sodium salts than NaCl at the same concentration. The ^{133}Cs chemical shift at 45 °C shows a small chemical shift dependency on the anion (Figures 44,45). These melt mixtures are saturated solutions. The ^{133}Cs NMR nucleus (Quad. moment = -3×10^{-3}, chemical shift range = 300 ppm) is more sensitive to environmental changes around the cation than is the ^{23}Na nucleus (Quad. moment = 0.12, chemical shift range = 30 ppm) (342). The ^{133}Cs chemical shift reflects the anion's ability to react with $Al_2Cl_7^-$ to produce $AlCl_4^-$, which reduces the acidity of the melt. Macial and Gray (340) showed by ^{27}Al NMR that addition of a tetramethylammonium iodide to an acidic melt produces $AlCl_3I^-$. Both this complex and $AlCl_4^-$ are generated from the reaction of tetramethylammonium iodide with $Al_2Cl_7^-$. Oxyanions have also been shown to react with $Al_2Cl_7^-$ to produce $AlCl_4^-$ (265-269,343). The ^{133}Cs resonance obtained from a 67 mole % $AlCl_3$ melt solution is concentration dependent. At concentrations below maximum CsCl solubility, the chemical shift is

Figure 44: Cesium-133 NMR spectra of cesium oxyanion salts in 67 mole % $AlCl_3$ BPC-$AlCl_3$ melt at 45 °C. All samples were inhomogeneous. The R corresponds to the reference band (0.01 M CsBr 20% D_2O/H_2O solution). The chemical shifts have not been corrected for the magnetic susceptibility of the melt.

a. 1.06 mole % CsPi

b. 1.11 mole % $CsNO_3$

c. 0.75 mole % Cs_2CO_3

d. 1.12 mole % $CsClO_4$

e. 0.88 mole % CsAc

f. 1.08 mole % Cs_2SO_4

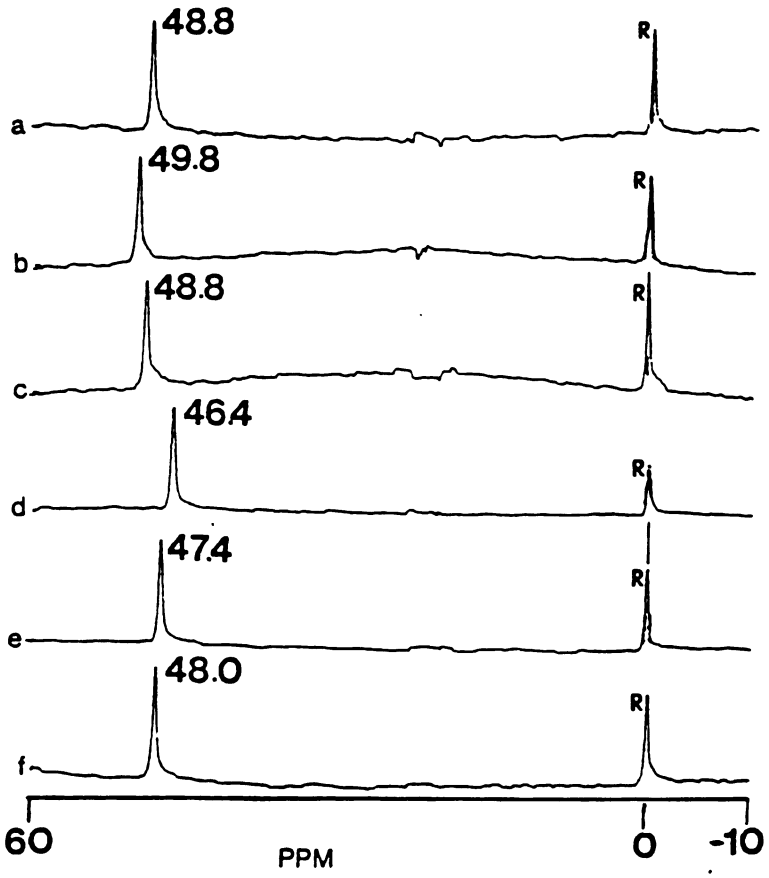
48.8
R
a
49.8
R
b
48.8
R
c
46.4
R
d
47.4
R
e
48.0
R
f
60
PPM
0
-10

Figure 45: Cesium-133 NMR spectra of several cesium salts in 67 mole % $AlCl_3$ BPC-$AlCl_3$ melts at 45 °C. All mixtures were inhomogeneous. The R corresponds to the reference band (0.01 M CsBr 20% D_2O/H_2O solution). The chemical shifts have not been corrected for the magnetic susceptibility of the melt.

a. 1.01 mole % CsSCN

b. 1.00 mole % $CsBPh_4$

c. 1.24 mole % CsF

d. 0.66 mole % CsCl

e. 0.84 mole % CsBr

f. 0.73 mole % CsI

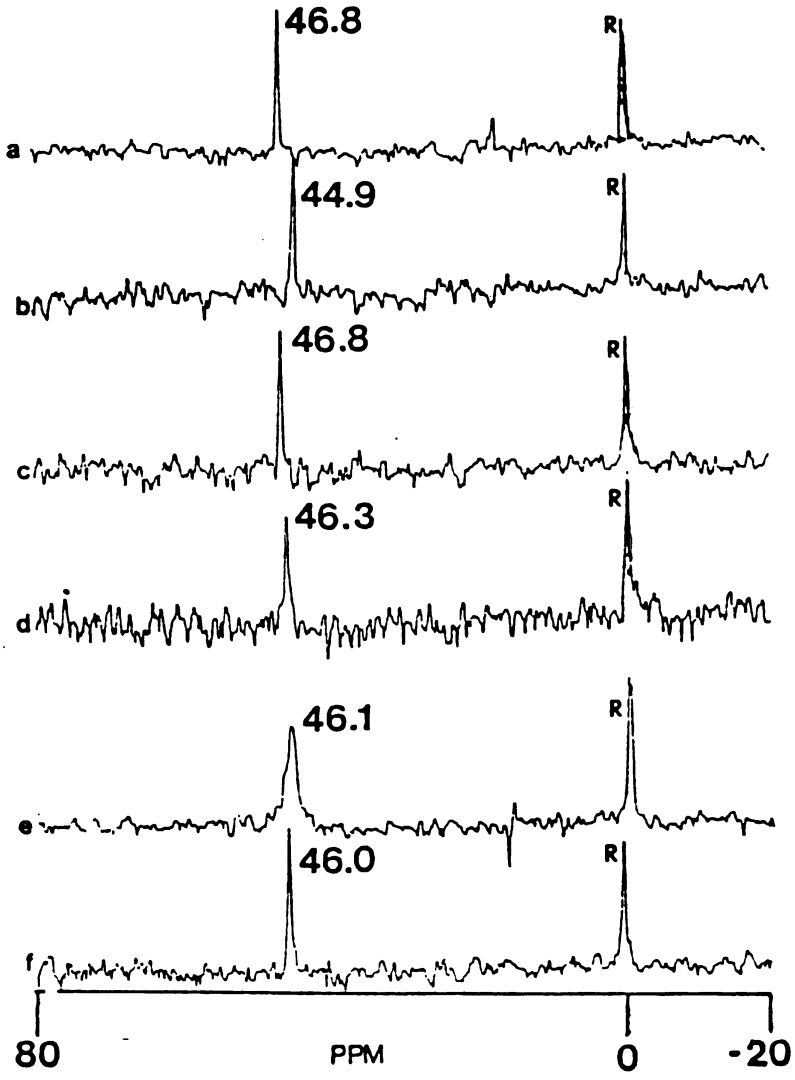
46.8
R
a
44.9
R
b
46.8
R
c
46.3
R
d
46.1
R
e
46.0
R
f
80
PPM
0
-20

upfield from the resonance obtained from a saturated CsCl solution, which indicates that this solution is less basic than the saturated solution (Figure 46). The ^{133}Cs band for a $CsBPh_4$ melt solution prepared from a 67 mole % $AlCl_3$ melt appears further upfield than any of the other melt solutions prepared with other cesium salts. The ^{133}Cs NMR measurements on the $CsBPh_4$ acidic melt solution indicate the BPh_4^- is less reactive toward $Al_2Cl_7^-$ then the other anions examined.

C. Anion Chemistry in Basic Melt

Two intense CN bands at 2075 and 2105 cm^{-1} are observed in the IR spectrum of the 0.99 mole % LiSCN prepared with a 45 mole % $AlCl_3$ BPC-$AlCl_3$ melt solutions (Figure 40). The same CN bands were observed in the IR spectrum obtained from a 0.95 mole % LiSCN prepared from a 45 mole % $AlCl_3$ 1-methyl-3-ethylimidazolium-$AlCl_3$ (MEIC-$AlCl_3$) melt solution (344). The IR spectrum of a 1.00 mole % LiSCN prepared from a 45 mole % $GaCl_3$ MEIC-$GaCl_3$ melt solution shows two intense CN bands at 2060 and 2070 cm^{-1} (344) (Figure 47). The 2070 cm^{-1} exists as a shoulder on the 2060 cm^{-1} band. These IR results indicate that the CN stretches are sensitive to the trichloride species ($AlCl_3$ or $GaCl_3$) used to prepare the melt. Therefore, the 2075 and 2105 cm^{-1} bands observed in the $AlCl_3$ melts result from SCN^- ions complexed to the aluminum(III) cation; SCN^- competes with chloride for coordination sites around the aluminum(III) cations. The position of the 2075 and 2105 cm^{-1} bands appear in the spectral regions attributed to complexes

Figure 46: Cesium-133 NMR spectra of CsCl solution in a 67 mole % $AlCl_3$ BPC-$AlCl_3$ melt at 45 °C. The R corresponds to the reference band (0.01 M CsBr 20% D_2O/H_2O solution). The chemical shifts have not been corrected for the magnetic susceptibility of the melt. The 0.66 mole % melt solution was not completely homogeneous.

a. 0.66 mole %

b. 0.25 mole %

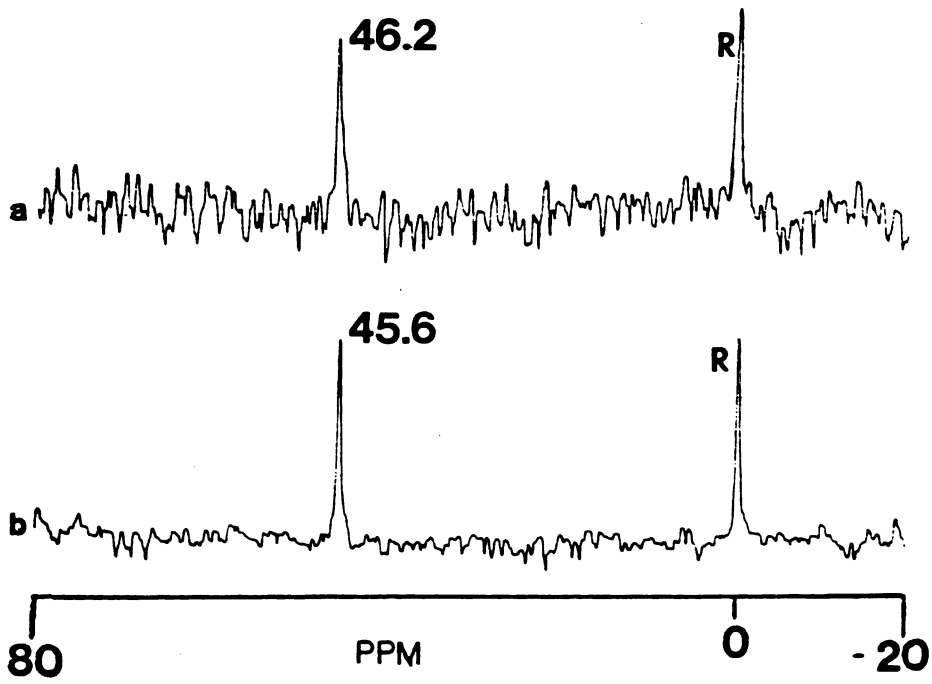
46.2
R
a
45.6
R
b
80
PPM
0
-20

Figure 47: Infrared absorption curve of 1.00 mole % LiSCN mixtures in a 45 mole % $GaCl_3$ MEIC-$GaCl_3$ melt.

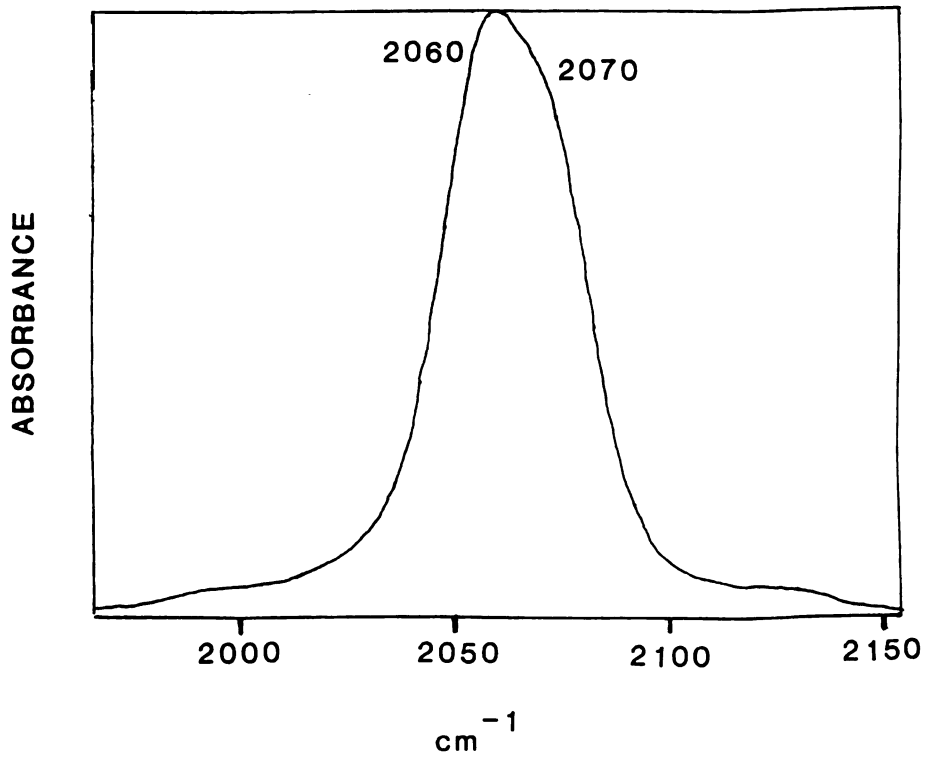
2060
2070
ABSORBANCE
2000
2050
2100
2150
cm⁻¹

where the metal cation interacts at the nitrogen and sulfur end of the SCN^- ion, respectively (325). Therefore, these bands may be assigned to the $AlCl_3NCS$ and $AlCl_3SCN$ complexes, respectively. Since the concentration of SCN^- is much lower than that of $AlCl_4^-$ (~1% of the total $AlCl_4^-$ concentration), aluminum(III) complexes containing more than one SCN^- ligand are not considered.

Vibrational studies were also carried out with other lithium salts ($LiNO_3$ and $LiClO_4$) whose anion vibrations were used to probe the interactions in the melt. The doubly degenerate $\nu_3(E')$ NO_3^- band is split, and only one band attributed to the triply degenerate $\nu_4(F_2)$ ClO_4^- band is observed in the IR spectra of $LiNO_3$ and $LiClO_4$ 45 mole % $AlCl_3$ melt solutions (Figure 48). In organic nonaqueous solvents, the C211 ligand forms complexes with the Li^+ and isolates the metal cation from any anion or solvent interactions. Lithium-7 NMR resonances obtained from melt solutions containing different lithium salts ($LiClO_4$, LiSCN, $LiNO_3$) and C211 did not show an anion dependence on the ^7Li chemical shift at 40 °C, which indicates that C211 has the same complexing behavior in basic melts as observed in organic solvents (Figure 49). The two chemical shifts listed in Figure 49 correspond to the measured chemical shift and the chemical shift corrected for the melt magnetic susceptibility. The chemical shift in the parentheses is the corrected chemical shift. The values in parentheses following the corrected chemical shifts is the error determined by error propagation methods. The bands identified by R correspond to the reference. The chemical shift of the complex,

Figure 48: Infrared absorption curves of different lithium salts in 45 mole % $AlCl_3$ BPC-$AlCl_3$ melt. Spectra were obtained at ambient temperature.

a. 1.04 mole % $LiClO_4$

b. 0.98 mole % $LiNO_3$

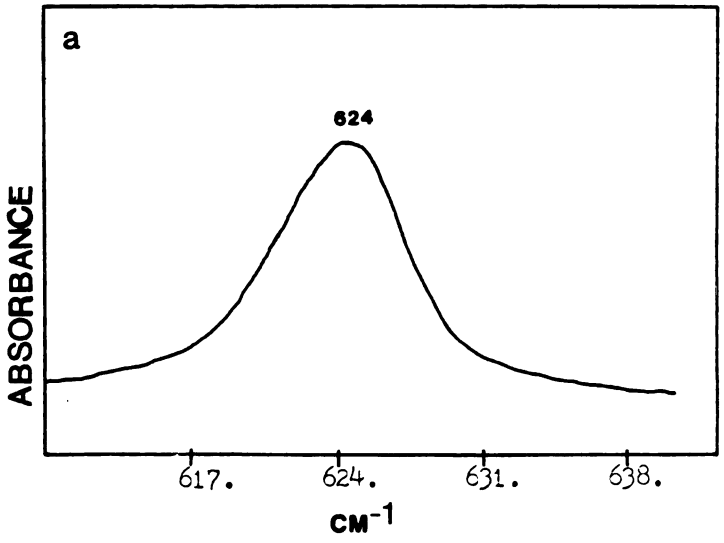
a
624
ABSORBANCE
617.
624.
631.
638.
CM-1

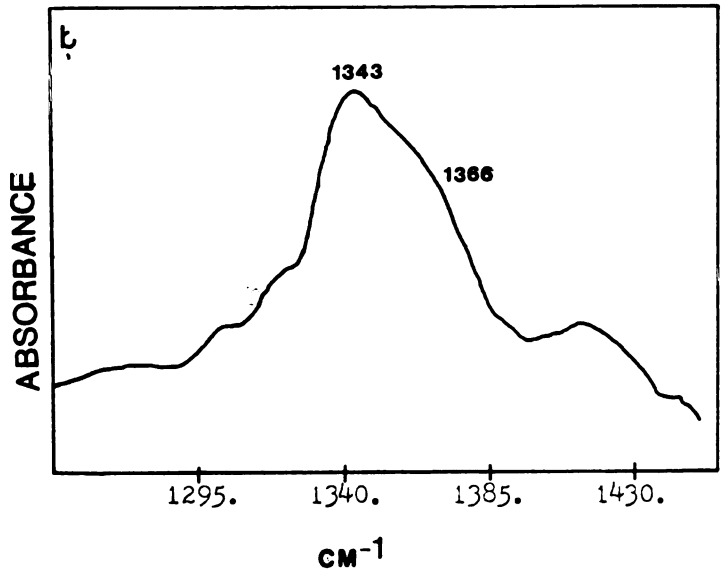
b
1343
1366
ABSORBANCE
1295.
1340.
1385.
1430.
CM-1

Figure 49: Lithium-7 NMR spectra of 45 mole % $AlCl_3$ BPC-$AlCl_3$ melts containing C211 and different lithium salts (MR = mole ratio) at 40 °C. The chemical shift in the parenthesis is the chemical shift of the C211 complex corrected for the magnetic susceptibility of the melt. The values in parentheses following the corrected chemical shifts is the error determined by error propagation methods.

a. 1.02 mole % $LiClO_4$, 1.67 mole % C211, MR = 1.6

b. 1.18 mole % LiSCN, 2.27 mole % C211, MR = 1.9

c. 1.07 mole % $LiNO_3$, 1.76 mole % C211, MR = 1.6

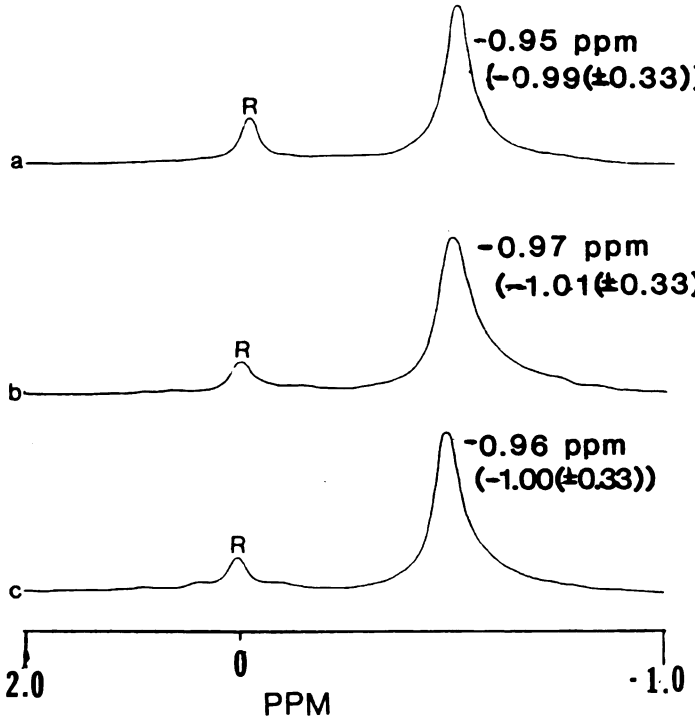
-0.95 ppm
(-0.99(±0.33))
R
a
-0.97 ppm
(-1.01(±0.33))
R
b
-0.96 ppm
(-1.00(±0.33))
R
c
2.0
0
-1.0
PPM

corrected for the magnetic susceptibility of the melt, is not equal to the corrected chemical shift for Li^+ C211 cryptate complexes measured in different organic solvents (-0.40(±0.03) ppm) (345). Therefore, the complexed Li^+ must not be totally shielded from interactions with Cl^- or $AlCl_4^-$ found in basic melt solutions. The vibrational bands of NO_3^- and ClO_4^- were unaffected by the addition of C211 to these melt solutions. The $\nu_3(E')$ NO_3^- bands were obscured by the presence of a C211 band at 1355 cm^{-1}. The IR spectrum of a 1.06 mole % $N(Bu)_4NO_3$ melt solution showed the same $\nu_3(E')$ bands as the IR spectrum obtained from a 0.99 mole % $LiNO_3$ melt solution. Also, the ^7Li chemical shift of the lithium salt solution in a 45 mole % $AlCl_3$ melt is concentration dependent but also independent of the anion of the salt added to the melt (337). These IR and NMR measurements suggest that only solvent anions, $AlCl_4^-$, and Cl^- coordinate to Li^+. Specifically the IR measurements show that NO_3^- like SCN^- competes with Cl^- for coordination sites on the aluminum(III) cation, while ClO_4^- does not. Since the splitting of the $\nu_3(E')$ NO_3^- bands is small for the $LiNO_3$ melt solution (Δ = 23 cm^{-1}), it suggests that the NO_3^- ligand complexes to an aluminum(III) cation through a single oxygen (327).

III. Complexation Studies in 45 mole % $AlCl_3$ Melt

A. Crown Ether Complexes in 45 mole % $AlCl_3$ Melt

For ^7Li NMR measurements, the concentration of 12C4, 15C5, 18C6, and B15C5 were varied keeping the alkali metal salt concentration constant to determine the formation constants of the respective crown

ether complexes with lithium chlorocomplexes in the 45 mole % $AlCl_3$ melt solution. Figure 50 shows the plots of ^7Li chemical shifts versus mole fraction at 40 °C obtained for these crown ether ligands. The error bars in Figure 50 correspond to ±2s, where s is the estimate of the error of the chemical shift measurements. The value for s is ±0.02 ppm. Previously, formation constants were reported but the monomer-dimer equilibrium was not accounted for (337). These measurements were refitted to the two site exchange model describing 1:1 complexation. The program calculated the formation constant and the ^7Li chemical shifts of the complexing species and the complex (Appendix 4-B). The log of the formation constants and the chemical shifts of the complexes are listed in Table 10, in columns two and three, respectively. The values in the parentheses are the standard deviations obtained from KINFIT linear least square program (299). The ^7Li chemical shift data obtained at different mole fractions were fit to a three site exchange model where the monomer-dimer equilibrium was accounted for. The fitting program calculated the $LiCl_2^-$ dimerization constant, the complexation constant, and the ^7Li chemical shifts of the monomer, dimer, and complex simultaneously (Appendix 4-B). Listed on the bottom of Table 10 are the log of the dimerization constants, and the chemical shifts corresponding to the monomer and dimer obtained from fitting this data to a three site exchange mechanism. The chemical shift measurements obtained at different LiCl concentrations were fitted simultaneously with the ^7Li chemical shift obtained from the mole ratio study.

Figure 50: Lithium-7 chemical shifts as a function of ligand/lithium ion mole ratio for the determination of formation constants of Li^+-crown complexes in 45 mole % $AlCl_3$ BPC-$AlCl_3$ melt at 45 °C. The error bars in this Figure correspond to ±2s, where s is the estimate of the error of the chemical shift measurements. The value for s is ±0.02 ppm. Solid lines are computer generated based on the formation of a 1:1 complex without consideration for the monomer-dimer equilibrium. Lithium-7 chemical shifts as a function of ligand/lithium ion mole ratio for the determination of formation constants of Li^+-crown complexes in 45 mole % $AlCl_3$ BPC-$AlCl_3$ melt at 45 °C -

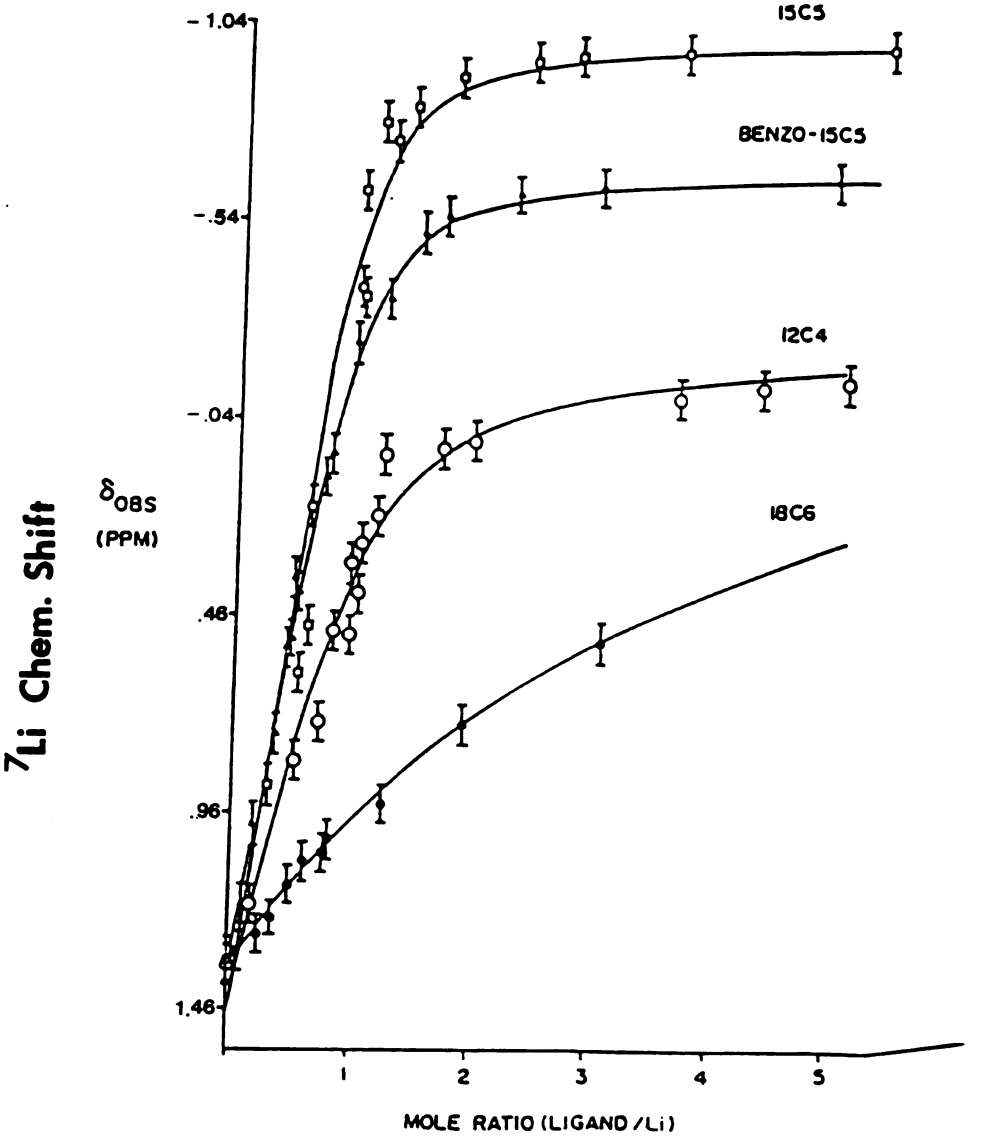
15C5
BENZO-15C5
12C4
18C6
-1.04
-.54
-.04
.46
.96
1.46
^{7}Li Chem. Shift
δ_{OBS}
(PPM)
1
2
3
4
5
MOLE RATIO (LIGAND/Li)

Table 10

Formation Constants for Crown Ethers Complexes in 45 mole % Melt and the Chemical Shifts of the Complexes at 40 °C

Ligand	log K_F	δc(PPM)	log K_F^{ca}	δc^c(PPM)	α
12C4	1.9(±0.1)	-0.20(±0.04)	2.5(±0.5)	-0.17(±0.03)	0.25
15C5	2.5(±0.2)	-1.00(±0.05)	3.9(±0.7)	-0.96(±0.02)	0.04
B15C5	2.4(±0.1)	-0.63(±0.03)	2.7(±0.2)	-0.63(±0.03)	0.50
18C6	0.6(±0.1)	-0.4(±0.2)	1.9(±0.4)	+0.15(±0.07)	0.05

[a] **12C4:** Log K_D = 2(±1), δ_M = 3(±1) ppm, δ_D = 1.1(±0.1) ppm
15C5: Log K_D = 4(±1), δ_M = 16(±22) ppm, δ_D = 1.15(±0.06) ppm
B15C5: Log K_D = 1.1(±0.6), δ_M = 1.7(±0.2) ppm, δ_D = 0.9(±0.2) ppm
18C6: Log K_D = 2.7(±0.7), δ_M = 4(±2) ppm, δ_D = 1.09(±0.03) ppm

$$2LiCl_2^- \leftrightarrow (LiCl_2^{2-})_2 \qquad (4\text{-}4)$$

$$LiCl_2^- + L \leftrightarrow LiCl_2^{2-} \cdot L \qquad (4\text{-}5)$$

Equation (4-5) describes the complexation of the crown ether ligand with the monomer. A poor fit was obtained when the dimer was taken as the complexing species; therefore, the complexing species is assumed to be the monomer. Table 10 also lists the formation constant and the chemical shift for the complex corrected for the monomer-dimer equilibrium; these are located in the fourth and fifth columns. Numerical values in parentheses are the standard deviations of the fits. These formation constants and chemical shifts are identified by the superscript c. The monomer-dimer correction causes the complex formation constants to increase. The values listed in the sixth column of Table 10 are the values for the fraction of LiCl existing as the monomer in the melt solution (346).

$$\alpha = \frac{[LiCl_2^-]}{C_T} = \frac{K_F}{K_F^C} \qquad (4\text{-}6)$$

The K_F and K_F^C terms correspond to the uncorrected and the corrected formation constants. The α values listed in Table 10 determined from the formation constant determined from fitting ^7Li chemical shifts are ± 0.40 from the calculated value ($\alpha = 0.10$). The calculated α value was determined from the concentration of LiCl in the melt and the monomer-dimer equilibrium constant.

One of the main factors affecting the stability of the crown ether

complexes is the relationship between the diameter of the cation and the size of the cavity. The predicted stability of the crown ether complexes depends on which ionic sizes are used, Pauling or electron density measurements (Table 11). Smetana and Popov (160) found for Li^+ in nonaqueous solvents, the electron density measurements provide a better size parameter than the Pauling values. The stability order of the Li^+ crown ether complexes, according to the electron density diameters, is: Li^+15C5 > Li^+12C4 > Li^+18C6. This behavior is observed in nonaqueous solvents (Table 12). The stability order of the crown ether complexes in 45 mole % $AlCl_3$ melt is: Li^+15C5 ≈ Li^+12C4 > Li^+18C6 (Table 10). The formation constant for the B15C5 complex in 45 mole % $AlCl_3$ melt was found to be larger than either the 12C4 or 18C6 complexes (Table 10). These comparisons were made using the formation constants obtained without the monomer-dimer correction. Correcting for the monomer-dimer equilibrium increases the error of the crown ether formation constants and does not allow for this distinction. Values are considered indistinguishable when their confident limits ($\bar{X}\pm 2s$) overlap.

Attachment of a benzene substituent to the 15C5 ring makes the crown ether less flexible, which reduces the formation constant of the crown ether complex. This is observed in $LiClO_4$ propylene carbonate solutions where the formation constant for B15C5 ($\log K_F = 3.77$) is less than that obtained for 15C5 ($\log K_F = 4.26$) at 25 °C. (347,348). The errors in the formation constants listed in Table 10 are too large to allow for this distinction in molten salt solutions.

Table 11

Ionic Diameters of Alkali Metal Cations and Ring Sizes of Some Crown Ethers

Cation	Cationic Diameters (Å) Pauling	Electron Density[a]	Crown Ether	Ring Size[b] (Å) Corey-Pauling-Koltun[b]	Fisher Hirschfelder Taylor[b]
Li^+	1.20	1.86	12C4	1.2	1.5
Na^+	1.90	2.34	15C5	1.7	2.2
K^+	2.66	2.89	18C6	2.6	3.2
Rb^+	2.96	3.28			
Cs^+	3.38	3.66			

[a] Reference 349

[b] Reference 350

Table 12

Log K_F and δ_c Values for Lithium Ion–Crown Complexes in 45 mole % $AlCl_3$ BPC–$AlCl_3$ Melts at 40 °C and in Various Nonaqueous Solvents at Ambient Temperatures

Ligand	Basic Melt		Pyridine[a]		Acetonitrile[a]		Acetone[a]	
	Log K_F	δ_c (PPM)	Log K_F	δ_c (PPM)	Log K_F	δ_c (PPM)	Log K_F	δ_c (PPM)
12C4	1.9	-0.20	0.70	-0.74	4.25	-1.04	1.62	-0.30
	±0.1	±0.04	±0.05	±0.26	±0.46	--	±0.03	--
15C5	2.5	-1.00	2.48	-1.15	>4	-1.79	3.59	-0.80
	±0.2	±0.05	±0.02	--	--	--	±0.08	--
B15C5	2.4	-0.63	--	--	--	--	--	--
	±0.1	±0.03	--	--	--	--	--	--
18C6	0.6	-0.4	0.62	-0.44	2.34	-1.32	1.50	-0.52
	±0.1	±0.2	±0.07	±0.30	±0.04	--	±0.02	--

Values with ± before them correspond to the standard deviation determined from the fit.

[a] Reference 160

The ^{7}Li chemical shifts give some information concerning the environment around the Li^{+} when complexed. In nonaqueous solutions, the chemical shifts of the Li^{+} complexed with a crown ether ligand are solvent-dependent (Table 12) (160). Complexes with Li^{+} still have coordination sites available for the solvent molecules, the anion, or both. Chemical shifts for the crown ether complexes in basic melt solutions can not be compared to the chemical shifts obtained for these complexes in other solvents, given in Table 12, because a different reference was used. However, the chemical shifts for the complexes in basic melt solutions parallel what was obtained in other solvents. For Li^{+} cryptates, the ligand encapsulates the cation in a cavity, and the cation is isolated from the solvent; the ^{7}Li chemical shift of the complex is solvent independent (345,351). In the 45 mole % $AlCl_3$ melt solution, the available coordination sites of the crown ether complex in the melt are occupied by either Cl^{-} or $AlCl_4^{-}$.

The ^{13}C chemical shifts of the crown ether carbons are sensitive to complexation. For 12C4 and 18C6, the ^{13}C NMR bands at 45 'C are shifted upfield when LiCl is added to the crown ether 45 mole % $AlCl_3$ melt solution. Figure 51 and 52 show the ^{13}C spectra of these solutions. Numerous bands exist in the ^{13}C spectra of the crown ether solution, and are attributed to the BP^{+}. The number by each band corresponds to the carbon as indicated by the illustrations in each Figure. The bands due to the crown are identified by an X, and the chemical shift is written by each band assigned to the crown ether. The bands identified by R correspond to the 8% $DMSO/D_2O$ reference.

Figure 51: Carbon-13 NMR spectra of 18C6 melt solutions (MR = mole ratio) prepared from 45 mole % $AlCl_3$ BPC-$AlCl_3$ at 45 °C. The chemical shift of the 18C6 band has not been corrected for the magnetic susceptibility of the melt.

a. 18C6, 1.00 mole % LiCl, MR = 2.96

b. 18C6, 2.66 mole % 18C6.

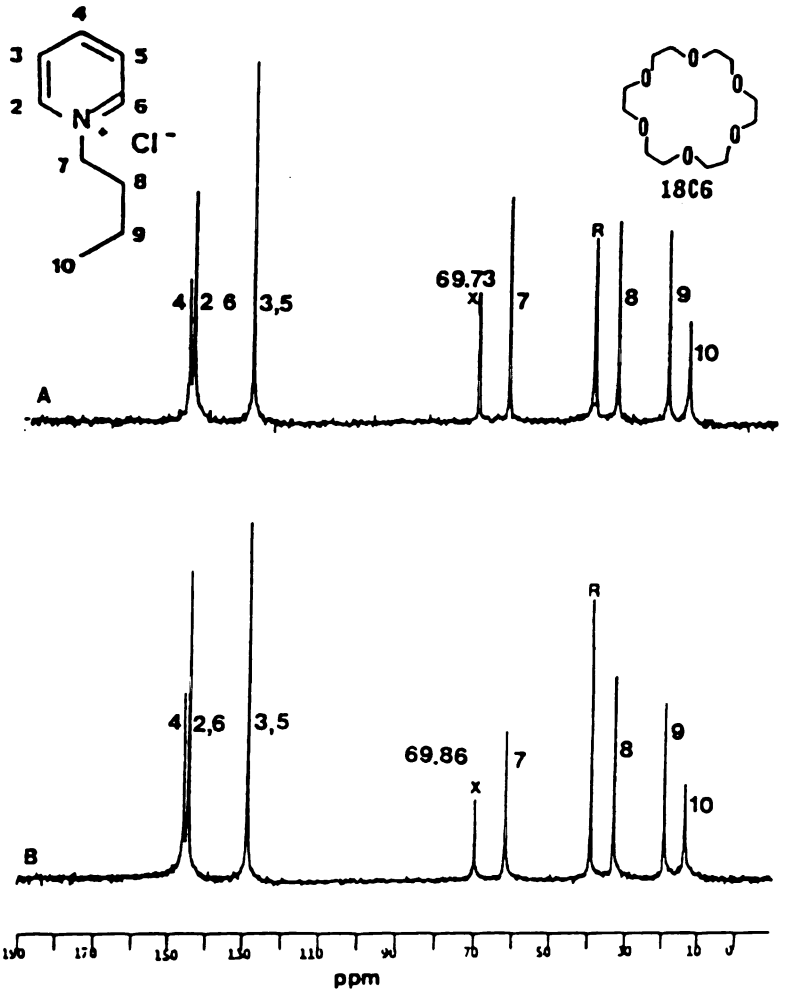
4
3
5
2
6
N
Cl⁻
7
8
9
10
18C6
4
2 6
3,5
69.73
X
7
R
8
9
10
A
4
2,6
3,5
69.86
X
7
R
8
9
10
B
ppm

Figure 52: Carbon-13 NMR spectra of 12C4 melt solutions (MR = mole ratio) prepared from 45 mole % $AlCl_3$ BPC-$AlCl_3$ at 45 °C. The chemical shift of the 12C4 band has not been corrected for the magnetic susceptibility of the melt.

a. 12C4, 1.00 mole % LiCl, MR = 3.53

b. 12C4, 3.35 mole % 12C4

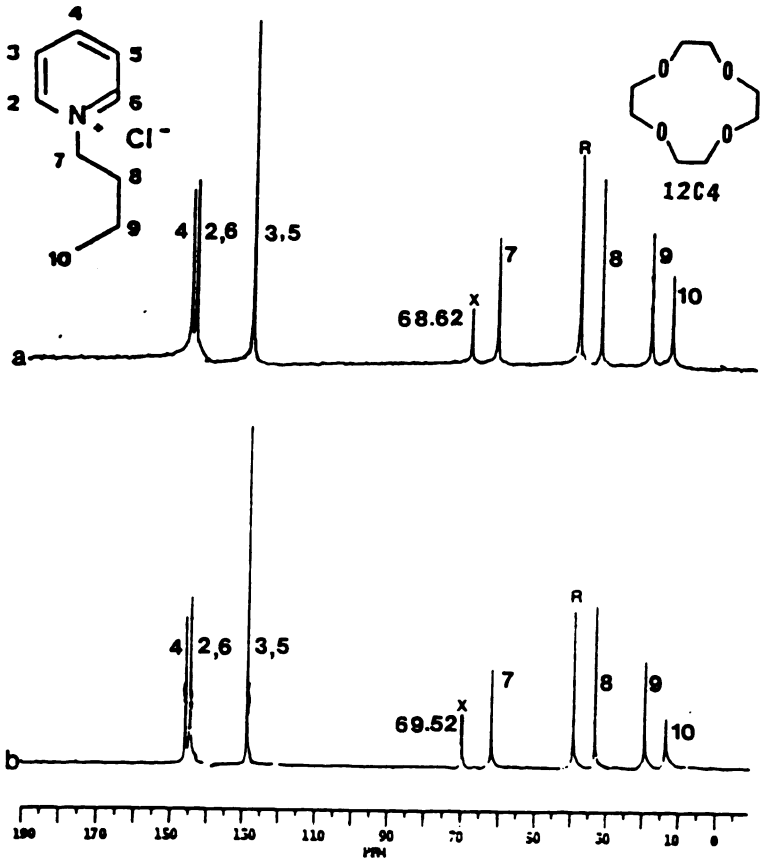
4
3
5
2
6
N
Cl⁻
7
8
9
10
12C4
4
2,6
3,5
68.62
X
7
R
8
9
10
a
4
2,6
3,5
69.52
X
7
R
8
9
10
b
190
170
150
130
110
90
70
50
30
10
0
PPM

Dale and coworkers (352,353) results on macrocyclic crown ethers containing only oxyethylene units, $(OCH_2CH_2)_n$, showed that the ^{13}C resonance shifts upfield on complexation attributed to conformational changes in the ligand that occur when the complex is formed. Upfield chemical shifts at 45 °C of the carbon adjacent to the ether oxygens were also observed for B15C5 when LiCl was added to the crown ether melt solution (Figures 53,54, Table 13). The precision of these ^{13}C measurements are ±0.06 ppm. The numbers by the ^{13}C resonance bands correspond to the carbons as indicated in the Figure. The ^{13}C NMR spectra of B15C5-LiCl melt solutions contain only three bands instead of four as observed for the uncomplexed ligand in the melt. The furthest downfield ether band consists of two overlapping bands due to C-3 and C-4. The differences in the chemical shifts of the aromatic carbons of the complexed and uncomplexed ligand reflect the changes in the electron density in the benzene carbon atoms of the ligand caused by complexation which may result from ligand conformational changes that occur on complexation. The chemical shift difference of the aromatic carbons are in the order C-5 › C-6 › C-7. The distance between the carbon 2p orbital and its nucleus is important for rationalizing ^{13}C chemical shifts (354). An increase in the electron density on a carbon atom expands the 2p orbital which decreases the paramagnetic screening constant. Therefore, adding electron density to a carbon atom should cause a upfield chemical shift. Neither induction or resonance effects could be used to explain the changes in the chemical shift of the aromatic carbons of B15C5 resulting from

Figure 53: Aromatic and aliphatic ether region of the ^{13}C spectrum of B15C5 melt solutions (MR = mole ratio) prepared from 45 mole % $AlCl_3$ BPC–$AlCl_3$ at 45 ^{o}C. The low intensity bands corresponding to B15C5 are identified by numbers.

a. B15C5, 1.00 mole %LiCl, MR = 1.19

b. B15C5, 0.90 mole % B15C5

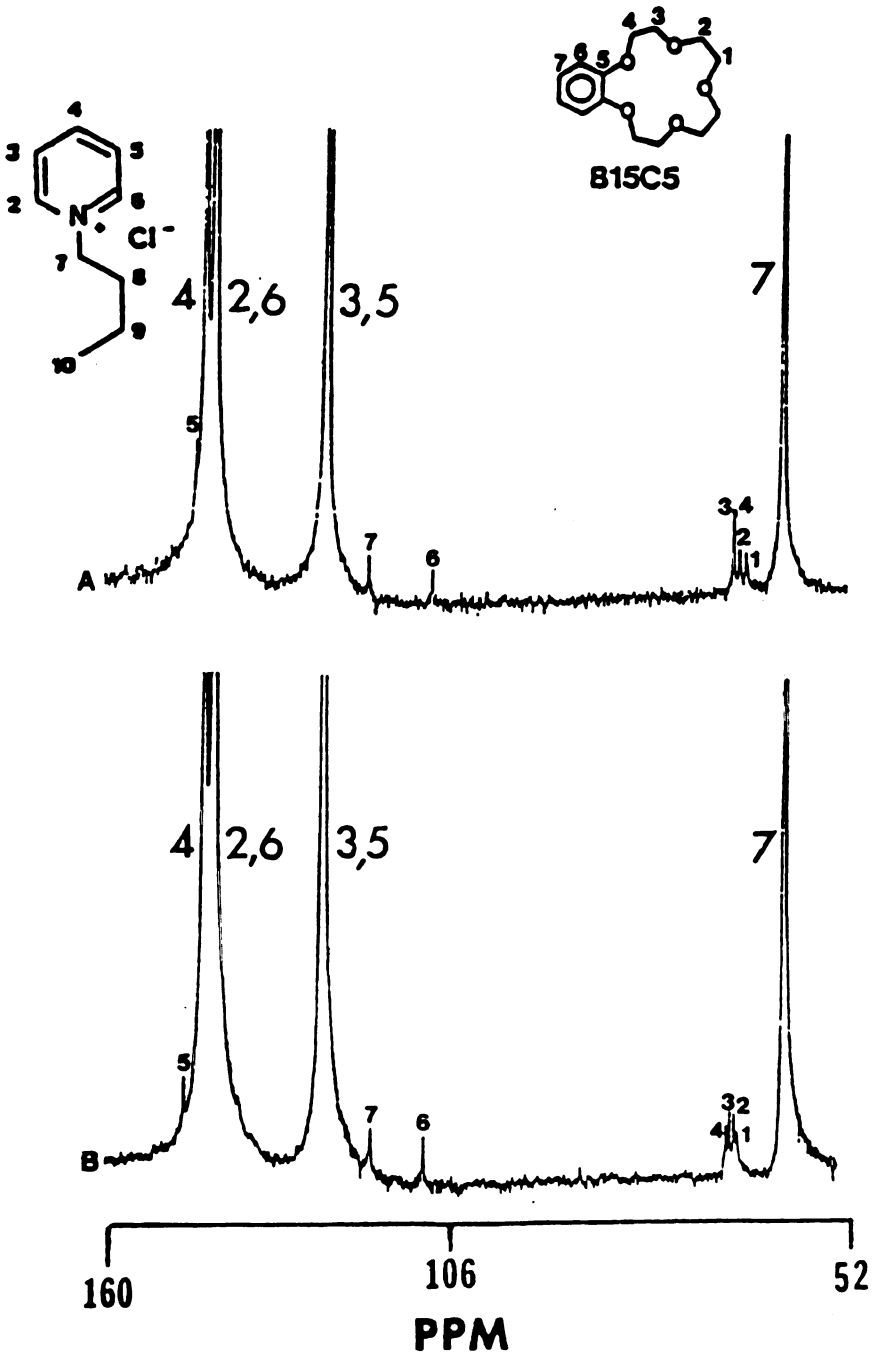
B15C5
Cl⁻
4
2,6
3,5
7
5
3,4
2
1
6
A
B
160
106
52
PPM

Figure 54: Aliphatic ether region of the ^{13}C spectrum of B15C5 melt solutions (MR = mole ratio) prepared from 45 mole % $AlCl_3$ BPC–$AlCl_3$ at 45 ^{o}C. The low intensity bands corresponding to B15C5 are identified by numbers.

a. B15C5, 1.00 mole %LiCl, MR = 1.19

b. B15C5, 0.90 mole % B15C5

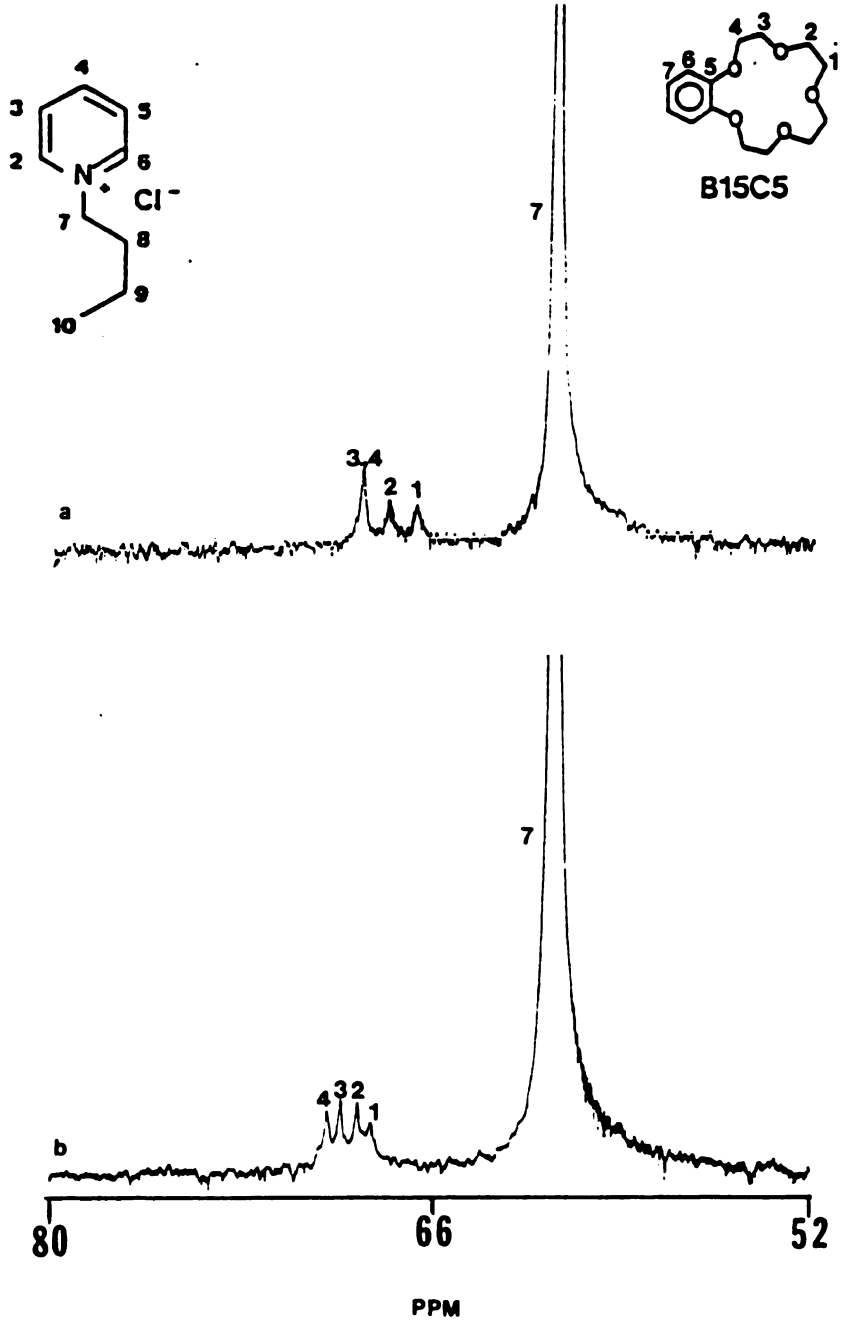
4
3
5
2
6
N
Cl⁻
7
8
9
10
4 3 2
7 6 5
1
B15C5
7
3 4
2
1
a
7
4 3 2
1
b
80
66
52
PPM

Table 13

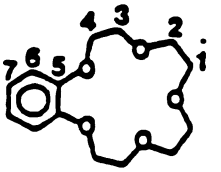

B15C5

Carbon-13 Chemical Shifts (PPM) of B15C5

in 45 mole % $AlCl_3$ BPC-$AlCl_3$ Melt at 45 °C

Sample	C-1	C-2	C-3	C-4	C-5	C-6	C-7
0.90 mole % B15C5	68.34	68.83	69.45	69.98	148.31	113.88	121.53
1.19 mole % B15C5-1.0 mole % LiCl	66.86	67.84	68.75	68.75	146.74	112.69	122.01
Difference	+1.48	+0.99	+0.70	+1.23	+1.57	+1.19	-0.48

Carbon-13 chemical shifts obtained from melt solutions have not been corrected for the magnetic susceptibility of the melt.

+ Difference = Addition of LiCl to the melt solution shifts the ^{13}C resonance upfield.

- Difference = Addition of LiCl to the melt solution shifts the ^{13}C resonance downfield.

complexation (355,356). Other effects such as magnetic anisotropy and electric field may also contribute to the observed chemical shift changes of the aromatic carbons. The magnetic anisotropy effect depends on the geometric relationship of the nucleus with respect to the magnetic anisotropic group (354). Since the complexed species is charged, electric field effects may also be important (354). The aromatic carbons of the benzene ring of B15C5 are not far enough from the C-O bond so that only one of these effects are predominant. For monosubstituted benzenes, the effect of substitution on the para carbon is explained by resonance effects (355,356). Due to its distance from the C-X bond other effects are absent.

In section I of this chapter, it was reported that ^{23}Na and ^{133}Cs resonances at 45 °C were not observed in basic or neutral melts. Addition of 15C5 to a series of NaCl melt mixtures prepared from 45 to 50 mole % $AlCl_3$ melts did not produce a ^{23}Na NMR signal at 45 °C from the melt solution. For CsCl melt mixtures over the same composition range, addition of either 18C6 or 21C7 produced a ^{133}Cs band in the spectrum. Figure 55 shows ^{133}Cs spectra obtained at 45 °C from the CsCl crown ether mixture in a 45 mole % $AlCl_3$ melt. Polyether 18C6 was also added to other 45 mole % mixtures containing different cesium salts. The appearance of a ^{133}Cs NMR resonance at 45 °C attributed to a Cs^+ complexed by 18C6 complex did not appear in every NMR spectrum obtained (Figures 56,57). The band identified as R in Figures 55-57 corresponds to the reference. The complexation chemistry is very slow. After three weeks of conditioning, the ^{133}Cs chemical shift had

Figure 55: Cesium-133 NMR spectra of crown ether complexes with cesium cations in 45 mole % $AlCl_3$ BPC-$AlCl_3$ melt at 45 °C (MR = mole ratio). The chemical shifts have not been corrected for the magnetic susceptibility of the melt. The R corresponds to the reference band (0.01 M CsBr 20% D_2O/H_2O solution). These NMR spectra were obtained on samples that were conditioned for three weeks.

a. 21C7, C(Cs) = 1.38 mole %, MR = 2.59

b. 18C6, C(Cs) = 1.49 mole %, MR = 1.83

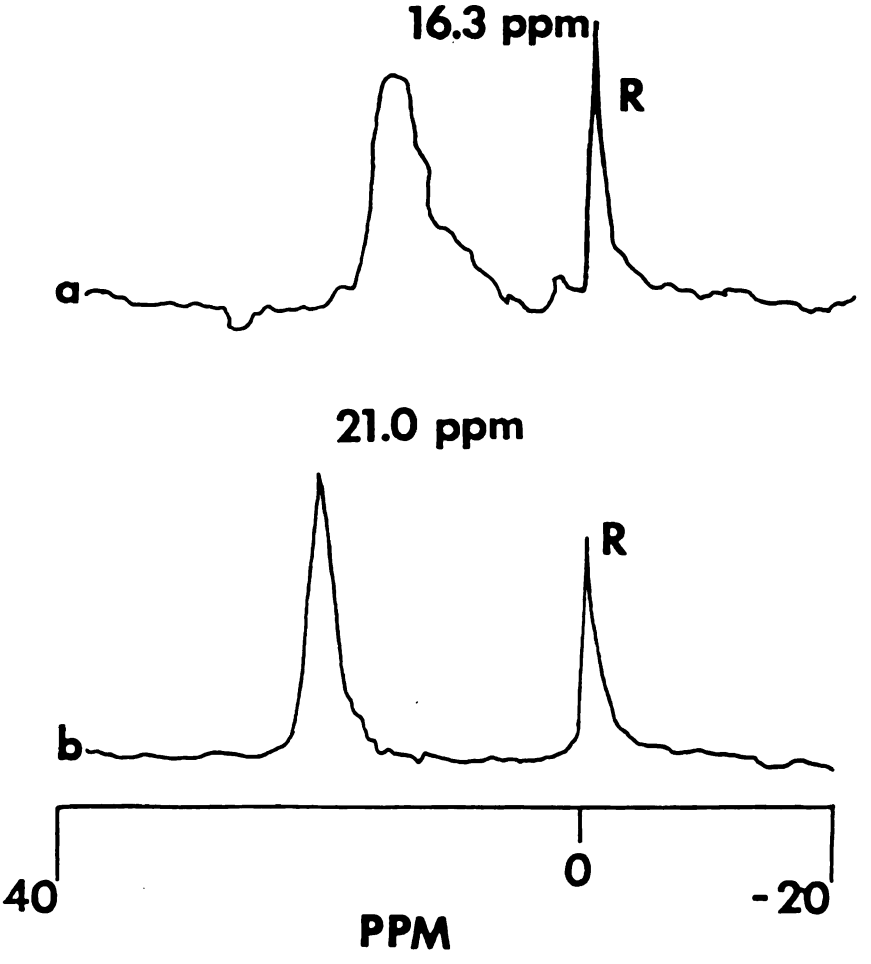
16.3 ppm
R
a
21.0 ppm
R
b
40
0
-20
PPM

Figure 56: Cesium-133 NMR spectra of several cesium salts in 67 mole % $AlCl_3$ BPC-$AlCl_3$ melt containing 18C6 (MR = mole ratio) at 45 °C. All samples were inhomogeneous. The R corresponds to the reference band (0.01 M CsBr 20% D_2O/H_2O solution). The chemical shifts have not been corrected for the magnetic susceptibility of the melt.

a. 0.81 mole % CsSCN, MR = 1.73

b. 0.56 mole % $CsBPh_4$, MR = 1.71

c. 0.78 mole % CsF, MR = 0.96

d. 1.48 mole % CsCl, MR = 0.98

e. 1.72 mole % CsBr, MR = 0.69

f 0.84 mole % CsI, MR = 1.10

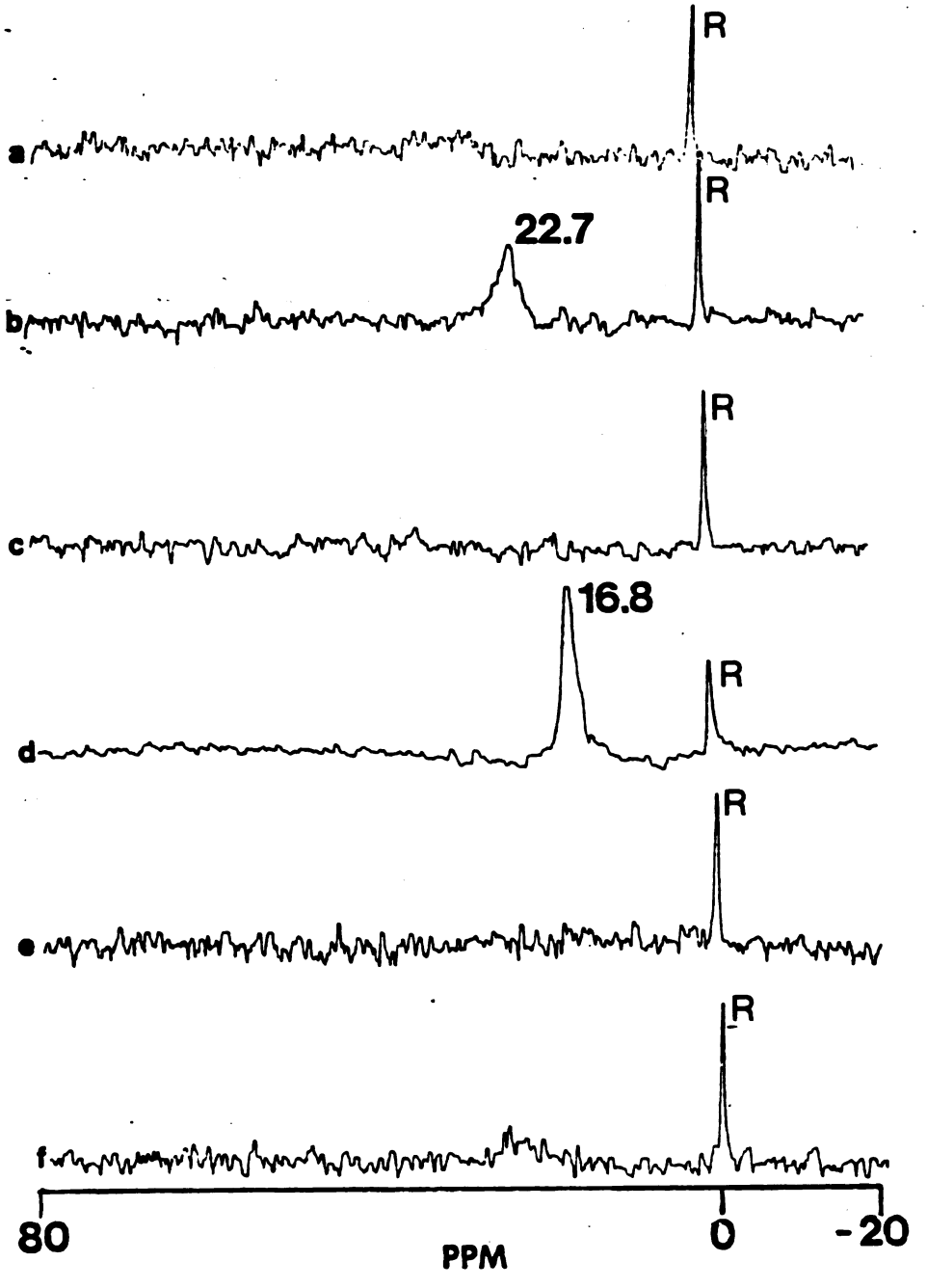
R
a
R
22.7
b
R
c
16.8
R
d
R
e
R
f
80
PPM
0
-20

Figure 57: Cesium-133 NMR spectra of cesium oxyanion salts in 67 mole % $AlCl_3$ BPC-$AlCl_3$ melt containing 18C6 (MR = mole ratio) at 45 ^{o}C. All mixtures were inhomogeneous. The R corresponds to the reference band (0.01 M CsBr 20% D_2O/H_2O solution). The chemical shifts have not been corrected for the magnetic susceptibility of the melt.

a. 0.83 mole % CsPi, MR = 1.36

b. 0.87 mole % $CsNO_3$, MR = 1.34

c. 0.94 mole % Cs_2CO_3, MR = 0.89

d. 0.83 mole % $CsClO_4$, MR = 1.09

e. 1.02 mole % CsAc, MR = 1.03

f. 1.11 mole % Cs_2SO_4, MR = 0.88

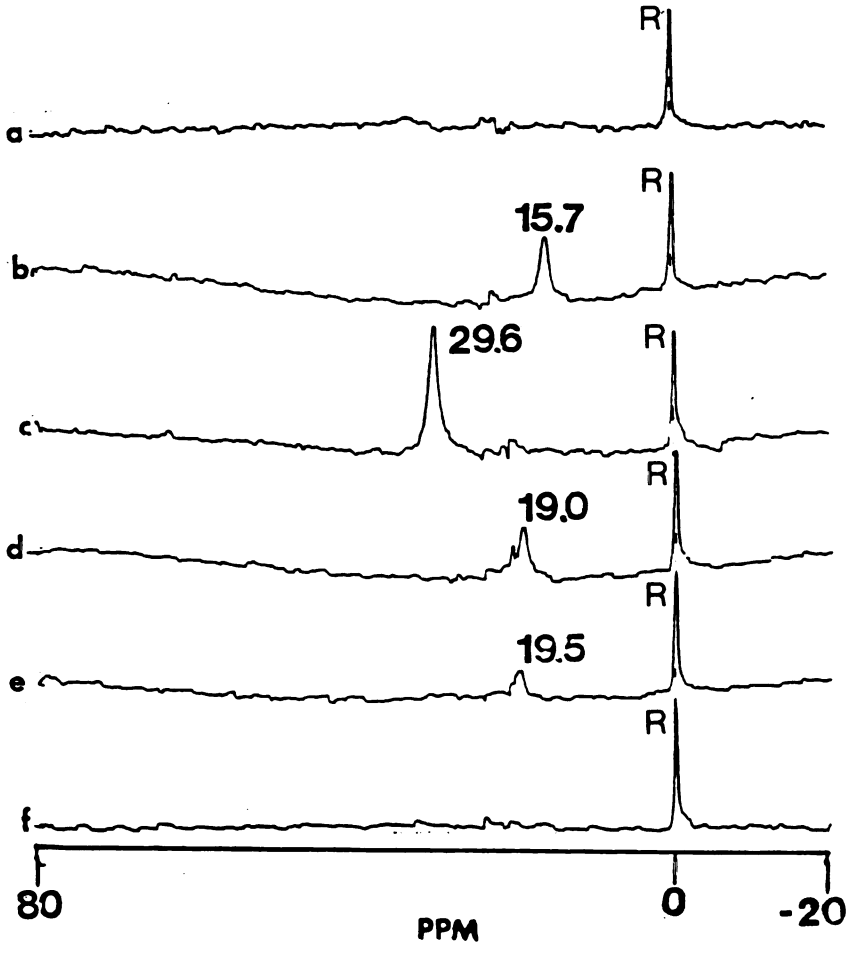
R
a
R
15.7
b
29.6
R
c
R
19.0
d
R
19.5
e
R
f
80
0
-20
PPM

not reached a stable value. This behavior is very similar to the that described by Pedersen (357) where $KMnO_4$ was made soluble in benzene by the addition of dicyclohexano-18C6.

B. Glyme Complexes in 45 mole % $AlCl_3$ Melt

The formation constants of several linear ethers with lithium chloroanionic complexes in 45 mole % $AlCl_3$ were obtained from a mole ratio study at 40 °C using ^7Li NMR (Figures 58-60). As a means of comparing results, similar measurements were carried out with the same glyme ligands in 2-butanone solutions at ambient temperature (Figure 61). The error of the ^7Li chemical shift measurements in these experiments was found to be ±0.02 ppm and ±0.01 ppm for melts and 2-butanone solutions, respectively. No error bars are included in these figures because they are too small to be observable. To obtain accurate measurements of formation constants in 45 mole % $AlCl_3$ melt, samples were prepared at mole ratios >20. The LiCl concentration for the triglyme (C(LiCl) = 0.69 mole %) study was larger than the LiCl concentration used for the pentaglyme (C(LiCl) = 0.20 mole %) and tetraglyme (C(LiCl)=0.19 mole %) studies. A melt solution of tetraglyme, containing 0.69 mole % LiCl and at mole ratios of greater than 17, turned cloudy. The mole ratio plots are shown in Figures 59-61. The curve does not begin to level off until the mole ratios exceed 10, which indicates that these complexes are weaker than those obtained with crown ether ligands. The ^7Li chemical shifts were fitted to a two-site exchange model to obtain conditional formation

Figure 58: Lithium-7 NMR chemical shifts for various ligand concentrations for the complexation of pentaglyme in 45 mole % $AlCl_3$ BPC-$AlCl_3$ at 40 °C. (C_{LiCl} = 0.20 mole %)

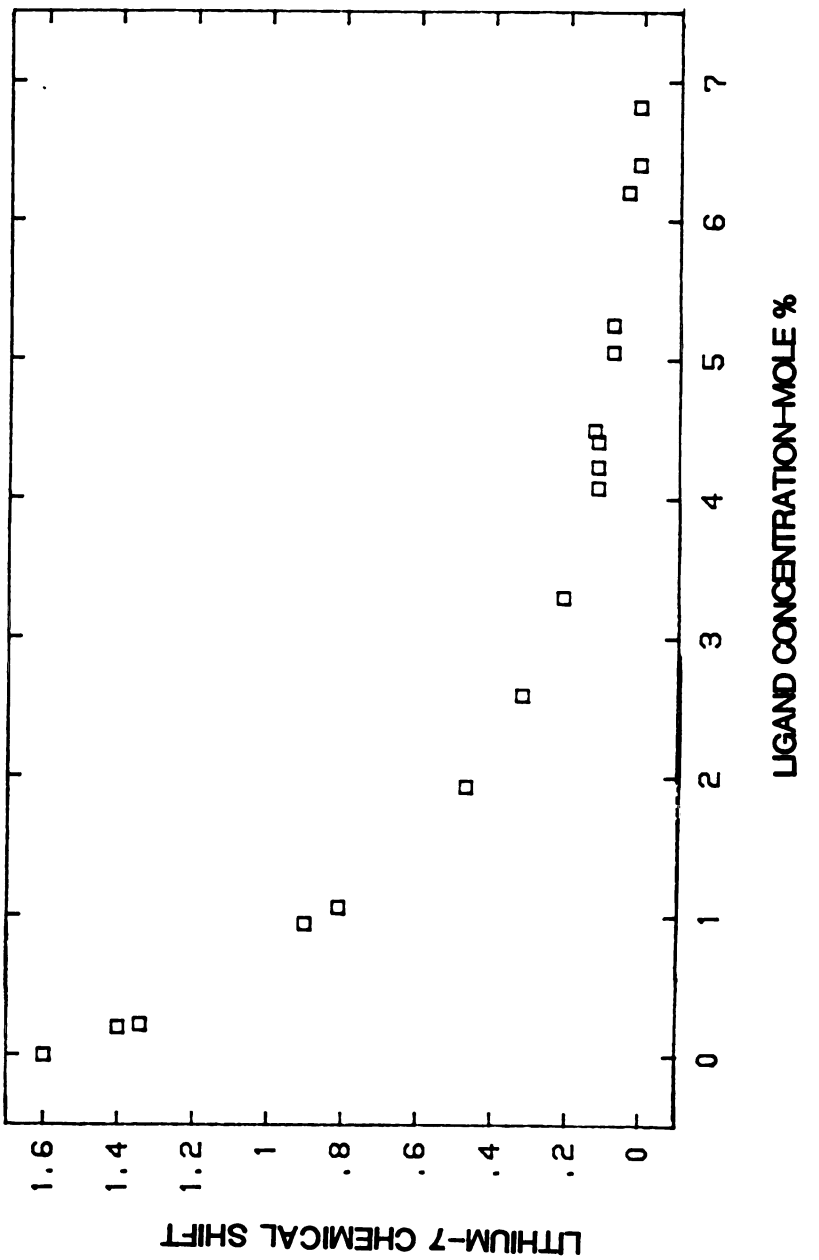
LITHIUM-7 CHEMICAL SHIFT
1.6
1.4
1.2
1
.8
.6
.4
.2
0
0
1
2
3
4
5
6
7
LIGAND CONCENTRATION-MOLE %

Figure 59: Lithium-7 NMR chemical shifts for various ligand concentrations for the complexation of tetraglyme in 45 mole % $AlCl_3$ BPC-$AlCl_3$ at 40 °C. (C_{LiCl} = 0.19 mole %)

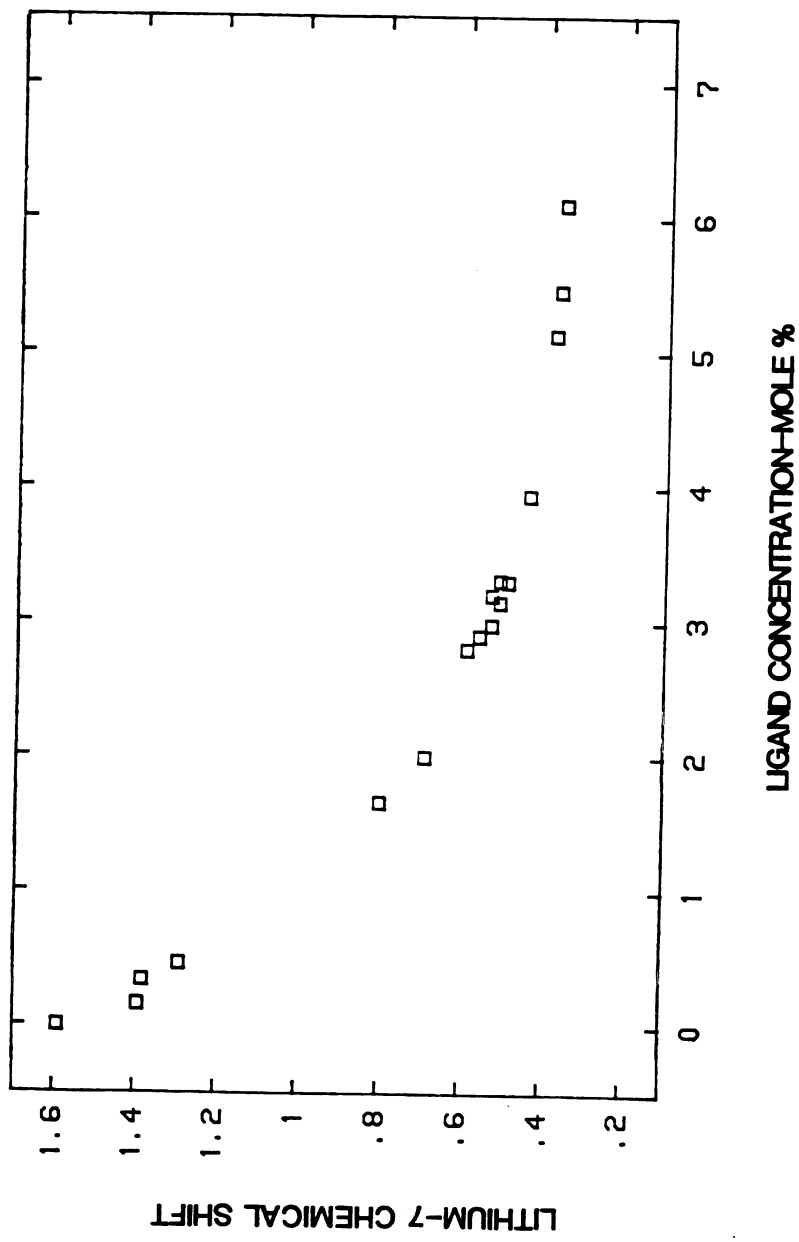
LITHIUM-7 CHEMICAL SHIFT
1.6
1.4
1.2
1
.8
.6
.4
.2
0
1
2
3
4
5
6
7
LIGAND CONCENTRATION-MOLE %

Figure 60: Lithium-7 NMR chemical shifts for various ligand concentrations for the complexation of triglyme in 45 mole % $AlCl_3$ BPC-$AlCl_3$ at 40 °C. (C_{LiCl} = 0.69 mole %)

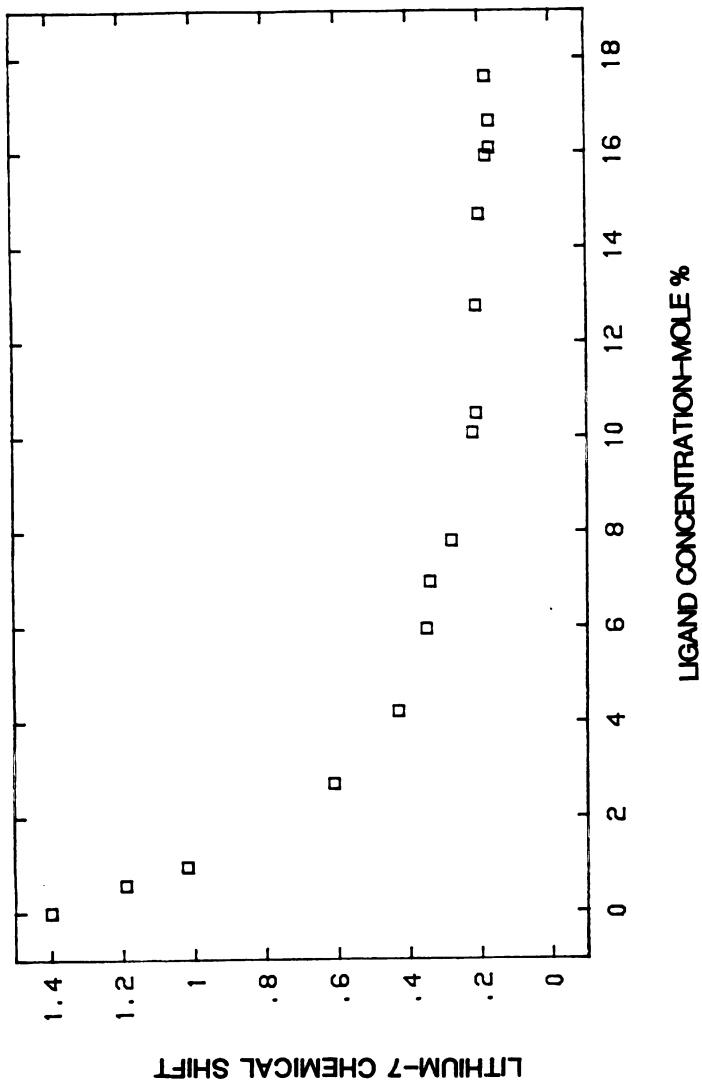
LITHIUM-7 CHEMICAL SHIFT
1.4
1.2
1
.8
.6
.4
.2
0
0
2
4
6
8
10
12
14
16
18
LIGAND CONCENTRATION-MOLE %

Figure 61: Lithium-7 chemical shifts for various ligand concentrations of three glymes in 2-butanone. (C_{LiBPh_4} = 0.01 M) Spectra were obtained at ambient temperature.

a. Triglyme (□)

b. Tetraglyme (○)

c. Pentaglyme (▷)

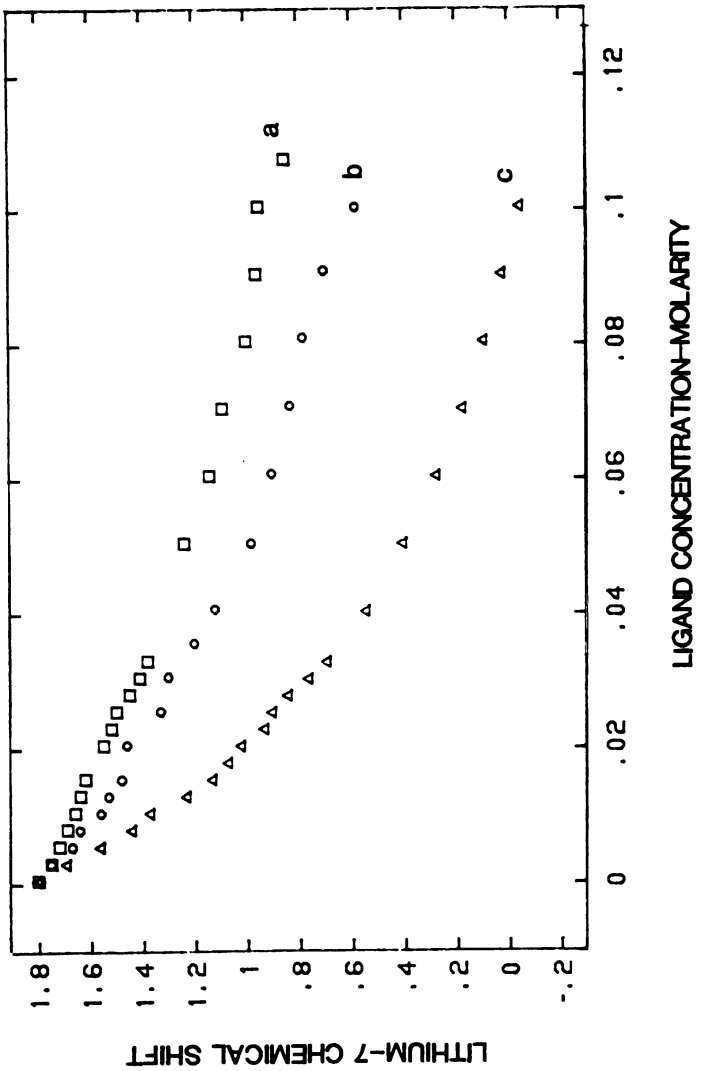
LITHIUM-7 CHEMICAL SHIFT
1.8
1.6
1.4
1.2
1
.8
.6
.4
.2
0
-.2
0
.02
.04
.06
.08
.1
.12
LIGAND CONCENTRATION-MOLARITY
a
b
c

constants. This assumes that the uncomplexed Li^+ exists in a single environment. These chemical shifts were also fitted to a three site exchange where the monomer-dimer equilibrium is accounted for. The fitting programs have been prevously described in Section III-A of this chapter. The complexing species was taken as $LiCl_2^-$. The same fitting programs used to fit the chemical shifts obtained from mole ratio studies with crown ethers were utilized (Appendix 4-B). The formation constants obtained by the three site exchange model represent a better measure of the stability of these ligands, since the monomer-dimer equilibrium is large (K_D = 630 $\underline{M}^{-1}$). In 2-butanone, $LiBPh_4$, which has a very small contact ion pairing constant (K_a = 2.6 $\underline{M}^{-1}$), was used; therefore, contact ion pairing does not significantly affect the formation constants obtained from the two site exchange model for complexation. Listed in Tables 14 and 15 are the formation constants and chemical shifts for the complexes obtained in 2-butanone and the 45 mole % $AlCl_3$ melt, respectively. Column four in Table 15 lists the corrected formation constants where the dimerization of LiCl is accounted for. The log of the dimerization constant and the chemical shifts corresponding to the monomer and dimer, which was also calculated by the fitting program are listed below Table 15. In Table 15, the seventh column lists the α values obtained from formation constants of complexation. The values give the fraction of LiCl existing as the monomer (346). The calculated α values are 0.21, 0.20, and 0.11 determined at 0.19, 0.20, and 0.69 mole % LiCl for tetraglyme, pentaglyme, and triglyme, respectively. The LiCl

Table 14

Formation Constants Obtained for Noncyclic Ligands at Ambient Temperature in 2-Butanone and for Crown Ethers in Acetone and also the Chemical Shifts of the Complexes

Ligands	$K_F(\underline{M}^{-1})$	δ_c (PPM)	$K_F^a(\underline{M}^{-1})$	Degree of Destability[b]
Triglyme	8(±1)	-0.3(±0.2)	42(±3)	0.19
Tetraglyme	10(±1)	-0.7(±0.2)	3890(±717)	0.0026
Pentaglyme	26(±1)	-0.82(±0.04)	32(±2)	0.81

[a] Formation constant for the cyclic analog in acetone.

[b] Ratio of formation constants for the glymes and the crown ethers.

Numerical values in the parentheses correspond to the standard deviations obtained from the fits.

Table 15

Formation Constants and Chemical Shifts
for Noncyclic Complexes in 45 mole % $AlCl_3$ BPC-$AlCl_3$ Melt at 40 °C

Ligands	$K_F(\underline{M}^{-1})$	δ_c (PPM)	$K_F^c(\underline{M}^{-1})^b$	δ_c^c (PPM)	Degree of Destabilization[a]	α
Triglyme	7.9(±0.6)	0.04(±0.02)	38(±6)	0.110(±0.005)	8.32	0.20
Tetraglyme	9.2(±0.9)	0.04(±0.04)	36(±12)	0.17(±0.02)	220.65	0.25
Pentaglyme	9.7(±0.7)	-0.34(±0.03)	45(±3)	-0.161(±0.008)	1.77	0.22

[a] Ratio of the formation constant of the crown ether ligand and the formation constant of the glyme ligand. The K's corrected for the monomer-dimer equilibrium were used.

Numerical values in the parentheses correspond to the standard deviations obtained from the fit.

[b] Triglyme: Log K_D = 2.4(±0.2), δ_M = 2.8(±0.3) ppm, δ_D = 1.08(±0.02) ppm
Tetraglyme: Log K_D = 2.5(±0.4), δ_M = 2.9(±0.6) ppm, δ_D = 1.14(±0.02) ppm
Pentaglyme: Log K_D = 2.71(±0.05), δ_M = 3.3(±0.1) ppm, δ_D = 1.12(±0.01) ppm

concentration and the monomer-dimer equilibrium constant were used in this calculation. The superscript c corresponds to the value obtained from the three site exchange model. The second to the last column in Table 14 lists the formation constants for the cyclic analogs in acetone.

Complexes obtained for the noncyclic ligands were weaker than those for the crown ether ligands in 2-butanone. The formation constants of 12C4, 15C5, and 18C6 have not been determined in 2-butanone, so the formation constants determined in acetone were used (160). For 15C5, the formation constant is >2 orders of magnitude larger than that obtained for tetraglyme (Table 14). For 12C4 and 18C6, the formation constants are within an order of magnitude of those determined for triglyme and pentaglyme. In 2-butanone solutions, the formation constant for the pentaglyme complex is measured accurately enough to distinguish its complexing ability from triglyme and tetraglyme. When comparisons are made between formation constants, they are considered distinguishable when their confident limits ($\bar{X}\pm 2s$) do not overlap. The stability of the glyme complexes with Li^+ in 2-butanone increases as the size of the ligand chain increases. A large increase in the formation constant occurs between the tetraglyme and pentaglyme. The increase in the formation constants in 2-butanone can be understood statistically by determining the number of different complexes that can occur with the ligand when oxygen atoms are coordinated to the Li^+ (358).

The corrected formation constants of the triglyme and pentaglyme ligands in the 45 mole % $AlCl_3$ are within an order of magnitude of the corrected formation constants obtained for 12C4 and 15C5 (Table 10,15). The corrected formation constant for the 15C5 complex is ~2 orders of magnitude greater the tetraglyme complex. The corrected formation constants could not be determined accurately enough by NMR to distinguish any difference in their complexing ability. The formation constants obtained without the monomer-dimer correction are not distinguishable either. The statistical criterion for determining whether values are indistinguishable has been presented in the previous paragraph. The corrected formation constants were obtained by simultaneously fitting the ^7Li chemical shifts obtained from mole ratio studies and LiCl concentration studies (Appendix 4-B). The relative errors in the formation constants increase for triglyme and tetraglyme and decreased for pentaglyme when utilizing this program.

C. Lariat Ethers Complexes in 45 mole % $AlCl_3$ Melt

The two lariats ethers ligands choosen for this study both contained a monoazo 15C5 ring with an ether side chain. The difference between the two ligands studied is that the ether side chains are of different lengths. Echegoyen and coworkers (359) have proposed that the complexation of lariat ethers involves two steps: (1) interaction with the side chain, (2) and an intermolecular reaction where the metal cation is embedded in the ring. The kinetic rate constants of complexation were obtained from ultrasonic

relaxation measurements; the kinetics of these processes are too fast to be obtained from NMR measurements.

The ^{7}Li chemical shift measurements obtained at 40 °C in 45 mole % $AlCl_3$ melt at different ligand concentrations indicates the formation of two different complexes with these ligands (Figures 62,63). The ^{7}Li chemical shift measurements from 45 mole % melt solutions were fitted to a mechanism which describes the formation of a 1:1 and a 2:1 complex.

$$LiCl_2^- + RN15C5 \rightleftharpoons LiCl_2^-RN15C5 + RN15C5 \rightleftharpoons LiCl_2^-(RN15C5)_2 \qquad (4\text{-}7)$$

The $LiCl_2^-RN15C5$ and $LiCl_2^-(RN15C5)_2$ complexes correspond to the 1:1 and 2:1 complexes, respectively. Addition of a second lariat ligand to the 1:1 complex gives the 2:1 complex. The second break in the chemical shifts versus ligand concentration plots occurs around 2:1 (Figures 62,63). In 45 mole % melt solutions, $LiCl_2^-$ forms dimers and it has been previously shown that $LiCl_2^-$ not $Li_2Cl_4^{2-}$ is the most favorable complexing species. The fitting program fitted simultaneously the chemical shift measurements obtained from the mole ratio and LiCl concentration study. The program determined seven unknowns; the dimerization and complexation constants and the chemical shifts of the complexes, the monomer, and the dimer (Appendix 4-B). Table 16 lists the formation constants for the methoxyethoxyethylmonoazo 15C5 and methoxyethylmonoazo 15C5 complexes with $LiCl_2^-$. The first K represents the formation constant for the

Figure 62: Lithium-7 NMR chemical shifts for various ligand concentrations for the complexation of methoxyethoxyethylmonoazo 15C5 in 45 mole % $AlCl_3$ BPC-$AlCl_3$ at 40 °C. (C_{LiCl} = 0.70 mole %)

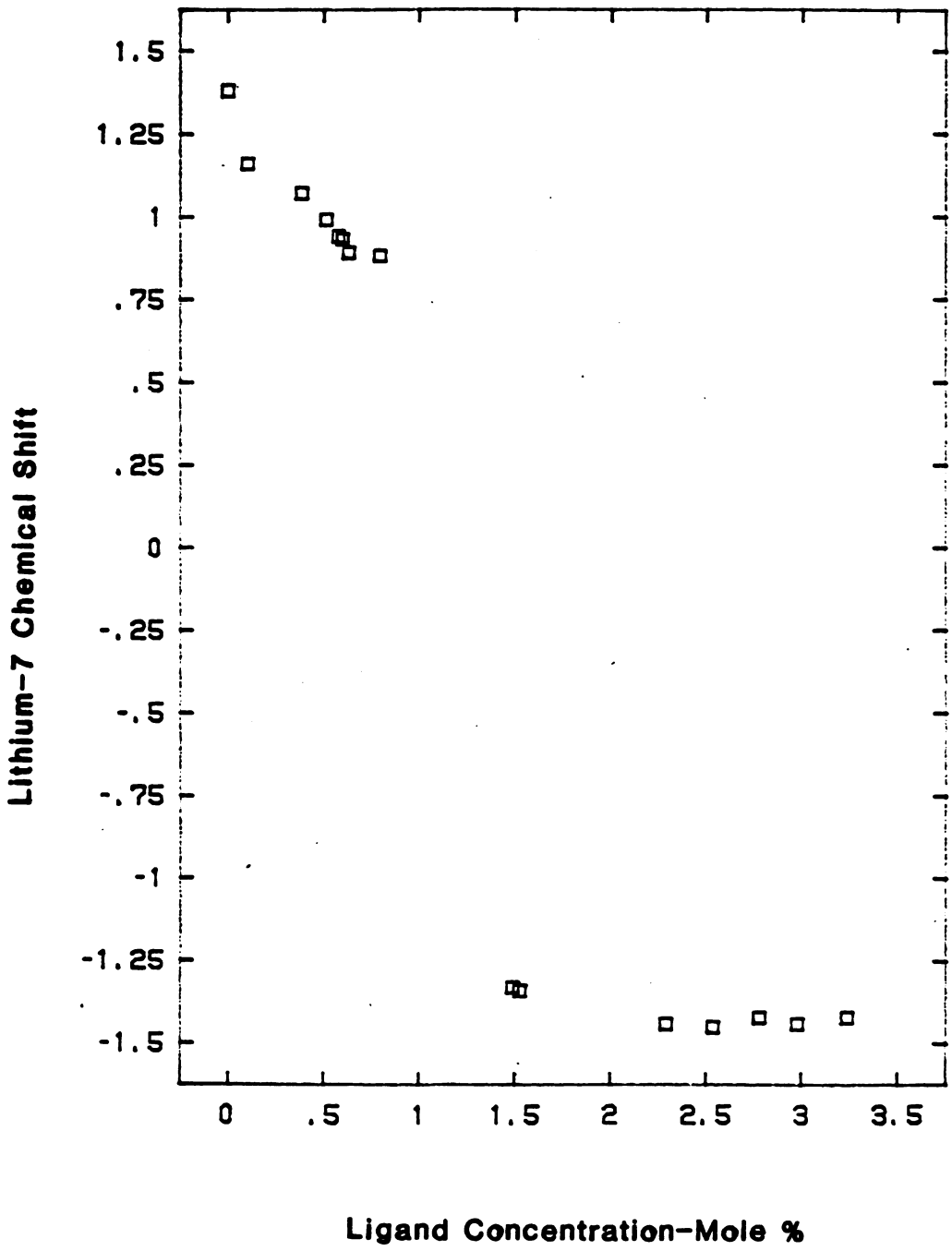
1.5
1.25
1
.75
.5
.25
0
-.25
-.5
-.75
-1
-1.25
-1.5
0
.5
1
1.5
2
2.5
3
3.5
Lithium-7 Chemical Shift
Ligand Concentration-Mole %

Figure 63: Lithium-7 NMR chemical shifts for various ligand concentrations for the complexation of methoxyethylmonoazo 15C5 in 45 mole % $AlCl_3$ BPC-$AlCl_3$ at 40 °C. (C_{LiCl} = 0.70 mole %)

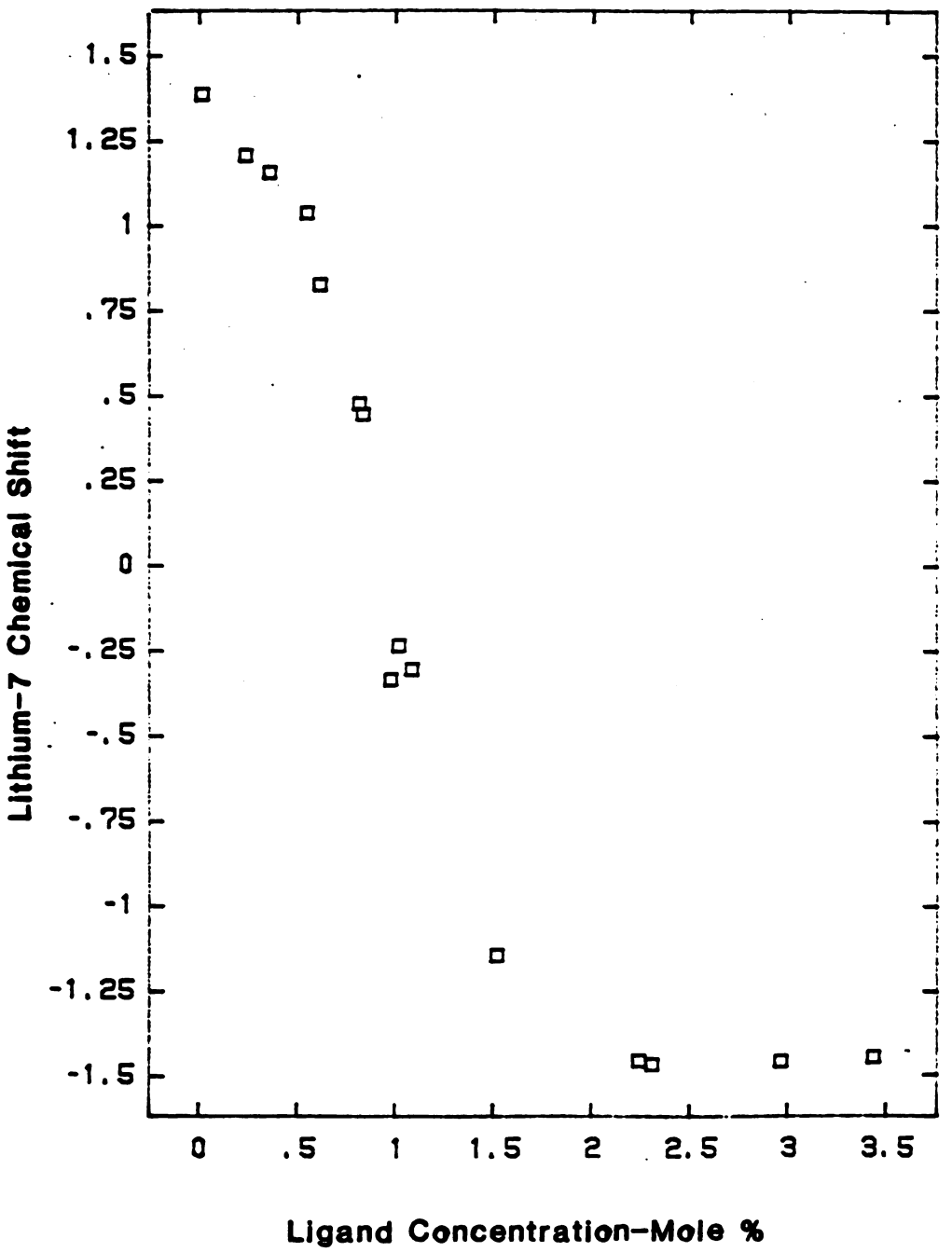
1.5
1.25
1
.75
.5
.25
0
-.25
-.5
-.75
-1
-1.25
-1.5
0
.5
1
1.5
2
2.5
3
3.5
Lithium-7 Chemical Shift
Ligand Concentration-Mole %

Table 16

Formation Constants Obtained for Lariat Ethers in 2-Butanone and 45 Mole % $AlCl_3$ Melt and also the Chemical Shifts of the Complexes

Ligand	Solvent	$K_F(\underline{M}^{-1})$	δ_C (PPM)
Methoxyethyl monoazo 15C5	2-butanone[a]	$1.3(\pm0.4) \times 10^3$	-1.3 (±0.1)
Methoxyethoxy ethylmonoaza 15C5	2-butanone[b]	$>10^5$	-1.00 (±0.02)
Methoxyethyl monoazo 15C5	45 mole % melt[c]	$>10^5$ $3.4(\pm0.8) \times 10^2$ $(2.6(\pm0.6) \times 10^3)$	0.71 (±0.02) -1.52 (±0.03)
Methoxyethoxy ethylmonoazo 15C5	45 mole % melt[c]	$>10^5$ $1.8(\pm0.8) \times 10^3$ $(1.4(\pm0.7) \times 10^4)$	0.80 (±0.03) -1.44 (±0.02)

[a] Formation constants determined at ambient temperatures.

[b] Formation constants determined at 50 °C.

[c] Formation constants determined at 40 °C. The fits were obtained by fitting simultaneously the chemical shifts obtained from the mole ratio and concentration studies. The dimerization constant and the chemical shifts of the monomer and dimer are given below for the two fits obtained from NMR measurements in melt solutions. The value in the parentheses corresponds to the formation constant in mole fraction units.

Methoxyethylmonoazo 15C5: Log K_D = 3(±2), δ_M = 3(±6) ppm, δ_D = 1.09(±0.08) ppm

Methoxyethoxyethylmonoazo 15C5: Log K_D = 6(±63), δ_M = 36(±2470) ppm, δ_D = 1.1(±0.1) ppm

1:1 complex and the second represents the formation of the 2:1 complex. The first K's for lariat complexes in basic melt are $>10^5$ $\underline{M}^{-1}$ and can not be determined accurately by NMR. Inorder to fit the chemical shifts obtained from the mole ratio studies with these ligands the precision of the variables had to be run in quad precision. The first K obtained from this fit is too large ($\sim10^{15}$) so the program terminates before completion at lower precisions.

Complexation studies with these lariat ligands were also carried out in 2-butanone. The salt choosen for this study was $LiBPh_4$, because of its small ion pairing constant (K_a = 2.6 $\underline{M}^{-1}$); therefore, no correction was necessary in the fitting program to account for contact ion pairing The formation constants are listed in Table 16. The fitting program was the same program used to obtain formation constants for crown ethers in basic melt and glyme ether in basic melts and 2-butanone solutions. The complexation constant for methoxyethoxyethylmonoazo 15C5 with Li^+ was measured at 50 °C because at room temperature, the kinetics of complexation was in intermediate exchange on the NMR time scale. This conclusion was arrived at from the ^7Li NMR spectra obtained below room temperature. Figure 64 shows that at -32 °C two peaks appear, which become more apparent as the temperature is further reduced. The NMR measurements obtained from 2-butanone solutions indicate only a two site exchange. Fitting the chemical shifts to a three site exchange mechanism as described by equation 4-7 produced too much correlation in the formation constants; therefore, accurate values could not be obtained.

Figure 64: Lithium-7 NMR spectra of a 0.02 M $LiBPh_4$ 2-butanone solution containing methoxyethoxyethylmonoazo 15C5 at different temperatures.

a. 23 °C

b. 9.4 °C

c. -13 °C

d. -32 °C

d. -51 °C

e. -73 °C

f. -91 °C

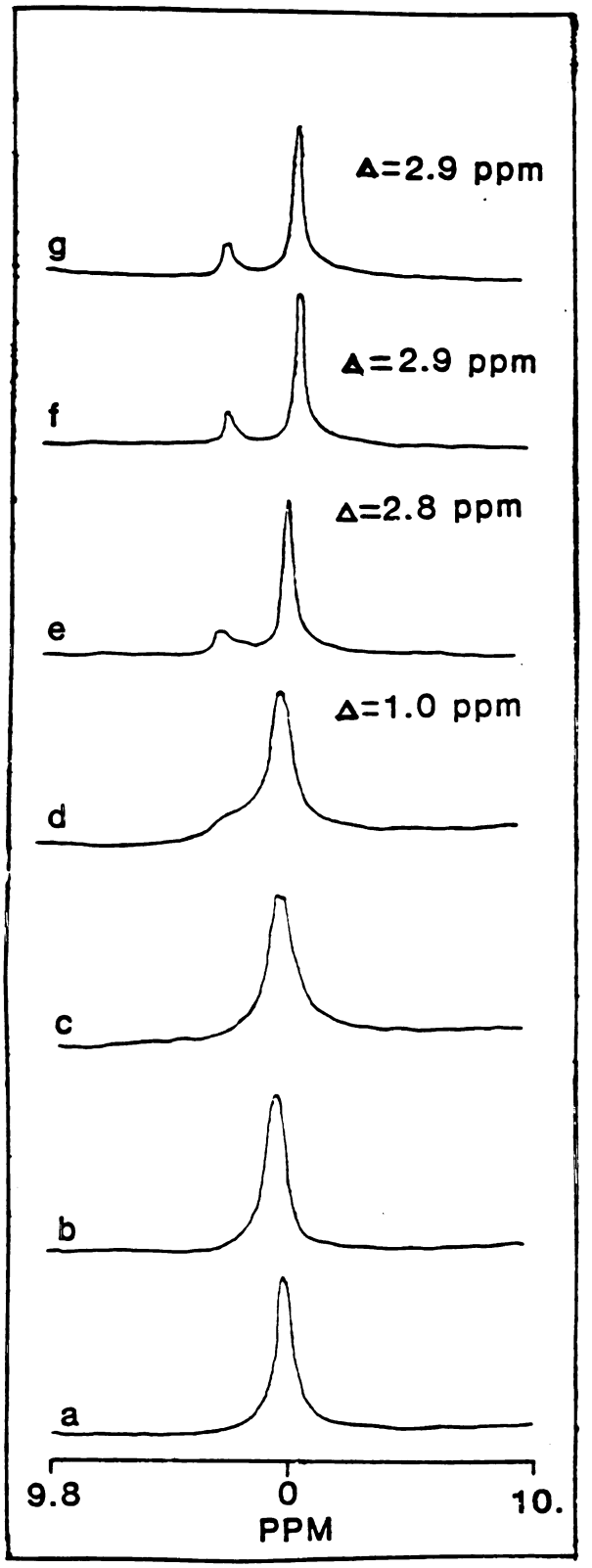
Δ=2.9 ppm
g
Δ=2.9 ppm
f
Δ=2.8 ppm
e
Δ=1.0 ppm
d
c
b
a
9.8
0
10.
PPM

IV. C

Th

soluti

sample

was f

additi

an al

alkali

determ

$AlCl_3$

Th

a crow

compon

a 45 m

single

45 mol

solutio

in the

The nur

$^{31}P^{+}$ as

ligand

to 5% .

corresp

line fo

equival

IV. Crown Ether Complexation Studies in Acidic Melt Solutions

The addition of a macrocyclic ligand to a 67 mole % $AlCl_3$ melt solution changes the color of the solution to black or brown after the sample has been conditioned at 70 °C for three weeks. When the sample was first prepared, no coloration of the melt was observed. The addition of macrocyclic ligands to a 67 mole % $AlCl_3$ melt containing an alkali metal salt (NaCl, CsCl) caused observable changes in the alkali NMR spectra. Carbon-13 NMR studies were carried out to determine the condition of the crown ether ligand in the 67 mole % $AlCl_3$ melt solution.

The color changes in the 67 mole % $AlCl_3$ melt solutions containing a crown ether ligand suggest a reaction between the ligand and the components of the melt. Carbon-13 NMR spectra obtained at 45 °C from a 45 mole % $AlCl_3$ melt solution containing either 18C6 or 12C4 show a single line. Figure 65 and 66 each contain two spectra, one for the 45 mole % $AlCl_3$ melt solution and the other, a 45 mole % $AlCl_3$ melt solution containing a crown ether ligand. Many intense bands appear in the ^{13}C spectra which correspond to the carbon of the BP^+ (224). The numbers by each ^{13}C band correspond to a particular carbon on the BP^+ as shown by the illustration in each figure. The bands due to the ligand are identified with an X. The chemical shifts are referenced to 5% TMS/$CDCl_3$. The bands designated with an R in Figures 65 and 66 correspond to the 8 % DMSO/D_2O reference. The appearance of a single line for the crown is expected because all of the carbons are in equivalent environments. These results indicate that crown ether

Figure 65: Carbon-13 NMR spectra of 45 mole % $AlCl_3$ BPC-$AlCl_3$ melt solutions at 45 °C. The bands identified by numbers are the carbons of the BP^+ cation. The band identified by R is the 8% DMSO/D_2O reference (39.02 ppm vs 5 mole % TMS chloroform-d). The chemical shift listed by the 12C4 band has not been corrected for the magnetic susceptibility of the melt.

a. 3.35 mole % 12C4, the x identifies the crown ether band, and its chemical shift is written by it.

b. 45 mole % melt.

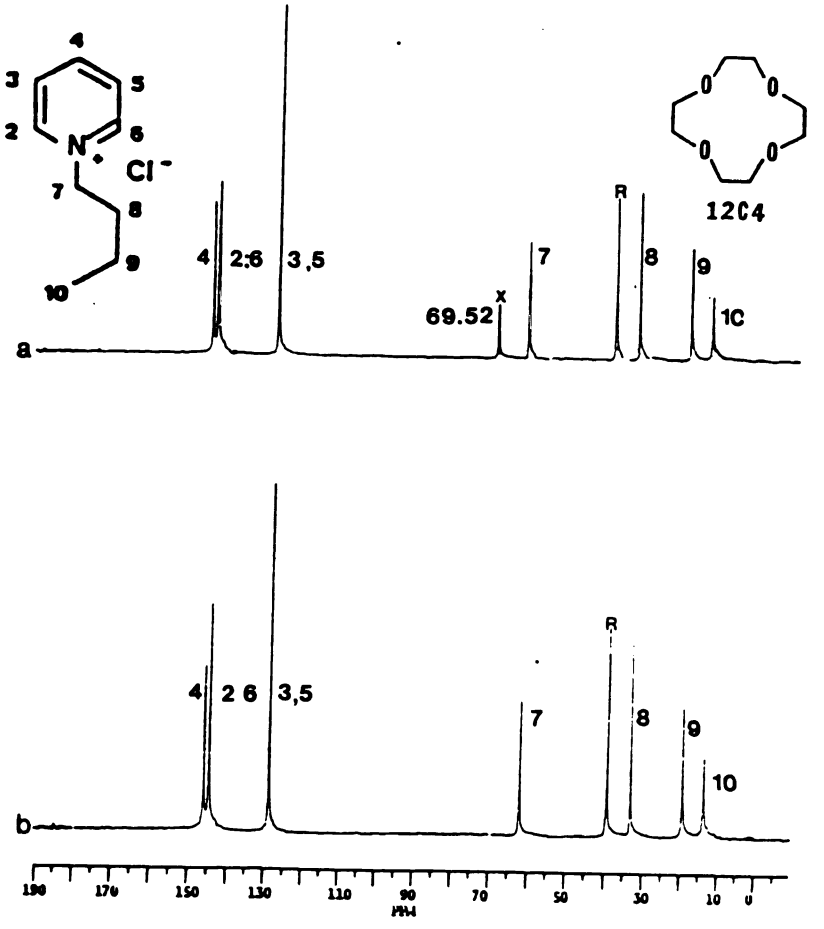
4
3
5
2
6
N
Cl⁻
7
8
9
10
12C4
4
2;6
3,5
69.52
X
7
R
8
9
10
a
4
2 6
3,5
7
R
8
9
10
b
190
170
150
130
110
90
70
50
30
10
0
PPM

Figure 66: Carbon-13 NMR spectra of 45 mole % $AlCl_3$ BPC-$AlCl_3$ melt solutions at 45 °C. The bands identified by numbers correspond to the carbons of the BP^+ cation. The band identified by R is the 8% DMSO/D_2O reference (39.02 ppm vs 5 % TMS chloroform-d). The chemical shift of the 18C6 band has not been corrected for the magnetic susceptibility of the melt.

a. 2.66 mole % 18C6, the x identifies the crown ether band, and its chemical shift is written by it.

b. 45 mole % melt.

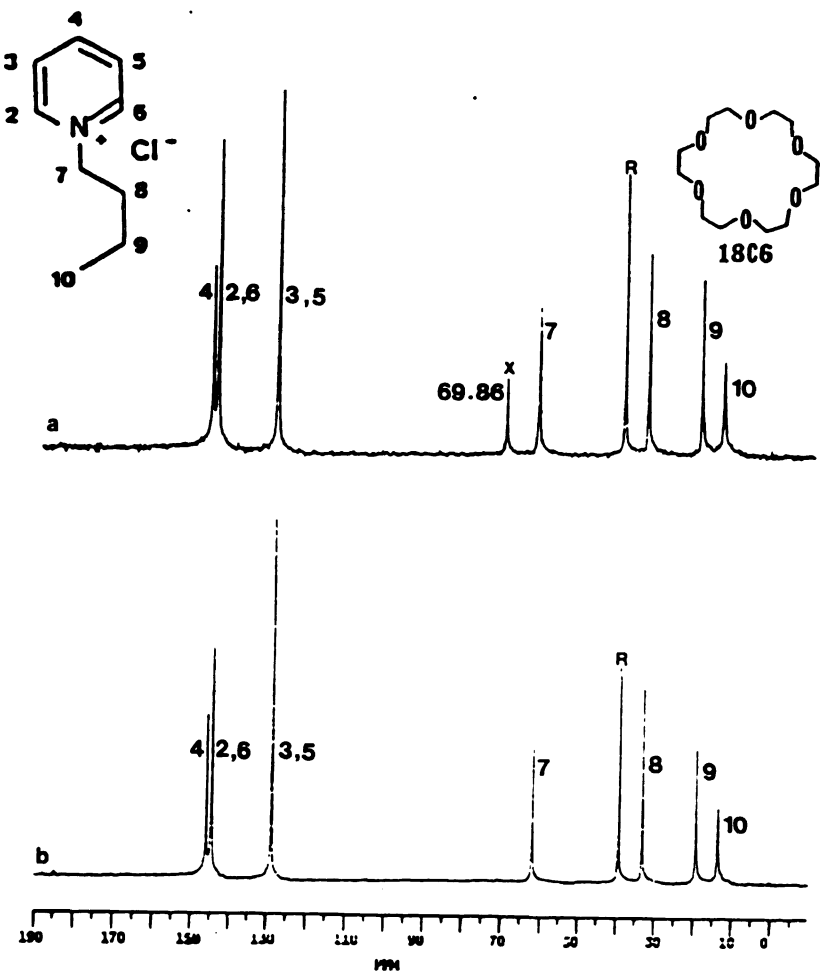
4
3
5
2
6
N
Cl⁻
7
8
9
10
18C6
4
2,6
3,5
69.86
X
7
R
8
9
10
a
4
2,6
3,5
7
R
8
9
10
b
190
170
150
130
110
90
70
50
30
10
0
PPM

ligan

$AlCl_4$

A

with

obtai

solut

aceto

an ir

ppm,

Al(CH

in F

Figur

addit

bands

the

two

the s

appea

both

linew

compl

titra

solut

broad

I

ligands are stable in basic melts; no reaction occurs with BP^+, $AlCl_4^-$, or Cl^-.

Aluminum-27 NMR studies showed that the $AlCl_4^-$ does not interact with 18C6 in acetonitrile. Figure 67 shows three ^{27}Al spectra obtained at ambient temperature of three different acetonitrile solutions each containing 0.10 M $AlCl_3$. In a 0.10 M $AlCl_3$ acetonitrile solution, three bands in the ^{27}Al spectrum are observed, an intense band at 101 ppm for $AlCl_4^-$ and weaker bands at -13 ppm, -23 ppm, and -35 ppm corresponding to $AlCl_2(CH_3CN)_4^+$, $AlCl(CH_3CN)_5^{2+}$, and $Al(CH_3CN)_6^{3+}$, respectively (Figure 67,68) (360). Another band appears in Figure 68 at -35 ppm due to $Al(CH_3CN)_6^{3+}$ which is not present in Figure 67 because of its low intensity at this concentration. The addition of 18C6 to a 0.10 M $AlCl_3$ acetonitrile solution produces new bands in the six coordinate spectral region at 9 ppm and -5 ppm, while the bands at -13 and -23 ppm decrease in intensity (Figure 68). The two kinds of 18C6 complexes occurring in acetonitrile solutions are the same except for the ligands that occupy the axial positions. It appears that the axial ligands are either 2 Cl^- or 2 CH_3CN because both bands associated with the complex have the same linewidth. The linewidths are listed in Figure 68 by the NMR bands due to the 18C6 complexes. The 0.10 M $AlCl_3$ solution was saturated with $N(CH_3)_4Cl$ to titrate all the cationic species to $AlCl_4^-$ (Figure 67). To this solution, an equimolar amount of 18C6 was added. No new bands or broadening of the 101 ppm $AlCl_4^-$ resonance was observed (Figure 67).

In 67 mole % $AlCl_3$ melt solutions, the $Al_2Cl_7^-$ is the major

Figure 67: Aluminum-27 NMR spectra of a series of 0.10 M $AlCl_3$ acetonitrile solutions. The ^{27}Al bands are identified by their chemical shifts which are not corrected for the magnetic susceptibility of the acetonitrile. Spectra were obtained at ambient temperature.

a. The $AlCl_3$ solution saturated with $N(CH_3)_4Cl$ containing 18C6 ($18C6/Al^{+3}$ = 2.00).

b. The $AlCl_3$ solution saturated with $N(CH_3)_4Cl$.

c. 0.10 M $AlCl_3$

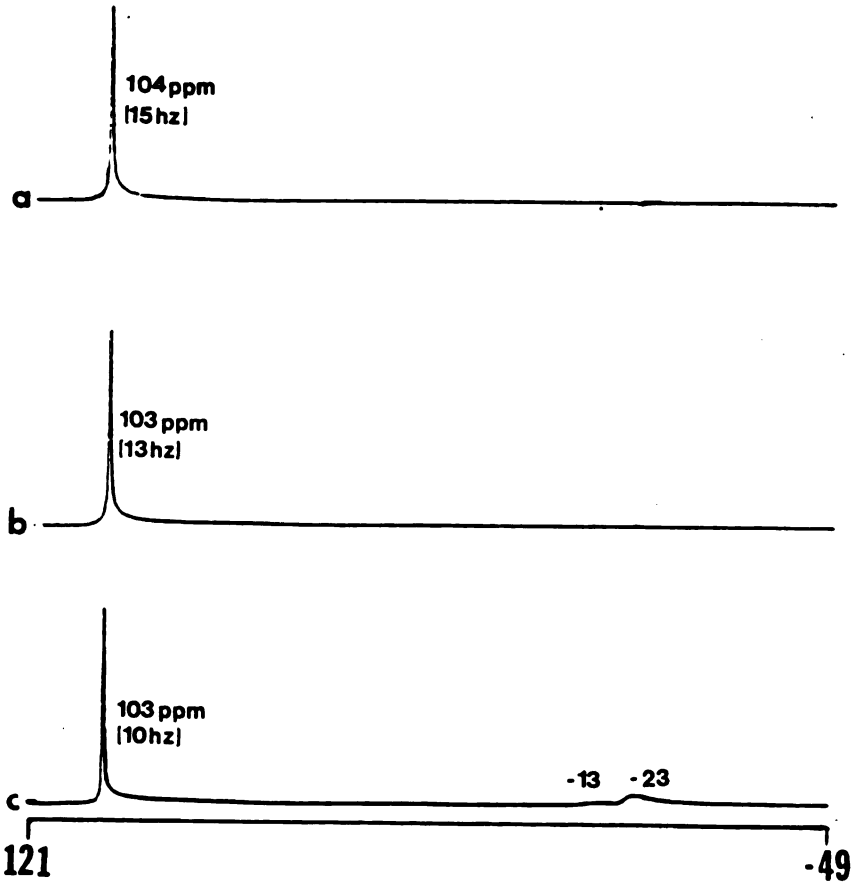
104 ppm
(15 hz)
a
103 ppm
(13 hz)
b
103 ppm
(10 hz)
-13
-23
c
121
-49
ppm

Figure 68: The effect in the ^{27}Al NMR spectra by varying the amount of 18C6 (MR = mole ratio) in 0.10 M $AlCl_3$ acetonitrile solutions. The chemical shifts have not been corrected for the magnetic susceptibility of acetonitrile. Spectra were obtained at ambient temperature.

a. MR = 1.59

b. MR = 1.21

c. MR = 0.80

d. MR = 0.40

e. MR = 0.10

f. MR = 0.00

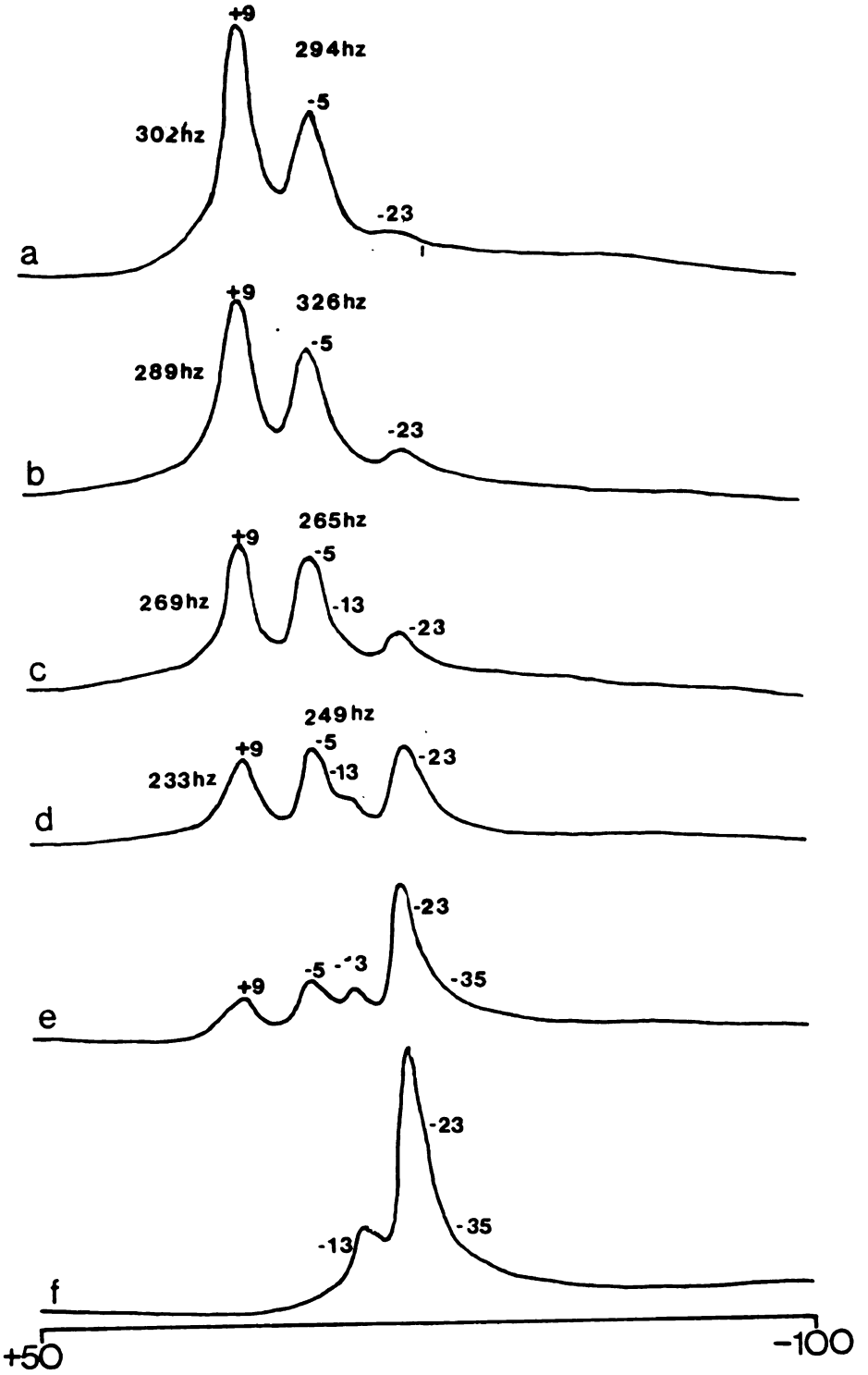
+9
294hz
-5
302hz
-23
a
+9
326hz
-5
289hz
-23
b
265hz
+9
-5
269hz
-13
-23
c
249hz
+9
-5
233hz
-13
-23
d
-23
+9
-5
-13
-35
e
-23
-13
-35
f
+50
-100
ppm

anionic species. A ^{13}C NMR spectrum at 45 ^{o}C of 12C4 melt solution prepared from 67 mole % $AlCl_3$ melt consists of many bands. Figures 69 and 70 show two regions of the ^{13}C NMR spectrum of this melt solution. These results indicate that 12C4 reacts with $Al_2Cl_7^-$ to produce many hydrocarbon fragments. The bands that are identified by numbers correspond to the BP^+. The other bands correspond to the products of the reaction with $Al_2Cl_7^-$.

Both B15C5 and DB18C6 melt solutions prepared with 67 mole % $AlCl_3$ melt are reddish brown as a result of the reaction with $Al_2Cl_7^-$. Carbon-13 NMR spectra obtained at 45 ^{o}C for the B15C5 solutions prepared from benzene and nitromethane contain three bands in the aromatic region (110–160 ppm) and four bands in the ether region (40–70 ppm) (Figures 72,72). The assignments of the B15C5 bands have been previously made by P. Boss (296). The number by the B15C5 ^{13}C NMR bands corresponds to the carbons labeled in the diagram of B15C5 found in the Figures. Table 17 lists the measured ^{13}C chemical shifts for B15C5 in nitromethane and benzene. The magnetic susceptibility of benzene and nitromethane were not available at 45 ^{o}C, so the correction was made using the unitless volumetric magnetic susceptibilities at 32 ^{o}C and 25 ^{o}C, respectively. Significant chemical shift differences occur among several carbons of the B15C5, which indicates a difference in the interaction of the ligand with benzene and nitromethane. Nitromethane forms a neutral molecule complex with crown ethers where the protons of the $-CH_3$ group are hydrogen bonded to the ether oxygens and benzene forms a complex with

Figure 69: Carbon-13 NMR spectrum of a 3.14 mole % 12C4-67 mole % melt solution at 45 °C. The bands identified by numbers are the carbons of the BP^+ cation. The other bands are due to decomposition products of 12C4.

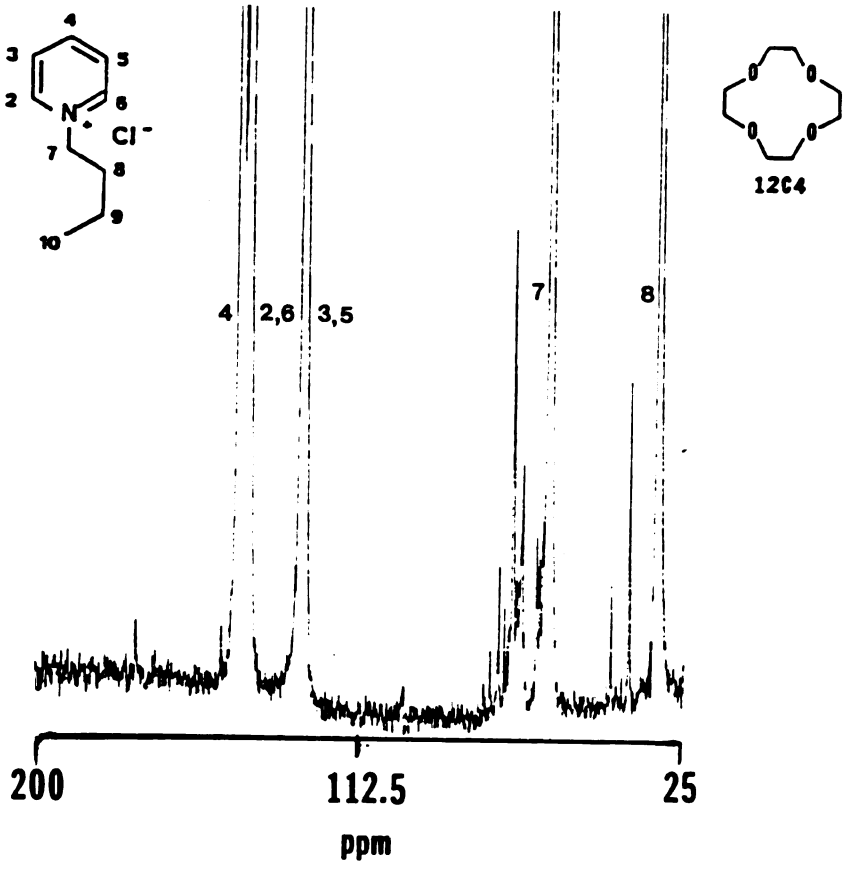
4
3
5
2
6
N+
Cl-
7
8
9
10
4
2,6
3,5
7
8
O
O
O
O
12C4
200
112.5
25
ppm

Figure 70: Limited ^{13}C NMR spectral region of a 3.14 mole % 12C4-67 mole % $AlCl_3$ BPC-$AlCl_3$ melt solution at 45 °C. The band identified by the number 7 corresponds to a carbon on the BP^+ cation. The other bands correspond to decomposition products of 12C4.

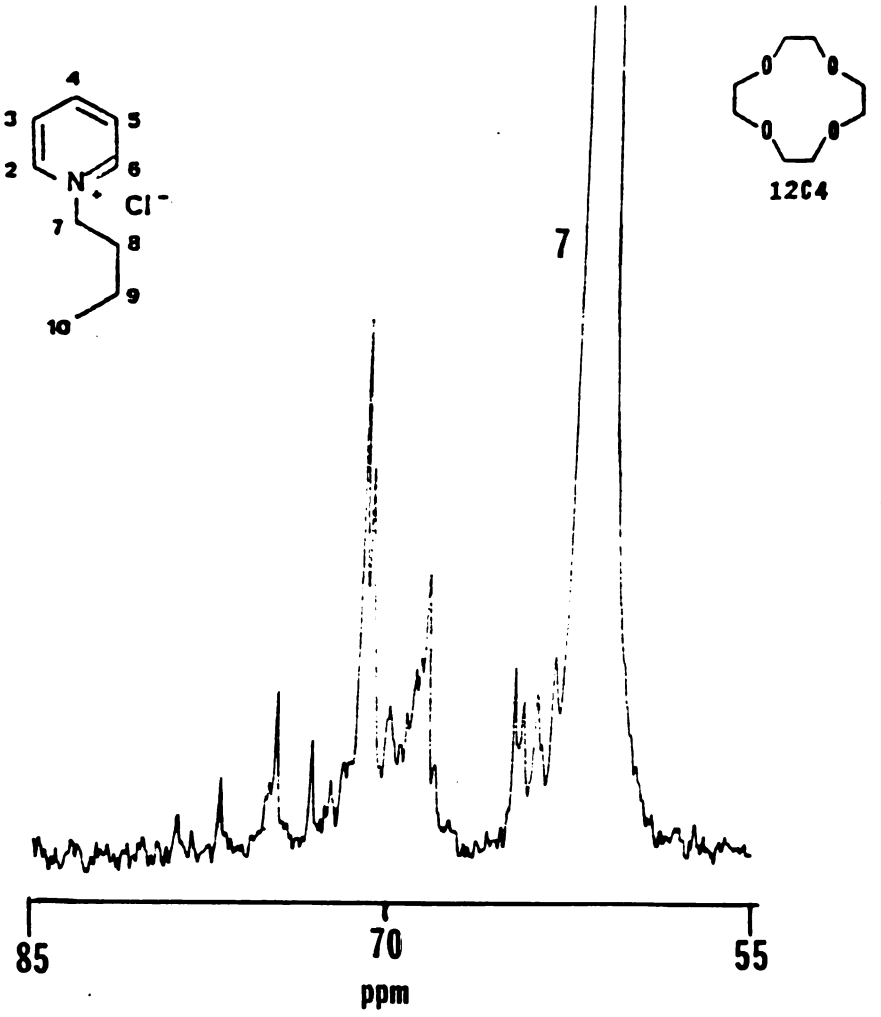
4
3
5
2
6
N+
Cl-
7
8
9
10
12C4
7
85
70
55
ppm

Figure 71: Carbon-13 NMR spectrum of a 0.15 M B15C5-C_6H_6 solution at 45 °C. The B identifies the benzene band (128.30 ppm vs 5% TMS chloroform-d reference), and the R corresponds to the reference (8% DMSO/D_2O, 39.02 ppm vs 5% TMS chloroform-d reference). The number by the low intensity bands identifies the carbon in the B15C5 ligand

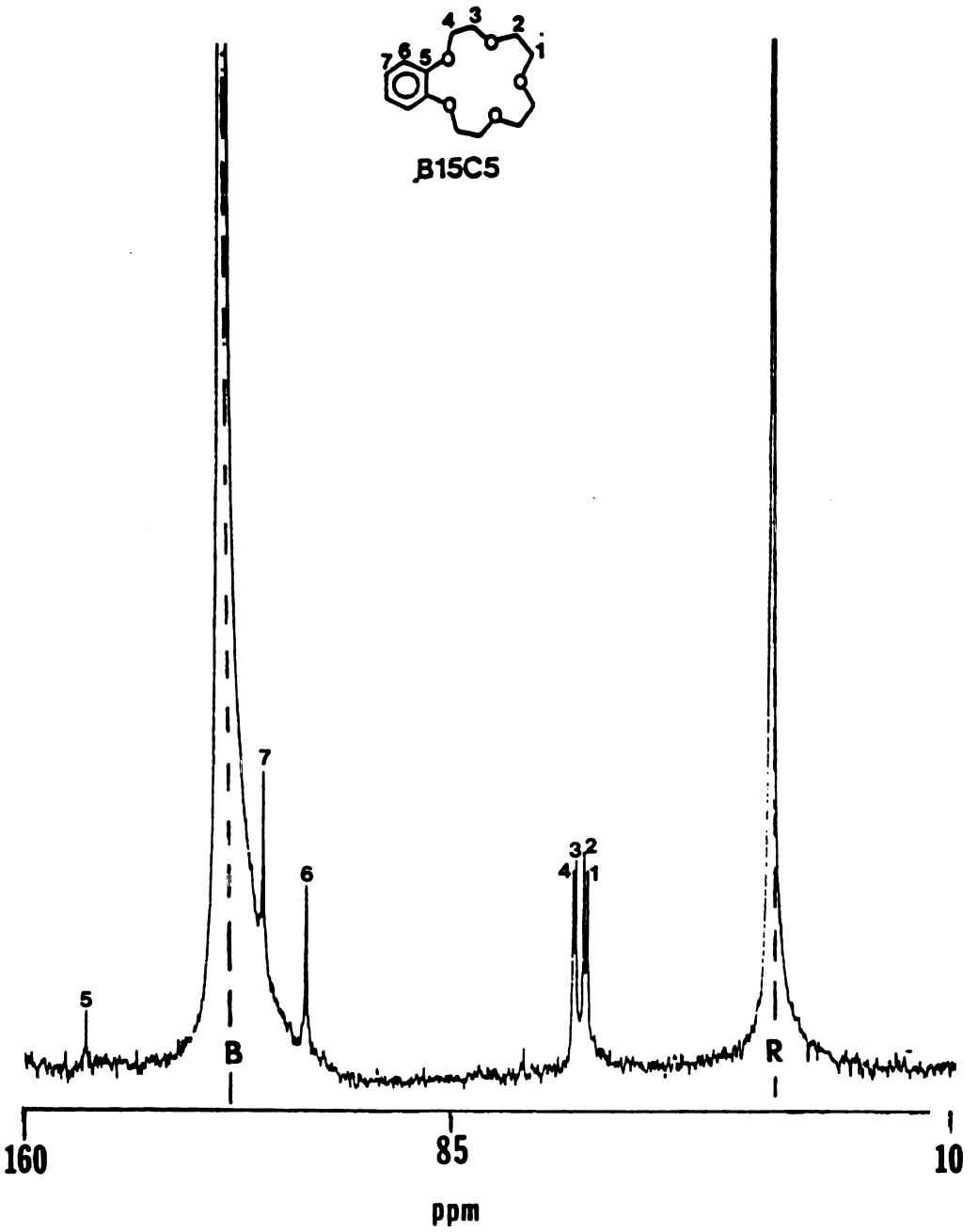
4 3 2
1
7 6 5
B15C5
7
6
3 2
4 1
5
B
R
160
85
10
ppm

Figure 72: Carbon-13 NMR spectrum of a 0.15 M B15C5-CH_3NO_2 solution at 45 °C. The N identifies the CH_3NO_2 band (63.19 ppm vs 5% TMS chloroform-d reference), and the R corresponds to the reference band (8% DMSO/D_2O, 39.02 ppm vs 5% TMS chloroform-d reference). The number by the low intensity bands identifies the carbon in the B15C5 ligand.

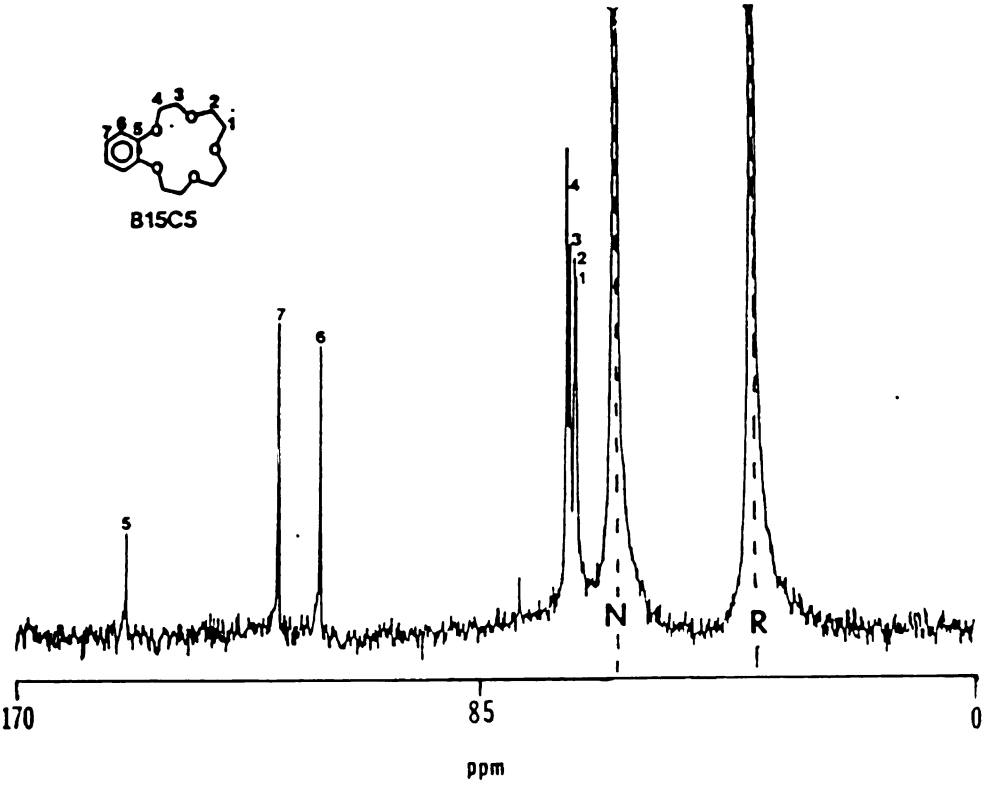
B15C5
4
3
2
1
7
6
5
N
R
170
85
0
ppm

Table 17

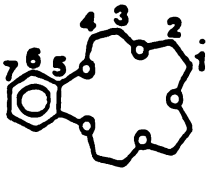

B15C5

Carbon-13 Chemical Shift Data (PPM) for

Solutions of B15C5 in Several Solvents at 45 °C

Sample	C-1	C-2	C-3	C-4	C-5	C-6	C-7
0.15 M B15C5 C_6H_6	68.74	69.33	70.65	71.09	149.43	114.02	120.81
0.15 M B15C5 CH_3NO_3	68.47	68.90	69.67	70.23	149.03	113.84	121.04
0.90 mole % B15C5 45 mole % melt	68.34	68.83	69.45	69.98	148.31	113.88	121.53
1.37 mole % B15C5 67 mole % melt	39.99	68.75	71.25	75.04	140.03	117.32	125.52

Carbon-13 chemical shifts obtained from melt solutions have not been corrected for the magnetic susceptibility of the melt. Those NMR measurements obtained in C_6H_6 and CH_3NO_3 have been corrected for the magnetic susceptibility of the solvent.

the benzene moiety of the B15C5 ligand (296). The precision of these ^{13}C measurements are ±0.06 ppm. The ^{13}C NMR spectra of acidic melt solutions consist of three bands in the aromatic region, three bands in the ether region, and another band shifted upfield from the ether region (39.99 ppm) (Figure 73). The shifted band is only observed when the 8 % DMSO/D_2O reference is not used; this band appears at the same position as the external reference. The chemical shifts of the carbon atoms of B15C5 for the 45 and 67 mole % $AlCl_3$ melt solution obtained at 45 °C are listed in Table 17. The chemical shift changes of the aromatic carbons indicate that the reaction between $Al_2Cl_7^-$ and B15C5 produces a change in the molecule which perturbs the electron density on the benzene ring. The carbon chemical shifts of the benzene carbons of B15C5 are different in basic melt than acidic melt (Table 17). Evans (361) reported that in THF, $AlCl_3$ attacks the oxygen ether atom and splits the THF ring. Splitting the ring of B15C5 by $Al_2Cl_7^-$ produces an aliphatic chloride and $ROAlCl_2$ species. The upfield band in the ^{13}C NMR spectrum of B15C5 appears in the aliphatic chloride region (40-70 ppm). In 67 mole % $AlCl_3$ melt solutions, the following reaction is proposed to occur:

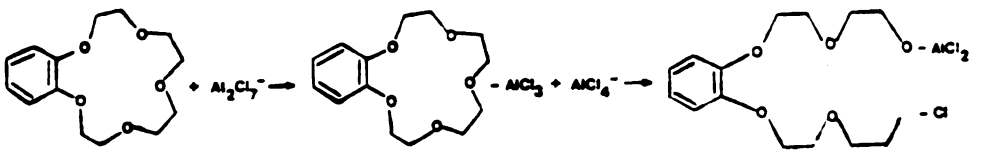

(4-8)

An ESR spectrum was obtained from 67 mole % $AlCl_3$ melt containing

Figure 73: Carbon-13 NMR spectrum of a 1.37 mole % B15C5 67 mole % $AlCl_3$ BPC-$AlCl_3$ melt solution at 45 °C. The bands identified by numbers are the carbons of the BP^+ cation. The bands with the chemical shifts written by them correspond to the bands of the B15C5 molecule. The chemical shifts have not been corrected for the magnetic susceptibility of the melt.

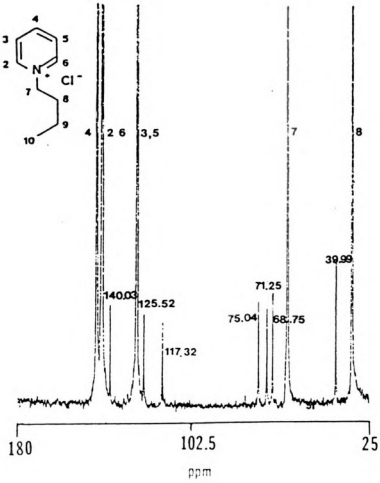
4
3
5
2
6
N
+
Cl -
7
8
9
10
4
2 6
3,5
7
8
140.03
125.52
117.32
75.04
71.25
68.75
39.99
180
102.5
25
ppm

12C4, B15C5, and DB18C6 solutions at -150 °C. The ESR spectrum indicated the presence of organic radicals (g = 2.00). Organic radicals all possess g values close to the g value for a free unbound electron (g = 2.002319). The addition of NaCl to the B15C5-67 mole % $AlCl_3$ melt solution produces a fine structure in the ESR spectrum (Figure 74). This indicates the formation of ion pairs which stabilize the radicals, slowing down the rate of electron exchange. Electron exchange occurs in B15C5-67 mole % $AlCl_3$ melt solutions to produce an ESR spectrum with fine structure. The fine structure in an ESR spectrum in solution results from a coupling of nuclei with spins >1/2. Hyperfine coupling constants cannot be measured directly from the spectra. For frozen melt solutions, this is not possible because all orientations of the molecule contribute to the spectral shape (Figure 74). The anisotropy in the hyperfine spectra distorts the ESR spectra in the melt, so the coupling constants cannot be obtained (362). Similar results were also obtained with DB18C6. The production of free radicals can be explained in B15C5 melt solutions by taking into the account the electrochemical properties of BP^+.

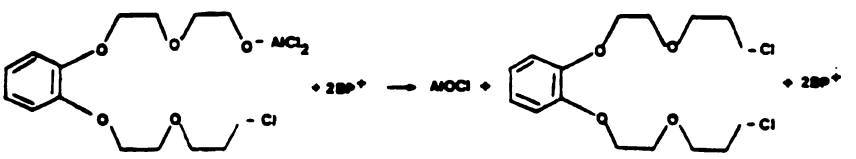

(4-9)

The B15C5 ligand is not totally decomposed as is the case for 12C4. The benzene units must prevent the decomposition reaction from going

Figure 74: Electron spin resonance spectra of B15C5 67 mole % $AlCl_3$ BPC-$AlCl_3$ melt solution at -150 °C (frequency = 9.51 Ghz). All B15C5 melt solutions were reddish-brown in color.

a. 1.24 mole % B15C5, 0.97 mole % NaCl (MR = 1.290)

b. 1.37 mole % B15C5

c. 67 mole % melt

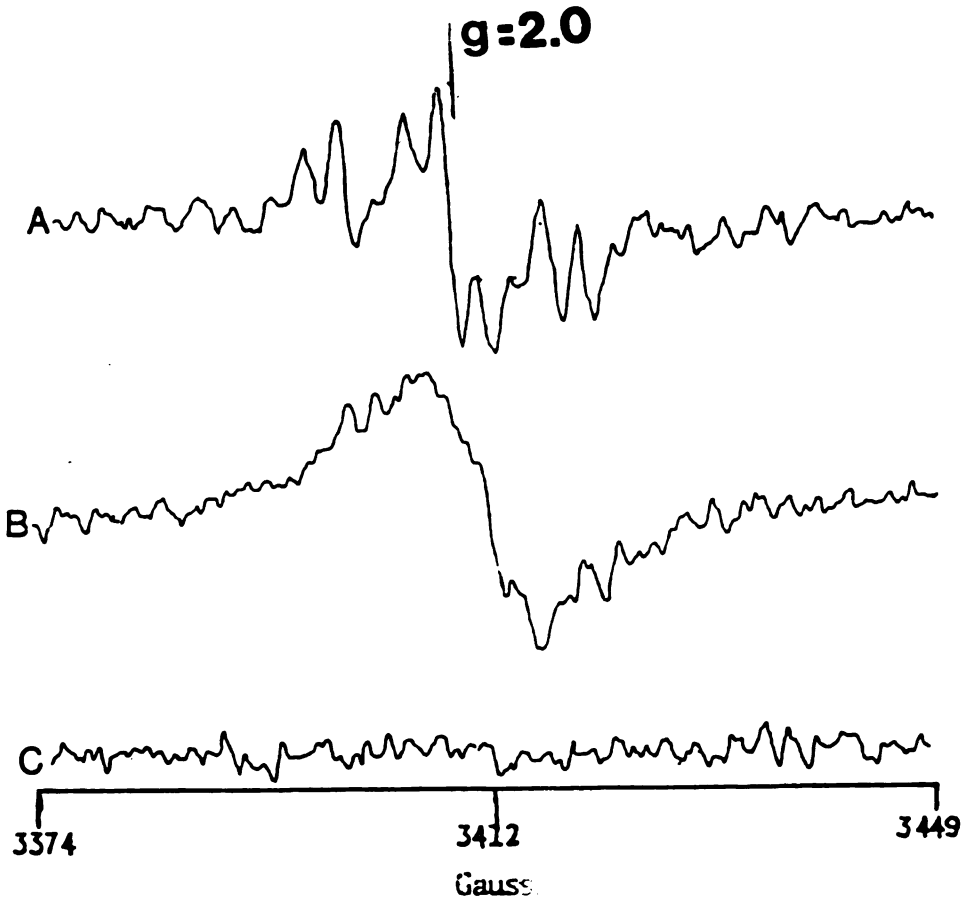
g=2.0
A
B
C
3374
3412
3449
Gauss

to completion.

The alkali metal NMR spectrum at 45 °C undergoes changes when the crown ethers or cryptands are added to a 67 mole % $AlCl_3$ melt containing an alkali metal salt. The ^{133}Cs and ^{23}Na lines shift downfield with the addition of the ligand (Figures 75,76). Since crown ethers contain oxygen, the reaction of $Al_2Cl_7^-$ reduces the acidity of the melt by production of $AlCl_4^-$. In 51 mole % $AlCl_3$ melt, the ^{23}Na NMR signal disappears with the addition of 15C5 (Figure 77). A change occurs in the environment around the Na^+; a more asymmetrical environment is produced around the Na^+ which causes the ^{23}Na NMR band to disappear when 15C5 is added to a NaCl acidic melt solution. These melt samples did not change color, which indicated very little decomposition; therefore, it can be concluded that the formation of a crown complex with Na^+ occurs at these low acidities.

V. Conclusion

Lithium cations are the only alkali metal cations whose salts are soluble in 45 mole % $AlCl_3$ melt. This has been attributed to the ability of Li^+ to form chloroanionic complexes ($LiCl_2^-$). The ^7Li chemical shift measurements at different concentrations indicate that the Li^+ exists in more than one environment. By fitting the chemical shifts, it was found that $LiCl_2^-$ forms dimers in 45 mole % $AlCl_3$ melts.

Salts of other alkali metal cations (Na^+, Cs^+) are not soluble in 45 mole % $AlCl_3$ melt because the cations do not form chloroanionic

Figure 75: Cesium-133 NMR spectra of CsCl solutions in 67 mole % $AlCl_3$ BPC-$AlCl_3$ melt at 45 ^{o}C. The ^{133}Cs band obtained in the melt is identified by its chemical shift and the band identified by R is the reference band (0.01 M CsBr 20% D_2O/H_2O). These solutions were not homogeneous, and the solutions containing the ligands were black. The chemical shifts listed have not been corrected for the magnetic susceptibility of the melt.

a. 0.66 mole % CsCl

b. 1.04 mole % CsCl ($18C6/Cs^+ = 1.2$)

c. 0.98 mole % CsCl ($C222/Cs^+ = 1.5$)

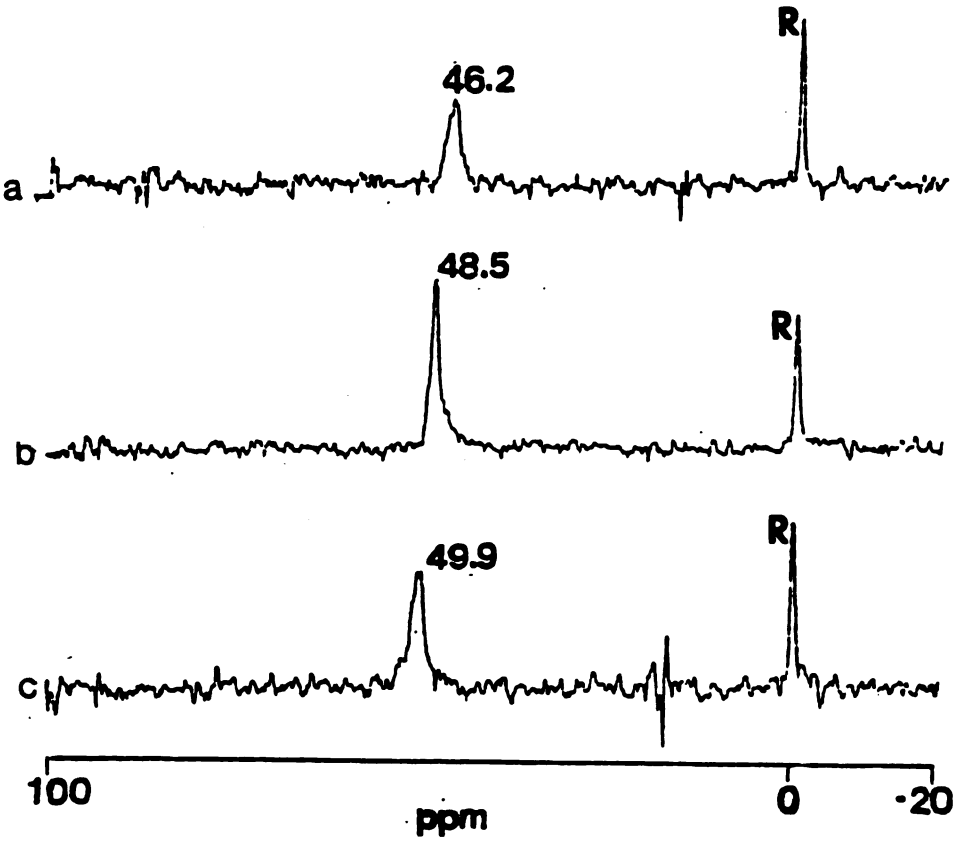
R
46.2
a
48.5
R
b
R
49.9
c
100
ppm
0
-20

Figure 76: Sodium-23 NMR spectra of 67 mole % $AlCl_3$ BPC-$AlCl_3$ melt solutions at 45 °C. The crown ether solutions (MR = mole ratio) were reddish-brown. The chemical shifts have not been corrected for the magnetic susceptibility of the melt.

a. DB18C6 (MR = 0.77), 0.99 NaCl

b. B15C5 (MR = 1.29), 0.97 mole % NaCl

c. 0.99 mole % NaCl

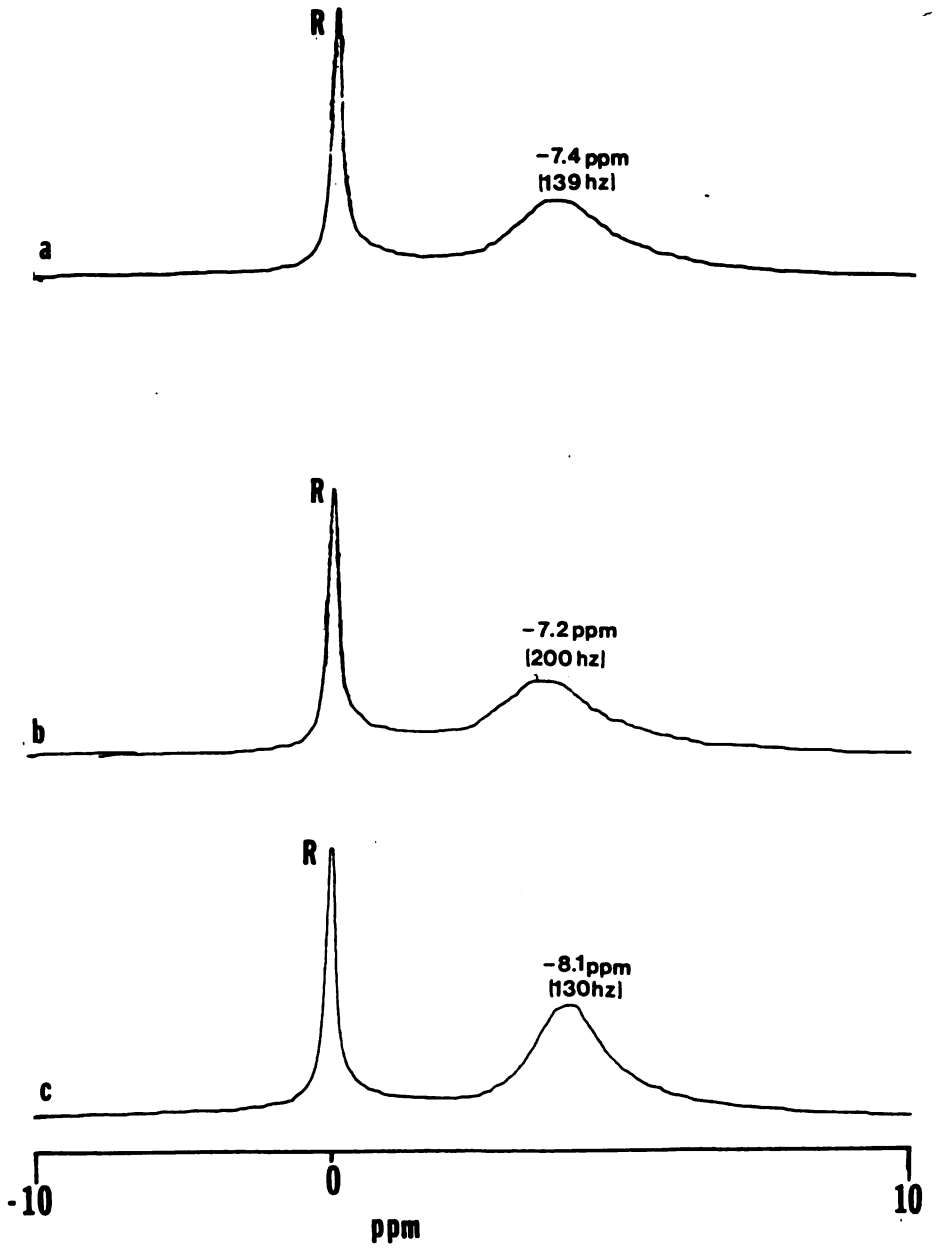
R
-7.4 ppm
(139 hz)
a
R
-7.2 ppm
(200 hz)
b
R
-8.1 ppm
(130 hz)
c
-10
0
10
ppm

Figure 77: Sodium-23 NMR spectra of NaCl melt solution prepared using 51 mole % $AlCl_3$ BPC-$AlCl_3$ melt solutions at 45 °C (MR = mole ratio). The chemical shift for the band in "a" has not been corrected for the magnetic susceptibility of the melt.

a. 1.02 mole % NaCl

b. 15C5 (MR = 1.89), 0.93 mole % NaCl

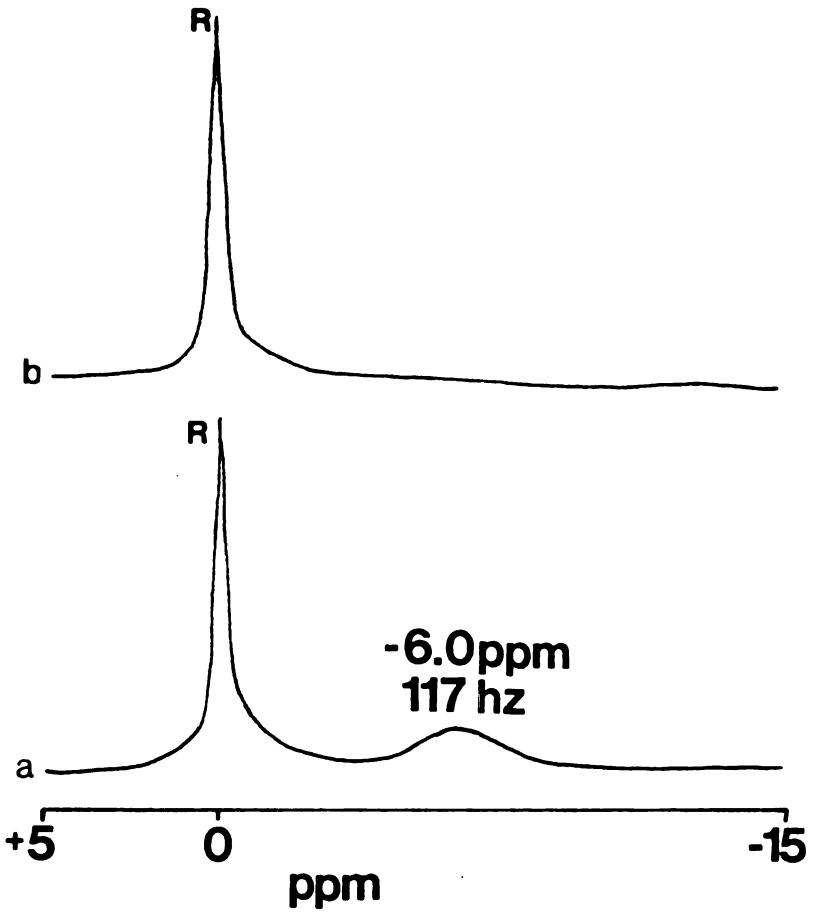
R
b
R
-6.0ppm
117 hz
a
+5
0
-15
ppm

complexes. Studies with sodium and cesium thiocyanates have shown that the anion is replaced with a Cl^- making the Na^+ and Cs^+ insoluble in the 45 mole % $AlCl_3$ melt. Both NMR and IR results indicates that both SCN^- and NO_3^- compete with Cl^- for coordination sites around the aluminum(III) cation, while ClO_4^- does not.

In acidic melts, all Li^+, Na^+, and Cs^+ metal salts studied were soluble. For NaCl and CsCl melt solutions, ^{23}Na and ^{133}Cs chemical shifts remain essentially constant up to 55 mole % $AlCl_3$ and then shift upfield. This has been attributed to an exchange of $Al_2Cl_7^-$ for $AlCl_4^-$ around the metal cation as the melt is made more acidic. Lithium-7 chemical shifts remain constant for all acidic melt mixtures, which indicates that the Li^+ environment is unaffected by the change in melt acidity.

Formation constants were measured for crown ethers, glymes, and lariat ether complexes in 45 mole % $AlCl_3$ using ^7Li NMR. The crown ether formation constants in 45 mole % melt for 15C5 and 12C4 complexes are larger than the 18C6 complex. The noncyclic ligands form weaker complexes than the crown ether ligands. The methoxyethylmonoazo 15C5 and methoxyethoxyethylmonoazo 15C5 ligands form stronger complexes with $LiCl_2^-$ than either 15C5 or tetraglyme. Also, 2:1 complexes are formed with these lariat ligands in 45 mole % melt.

In acidic melts, the complexing capability of crown ether ligands depends on the $Al_2Cl_7^-$ concentration. In 51 mole % $AlCl_3$ melt, the ^{23}Na NMR indicates that Na^+ forms a complex with 15C5 after three weeks of conditioning. In 67 mole % $AlCl_3$, the ether ligands were decomposed by $Al_2Cl_7^-$ after three weeks of conditioning.

A P P E N D I C E S

APPENDIX 1

^{7}Li CHEMICAL SHIFT AND ^{35}Cl LINEWIDTH MEASUREMENTS

^{7}Li Chemical Shifts for LiI 2-Butanone

Concentration (±0.003)* (M)	Chemical Shift (±0.01)* (PPM)
0.010	1.69
0.020	1.67
0.030	1.63
0.040	1.64
0.050	1.61
0.060	1.61
0.070	1.61
0.080	1.58
0.090	1.60
0.100	1.58
0.125	1.57
0.150	1.56
0.175	1.58
0.200	1.53
0.250	1.52
0.300	1.49
0.350	1.47
0.400	1.47
0.450	1.45
0.500	1.43
0.573	1.42

*Estimate of error used in the fitting program.

^{7}Li Chemical Shifts for LiPi 2-Butanone

Concentration (±0.003)* (M)	Chemical Shift (±0.01)* (PPM)
0.010	1.39
0.020	1.37
0.031	1.36
0.041	1.35
0.051	1.35
0.061	1.35
0.071	1.35
0.082	1.35
0.092	1.34
0.102	1.33
0.125	1.33
0.150	1.33
0.200	1.31
0.250	1.30
0.275	1.30
0.300	1.30
0.350	1.29
0.400	1.28
0.450	1.28
0.500	1.27

*Estimate of error used in the fitting program.

^{7}Li Chemical Shifts for $LiAsF_6$ 2-Butanone

Concentration (±0.003)* (M)	Chemical Shift (±0.01)* (PPM)
0.010	1.79
0.020	1.78
0.030	1.77
0.040	1.76
0.050	1.75
0.060	1.76
0.070	1.75
0.080	1.74
0.090	1.73
0.100	1.72
0.124	1.71
0.150	1.70
0.200	1.69
0.249	1.67
0.299	1.65
0.349	1.64
0.398	1.63
0.448	1.61
0.497	1.59
0.528	1.58

*Estimate of error used in the fitting program.

^{7}Li Chemical Shifts for $LiCF_3CO_2$ 2-Butanone

Concentration (±0.003)* (M)	Chemical Shift (±0.01)* (PPM)
0.010	0.77
0.020	0.75
0.030	0.74
0.040	0.74
0.050	0.74
0.060	0.74
0.070	0.73
0.080	0.74
0.090	0.73
0.100	0.73
0.150	0.73
0.200	0.72
0.250	0.72
0.300	0.71
0.350	0.70
0.400	0.70
0.450	0.70
0.500	0.70
0.601	0.69
0.650	0.68

*Estimate of error used in the fitting program.

^{7}Li Chemical Shifts for LiB(Ph)$_4$ 2-Butanone

Concentration (±0.003)* (M)	Chemical Shift (±0.01)* (PPM)
0.010	1.77
0.020	1.75
0.030	1.74
0.040	1.73
0.050	1.73
0.060	1.72
0.071	1.71
0.080	1.69
0.090	1.70
0.100	1.64
0.150	1.62
0.200	1.57
0.250	1.56
0.300	1.51
0.350	1.48
0.400	1.46
0.500	1.40
0.600	1.35
0.700	1.30

*Estimate of error used in the fitting program.

^{7}Li Chemical Shifts for $LiClO_4$ 2-Butanone

Concentration (±0.003)* (M)	Chemical Shift (±0.01)* (PPM)
0.010	1.43
0.020	1.36
0.030	1.32
0.040	1.29
0.050	1.27
0.060	1.26
0.070	1.23
0.080	1.23
0.090	1.21
0.100	1.20
0.200	1.14
0.250	1.13
0.300	1.11
0.400	1.08
0.500	1.05
0.600	1.02
0.700	1.00
0.750	0.99
0.800	0.97
0.900	0.95
1.000	0.92

*Estimate of error used in the fitting program.

^{7}Li Chemical Shifts for LiSCN 2-Butanone

Concentration (±0.003)* (M)	Chemical Shift (±0.01)* (PPM)	
0.010	0.37	
0.020	0.35	
0.030	0.31	0.32
0.040	0.31	0.32
0.050	0.32	
0.060	0.30	0.33
0.070	0.31	
0.080	0.30	0.32
0.090	0.31	
0.100	0.29	
0.150	0.29	
0.200	0.29	
0.250	0.28	
0.300	0.27	
0.350	0.27	
0.400	0.27	
0.500	0.26	
0.600	0.25	
0.650	0.24	
0.700	0.23	
0.780	0.23	
0.800	0.22	

*Estimate of error used in the fitting program.

^{35}Cl Linewidths as a Function of $LiClO_4$ Concentration in 2-Butanone at 25°

Concentration (±0.003) (M)	η(centapoise)	Linewidths (hz)
0.010	0.45	14. (±1.)
0.020	0.46	31. (±1.)
0.030	0.47	35. (±1.)
0.040	0.48	30. (±1.)
0.050	0.49	36. (±1.)
0.060	0.49	31. (±1.)
0.070	0.50	33. (±1.)
0.080	0.50	37. (±8.)
0.090	0.51	33. (±1.)
0.100	0.51	38. (±4.)
0.200	0.54	44. (±4.)
0.250	0.55	35. (±5.)
0.300	0.56	43. (±4.)
0.400	0.59	47. (±4.)
0.500	0.61	47. (±4.)
0.600	0.65	48. (±2.)
0.700	0.68	53. (±4.)
0.750	0.71	40. (±5.)
0.800	0.73	49. (±2.)
0.900	0.78	47. (±4.)
1.000	0.84	47. (±1.)
1.200	0.97	46. (±2.)
1.400	1.14	44. (±4.)
1.600	1.33	45. (±2.)
1.800	1.55	55. (±3.)
2.000	1.81	54. (±6.)

η(centapoise) (2-Butanone) = 0.41

*Values in parentheses corresponds to the errors used in the fitting program. Values were obtained from several linewidth measurements. The constants for the fit of the viscosity curve are:

A_η=1.1(±0.9)
B_η=-1.(±1.)
D_η=1.0(±0.4)

The equation used for this calculation is found in the experimental section, Chapter II.

^{7}Li Chemical Shifts as a Function of Pentaglyme Concentration in 2-Butanone

$C(LiBPh_4)$ = 0.01 M

Concentration (±0.0001)* (M)	Chemical Shift (±0.01)* (PPM)
0.0	1.80
0.0025	1.69
0.0050	1.56
0.0075	1.44
0.0100	1.37
0.0125	1.23
0.0150	1.13
0.0175	1.07
0.0200	1.02
0.0225	0.93
0.0250	0.90
0.0275	0.84
0.0300	0.76
0.0325	0.69
0.0400	0.54
0.0501	0.40
0.0601	0.27
0.0701	0.17
0.0801	0.09
0.0901	0.02
0.1001	-0.05

*Estimate of error used in the fitting program.

^{7}Li Chemical Shifts as a Function of Triglyme Concentration in 2-Butanone

$C(LiBPh_4)$ = 0.01 M

Concentration (±0.0001)* (M)	Chemical Shift (±0.01)* (PPM)
0.0	1.80
0.0025	1.75
0.0050	1.72
0.0075	1.69
0.0100	1.66
0.0125	1.64
0.0150	1.62
0.0200	1.55
0.0225	1.52
0.0250	1.50
0.0275	1.45
0.0300	1.41
0.0325	1.38
0.0500	1.24
0.0600	1.14
0.0700	1.09
0.0800	1.00
0.0900	0.96
0.1000	0.95
0.1071	0.85

*Estimate of error used in the fitting program.

^{7}Li Chemical Shifts as a Function of Tetraglyme Concentration in 2-Butanone

$C(LiBPh_4)$ = 0.01 M

Concentration (±0.0001)* (M)	Chemical Shift (±0.01)* (PPM)
0.0	1.79
0.0025	1.75
0.0050	1.67
0.0075	1.64
0.0100	1.56
0.0125	1.53
0.0150	1.48
0.0201	1.46
0.0251	1.33
0.0302	1.30
0.0352	1.20
0.0403	1.12
0.0501	0.98
0.0604	0.90
0.0705	0.83
0.0806	0.78
0.0906	0.70
0.1000	0.58

*Estimate of error used in the fitting program.

^{7}Li Chemical Shifts as a Function of Methoxyethoxyethylmonoazo 15C5 Concentration in 2-Butanone at 50 °C

$C(LiBPh_4)$ = 0.01 M

Concentration (±0.0001)* (M)	Chemical Shift (±0.01)* (PPM)
0.0	1.79
0.0020	1.48
0.0040	0.78
0.0060	0.27
0.0080	-0.42
0.0090	-0.82
0.0100	-0.93
0.0110	-0.98
0.0120	-1.02
0.0140	-0.97
0.0160	-1.01
0.0180	-1.00
0.0200	-1.01

*Estimate of error used in the fitting program.

^{7}Li Chemical Shifts as a Function of Methyoxyethylmonoazo 15C5 Concentration in 2-Butanone

$C(LiBPh_4)$ = 0.01 M

Concentration (±0.0001)* (M)	Chemical Shift (±0.01)* (PPM)
0.0	1.79
0.0005	1.71
0.0010	1.58
0.0015	1.48
0.0020	1.35
0.0025	1.25
0.0030	0.97
0.0035	1.13
0.0040	0.92
0.0045	0.83
0.0050	0.73
0.0063	0.42
0.0075	0.12
0.0088	-0.18
0.0100	-0.44
0.0113	-0.65
0.0125	-0.79
0.0138	-0.95
0.0151	-0.95
0.0176	-1.02
0.0201	-1.02

*Estimate of error used in the fitting program.

^{7}Li Chemical Shifts for $LiNO_3$ Pyridine

Concentration (±0.003)* (M)	Chemical Shift (±0.01)* (PPM)
0.001	2.37
0.002	2.35
0.003	2.32
0.005	2.32
0.007	2.33
0.009	2.32
0.010	2.32
0.020	2.31
0.029	2.30
0.040	2.30
0.050	2.28
0.060	2.28
0.069	2.27
0.087	2.27
0.100	2.26
0.150	2.23
0.200	2.22
0.279	2.19
0.319	2.19
0.411	2.16
0.479	2.14
0.550	2.12
0.639	2.11
0.679	2.10
0.720	2.10
0.760	2.08, 2.09
0.800	2.07

*Estimate of error used in the fitting program.

^{7}Li Chemical Shifts for LiPi Pyridine

Concentration (M)	Chemical Shifts (PPM)
0.010	2.18
0.020	2.16
0.030	2.16
0.040	2.16
0.050	2.16
0.060	2.17
0.070	2.17
0.080	2.16
0.090	2.16
0.100	2.15
0.125	2.15
0.150	2.15
0.200	2.14
0.225	2.15
0.250	2.14
0.300	2.14
0.350	2.13
0.400	2.13
0.450	2.13
0.500	2.12

^{7}Li Chemical Shifts for $LiClO_4$ Pyridine

Concentration (±0.003)* (M)	Chemical Shift (±0.01)* (PPM)
0.010	2.39
0.020	2.36
0.030	2.34
0.040	2.33
0.050	2.32
0.060	2.31
0.070	2.30
0.080	2.30
0.090	2.29
0.100	2.29
0.125	2.28
0.150	2.26
0.200	2.25
0.225	2.24
0.250	2.23
0.300	2.21
0.350	2.19
0.400	2.19
0.450	2.17
0.500	2.16

*Estimate of error used in the fitting program.

^{7}Li Chemical Shifts for LiSCN Pyridine

Concentration (±0.003)* (M)	Chemical Shift (±0.01)* (PPM)			
0.010	1.60	1.60	1.59	
0.020	1.57	1.58	1.57	
0.030	1.56	1.58	1.56	
0.040	1.56	1.57	1.55	1.56
0.050	1.56	1.58	1.55	1.56
0.060	1.55	1.56	1.54	1.56
0.070	1.55	1.56	1.55	1.56
0.080	1.55	1.56	1.55	1.55
0.090	1.56	1.56	1.54	1.55
0.100	1.56	1.53	1.55	
0.150	1.53	1.54		
0.200	1.52	1.50	1.54	
0.250	1.51	1.53		
0.280	1.52			
0.300	1.51	1.52		
0.320	1.51			
0.350	1.50	1.51		
0.400	1.50	1.49	1.50	
0.450	1.48			
0.480	1.49			
0.500	1.47	1.48		
0.550	1.46			
0.560	1.47			
0.600	1.45	1.48		
0.640	1.46			
0.650	1.44			
0.700	1.44	1.46		
0.720	1.45			
0.750	1.43			
0.760	1.44			
0.800	1.44	1.43	1.45	

*Estimate of error used in the fitting program.

^{7}Li Chemical Shifts for LiCl Pyridine

Concentration (±0.003)* (M)	Chemical Shift (±0.01)* (PPM)
0.001	2.99
0.002	2.97
0.004	2.99
0.005	2.98
0.007	2.98
0.009	2.97
0.012	2.98
0.022	2.96
0.029	2.93
0.045	2.93, 2.94
0.049	2.92
0.060	2.90
0.070	2.89
0.091	2.88, 2.89
0.111	2.87, 2.89
0.150	2.83
0.206	2.82
0.279	2.78
0.319	2.77
0.438	2.74
0.478	2.72
0.548	2.71
0.638	2.68
0.680	2.67
0.718	2.66
0.758	2.66, 2.66
0.800	2.65
0.850	2.64

*Estimate of error used in the fitting program. The first six data points were not included in the fitting program.

^{35}Cl Linewidths as a Function of LiCl Concentration in Pyridine at 25 °C

Concentration (±0.003) (M)	η(centapoise)	Linewidths (hz)
0.020	0.88	376. (±17.)
0.040	0.89	456. (±34.)
0.060	0.89	513. (±46.)
0.080	0.90	539. (±84.)
0.090	0.90	571. (±55.)
0.100	0.91	525. (±13.)
0.125	0.92	556. (±48.)
0.150	0.94	591. (±2.)
0.200	0.96	585. (±27.)
0.250	0.99	669. (±35.)
0.300	1.02	706. (±4.)
0.350	1.05	685. (±31.)
0.400	1.08	723. (±47.)
0.450	1.12	723. (±63.)
0.500	1.15	746. (±40.)
0.600	1.22	810. (±41.)
0.700	1.30	789. (±71.)
0.800	1.38	879. (±148.)

η(centapoise) (Pyridine) = 0.88

*Values in parentheses correspond to the errors used in the fitting program. Values were obtained for several linewidth measurements. The constants for the fit of the viscosity curve are:

A_η=-0.1(±0.1)
B_η=0.6(±0.4)
D_η=0.2(±0.3)

The equation used for this calculation is found in the experimental section, Chapter II.

^{35}Cl Linewidths as a Function of $LiClO_4$ Concentration in Pyridine at 25 °C

Concentration (±0.003) (M)	η(centapoise)	Linewidths (hz)
0.020	0.88	24. (±3.)
0.040	0.90	38. (±3.)
0.060	0.91	39. (±3.)
0.080	0.92	40. (±1.)
0.100	0.94	42. (±2.)
0.125	0.95	40. (±1.)
0.150	0.97	44. (±2.)
0.175	0.99	44. (±4.)
0.200	1.01	41. (±1.)
0.225	1.03	44. (±1.)
0.250	1.05	43. (±1.)
0.275	1.07	41. (±4.)
0.300	1.09	50. (±1.)
0.325	1.10	49. (±1.)
0.350	1.13	45. (±2.)
0.375	1.15	46. (±2.)
0.400	1.18	44. (±1.)
0.425	1.20	47. (±2.)
0.450	1.22	48. (±2.)
0.500	1.27	48. (±3.)

η(centapoise) (Pyridine) = 0.88

*Values in parentheses correspond to the errors used in fitting program. Values were obtained for several linewidth measurements. The constants obtained from the fit of the viscosities are:

A_η=-0.08(±0.02)
B_η=0.84(±0.07)
D_η=0.27(±0.08)

The equation used for this calculation is found in the experimental section, Chapter II.

^{7}Li Chemical Shifts as a Function of Tetraglyme Concentration in 45 Mole % Melt at 40 °C

C(LiCl) = 0.19 mole %

Concentration (±0.01)* (mole %)	Chemical Shift (±0.02)* (PPM)
0.0	1.59
0.16	1.39
0.34	1.38
0.46	1.29
1.66	0.80
2.00	0.69
2.80	0.59
2.90	0.56
2.98	0.53
3.15	0.51
3.20	0.53
3.30	0.49
3.31	0.51
3.94	0.44
5.13	0.38
5.46	0.37
6.10	0.36

*Estimate of error used in the fitting program.

^{7}Li Chemical Shifts as a Function of B15C5 Concentration in 45% Melt at 40°C

C(LiCl) = 1.0 mole %

Concentration (±0.01)* (mole %)	Chemical Shift (±0.02)* (PPM)
0.0	1.34
0.10	1.16
0.16	0.96
0.33	0.76
0.42	0.55
0.46	0.52
0.47	0.36
0.52	0.36
0.75	0.06
0.77	-0.03
0.95	-0.22
1.22	-0.34
1.49	-0.43
1.71	-0.55
2.28	-0.54
3.03	-0.62
5.05	-0.63

*Estimate of error used in the fitting program.

^{7}Li Chemical Shifts as a Function of Triglyme Concentration in 45 Mole % Melt at 40 °C

C(LiCl) = 0.69 mole %

Concentration (±0.01)* (mole %)	Chemical Shift (±0.02)* (PPM)
0.0	1.40
0.57	1.19
0.95	1.02
2.71	0.61
4.23	0.43
5.96	0.35
6.96	0.34
7.82	0.28
10.09	0.22
10.50	0.21
12.76	0.21
14.69	0.20
15.93	0.18
16.09	0.17
16.66	0.17
17.61	0.18

*Estimate of error used in the fitting program.

^{7}Li Chemical Shifts as a Function of 18C6 Concentration in 45 Mole % Melt at 40 °C

C(LiCl) = 1.00 mole %

Concentration (±0.01)* (mole %)	Chemical Shift (±0.02)* (PPM)
0.0	1.35
0.08	1.31
0.23	1.27
0.34	1.23
0.49	1.14
0.55	1.13
0.57	1.08
0.76	1.06
0.82	1.03
1.26	0.93
1.91	0.74
3.08	0.52

*Estimate of error used in the fitting program.

C(LiCl)

Concent

*Estim

^{7}Li Chemical Shifts as a Function of Pentaglyme Concentration in 45 Mole % Melt at 40 °C

C(LiCl) = 0.20 mole %

Concentration (±0.01)* (mole %)	Chemical Shift (±0.02)* (PPM)
0.0	1.60
0.20	1.40
0.22	1.34
0.94	0.90
1.06	0.81
1.93	0.47
2.59	0.32
3.29	0.21
4.08	0.12
4.23	0.12
4.41	0.12
4.49	0.12
5.05	0.08
5.25	0.08
6.20	0.04
6.40	0.01
6.82	0.01

*Estimate of error used in the fitting program.

^{7}Li Chemical Shifts as a Function of 12C4 Concentration in 45 Mole % Melt at 40 °C

C(LiCl) = 1.00 mole %

Concentration (±0.01)* (mole %)	Chemical Shift (±0.02)* (PPM)
0.0	1.35
0.16	1.19
0.49	0.83
0.52	0.84
0.54	0.75
0.60	0.89
0.68	0.73
0.94	0.33
1.00	0.41
1.02	0.28
1.14	0.21
1.19	0.06
1.70	0.04
1.96	0.02
3.67	-0.09
4.37	-0.12
5.14	-0.12
13.23	-0.26

*Estimate of error used in the fitting program.

^{7}Li Chemical Shifts as a Function of Methoxyethoxyethylmonoazo 15C5 Concentration in 45 Mole % Melt at 40 °C

C(LiCl) = 0.70 mole %

Concentration (±0.01)* (mole %)	Chemical Shift (±0.02)* (PPM)
0.0	1.38
0.10	1.16
0.38	1.07
0.51	0.99
0.58	0.94
0.60	0.93
0.63	0.89
0.79	0.88
1.49	-1.33
1.53	-1.34
2.29	-1.44
2.54	-1.45
2.78	-1.42
2.98	-1.44
3.24	-1.42

*Estimate of error used in the fitting program.

^{7}Li Chemical Shifts as a Function of Methoxyethylmonoazo 15C5 Concentration in 45 Mole % Melt at 40 °C

C(LiCl) = 0.70 mole %

Concentration (±0.01)* (mole %)	Chemical Shift (±0.02)* (PPM)
0.0	1.38
0.22	1.20
0.34	1.15
0.53	1.03
0.60	0.82
0.80	0.47
0.82	0.44
0.97	-0.34
1.00	-0.24
1.07	-0.31
1.51	-1.15
2.23	-1.46
2.30	-1.47
2.95	-1.47
3.43	-1.45

*Estimate of error used in the fitting program.

^{7}Li Chemical Shifts as a Function of LiCl Concentration in 45 Mole % Melt at 40 °C

Concentration (±0.00001)* (mole %)	Chemical Shift (±0.05)* (PPM)
0.1062	1.80
0.2243	1.61
0.2646	1.55
0.2972	1.56
0.3634	1.51
0.3989	1.52
0.4006	1.49
0.4412	1.47
0.4808	1.46
0.4910	1.45
0.5194	1.45
0.5651	1.44
0.6211	1.41
0.6677	1.40
0.7203	1.39
0.7258	1.38
0.7903	1.37
0.8450	1.39
0.8929	1.39
0.9507	1.37
1.0192	1.37
1.1131	1.34
1.2319	1.32
1.3128	1.32
1.3993	1.31
1.5051	1.31
1.6136	1.32
1.6975	1.30
1.9363	1.29
1.9608	1.27
1.9737	1.29
2.0099	1.29
2.0434	1.29

*Estimate of error used in the fitting program.

APPENDIX 2
VISCOSITY MEASUREMENTS

Viscosity Measurements for Pyridine and 2-Butanone Solutions at 25 °C

I. $LiClO_4$-Pyridine

Concentration (±0.0001) (M)	η(centapoise)	Time (seconds)
0.0000	0.88(±0.02)	54.71(±0.09)
0.0199	0.88(±0.02)	54.92(±0.02)
0.0800	0.92(±0.02)	57.37(±0.06)
0.9991	0.94(±0.02)	58.42(±0.02)
0.2500	1.04(±0.02)	65.13(±0.05)
0.5470	1.30(±0.02)	81.62(±0.05)

ρ(pyridine)=0.9782 g/cm^3

II. LiCl-Pyridine

Concentration (±0.0001) (M)	η(centapoise)	Time (seconds)
0.0000	0.88(±0.02)	54.71(±0.09)
0.0399	0.88(±0.02)	55.08(±0.08)
0.0800	0.89(±0.02)	55.46(±0.04)
0.2000	0.99(±0.02)	62.0(±0.6)
0.4000	1.06(±0.02)	66.15(±0.03)
0.8080	1.38(±0.03)	86.51(±0.02)

ρ(pyridine)=0.9782 g/cm^3

III. $LiClO_4$-2-Butanone

Concentration (±0.0001) (M)	η(centapoise)	Time (seconds)
0.0000	0.41(±0.01)	31.22(±0.05)
0.0496	0.42(±0.01)	32.15(±0.06)
0.0996	0.43(±0.01)	33.10(±0.05)
0.4980	0.72(±0.01)	54.9(±0.1)
0.9961	0.76(±0.01)	58.0(±0.2)
1.4965	1.10(±0.02)	84.2(±0.1)
2.3166	2.40(±0.04)	183.1(±0.4)

ρ(2-butanone)=0.7997 g/cm^3

(H_2O: Times (seconds)=55.00(±0.01), 53.49(±0.03))

Error in the parenthesis were calculated from several measurements.

APPENDIX 3

ELECTRICAL CONDUCTANCE MEASUREMENTS

Conductance Measurements in Pyridine Solutions at 25 °C

Concentration (M X 10^{+3}) (±0.00003)	Λ (cm^2/ohm mol)	Concentration (M X 10^{+3}) (±0.00003)	Λ (cm^2/ohm mol)
$LiNO_3$		LiCl	
1.43	5.3 (±0.1)	1.30	1.0 (±0.1)
2.00	4.73 (±0.07)	2.00	0.9 (±0.1)
3.00	3.96 (±0.04)	3.00	0.77 (±0.07)
4.00	3.50 (±0.03)	4.00	0.70 (±0.05)
5.00	3.18 (±0.02)	5.00	0.65 (±0.04)
6.00	2.95 (±0.02)	6.00	0.63 (±0.03)
7.00	2.76 (±0.01)	7.00	0.60 (±0.03)
7.80	2.65 (±0.01)	8.00	0.58 (±0.03)
10.14	2.147 (±0.007)	9.92	0.55 (±0.02)
LiSCN		$LiClO_4$	
2.00	5.29 (±0.08)	1.19	44. (±1.)
3.00	4.41 (±0.05)	1.99	39.6 (±0.7)
4.00	3.94 (±0.03)	2.99	36.4 (±0.4)
5.01	3.63 (±0.02)	3.99	34.2 (±0.3)
6.01	3.39 (±0.02)	5.00	32.6 (±0.2)
7.01	3.19 (±0.01)	6.00	31.5 (±0.2)
8.00	3.04 (±0.01)	7.00	30.4 (±0.1)
10.25	2.741 (±0.009)	8.05	29.6 (±0.1)
		9.92	28.86 (±0.09)
LiPi			
2.01	11.9 (±0.2)		
3.03	10.4 (±0.1)		
4.02	9.37 (±0.07)		
5.03	8.67 (±0.05)		
6.04	8.15 (±0.04)		
7.04	7.75 (±0.03)		
8.05	7.42 (±0.03)		
10.06	6.92 (±0.02)		

Conductance Measurements in 2-Butanone Solutions at 25 °C

Concentration (M X 10^{+3}) (±0.00003)	Λ (cm^2/ohm mol)	Concentration (M X 10^{+3}) (±0.00003)	Λ (cm^2/ohm mol)
LiI		$LiAsF_6$	
1.00	111. (±3.)	1.16	122. (±3.)
2.00	100. (±2.)	2.00	116. (±2.)
3.00	94. (±1.)	3.00	111. (±1.)
4.00	88.7 (±0.7)	4.00	107.2 (±0.9)
5.00	85.0 (±0.6)	5.00	104.1 (±0.7)
6.00	82.0 (±0.5)	6.00	102.1 (±0.5)
6.99	75.9 (±0.4)	7.00	100.0 (±0.5)
8.00	73.6 (±0.4)	8.00	98.0 (±0.4)
10.76	66.1 (±0.3)	9.20	96.1 (±0.3)
$LiCF_3CO_2$		$LiBPh_4$	
1.12	7.1 (±0.2)	0.50	90. (±6.)
2.00	6.9 (±0.1)	1.00	86. (±3.)
3.00	6.57 (±0.07)	1.50	84. (±2.)
4.00	6.33 (±0.05)	2.05	79. (±1.)
5.00	6.14 (±0.04)	3.00	78.8 (±0.8)
6.00	5.96 (±0.03)	4.00	76.5 (±0.6)
7.00	5.71 (±0.02)	5.00	74.6 (±0.5)
8.00	5.50 (±0.02)	6.00	73.2 (±0.4)
10.40	5.14 (±0.02)	7.00	71.9 (±0.3)
		8.00	70.2 (±0.3)
		10.14	68.9 (±0.2)
LiSCN		LiPi	
1.25	20.8 (±0.5)	1.00	42. (±1.)
1.99	16.6 (±0.3)	2.01	33.8 (±0.5)
2.99	14.0 (±0.1)	3.01	28.4 (±0.3)
3.98	12.5 (±0.1)	4.01	25.5 (±0.2)
5.08	11.54 (±0.07)	5.01	23.4 (±0.1)
5.77	10.97 (±0.06)	6.01	21.8 (±0.1)
6.77	10.26 (±0.05)	7.04	20.67 (±0.09)
8.06	9.78 (±0.04)	8.04	19.56 (±0.08)
10.06	9.21 (±0.03)	9.80	18.37 (±0.06)

Conductance Measurements in 2-Butanone Solutions at 25 °C

Concentration ($M \times 10^{+3}$) (±0.00003)	Λ (cm^2/ohm mol)
	$LiClO_4$
0.52	113. (±7.)
1.03	104. (±3.)
1.55	97. (±2.)
2.07	93. (±1.)
2.99	87.7 (±0.9)
4.00	82.3 (±0.6)
5.00	78.3 (±0.5)
6.00	75.6 (±0.4)
7.00	72.3 (±0.3)
8.00	70.0 (±0.3)
10.49	65.5 (±0.2)

APPENDIX 4

DESCRIPTION OF COMPUTER PROGRAMS AND SUBROUTINE EQUATIONS

A. Determination of Association Constants by the NMR Technique

The equilibria that describe ionic association in solution are represented by:

$$M^+ + X^- \rightleftharpoons M^+SX^- \rightleftharpoons M^+X^- \rightleftharpoons (MX)_n \qquad \text{(A-1)}$$

which involves the formation of solvent separated ion pairs (M^+SX^-), contact ion pairs (M^+X^-), and aggregates ($(MX)_n$). Chemical shifts or linewidths measurements are sensitive only to the formation of M^+X^- and $(MX)_n$. Therefore, the only equilibrium constants than can be obtained from NMR measurements are:

$$M^+ + X^- \rightleftharpoons M^+X^- \qquad \text{(A-2)}$$

$$M^+SX^- \rightleftharpoons M^+X^- \qquad \text{(A-3)}$$

$$M^+X^- \rightleftharpoons (MX)_n \qquad \text{(A-4)}$$

For ion pairing processes in solutions where both solvent separated ion pairs and free ion exist, the free M^+ concentration is taken as the sum of the concentration of free M^+ and solvent separated ion pairs.

The thermodynamic equilibrium constant for contact ion pairing, represented by equation A-2, can be expressed as:

$$K_a = \frac{a_{M^+X^-}}{a_{M^+}\, a_{X^-}} = \frac{(1 - \alpha)}{C_T \alpha^2 f_\pm^2} \qquad \text{(A-5)}$$

where C_T is the total salt concentration, the $f_\pm$ is the mean activity coefficient for the ions in solution. When the ions exist as solvent separated ion pairs, $f_\pm = 1$. The $f_\pm$ value was calculated using the Debye-Hückel equation:

$$f_\pm = \exp \frac{-4.19764 \times 10^6 \, |Z_+Z_-| \, \sqrt{I}}{(\epsilon T)^{3/2} \left| 1.0 + \frac{50.29 \, a\sqrt{I}}{(\epsilon T)^{1/2}} \right|} \qquad \text{(A-6)}$$

in which Z_+ and Z_- are charges on the ions, ϵ is the dielectric constant of the solvent, T is the absolute temperature, a is the closed distance of approach in Angstroms, and I is the ionic strength of the solution.

The observed chemical shift for the contact ion pairing process has been written as a population average chemical shift which is:

$$\delta_{OBS} = \delta_{M^+}X_{M^+} + \delta_{MX}X_{MX} \qquad \text{(A-7)}$$

where δ_{M^+} and δ_{MX} are the chemical shifts of the free ion and contact ion pair, and X_{M^+} and X_{MX} are the mole fractions of the free ion and contact ion pair. Using the mass balance equations, C_T^M, A-5, and A-6, the concentration of free M^+ (C_{M^+}) can be calculated:

$$C_T^M = C_{M^+} + C_{MX} \qquad \text{(A-8)}$$

$$C_{M^+} = \frac{-1 + \sqrt{1. + 4K_a f_\pm^2 C_T^M}}{2K_a f_\pm^2} \qquad \text{(A-9)}$$

The free M^+ concentration, obtained from equation A-9, is used to calculate the mole ratios of the free ions and ion pair which are then substituted into equation A-7 to produce the chemical shift equation that can be represented by:

$$\delta_{OBS} = \frac{-1. + (1 + 4K_a C_T^M f_\pm^2)^{1/2}}{2K_a C_T^M f_\pm^2} (\delta_f - \delta_{ip}) + \delta_{ip} \qquad \text{(A-10)}$$

where δ_{ip} and δ_f are the chemical shift of the ion pair and free ion, respectively.

For fitting linewidth measurements ($\Delta\nu_{1/2}$), equation A-10 can also be used by substituting linewidths for chemical shifts. Four data sets are used in KINFIT, one for the chemical shifts (ppm) or linewidths, (hz) and another for the molar concentrations. The other two data sets are the variances of the NMR measurements and the concentrations. For two site exchange model, the maximum number of unknowns is four.

$$\begin{aligned} U(1) &= \delta_{M^+} \text{ or } \Delta\nu_{1/2} \qquad & U(4) &= \text{a parameter} \\ U(2) &= \delta_{M^+X^-} \text{ or } \Delta\nu_{1/2} & & \\ U(3) &= K_a & & \end{aligned} \qquad \text{(A-11)}$$

When the chemical shift measurements were fit using four unknowns, a large correlation occurred with the values obtained from the fit. To elliminate this problem, the a parameter was set equal to the Bjerrum distance or the distances determined for the crystallographic radii, which reduces the number of unknowns to three. When linewidths were

available, both chemical shifts and linewidths were fitted simultaneously. This produced a problem with five unknowns. The expression represented by equation A-10 can be used to represent a dimerization process as long as the mean activity coefficient, $f_{\pm}$, is set to one and the mole ratio of the dimers is multiplied by two to account for two Li^+ per dimer.

In some cases, the two site exchange model does not fit the NMR data very well. An additional equilibrium was added and the NMR data was refitted. The mathematical equation for a three site exchange model is represented by a polynomial of higher order than two. A fourth order polynomial is derived by substituting the expressions derived from the equilibrium constants for two of the three terms in the mass balance equation. The EQN subroutine was used to evaluate the roots of a fourth order polynomial. The coefficients of each term of the polynomial starting with the fourth order term are represented in the programs as A1, B, C, D and E. The polynomial program determined the smallest positive root.

```
      SUBROUTINE EQN
      COMMON KOUNT,ITAPE,JTAPE,IWT,LAP,XINCR,NOPT,NOVAR,NOUNK
     1,X,U,ITMAX,WTX,TEST,I,AV,RESID,IAR,EPS,ITYP,XX,RXTYP
     2,DX1I,FOP,FO,FU,P,ZL,TO,EIGVAL,XST,T,DT,L,M,JJJ,Y,DY
     3,VECT,NCST,CONST,NDAT,JDAT,MOPT,LOPT,YYY,CONSTS
      COMMON/FREDT/IMETH
      COMMON/POINT/KOPT,JOPT,XXX
      DIMENSION X(4,300),U(20),WTX(4,300),XX(4),FOP(300)
     1,FO(300),FU(300),P(20,21),VECT(20,21),ZL(300)
     2,TO(20),EIGVAL(20),XST(300),Y(10),DY(10),CONSTS(50,16)
     3,NCST(50),ISMIN(50),RXTYP(50),DX1I(50),IRX(50)
     4,MOPT(50),LOPT(50),YYY(50),CONST(16),XXX(15)
      GO TO (2,3,4,5,1,7,8,9,10,11,12)  ITYP
    1 CONTINUE
      ITAPE=60
      JTAPE=61
      RETURN
    7 CONTINUE
      NOUNK=3
      NOVAR=2
      RETURN
    8 CONTINUE
      RETURN
    2 CONTINUE
C     **********************************
C     TWO SITE EXCHANGE
C     ACTIVITY CORRECTION
C     CONTACT ION PAIRING
C     CHEMICAL SHIFTS
C     LiI, LiBPh4, LiAsF6 IN 2-BUTANONE
C     **********************************
C     U(1)=CHEMICAL SHIFT OF ION PAIR-PPM
C     U(2)=ION PAIRING CONSTANT-M^-1
C     U(3)=CHEMICAL SHIFT OF SOLVATED CATION-PPM
C     **********************************
C     CONST(1)=(DIELECTRIC CONSTANT*TEMPERATURE)**1/2
C     CONST(2)=ION SIZE PARAMETER-ANGSTROM
C     **********************************
C     XX(1)=SALT CONCENTRATION-MOLARITY
C     XX(2)=LITHIUM CHEMICAL SHIFTS-PPM
C     **********************************
C     ALPH=DEGREE OF DISSOCIATION
C     STREN=IONIC STRENGTH
C     GAMA,GAMAN=ACTIVITY COEFFICIENT
C     **********************************
      U(2)=ABS(U(2))
      GAMA=1.0
 1000 CONTINUE
      ARGM=1.0+4.0*U(2)*XX(1)*(GAMA**2.)
```

```
      IF(U(2).EQ.0.0)GO TO 55
      ALPH=(-1.+SQRT(ARGM))/(2.0*U(2)*XX(1)*(GAMA**2.))
      GO TO 58
   55 ALPH=1.0
   58 CONTINUE
      STREN=XX(1)*ALPH
      IF(STREN.LT.0.0)GO TO 100
      GO TO 200
  100 STREN=0.0
  200 CONTINUE
      AA=-4197640.0*SQRT(STREN)
      BB=CONST(1)**3
      CC=1.0+((50.29*CONST(2)*SQRT(STREN))/CONST(1))
      DD=BB*CC
      GAMAN=EXP(AA/DD)
      IF(STREN.EQ.0.0)GO TO 71
      GO TO 72
   71 GAMA=GAMAN
      GO TO 1000
   72 CONTINUE
      IF(GAMAN.LT.0.0)GO TO 300
      IF(GAMAN.EQ.0.0)GO TO 300
      MAR=1
      GO TO 400
  300 GAMAN=0.0
      MAR=0
  400 CONTINUE
      IF(MAR.EQ.0)GO TO 1000
      RAT=((GAMAN-GAMA)/GAMAN)
      RAT=ABS(RAT)
      GAMA=GAMAN
      IF(RAT.GT.0.00001)GO TO 1000
      CONK=U(2)*(GAMA**2.)
      IF(CONK.EQ.0.0)GO TO 31
      F=4.0*CONK*XX(1)
      CALC=(((-1.0+SQRT(1.0+F))*(U(3)-U(1)))/(2.*CONK*XX(1)))+U(1)
      GO TO 37
   31 CALC=U(3)
   37 CONTINUE
      IF(IMETH.NE.-1)GO TO 35
      RETURN
   35 CONTINUE
      RESID=CALC-XX(2)
      IF(LAP.NE.3)GO TO 600
      WRITE(JTAPE,53)XX(1),ALPH,GAMA
   53 FORMAT(5X,3E10.4)
  600 CONTINUE
      RETURN
    3 CONTINUE
```

```
      RETURN
    4 CONTINUE
      RETURN
    5 CONTINUE
      IF(IMETH.NE.-1)GO TO 20
      RETURN
   20 CONTINUE
      RETURN
    9 CONTINUE
      RETURN
   10 CONTINUE
      RETURN
   11 CONTINUE
      RETURN
   12 CONTINUE
      RETURN
   13 CONTINUE
      RETURN
      END
```

```
      SUBROUTINE EQN
      COMMON KOUNT,ITAPE,JTAPE,IWT,LAP,XINCR,NOPT,NOVAR,NOUNK
     1,X,U,ITMAX,WTX,TEST,I,AV,RESID,IAR,EPS,ITYP,XX,RXTYP
     2,DX1I,FOP,FO,FU,P,ZL,TO,EIGVAL,XST,T,DT,L,M,JJJ,Y,DY
     3,VECT,NCST,CONST,NDAT,JDAT,MOPT,LOPT,YYY,CONSTS
      COMMON/FREDT/IMETH
      COMMON/POINT/KOPT,JOPT,XXX
      DIMENSION X(4,300),U(20),WTX(4,300),XX(4),FOP(300)
     1,FO(300),FU(300),P(20,21),VECT(20,21),ZL(300)
     2,TO(20),EIGVAL(20),XST(300),Y(10),DY(10),CONSTS(50,16)
     3,NCST(50),ISMIN(50),RXTYP(50),DX1I(50),IRX(50)
     4,MOPT(50),LOPT(50),YYY(50),CONST(16),XXX(15)
      GO TO (2,3,4,5,1,7,8,9,10,11,12)  ITYP
    1 CONTINUE
      ITAPE=60
      JTAPE=61
      RETURN
    7 CONTINUE
      NOUNK=2
      NOVAR=2
      RETURN
    8 CONTINUE
      RETURN
    2 CONTINUE
C     **********************************
C     TWO SITE EXCHANGE
C     ACTIVITY CORRECTION
C     CONTACT ION PAIRING
C     CHEMICAL SHIFTS
C     LiI IN 2-BUTANONE
C     **********************************
C     U(1)=CHEMICAL SHIFT OF ION PAIR-PPM
C     U(2)=ION PAIRING CONSTANT-M^-1
C     **********************************
C     CONST(1)=(DIELECTRIC CONSTANT*TEMPERATURE)**1/2
C     CONST(2)=ION SIZE PARAMETER-ANGSTROM
C     CONST(3)=CHEMICAL SHIFT OF SOLVATED CATION-PPM
C     **********************************
C     XX(1)=SALT CONCENTRATION-MOLARITY
C     XX(2)=LITHIUM CHEMICAL SHIFTS-PPM
C     **********************************
C     ALPH=DEGREE OF DISSOCIATION
C     STREN=IONIC STRENGTH
C     GAMA,GAMAN=ACTIVITY COEFFICIENT
C     **********************************
      U(2)=ABS(U(2))
      GAMA=1.0
 1000 CONTINUE
      ARGM=1.0+4.0*U(2)*XX(1)*(GAMA**2.)
```

```
      IF(U(2).EQ.0.0)GO TO 55
      ALPH=(-1.+SQRT(ARGM))/(2.0*U(2)*XX(1)*(GAMA**2.))
      GO TO 58
   55 ALPH=1.0
   58 CONTINUE
      STREN=XX(1)*ALPH
      IF(STREN.LT.0.0)GO TO 100
      GO TO 200
  100 STREN=0.0
  200 CONTINUE
      AA=-4197640.0*SQRT(STREN)
      BB=CONST(1)**3
      CC=1.0+((50.29*CONST(2)*SQRT(STREN))/CONST(1))
      DD=BB*CC
      GAMAN=EXP(AA/DD)
      IF(STREN.EQ.0.0)GO TO 71
      GO TO 72
   71 GAMA=GAMAN
      GO TO 1000
   72 CONTINUE
      IF(GAMAN.LT.0.0)GO TO 300
      IF(GAMAN.EQ.0.0)GO TO 300
      MAR=1
      GO TO 400
  300 GAMAN=0.0
      MAR=0
  400 CONTINUE
      IF(MAR.EQ.0)GO TO 1000
      RAT=((GAMAN-GAMA)/GAMAN)
      RAT=ABS(RAT)
      GAMA=GAMAN
      IF(RAT.GT.0.0001)GO TO 1000
      CONK=U(2)*(GAMA**2.)
      IF(CONK.EQ.0.0)GO TO 31
      F=4.0*CONK*XX(1)
      CALC=(((-1.0+SQRT(1.0+F))*(CONST(3)-U(1)))/
     1(2.*CONK*XX(1)))+U(1)
      GO TO 37
   31 CALC=CONST(3)
   37 CONTINUE
      IF(IMETH.NE.-1)GO TO 35
      RETURN
   35 CONTINUE
      RESID=CALC-XX(2)
      IF(LAP.NE.3)GO TO 600
      WRITE(JTAPE,53)XX(1),ALPH,GAMA
   53 FORMAT(5X,3E10.4)
  600 CONTINUE
      RETURN
```

```
  3 CONTINUE
    RETURN
  4 CONTINUE
    RETURN
  5 CONTINUE
    IF(IMETH.NE.-1)GO TO 20
    RETURN
 20 CONTINUE
    RETURN
  9 CONTINUE
    RETURN
 10 CONTINUE
    RETURN
 11 CONTINUE
    RETURN
 12 CONTINUE
    RETURN
 13 CONTINUE
    RETURN
    END
```

```
      SUBROUTINE EQN
      COMMON KOUNT,ITAPE,JTAPE,IWT,LAP,XINCR,NOPT,NOVAR,NOUNK
     1,X,U,ITMAX,WTX,TEST,I,AV,RESID,IAR,EPS,ITYP,XX,RXTYP
     2,DX1I,FOP,FO,FU,P,ZL,TO,EIGVAL,XST,T,DT,L,M,JJJ,Y,DY
     3,VECT,NCST,CONST,NDAT,JDAT,MOPT,LOPT,YYY,CONSTS
      COMMON/FREDT/IMETH
      COMMON/POINT/KOPT,JOPT,XXX
      DIMENSION X(4,300),U(20),WTX(4,300),XX(4),FOP(300)
     1,FO(300),FU(300),P(20,21),VECT(20,21),ZL(300)
     2,TO(20),EIGVAL(20),XST(300),Y(10),DY(10),CONSTS(50,16)
     3,NCST(50),ISMIN(50),RXTYP(50),DX1I(50),IRX(50)
     4,MOPT(50),LOPT(50),YYY(50),CONST(16),XXX(15)
      GO TO (2,3,4,5,1,7,8,9,10,11,12)  ITYP
    1 CONTINUE
      ITAPE=60
      JTAPE=61
      RETURN
    7 CONTINUE
      NOUNK=5
      NOVAR=2
      RETURN
    8 CONTINUE
      RETURN
    2 CONTINUE
C     **********************************
C     TWO SITE EXCHANGE
C     ACTIVITY CORRECTION
C     CONTACT ION PAIRING
C     CHEMICAL SHIFTS AND LINEWIDTHS
C     LiClO4-2-BUTANONE
C     **********************************
C     U(1)=CHEMICAL SHIFT OF ION PAIR-PPM
C     U(2)=CHEMICAL SHIFT OF SOLVATE ION-PPM
C     U(3)=ION PAIRING CONSTANT-M^-1
C     U(4)=LINEWIDTH OF SOLVATED ION-HERTZ
C     U(5)=LINEWIDTH OF ION PAIR-HERTZ
C     **********************************
C     CONSTS(1,1)=CONSTS(2,1)=(DIELECTRIC CONSTANT*TEMPERATURE)**1/2
C     CONSTS(1,2)=CONSTS(2,2)=ION SIZE PARAMETER-ANGSTROM
C     **********************************
C     XX(1)=SALT CONCENTRATION-MOLARITY
C     XX(2)=LITHIUM-7 CHEMICAL SHIFTS-DATA SET 1-PPM
C     XX(2)=CHLORINE-35 LINEWIDTHS-DATA SET 2-HERTZ
C     **********************************
C     ALPH=DEGREE OF DISSOCIATION
C     STREN=IONIC STRENGTH
C     GAMA,GAMAN= ACTIVITY COEFFICIENT
C     **********************************
      U(3)=ABS(U(3))
```

```
      GAMA=1.0
      GO TO (1000,1001)JDAT
1000  CONTINUE
      AA1=CONSTS(1,1)
      BB1=CONSTS(1,2)
      CC1=U(2)
      DD1=U(1)
      GO TO 500
1001  CONTINUE
      AA1=CONSTS(2,1)
      BB1=CONSTS(2,2)
      CC1=U(4)
      DD1=U(5)
500   CONTINUE
      ARGM=1.0+4.0*U(3)*XX(1)*(GAMA**2.0)
      IF(U(3).EQ.0.0)GO TO 55
      ALPH=(-1.0+SQRT(ARGM))/(2.0*U(3)*XX(1)*(GAMA**2.))
      GO TO 58
   55 ALPH=1.0
   58 CONTINUE
      STREN=XX(1)*ALPH
      IF(STREN.LT.0.0)GO TO 100
      GO TO 200
  100 STREN=0.0
  200 CONTINUE
      AA=-4197640.0*SQRT(STREN)
      BB=AA1**3
      CC=1.0+((50.29*BB1*SQRT(STREN))/AA1)
      DD=BB*CC
      GAMAN=EXP(AA/DD)
      IF(STREN.EQ.0.0)GO TO 71
      GO TO 72
   71 GAMA=GAMAN
      GO TO 1000
   72 CONTINUE
      IF(GAMAN.LT.0.0)GO TO 300
      IF(GAMAN.EQ.0.0)GO TO 300
      MAR=1
      GO TO 400
  300 GAMAN=0.0
      MAR=0
  400 CONTINUE
      IF(MAR.EQ.0)GO TO 1000
      RAT=((GAMAN-GAMA)/GAMAN)
      RAT=ABS(RAT)
      GAMA=GAMAN
      IF(RAT.GT.0.00001)GO TO 500
      CONK=U(3)*(GAMA**2)
      IF(CONK.EQ.0.0)GO TO 31
```

```
      F=4.0*CONK*XX(1)
      CALC=(((-1.0+SQRT(1.0+F))*(CC1-DD1))/(2.0*CONK*XX(1)))+DD1
      GO TO 37
   31 CALC=CC1
   37 CONTINUE
      IF(IMETH.NE.-1)GO TO 35
      RETURN
   35 CONTINUE
      RESID=CALC-XX(2)
      RETURN
    3 CONTINUE
      RETURN
    4 CONTINUE
      RETURN
    5 CONTINUE
      IF(IMETH.NE.-1)GO TO 20
      RETURN
   20 CONTINUE
      RETURN
    9 CONTINUE
      RETURN
   10 CONTINUE
      RETURN
   11 CONTINUE
      RETURN
   12 CONTINUE
      RETURN
   13 CONTINUE
      RETURN
      END
```

```
      SUBROUTINE EQN
      COMMON KOUNT,ITAPE,JTAPE,IWT,LAP,XINCR,NOPT,NOVAR,NOUNK
     1,X,U,ITMAX,WTX,TEST,I,AV,RESID,IAR,EPS,ITYP,XX,RXTYP
     2,DX1I,FOP,FO,FU,P,ZL,TO,EIGVAL,XST,T,DT,L,M,JJJ,Y,DY
     3,VECT,NCST,CONST,NDAT,JDAT,MOPT,LOPT,YYY,CONSTS
      COMMON/FREDT/IMETH
      COMMON/POINT/KOPT,JOPT,XXX
      DIMENSION X(4,300),U(20),WTX(4,300),XX(4),FOP(300)
     1,FO(300),FU(300),P(20,21),VECT(20,21),ZL(300)
     2,TO(20),EIGVAL(20),XST(300),Y(10),DY(10),CONSTS(50,16)
     3,NCST(50),ISMIN(50),RXTYP(50),DX1I(50),IRX(50)
     4,MOPT(50),LOPT(50),YYY(50),CONST(16),XXX(15)
      GO TO (2,3,4,5,1,7,8,9,10,11,12)  ITYP
    1 CONTINUE
      ITAPE=60
      JTAPE=61
      RETURN
    7 CONTINUE
      NOUNK=4
      NOVAR=2
      RETURN
    8 CONTINUE
      RETURN
    2 CONTINUE
C     **********************************
C     TWO SITE EXCHANGE
C     ACTIVITY CORRECTION
C     CONTACT ION PAIRING
C     CHEMICAL SHIFTS AND LINEWIDTHS
C     LiClO4-2-BUTANONE
C     **********************************
C     U(1)=CHEMICAL SHIFT OF ION PAIR-PPM
C     U(2)=ION PAIRING CONSTANT-M-1
C     U(3)=LINEWIDTH OF SOLVATED ION-HERTZ
C     U(4)=LINEWIDTH OF ION PAIR-HERTZ
C     **********************************
C     CONSTS(1,1)=CONSTS(1,2)=(DIELECTRIC CONSTANT*TEMPERATURE)**1/2
C     CONSTS(2,1)=CONSTS(2,2)=ION SIZE PARAMETER-ANGSTROM
C     CONSTS(3,1)=CHEMICAL SHIFT OF SOLVATED CATION-PPM
C     **********************************
C     XX(1)=SALT CONCENTRATION-MOLARITY
C     XX(2)=LITHIUM-7 CHEMICAL SHIFTS-DATA SET 1-PPM
C     XX(2)=CHLORINE-35 LINEWIDTHS-DATA SET 2-HERTZ
C     **********************************
C     ALPH=DEGREE OF DISSOCIATION
C     STREN=IONIC STRENGTH
C     GAMA,GAMAN= ACTIVITY COEFFICIENT
C     **********************************
      U(2)=ABS(U(2))
      GAMA=1.0
```

```
      GO TO (1000,1001)JDAT
1000  CONTINUE
      AA1=CONSTS(1,1)
      BB1=CONSTS(1,2)
      CC1=CONSTS(1,3)
      DD1=U(1)
      GO TO 500
1001  CONTINUE
      AA1=CONSTS(2,1)
      BB1=CONSTS(2,2)
      CC1=U(3)
      DD1=U(4)
500   CONTINUE
      ARGM=1.0+4.0*U(2)*XX(1)*(GAMA**2.0)
      IF(U(2).EQ.0.0)GO TO 55
      ALPH=(-1.0+SQRT(ARGM))/(2.0*U(2)*XX(1)*(GAMA**2.))
      GO TO 58
   55 ALPH=1.0
   58 CONTINUE
      STREN=XX(1)*ALPH
      IF(STREN.LT.0.0)GO TO 100
      GO TO 200
  100 STREN=0.0
  200 CONTINUE
      AA=-4197640.0*SQRT(STREN)
      BB=AA1**3
      CC=1.0+((50.29*BB1*SQRT(STREN))/AA1)
      DD=BB*CC
      GAMAN=EXP(AA/DD)
      IF(STREN.EQ.0.0)GO TO 71
      GO TO 72
   71 GAMA=GAMAN
      GO TO 1000
   72 CONTINUE
      IF(GAMAN.LT.0.0)GO TO 300
      IF(GAMAN.EQ.0.0)GO TO 300
      MAR=1
      GO TO 400
  300 GAMAN=0.0
      MAR=0
  400 CONTINUE
      IF(MAR.EQ.0)GO TO 1000
      RAT=((GAMAN-GAMA)/GAMAN)
      RAT=ABS(RAT)
      GAMA=GAMAN
      IF(RAT.GT.0.000001)GO TO 500
      CONK=U(2)*(GAMA**2)
      IF(CONK.EQ.0.0)GO TO 31
      F=4.0*CONK*XX(1)
```

```
      CALC=(((-1.0+SQRT(1.0+F))*(CC1-DD1))/(2.0*CONK*XX(1)))+DD1
      GO TO 37
   31 CALC=CC1
   37 CONTINUE
      IF(IMETH.NE.-1)GO TO 35
      RETURN
   35 CONTINUE
      RESID=CALC-XX(2)
      RETURN
    3 CONTINUE
      RETURN
    4 CONTINUE
      RETURN
    5 CONTINUE
      IF(IMETH.NE.-1)GO TO 20
      RETURN
   20 CONTINUE
      RETURN
    9 CONTINUE
      RETURN
   10 CONTINUE
      RETURN
   11 CONTINUE
      RETURN
   12 CONTINUE
      RETURN
   13 CONTINUE
      RETURN
      END
```

```
      SUBROUTINE EQN
      COMMON KOUNT,ITAPE,JTAPE,IWT,LAP,XINCR,NOPT,NOVAR
     1,NOUNK,X,U,ITMAX,WTX,TEST,I,AV,RESID,IAR,EPS,
     2ITYP,XX,RXTYP,DX1I,FOP,FO,FU,P,ZL,TO,EIGVAL
     3,XST,T,DT,L,M,JJJ,Y,DY,VECT,NCST,CONST,NDAT
     4,JDAT,MOPT,LOPT,3YYY,CONSTS
      COMMON/FREDT/IMETH
      COMMON/POINT/KOPT,JOPT,XXX
      DIMENSION X(4,300),U(20),WTX(4,300),XX(4),FOP(300)
     1,FO(300),FU(300)1,P(20,21),VECT(20,21),ZL(300),TO(20)
     2,EIGVAL(20),XST(300),Y(10),DY(10),CONSTS(50,16)
     3,NCST(50),ISMIN(50),RXTYP(50),DX1I(50)
     4,IRX(50),MOPT(50),LOPT(50),YYY(50),CONST(16),XXX(15)
      GO TO (2,3,4,5,1,7,8,9,10,11,12)  ITYP
    1 CONTINUE
      ITAPE=60
      JTAPE=61
      RETURN
    7 CONTINUE
      NOUNK=5
      NOVAR=2
      RETURN
    8 CONTINUE
      RETURN
    2 CONTINUE
C     ********************************************
C     TWO SITE EXCHANGE
C     NO ACTIVITY CORRECTION
C     CONTACT ION PAIRING
C     CHEMICAL SHIFTS AND LINEWIDTHS
C     LiClO4-PYRIDINE
C     SOLUTION TO A SECOND ORDER POLYNOMIAL
C     ********************************************
C     U(1)=ION PAIRING CONSTANT-M^-1
C     U(2)=CHEMICAL SHIFT OF CONTACT ION PAIR-PPM
C     U(3)=LINEWIDTH OF SOLVATED ION-HERTZ
C     U(4)=LINEWIDTH OF CONTACT ION PAIR-HERTZ
C     U(5)=CHEMICAL SHIFT OF SOLVATED ION-PPM
C     ********************************************
C     XX(1)=SALT CONCENTRATION-MOLARITY
C     XX(2)=LITHIUM-7 CHEM SHIFTS-DATA SET I-PPM
C     XX(3)=CHLORINE-35 LINEWIDTHS-DATA SET II-HERTZ
C     ********************************************
C     FREEL=FREE LITHIUM ION CONCENTRATION
C     LFLAG=FLAG
C     FLAG=FLAG
C     XMAR=INCREMENT FOR INTERVAL
C     XCON=CONTROLS INTERVAL FOR FREEL AXIS
C     A1,B,C,D,E=COEFFICIENTS IN POLYNOMIAL
```

```
C     ************************************************
      U(1)=ABS(U(1))
      IF(U(2).LT.-3.0)U(2)=-3.0
      IF(U(3).LT. 0.0)U(3)=0.0
      VALUE3=1.0
      LFLAG=0
      XCON=5.0
      FLAG=0.0
      XMAR=10.0
 1000 CONTINUE
C     ******************************************
C     ENTERING COEFFICIENTS
C     ******************************************
      A1=0.0
      B=0.0
      C=U(1)/XX(1)
      D=1.0/XX(1)
      E=-1.0
  573 CONTINUE
      VALUE1=XX(1)
      FREEL0=0.0
      FREEL1=0.00
      VALUE1=E
      XVAL=(ABS(E)/C)**0.5
      FREEL2=XVAL/XCON
 2005 CONTINUE
      VALUE2=A1*(FREEL2**4.0)+B*(FREEL2**3.0)+C*(FREEL2**2.0)
     1+D*(FREEL2)+E
      IF(LFLAG.EQ.1)GO TO 81
      IF(VALUE2.LT.0.0)GO TO 2000
      GO TO 82
   81 IF(VALUE2.GT.0.0)GO TO 2000
   82 CONTINUE
      IF(VALUE2.EQ.0.0)GO TO 2001
 2004 CONTINUE
      LFLAG=0
      FLAG=0.0
      FREEL3=(FREEL2-FREEL1)/(VALUE1-VALUE2)*VALUE1+FREEL1
      IF(ABS((FREEL3-FREEL0)/FREEL3).LT.0.0000001)GO TO 2002
      VALUE5=A1*(FREEL3**4.0)+B*(FREEL3**3.0)+C*(FREEL3**2.0)
     1+D*(FREEL3)+E
      VALUE6=VALUE5-VALUE3
      RAT=ABS(VALUE6/VALUE3)
      VALUE3=VALUE5
      VALUE4=ABS(VALUE5)
      IF(VALUE4.GT.0.0000001)GO TO 91
      XCON=5.0
      IF(RAT.LT.0.000000001)GO TO 2002
      IF(VALUE3.LT.0.0)GO TO 2003
```

```
      VALUE2=VALUE3
      FREEL2=FREEL3
      FREEL0=FREEL3
      GO TO 2004
2003  CONTINUE
      VALUE1=VALUE3
      FREEL1=FREEL3
      GO TO 2004
2000  CONTINUE
      FREELL=FREEL1
      VALUELL=VALUE1
      VALUE1=VALUE2
      FREEL1=FREEL2
      IF(LFLAG.EQ.1)GO TO 89
      IF(VALUELL.GT.VALUE1)GO TO 2220
      IF(FLAG.EQ.1.0)GO TO 2225
   89 CONTINUE
      IF(LFLAG.EQ.0)GO TO 85
      FREEL2=FREEL1-XVAL/XCON
      GO TO 86
   85 CONTINUE
      FREEL2=FREEL1+XVAL/XCON
   86 CONTINUE
      IF(FREEL1.GT.XX(1))GO TO 2006
      GO TO 2005
2220  DEL=(ABS(FREELL-FREEL1))/XMAR
      XMAR=XMAR*10.0
      FREEL2=FREELL+DEL
      FREEL1=FREELL
      VALUE1=VALUELL
      FLAG=1.0
      GO TO 2005
2225  DEL=DEL/5.0
      XMAR=10.0
      FREEL2=FREEL1+DEL
      GO TO 2005
2001  CONTINUE
      FREEL=FREEL2
      GO TO 95
   91 CONTINUE
      XCON=XCON*5.0
      IF(VALUE3.LT.0.0)GO TO 21
      LFLAG=1
      FREEL1=FREEL3
      VALUE1=VALUE3
      FREEL2=FREEL1-XVAL/XCON
      GO TO 2005
   21 FREEL1=FREEL3
      VALUE1=VALUE3
```

```
      FREEL2=FREEL1+XVAL/XCON
      GO TO 2005
 2002 CONTINUE
      FREEL=FREEL3
   95 CONTINUE
      TOTAL=XX(1)
      XF=FREEL/TOTAL
      XIP=1.0-XF
      GO TO 574
 2006 CONTINUE
      WRITE(JTAPE,996)
  996 FORMAT(5X,50H**********************
     1 WARNING **********************,/,
     215X,50H************ NO POSITIVE "VALUE" FOUND *************)
 2008 CONTINUE
      FREEL=0.0
  574 CONTINUE
      GO TO (111,1112) JDAT
  111 CALC=(U(5)-U(2))*XF+U(2)
      GO TO 36
 1112 CALC=(U(3)-U(4))*XF+U(4)
   36 CONTINUE
      IF(IMETH.NE.-1)GO TO 35
      RETURN
   35 CONTINUE
      RESID=CALC-XX(2)
      RETURN
    3 CONTINUE
      RETURN
    4 CONTINUE
      RETURN
    5 CONTINUE
      IF(IMETH.NE.-1)GO TO 20
      RETURN
   20 CONTINUE
      RETURN
    9 CONTINUE
      RETURN
   10 CONTINUE
      RETURN
   11 CONTINUE
      RETURN
   12 CONTINUE
      RETURN
   13 CONTINUE
      RETURN
      END
```

```
      SUBROUTINE EQN
      COMMON KOUNT,ITAPE,JTAPE,IWT,LAP,XINCR,NOPT,NOVAR
     1,NOUNK,X,U,ITMAX,WTX,TEST,I,AV,RESID,IAR,EPS,
     2ITYP,XX,RXTYP,DX1I,FOP,FO,FU,P,ZL,TO,EIGVAL
     3,XST,T,DT,L,M,JJJ,Y,DY,VECT,NCST,CONST,NDAT
     4,JDAT,MOPT,LOPT,3YYY,CONSTS
      COMMON/FREDT/IMETH
      COMMON/POINT/KOPT,JOPT,XXX
      DIMENSION X(4,300),U(20),WTX(4,300),XX(4),FOP(300)
     1,FO(300),FU(300)1,P(20,21),VECT(20,21),ZL(300),TO(20)
     2,EIGVAL(20),XST(300),Y(10),DY(10),CONSTS(50,16)
     3,NCST(50),ISMIN(50),RXTYP(50),DX1I(50)
     4,IRX(50),MOPT(50),LOPT(50),YYY(50),CONST(16),XXX(15)
      GO TO (2,3,4,5,1,7,8,9,10,11,12)  ITYP
    1 CONTINUE
      ITAPE=60
      JTAPE=61
      RETURN
    7 CONTINUE
      NOUNK=8
      NOVAR=2
      RETURN
    8 CONTINUE
      RETURN
    2 CONTINUE
C     **********************************************
C     THREE SITE EXCHANGE
C     NO ACTIVITY CORRECTION
C     CONTACT ION PAIRING AND DIMERIZATION
C     CHEMICAL SHIFTS AND LINEWIDTHS
C     LiClO4-PYRIDINE
C     SOLUTIONS TO A FOURTH ORDER POLYNOMIAL
C     **********************************************
C     U(1)=ION PAIRING CONSTANT-M^-1
C     U(2)=DIMERIZATION CONSTANT-M^-1
C     U(3)=CHEMICAL SHIFT OF ION PAIR-PPM
C     U(4)=CHEMICAL SHIFT OF DIMER-PPM
C     U(5)=LINEWIDTH OF SOLVATED ANION-HERTZ
C     U(6)=LINEWIDTH OF ION PAIR-HERTZ
C     U(7)=LINEWIDTH OF DIMER-HERTZ
C     U(8)=CHEMICAL SHIFT OF SOLVATED CATION-PPM
C     **********************************************
C     XX(1)=SALT CONCENTRATION-MOLARITY
C     XX(2)=LITHIUM-7 CHEM SHIFTS-DATA SET I-PPM
C     XX(3)=CHLORINE-35 LINEWIDTHS-DATA SET II-HERTZ
C     **********************************************
C     FREEL=FREE LITHIUM ION CONCENTRATION
C     LFLAG=FLAG
C     FLAG=FLAG
```

```
C      XMAR=INCREMENT FOR INTERVAL
C      XCON=CONTROLS INTERVAL FOR FREEL AXIS
C      A1,B,C,D,E=COEFFICIENTS IN POLYNOMIAL
C      ***********************************************
       U(1)=ABS(U(1))
       U(2)=ABS(U(2))
       IF(U(2).GT.U(1))U(1)=U(2)
       IF(U(4).LT.-3.0)U(4)=-3.0
       IF(U(3).LT.-3.0)U(3)=-3.0
       IF(U(4).GT.U(3))U(4)=U(3)
       IF(U(5).LT.0.0)U(5)=0.0
       VALUE3=1.0
       LFLAG=0
       XCON=5.0
       FLAG=0.0
       XMAR=10.0
 1000 CONTINUE
C      *****************************************
C      ENTERING COEFFICIENTS
C      *****************************************
       A1=(2.*U(2)*(U(1)**2))/XX(1)
       B=0.0
       C=U(1)/XX(1)
       D=1.0/XX(1)
       E=-1.0
  573 CONTINUE
       VALUE1=XX(1)
       FREEL0=0.00
       FREEL1=0.00
       VALUE1=E
       XVAL=(ABS(E)/C)**0.5
       FREEL2=XVAL/XCON
 2005 CONTINUE
       VALUE2=A1*(FREEL2**4.0)+B*(FREEL2**3.0)+C*(FREEL2**2.0)
      1+D*(FREEL2)+E
       IF(LFLAG.EQ.1)GO TO 81
       IF(VALUE2.LT.0.0)GO TO 2000
       GO TO 82
   81 IF(VALUE2.GT.0.0)GO TO 2000
   82 CONTINUE
       IF(VALUE2.EQ.0.0)GO TO 2001
 2004 CONTINUE
       LFLAG=0
       FLAG=0.0
       FREEL3=(FREEL2-FREEL1)/(VALUE1-VALUE2)*VALUE1+FREEL1
       IF(ABS((FREEL3-FREEL0)/FREEL3).LT.0.0000001)GO TO 2002
       VALUE5=A1*(FREEL3**4.0)+B*(FREEL3**3.0)+C*(FREEL3**2.0)
      1+D*(FREEL3)+E
       VALUE6=VALUE5-VALUE3
```

```
      RAT=ABS(VALUE6/VALUE3)
      VALUE3=VALUE5
      VALUE4=ABS(VALUE5)
      IF(VALUE4.GT.0.0000001)GO TO 91
      XCON=5.0
      IF(RAT.LT.0.000000001)GO TO 2002
      IF(VALUE3.LT.0.0)GO TO 2003
      VALUE2=VALUE3
      FREEL2=FREEL3
      FREEL0=FREEL3
      GO TO 2004
2003  CONTINUE
      VALUE1=VALUE3
      FREEL1=FREEL3
      GO TO 2004
2000  CONTINUE
      FREELL=FREEL1
      VALUELL=VALUE1
      VALUE1=VALUE2
      FREEL1=FREEL2
      IF(LFLAG.EQ.1)GO TO 89
      IF(VALUELL.GT.VALUE1)GO TO 2220
      IF(FLAG.EQ.1.0)GO TO 2225
   89 CONTINUE
      IF(LFLAG.EQ.0)GO TO 85
      FREEL2=FREEL1-XVAL/XCON
      GO TO 86
   85 CONTINUE
      FREEL2=FREEL1+XVAL/XCON
   86 CONTINUE
      IF(FREEL1.GT.XX(1))GO TO 2006
      GO TO 2005
2220  DEL=(ABS(FREELL-FREEL1))/XMAR
      XMAR=XMAR*10.0
      FREEL2=FREELL+DEL
      FREEL1=FREELL
      VALUE1=VALUELL
      FLAG=1.0
      GO TO 2005
2225  DEL=DEL/5.0
      XMAR=10.0
      FREEL2=FREEL1+DEL
      GO TO 2005
2001  CONTINUE
      FREEL=FREEL2
      GO TO 95
   91 CONTINUE
      XCON=XCON*5.0
      IF(VALUE3.LT.0.0)GO TO 21
```

```
      LFLAG=1
      FREEL1=FREEL3
      VALUE1=VALUE3
      FREEL2=FREEL1-XVAL/XCON
      GO TO 2005
   21 FREEL1=FREEL3
      VALUE1=VALUE3
      FREEL2=FREEL1+XVAL/XCON
      GO TO 2005
 2002 CONTINUE
      FREEL=FREEL3
   95 CONTINUE
      TOTAL=XX(1)
      XF=FREEL/TOTAL
      XIP=(U(1)*(FREEL**2))/TOTAL
      GO TO 574
 2006 CONTINUE
      WRITE(JTAPE,996)
  996 FORMAT(5X,50H********************* WARNING
     1 **********************,/,
     215X,50H************ NO POSITIVE "VALUE" FOUND *************)
 2008 CONTINUE
      FREEL=0.0
  574 CONTINUE
      GO TO (111,1112) JDAT
  111 CALC=(U(8)-U(4))*XF+(U(3)-U(4))*XIP+U(4)
      GO TO 36
 1112 CALC=XF*(U(5)-U(7))+XIP*(U(6)-U(7))+U(7)
   36 CONTINUE
      IF(IMETH.NE.-1)GO TO 35
      RETURN
   35 CONTINUE
      RESID=CALC-XX(2)
      RETURN
    3 CONTINUE
      RETURN
    4 CONTINUE
      RETURN
    5 CONTINUE
      IF(IMETH.NE.-1)GO TO 20
      RETURN
   20 CONTINUE
      RETURN
    9 CONTINUE
      RETURN
   10 CONTINUE
      RETURN
   11 CONTINUE
      RETURN
```

```
12 CONTINUE
   RETURN
13 CONTINUE
   RETURN
   END
```

```
      SUBROUTINE EQN
      COMMON KOUNT,ITAPE,JTAPE,IWT,LAP,XINCR,NOPT,NOVAR
     1,NOUNK,X,U,ITMAX,WTX,TEST,I,AV,RESID,IAR,EPS
     2,ITYP,XX,RXTYP,DX1I,FOP,FO,FU,P,ZL,TO,EIGVAL
     3,XST,T,DT,L,M,JJJ,Y,DY,VECT,NCST,CONST,NDAT
     4,JDAT,MOPT,LOPT,YYY,CONSTS
      COMMON/FREDT/IMETH
      COMMON/POINT/KOPT,JOPT,XXX
      DIMENSION X(4,300),U(20),WTX(4,300),XX(4),FOP(300)
     1,FO(300),FU(300),P(20,21),VECT(20,21),ZL(300),TO(20)
     2,EIGVAL(20),XST(300),Y(10),DY(10),CONSTS(50,16)
     3,NCST(50),ISMIN(50),RXTYP(50),DX1I(50)
     4,IRX(50),MOPT(50),LOPT(50),YYY(50),CONST(16),XXX(15)
      GO TO (2,3,4,5,1,7,8,9,10,11,12)  ITYP
    1 CONTINUE
      ITAPE=60
      JTAPE=61
      RETURN
    7 CONTINUE
      NOUNK=7
      NOVAR=2
      RETURN
    8 CONTINUE
      RETURN
    2 CONTINUE
C     ********************************************
C     THREE SITE EXCHANGE
C     WITH ACTIVITY CORRECTION
C     CONTACT ION PAIRING AND DIMERIZATION
C     CHEMICAL SHIFTS AND LINEWIDTHS
C     LiClO4-2-BUTANONE
C     SOLUTIONS TO A FOURTH ORDER POLYNOMIAL
      ********************************************
C     U(1)=ION PAIRING CONSTANT-M^-1
C     U(2)=DIMERIZATION CONSTANT-M^-1
C     U(3)=CHEMICAL SHIFT OF ION PAIR-PPM
C     U(4)=CHEMICAL SHIFT OF DIMER-PPM
C     U(5)=LINEWIDTH OF SOLVATED ANION-HERTZ
C     U(6)=LINEWIDTH OF ION PAIR-HERTZ
C     U(7)=LINEWIDTH OF DIMER-HERTZ
C     ********************************************
C     CONSTS(1,1)=CONSTS(2,1)=(DIELECTRIC CONSTANT*TEMPERATURE)**1/2
C     CONSTS(1,2)=CONSTS(2,2)=ION SIZE PARAMETER-ANGSTROM
C     CONSTS(1,3)=CHEMICAL SHIFT OF SOLVATED CATION-PPM
C     ********************************************
C     XX(1)=SALT CONCENTRATION-MOLARITY
C     XX(2)=LITHIUM-7 CHEM SHIFTS-DATA SET I-PPM
C     XX(2)=CHLORINE-35 LINEWIDTHS-DATA SET II-HERTZ
C     ********************************************
```

```
C     FREEL=FREE LITHIUM ION CONCENTRATION
C     LFLAG=FLAG
C     FLAG=FLAG
C     XMAR=INCREMENT FOR INTERVAL
C     XCON=CONTROLS INTERVAL FOR FREEL AXIS
C     A1,B,C,D,E=COEFFICIENTS IN POLYNOMIAL
C     ********************************************
      U(1)=ABS(U(1))
      U(2)=ABS(U(2))
      IF(U(2).GT.U(1))U(1)=U(2)
      IF(U(3).LT.-3.0)U(3)=-3.0
      IF(U(4).LT.-3.0)U(4)=-3.0
      IF(U(4).GT.U(3))U(4)=U(3)
      IF(U(5).LT.0.0)U(5)=0.0
      GAMA=1.0
      VALUE3=1.0
      LFLAG=0
      XCON=5.0
      FLAG=0.0
      XMAR=10.0
 1000 CONTINUE
C     ************************************
C     ENTERING COEFFICIENTS FOR POLYNOMIAL
C     ************************************
      A1=(2.*U(2)*(U(1)**2))/XX(1)
      B=0.0
      C=U(1)/XX(1)
      D=1.0/XX(1)
      E=-1.0
  573 CONTINUE
      VALUE1=XX(1)
      FREEL0=0.0
      FREEL1=0.00
      VALUE1=E
      XVAL=(ABS(E)/C)**0.5
      FREEL2=XVAL/XCON
 2005 CONTINUE
      VALUE2=A1*(FREEL2**4.0)+B*(FREEL2**3.0)+C*(FREEL2**2.0)
     1+D*(FREEL2)+E
      IF(LFLAG.EQ.1)GO TO 81
      IF(VALUE2.LT.0.0)GO TO 2000
      GO TO 82
   81 IF(VALUE2.GT.0.0)GO TO 2000
   82 CONTINUE
      IF(VALUE2.EQ.0.0)GO TO 2001
 2004 CONTINUE
      LFLAG=0
      FLAG=0.0
      FREEL3=(FREEL2-FREEL1)/(VALUE1-VALUE2)*VALUE1+FREEL1
```

```
      IF(ABS((FREEL3-FREEL0)/FREEL3).LT.0.0000001)GO TO 2002
      VALUE5=A1*(FREEL3**4.0)+B*(FREEL3**3.0)+C*(FREEL3**2.0)
     1+D*(FREEL3)+E
      VALUE6=VALUE5-VALUE3
      RAT=ABS(VALUE6/VALUE3)
      VALUE3=VALUE5
      VALUE4=ABS(VALUE5)
      IF(VALUE4.GT.0.0000001)GO TO 91
      XCON=5.0
      IF(RAT.LT.0.000000001)GO TO 2002
      IF(VALUE3.LT.0.0)GO TO 2003
      VALUE2=VALUE3
      FREEL2=FREEL3
      FREEL0=FREEL3
      GO TO 2004
2003  CONTINUE
      VALUE1=VALUE3
      FREEL1=FREEL3
      GO TO 2004
2000  CONTINUE
      FREELL=FREEL1
      VALUELL=VALUE1
      VALUE1=VALUE2
      FREEL1=FREEL2
      IF(LFLAG.EQ.1)GO TO 89
      IF(VALUELL.GT.VALUE1)GO TO 2220
      IF(FLAG.EQ.1.0)GO TO 2225
   89 CONTINUE
      IF(LFLAG.EQ.0)GO TO 85
      FREEL2=FREEL1-XVAL/XCON
      GO TO 86
   85 CONTINUE
      FREEL2=FREEL1+XVAL/XCON
   86 CONTINUE
      IF(FREEL1.GT.XX(1))GO TO 2006
      GO TO 2005
2220  DEL=(ABS(FREELL-FREEL1))/XMAR
      XMAR=XMAR*10.0
      FREEL2=FREELL+DEL
      FREEL1=FREELL
      VALUE1=VALUELL
      FLAG=1.0
      GO TO 2005
2225  DEL=DEL/5.0
      XMAR=10.0
      FREEL2=FREEL1+DEL
      GO TO 2005
2001  CONTINUE
      FREEL=FREEL2
```

```
      GO TO 95
   91 CONTINUE
      XCON=XCON*5.0
      IF(VALUE3.LT.0.0)GO TO 21
      LFLAG=1
      FREEL1=FREEL3
      VALUE1=VALUE3
      FREEL2=FREEL1-XVAL/XCON
      GO TO 2005
   21 FREEL1=FREEL3
      VALUE1=VALUE3
      FREEL2=FREEL1+XVAL/XCON
      GO TO 2005
 2002 CONTINUE
      FREEL=FREEL3
   95 CONTINUE
      GO TO (114,113) JDAT
  113 BB1=CONSTS(2,1)
      AA1=CONSTS(2,2)
      GO TO 49
  114 BB1=CONSTS(1,1)
      AA1=CONSTS(1,2)
   49 CONTINUE
      ALPH=FREEL/XX(1)
      STREN=XX(1)*ALPH
      AA=-4197640.0*SQRT(STREN)
      BB=AA1**3
      CC=1.0+((50.29*BB1*SQRT(STREN))/AA1)
      DD=BB*CC
      GAMAN=EXP(AA/DD)
      GAMA=GAMAN
      FREEL=FREEL/(GAMA)
      CONK=U(1)*(GAMA**2.0)
      FRIP=CONK*(FREEL**2.0)
      TOTAL=XX(1)
      XF=FREEL/TOTAL
      XIP=FRIP/XX(1)
      GO TO 574
 2006 CONTINUE
      WRITE(JTAPE,996)
  996 FORMAT(5X,50H********************** WARNING
     1 **********************,/,15X,50H************ NO POSITIVE "VALUE"
     2 FOUND ************)
 2008 CONTINUE
      FREEL=0.0
  574 CONTINUE
      GO TO (111,1112) JDAT
  111 CALC=(CONSTS(1,3)-U(4))*XF+(U(3)-U(4))*XIP+U(4)
      GO TO 36
```

```
1112 CALC=XF*(U(5)-U(7))+XIP*(U(6)-U(7))+U(7)
  36 CONTINUE
     IF(IMETH.NE.-1)GO TO 35
     RETURN
  35 CONTINUE
     RESID=CALC-XX(2)
     RETURN
   3 CONTINUE
     RETURN
   4 CONTINUE
     RETURN
   5 CONTINUE
     IF(IMETH.NE.-1)GO TO 20
     RETURN
  20 CONTINUE
     RETURN
   9 CONTINUE
     RETURN
  10 CONTINUE
     RETURN
  11 CONTINUE
     RETURN
  12 CONTINUE
     RETURN
  13 CONTINUE
     RETURN
     END
```

```
      SUBROUTINE EQN
      COMMON KOUNT,ITAPE,JTAPE,IWT,LAP,XINCR,NOPT,NOVAR,NOUNK
     1,X,U,ITMAX,WTX,TEST,I,AV,RESID,IAR,EPS,ITYP,XX,RXTYP
     2,DX1I,FOP,FO,FU,P,ZL,TO,EIGVAL,XST,T,DT,L,M,JJJ,Y,DY
     3,VECT,NCST,CONST,NDAT,JDAT,MOPT,LOPT,YYY,CONSTS
      COMMON/FREDT/IMETH
      COMMON/POINT/KOPT,JOPT,XXX
      DIMENSION X(4,300),U(20),WTX(4,300),XX(4),FOP(300)
     1,FO(300),FU(300),P(20,21),VECT(20,21),ZL(300)
     2,TO(20),EIGVAL(20),XST(300),Y(10),DY(10),CONSTS(50,16)
     3,NCST(50),ISMIN(50),RXTYP(50),DX1I(50),IRX(50)
     4,MOPT(50),LOPT(50),YYY(50),CONST(16),XXX(15)
      GO TO (2,3,4,5,1,7,8,9,10,11,12)  ITYP
    1 CONTINUE
      ITAPE=60
      JTAPE=61
      RETURN
    7 CONTINUE
      NOUNK=3
      NOVAR=2
      RETURN
    8 CONTINUE
      RETURN
    2 CONTINUE
C     **********************************
C     TWO SITE EXCHANGE
C     DIMERIZATION
C     CHEMICAL SHIFTS
C     LiPi, LiCF3CO2, LiSCN IN 2-BUTANONE
C     LiNO3, LiSCN IN PYRIDINE
C     **********************************
C     U(1)=DIMERIZATION CONSTANT-M-1
C     U(2)=CHEMICAL SHIFT OF ION PAIR-PPM
C     U(3)=CHEMICAL SHIFT OF DIMER-PPM
C     **********************************
C     XX(1)=SALT CONCENTRATION-MOLARITY
C     XX(2)=LITHIUM-7 CHEMICAL SHIFTS-PPM
C     **********************************
C     ALPH=DEGREE OF DISSOCIATION
C     **************************************
      U(1)=ABS(U(1))
      ARG=1.0+8.0*U(1)*XX(1)
      IF(U(1).EQ.0.00)GO TO 55
      ALPH=(-1.0+SQRT(ARG))/(4.0*U(1)*XX(1))
      CALC=ALPH*(U(2)-U(3))+U(3)
      GO TO 37
   55 CALC=U(2)
   37 CONTINUE
      IF(IMETH.NE.-1)GO TO 35
```

35

3

4

5

20

9

10

11

12

13

```
      RETURN
   35 CONTINUE
      RESID=CALC-XX(2)
      RETURN
    3 CONTINUE
      RETURN
    4 CONTINUE
      RETURN
    5 CONTINUE
      IF(IMETH.NE.-1)GO TO 20
      RETURN
   20 CONTINUE
      RETURN
    9 CONTINUE
      RETURN
   10 CONTINUE
      RETURN
   11 CONTINUE
      RETURN
   12 CONTINUE
      RETURN
   13 CONTINUE
      RETURN
      END
```

```
      SUBROUTINE EQN
      COMMON KOUNT,ITAPE,JTAPE,IWT,LAP,XINCR,NOPT,NOVAR,NOUNK
     1,X,U,ITMAX,WTX,TEST,I,AV,RESID,IAR,EPS,ITYP,XX,RXTYP
     2,DX1I,FOP,FO,FU,P,ZL,TO,EIGVAL,XST,T,DT,L,M,JJJ,Y,DY
     3,VECT,NCST,CONST,NDAT,JDAT,MOPT,LOPT,YYY,CONSTS
      COMMON/FREDT/IMETH
      COMMON/POINT/KOPT,JOPT,XXX
      DIMENSION X(4,300),U(20),WTX(4,300),XX(4),FOP(300)
     1,FO(300),FU(300)1,P(20,21),VECT(20,21),ZL(300)
     2,TO(20),EIGVAL(20),XST(300),Y(10),DY(10),CONSTS(50,16)
     3,NCST(50),ISMIN(50),RXTYP(50),DX1I(50),IRX(50)
     4,MOPT(50),LOPT(50),YYY(50),CONST(16),XXX(15)
      GO TO (2,3,4,5,1,7,8,9,10,11,12)  ITYP
    1 CONTINUE
      ITAPE=60
      JTAPE=61
      RETURN
    7 CONTINUE
      NOUNK=5
      NOVAR=2
      RETURN
    8 CONTINUE
      RETURN
    2 CONTINUE
C     **********************************
C     TWO SITE EXCHANGE
C     DIMERIZATION
C     NO ACTIVITY CORRECTION
C     CHEMICAL SHIFTS AND LINEWIDTHS
C     LiCl-PYRIDINE
C     **********************************
C     U(1)=CHEMICAL SHIFT OF DIMER-PPM
C     U(2)=CHEMICAL SHIFT OF ION PAIR-PPM
C     U(3)=DIMERIZATION CONSTANT-M^-1
C     U(4)=LINEWIDTH OF ION PAIR-HERTZ
C     U(5)=LINEWIDTH OF DIMER-HERTZ
C     **********************************
C     XX(1)=SALT CONCENTRATION-MOLARITY
C     XX(2)=LITHIUM-7 CHEMICAL SHIFTS-DATA SET 1-PPM
C     XX(2)=CHLORINE-35 LINEWIDTHS-DATA SET 2-HERTZ
C     **********************************
C     ALPH=DEGREE OF DISSOCIATION
C     **********************************
      U(3)=ABS(U(3))
      GO TO (1000,1001)JDAT
 1001 CONTINUE
      CC1=U(2)
      DD1=U(1)
      GO TO 500
```

```
1001 CONTINUE
     CC1=U(4)
     DD1=U(5)
 500 CONTINUE
     ARGM=1.0+8.0*U(3)*XX(1)
     ALPH=(-1.0+SQRT(ARGM))/(4.0*U(3)*XX(1))
     CALC=ALPH*(CC1-DD1)+DD1
     IF(IMETH.NE.-1)GO TO 35
     RETURN
  35 CONTINUE
     RESID=CALC-XX(2)
     RETURN
   3 CONTINUE
     RETURN
   4 CONTINUE
     RETURN
   5 CONTINUE
     IF(IMETH.NE.-1)GO TO 20
     RETURN
  20 CONTINUE
     RETURN
   9 CONTINUE
     RETURN
  10 CONTINUE
     RETURN
  11 CONTINUE
     RETURN
  12 CONTINUE
     RETURN
  13 CONTINUE
     RETURN
     END
```

```
      SUBROUTINE EQN
      COMMON KOUNT,ITAPE,JTAPE,IWT,LAP,XINCR,NOPT,NOVAR
     1,NOUNK,X,U,ITMAX,WTX,TEST,I,AV,RESID,IAR,EPS
     2,ITYP,XX,RXTYP,DX1I,FOP,FO,FU,P,ZL,TO,EIGVAL
     3,XST,T,DT,L,M,JJJ,Y,DY,VECT,NCST,CONST,NDAT
     4,JDAT,MOPT,LOPT,YYY,CONSTS
      COMMON/FREDT/IMETH
      COMMON/POINT/KOPT,JOPT,XXX
      DIMENSION X(4,300),U(20),WTX(4,300),XX(4),FOP(300)
     1,FO(300),FU(300),P(20,21),VECT(20,21),ZL(300),TO(20)
     2,EIGVAL(20),XST(300),Y(10),DY(10),CONSTS(50,16)
     3,NCST(50),ISMIN(50),RXTYP(50),DX1I(50)
     4,IRX(50),MOPT(50),LOPT(50),YYY(50),CONST(16),XXX(15)
      GO TO (2,3,4,5,1,7,8,9,10,11,12)  ITYP
    1 CONTINUE
      ITAPE=60
      JTAPE=61
      RETURN
    7 CONTINUE
      NOUNK=5
      NOVAR=2
      RETURN
    8 CONTINUE
      RETURN
    2 CONTINUE
C     ********************************************
C     THREE SITE EXCHANGE
C     NO ACTIVITY CORRECTION
C     DIMERIZATION AND TETRAMER FORMATION
C     LISCN-2-BUTANONE
C     SOLUTION TO A FOURTH ORDER POLYNOMIAL
C     ********************************************
C     U(1)=DIMERIZATION CONSTANT-M^-1
C     U(2)=TETRAMER FORMATION CONSTANT-M^-1
C     U(3)=CHEMICAL SHIFT OF ION PAIR-PPM
C     U(4)=CHEMICAL SHIFT OF DIMER-PPM
C     U(5)=CHEMICAL SHIFT OF TETRAMER-PPM
C     ********************************************
C     XX(1)=SALT CONCENTRATION-MOLARITY
C     XX(2)=LITHIUM-7 CHEMICAL SHIFTS-PPM
C     ********************************************
C     FREEL=ION PAIR CONCENTRATION
C     LFLAG=FLAG
C     FLAG=FLAG
C     XMAR=INCREMENT FOR INTERVAL
C     XCON=CONTROLS INTERVAL FOR FREEL AXIS
C     A1,B,C,D,E=COEFFICIENTS IN FOURTH ORDER POLYNOMIAL
C     ********************************************
      U(1)=ABS(U(1))
```

```
      U(2)=ABS(U(2))
      IF(U(2).GT.U(1))U(1)=U(2)
      IF(U(4).LT.-3.0)U(4)=-3.0
      IF(U(5).LT.-3.0)U(5)=-3.0
      IF(U(5).GT.U(4))U(5)=U(4)
      VALUE3=1.0
      LFLAG=0
      XCON=5.0
      FLAG=0.0
      XMAR=10.0
 1000 CONTINUE
C     **********************
C     ENTER COEFFICIENTS
C     **********************
      A1=(4.0*U(2)*(U(1)**2))/XX(1)
      B=0.0
      C=(2.0*U(1))/XX(1)
      D=1.0/XX(1)
      E=-1.0
  573 CONTINUE
      VALUE1=XX(1)
      FREEL0=0.0
      FREEL1=0.00
      VALUE1=E
      XVAL=(ABS(E)/C)**0.5
      FREEL2=XVAL/XCON
 2005 CONTINUE
      VALUE2=A1*(FREEL2**4.0)+B*(FREEL2**3.0)+C*(FREEL2**2.0)
     1+D*(FREEL2)+E
      IF(LFLAG.EQ.1)GO TO 81
      IF(VALUE2.LT.0.0)GO TO 2000
      GO TO 82
   81 IF(VALUE2.GT.0.0)GO TO 2000
   82 CONTINUE
      IF(VALUE2.EQ.0.0)GO TO 2001
 2004 CONTINUE
      LFLAG=0
      FLAG=0.0
      FREEL3=(FREEL2-FREEL1)/(VALUE1-VALUE2)*VALUE1+FREEL1
      IF(ABS((FREEL3-FREEL0)/FREEL3).LT.0.0000001)GO TO 2002
      VALUE5=A1*(FREEL3**4.0)+B*(FREEL3**3.0)+C*(FREEL3**2.0)
     1+D*(FREEL3)+E
      VALUE6=VALUE5-VALUE3
      RAT=ABS(VALUE6/VALUE3)
      VALUE3=VALUE5
      VALUE4=ABS(VALUE5)
      IF(VALUE4.GT.0.0000001)GO TO 91
      XCON=5.0
      IF(RAT.LT.0.000000001)GO TO 2002
```

```
      IF(VALUE3.LT.0.0)GO TO 2003
      VALUE2=VALUE3
      FREEL2=FREEL3
      FREEL0=FREEL3
      GO TO 2004
2003  CONTINUE
      VALUE1=VALUE3
      FREEL1=FREEL3
      GO TO 2004
2000  CONTINUE
      FREELL=FREEL1
      VALUELL=VALUE1
      VALUE1=VALUE2
      FREEL1=FREEL2
      IF(LFLAG.EQ.1)GO TO 89
      IF(VALUELL.GT.VALUE1)GO TO 2220
      IF(FLAG.EQ.1.0)GO TO 2225
   89 CONTINUE
      IF(LFLAG.EQ.0)GO TO 85
      FREEL2=FREEL1-XVAL/XCON
      GO TO 86
   85 CONTINUE
      FREEL2=FREEL1+XVAL/XCON
   86 CONTINUE
      IF(FREEL1.GT.XX(1))GO TO 2006
      GO TO 2005
2220  DEL=(ABS(FREELL-FREEL1))/XMAR
      XMAR=XMAR*10.0
      FREEL2=FREELL*DEL
      FREEL1=FREELL
      VALUE1=VALUELL
      FLAG=1.0
      GO TO 2005
2225  DEL=DEL/5.0
      XMAR=10.0
      FREEL2=FREEL1+DEL
      GO TO 2005
2001  CONTINUE
      FREEL=FREEL2
      GO TO 95
   91 CONTINUE
      XCON=XCON*5.0
      IF(VALUE3.LT.0.0)GO TO 21
      LFLAG=1
      FREEL1=FREEL3
      VALUE1=VALUE3
      FREEL2=FREEL1-XVAL/XCON
      GO TO 2005
   21 FREEL1=FREEL3
```

```
      VALUE1=VALUE3
      FREEL2=FREEL1+XVAL/XCON
      GO TO 2005
 2002 CONTINUE
      FREEL=FREEL3
   95 CONTINUE
      TOTAL=XX(1)
      XIP=FREEL/TOTAL
      XD=(U(1)*(FREEL**2))/TOTAL
      XD=XD*2.0
      XT=1.0-XD-XIP
      GO TO 574
 2006 CONTINUE
      WRITE(JTAPE,996)
  996 FORMAT(5X,50H********************* WARNING
     1 **********************,/,15X,50H************ NO POSITIVE
     2 "VALUE" FOUND *************)
 2008 CONTINUE
      FREEL=0.0
  574 CONTINUE
      CALC=XIP*U(3)+XD*U(4)+XT*U(5)
      IF(IMETH.NE.-1)GO TO 35
      RETURN
   35 CONTINUE
      RESID=CALC-XX(2)
      RETURN
    3 CONTINUE
      RETURN
    4 CONTINUE
      RETURN
    5 CONTINUE
      IF(IMETH.NE.-1)GO TO 20
      RETURN
   20 CONTINUE
      RETURN
    9 CONTINUE
      RETURN
   10 CONTINUE
      RETURN
   11 CONTINUE
      RETURN
   12 CONTINUE
      RETURN
   13 CONTINUE
      RETURN
      END
```

B.

neut

and

pro

cha

cor

tak

spe

spe

mus

che

fas

resp

B. Determination of Complex Formation Constants from NMR Measurements

The equilibrium for a one-to-one complexing reaction with a neutral ligand can be expressed as:

$$M^+ + L \rightleftharpoons ML^+ \qquad \text{(B-1)}$$

and the thermodynamic equilibrium constant will be:

$$K_F = \frac{(ML^+)}{(M^+)(L)} \qquad \text{(B-2)}$$

The Debye-Hückel mean activity coefficient is a function of the product of the absolute value of the charges on the ions. Since the charge on the complexing ion and the complex are the same, no activity correction is necessary. In equation B-1, the complexing species is taken to be a metal cation; however, this can be taken to be any species that will complex with a neutral ligand. When the complexing species is involved in other reactions in solution, these processes must be accounted for.

The observed chemical shift is a mass average of the individual chemical shift of the species involved in the reaction, assuming a fast exchange process occurs between two sites or three sites with respect to the NMR time scale.

$$\delta_{OBS} = X_{M^+}\delta_{M^+} + X_{ML}\delta_{ML} \qquad \text{(B-3)}$$

$$\delta_{OBS} = X_{M^+}\delta_{M^+} + X_{ML^+}\delta_{ML} + X_X\delta_X \qquad \text{(B-4)}$$

The

specie

the c

specie

C

using

ligan

wher

ion

sub

δ_O =

chem

a st

const

molar

excha

unknow

The δ_{M^+}, δ_{ML^+}, and δ_X are the chemical shift of the complexing species, complex, and additional site produced by a side reaction with the complexing species, and X is the mole ratio of the different species specified by the subscript.

Considering the problem represented by B-1, two site exchange, using the mass balance equation for the complexing species and the ligand, the free metal (C_{M^+}) can be calculated and is given by:

$$C_{M^+} = \frac{(-K_F C_L^T + K_F C_M^T - 1) - \sqrt{(K_F C_L^T - K_F C_M^T + 1)^2 - 4K_F C_M^T}}{2K_F} \quad \text{(B-5)}$$

where the C^T_L and C^T_M are the total concentrations of the complexing ion and the ligand. The chemical shift equation used in the subroutine is calculated using B-3 and B-5 which is given by:

$$\delta_O = \frac{(K_F C_M^T - K_F C_L^T - 1) + \sqrt{(K_F^2 C_L^{T^2} + K_F^2 C_M^{T^2} - 2K_F^2 C_L^T C_M^T + 2K_F C_L^T + 2K_F C_M^T + 1)}\ (\delta_F - \delta_{ML})}{2K_F C_M^T} + \delta_{ML} \quad \text{(B-6)}$$

To obtain formation constants for a 1:1 complexation reaction, the chemical shifts at different ligand concentrations are measured versus a stable reference keeping the concentration of the complexing species constant. Four data sets exist, one each for the chemical shifts, molar concentrations of the ligand, and their variances. The two site exchange program for the 1:1 complexation reaction contains three unknowns and one constant which are:

U(1) = K_F U(3) = δ (chemical shift of the complexing species in solution)

U(2) = δ_{ML} constant(1) = C^T_M

The program for the three site exchange mechanism allows for the calculation of a formation constant taking into account a side reaction. The EQN subroutine contains a loop where the concentration of the complex and the complexing species are determined sequentially considering first the complexing reaction followed by the side reaction. The program remains in a the loop as long as there exists a large difference in the concentration of the species obtained from two sequential runs. Once out of the loop, the concentrations of the different species are used to calculate the chemical shifts based on the values assigned to the unknowns. This problem contains five unknowns and one constant which are:

U(1) = K (side reaction) U(3) = δ (Salt Conc = ∞)

U(2) = δ (Salt Conc = 0) U(4) = K_F

U(5) = δ_{ML} constant(1) = C^T_M

This programs was used to obtain formation constants for $LiCl_2^-$ crown ether and glyme complexes in 45 mole % $AlCl_3$ melt taking into account the dimerization of $LiCl_2^-$.

The program which describes a four site exchange mechanisms allows for the calculation of formation constants for two different complexes

taking into account a side reaction. The equations used in the fitting program to fit the chemical shifts obtained from the mole ratio study were derived from equilibrium constants for the formation of two different complexes with the ligand and the side reaction. The program then goes into a loop calculating the concentrations of each complex until the concentration of one of the complexing specie reaches a stable value. Then, the program recalculates the complexing species resulting from the side reaction and goes into another loop until the concentration of the complexing species reaches a stable value. This problem contains seven unknowns and one constant which are:

U(1) = K_F(Complex 1)	U(5) = K (side reaction)
U(2) = K_F(Complex 2)	U(6) = δ (Salt Conc = 0)
U(3) = δ_{ML1}	U(7) = δ (Salt Conc = ∞)
U(4) = δ_{ML2}	constant(1) = C^T_M

This program was used to obtain formation constants for $LiCl_2^-$ lariat ether complexes in 45 mole % melt. The KINFIT program on the VAX-11/780 computer was used to fit this data. This program fitted the data to mechanism which describes the formation of a 1:1 and a 2:1 complex. The dimerization of $LiCl_2^-$ was taken as the side reaction.

```
      SUBROUTINE EQN
      COMMON KOUNT,ITAPE,JTAPE,IWT,LAP,XINCR,NOPT,NOVAR,NOUNK
     1,X,U,ITMAX,WTX,TEST,I,AV,RESID,IAR,EPS,ITYP,XX,RXTYP
     2,DX1I,FOP,FO,FU,P,ZL,TO,EIGVAL,XST,T,DT,L,M,JJJ,Y,DY
     3,VECT,NCST,CONST,NDAT,JDAT,MOPT,LOPT,YYY,CONSTS
      COMMON/FREDT/IMETH
      COMMON/POINT/KOPT,JOPT,XXX
      DIMENSION X(4,300),U(20),WTX(4,300),XX(4),FOP(300)
     1,FO(300),FU(300),P(20,21),VECT(20,21),ZL(300)
     2,TO(20),EIGVAL(20),XST(300),Y(10),DY(10),CONSTS(50,16)
     3,NCST(50),ISMIN(50),RXTYP(50),DX1I(50),IRX(50)
     4,MOPT(50),LOPT(50),YYY(50),CONST(16),XXX(15)
      GO TO (2,3,4,5,1,7,8,9,10,11,12)  ITYP
    1 CONTINUE
      ITAPE=60
      JTAPE=61
      RETURN
    7 CONTINUE
      NOUNK=3
      NOVAR=2
      RETURN
    8 CONTINUE
      RETURN
    2 CONTINUE
C     ***************************************************
C     1:1 COMPLEXATION IN BASIC MELT AND 2-BUTANONE
C     ***************************************************
C     XX(1)=LIGAND CONCENTRATION-MOLE FRACTION OR MOLARITY
C     XX(2)=LITHIUM-7 CHEMICAL SHIFTS-PPM
C     ***************************************************
C     CONST(1)=CONCENTRATION OF LiCl OR LIBPh4-MOLARITY
C     ***************************************************
C     U(1)=COMPLEXATION CONSTANT-M^-1 or (MOLE FRACTION)^-1
C     U(2)=CHEMICAL SHIFT OF COMPLEX-PPM
c     U(3)=CHEMICAL SHIFT OF COMPLEXING SPECIES-PPM
C     ***************************************************
C     FREEM=CONCENTRATION OF UNCOMPLEXED METAL CATION
C     XC1=CONCENTRATION OF COMPLEX
C     ***************************************************
      U(1)=ABS(U(1))
      A1=-U(1)*CONST(1)-U(1)*XX(1)-1.0
      A2=4.0*(U(1)**2.)*CONST(1)*XX(1)
      XC1=(-A1-SQRT((A1**2.)-A2))/(2.0*U(1))
      FREEM=CONST(1)-XC1
      XF=FREEM/CONST(1)
      X1C=XC1/CONST(1)
      CALC=XF*U(3)+X1C*U(2)
      IF(IMETH.NE.-1)GO TO 35
      RETURN
```

```
35 CONTINUE
   RESID=CALC-XX(2)
   RETURN
 3 CONTINUE
   RETURN
 4 CONTINUE
   RETURN
 5 CONTINUE
   IF(IMETH.NE.-1)GO TO 20
   RETURN
20 CONTINUE
   RETURN
 9 CONTINUE
   RETURN
10 CONTINUE
   RETURN
11 CONTINUE
   RETURN
12 CONTINUE
   RETURN
13 CONTINUE
   RETURN
   END
```

```
      SUBROUTINE EQN
      COMMON KOUNT,ITAPE,JTAPE,IWT,LAP,XINCR,NOPT,NOVAR,NOUNK
     1,X,U,ITMAX,WTX,TEST,I,AV,RESID,IAR,EPS,ITYP,XX,RXTYP
     2,DX1I,FOP,FO,FU,P,ZL,TO,EIGVAL,XST,T,DT,L,M,JJJ,Y,DY
     3,VECT,NCST,CONST,NDAT,JDAT,MOPT,LOPT,YYY,CONSTS
      COMMON/FREDT/IMETH
      COMMON/POINT/KOPT,JOPT,XXX
      DIMENSION X(4,300),U(20),WTX(4,300),XX(4),FOP(300)
     1,FO(300),FU(300),P(20,21),VECT(20,21),ZL(300)
     2,TO(20),EIGVAL(20),XST(300),Y(10),DY(10),CONSTS(50,16)
     3,NCST(50),ISMIN(50),RXTYP(50),DX1I(50),IRX(50)
     4,MOPT(50),LOPT(50),YYY(50),CONST(16),XXX(15)
      GO TO (2,3,4,5,1,7,8,9,10,11,12)  ITYP
    1 CONTINUE
      ITAPE=60
      JTAPE=61
      RETURN
    7 CONTINUE
      NOUNK=5
      NOVAR=2
      RETURN
    8 CONTINUE
      RETURN
    2 CONTINUE
C     ****************************************************
C     1:1 COMPLEXATION IN BASIC MELT
C     CORRECTION FOR DIMERIZATION OF LICl2-
C     ****************************************************
C     XX(1)=LICL CONCENTRATION-DATA SET I
C     XX(2)=LITHIUM-7 CHEMICAL SHIFTS-DATA SET I-PPM
C     XX(1)=LIGAND CONCENTRATION-DATA SET II-MOLE FRACTION
C     XX(2)=LITHIUM-7 CHEMICAL SHIFTS-DATA SET II-PPM
C     ************************************************
C     CONSTS(2,1)=LICL CONCENTRATION-MOLE FRACTION
C     ************************************************
C     U(1)=DIMERIZATION CONSTANT-(MOLE FRACTION)-1
C     U(2)=CHEMICAL SHIFT OF MONOMER-PPM
C     U(3)=CHEMICAL SHIFT OF DIMER-PPM
C     U(4)=COMPLEXATION CONSTANT-(MOLE FRACTION)-1
C     U(5)=CHEMICAL SHIFT OF COMPLEX-PPM
C     ************************************************
C     CM, FREEM, FREEM1 = CONCENTRATION OF LiCl2-
C     CD, FCHANG = CONCENTRATION OF Li2Cl4 2-
C     B2, B5 = CONCENTRATION OF COMPLEX
C     FREEL, FREEL1 = CONCENTRATION OF UNCOMPLEXED LIGAND
C     ************************************************
      U(1)=ABS(U(1))
      U(4)=ABS(U(4))
      GO TO (1501,1502)JDAT
```

```
1501 CONTINUE
     CA=4.0*U(1)*XX(1)+1.0
     CB=16.0*(U(1)**2)*(XX(1)**2)
     CC=CA-SQRT((CA**2)-CB)
     CD=CC/(8.0*U(1))
     CM=XX(1)-(2.0*CD)
     XM=CM/XX(1)
     XD=1.0-XM
     CALC=XM*U(2)+XD*U(3)
     IF(IMETH.NE.-1)GO TO 35
     RETURN
1502 CONTINUE
     CA=4.0*U(1)*CONSTS(2,1)+1.0
     CB=16.0*(U(1)**2)*(CONSTS(2,1)**2)
     CC=CA-SQRT((CA**2)-CB)
     CD=CC/(8.0*U(1))
     CM=CONSTS(2,1)-(2.0*CD)
     IF(XX(1).EQ.0.00)GO TO 1500
     B=U(4)*XX(1)+U(4)*CM+1.0
     B1=4.0*(U(4)**2)*XX(1)*CM
     B2=(B-SQRT((B**2)-B1))/(2.0*U(4))
     FREEM=CM-B2
     FREEL=XX(1)-B2
     IF(FREEL.LT.0.0)FREEM=0.0
2000 CONTINUE
     C=4.0*U(1)*FREEM+1.0
     C1=(C**2)-16.0*(U(1))*(U(1)*(FREEM**2)-CD)
     FCHANG=(C-SQRT(C1))/(8.0*U(1))
     CD= CD+FCHANG
     FREEM=FREEM-(2.0*FCHANG)
     B3=(U(4)*FREEM)+(U(4)*FREEL)+1.0
     B4=(B3**2)-4.0*(U(4))*(U(4)*FREEM*FREEL-B2)
     B5=(B3-SQRT(B4))/(2.0*U(4))
     FREEL1=FREEL-B5
     FREEM1=FREEM-B5
     B2=B2+B5
     RAT=(FREEL1-FREEL)/FREEL
     RAT=ABS(RAT)
     FREEL=FREEL1
     FREEM=FREEM1
     IF(RAT.LT.0.00001)GO TO 1000
     GO TO 2000
1000 CONTINUE
     XM=FREEM/CONSTS(2,1)
     XD=(2.0*CD)/CONSTS(2,1)
     XC1=1.0-XM-XD
     CALC=XM*U(2)+XD*U(3)+XC1*U(5)
     GO TO 36
1500 XM=CM/CONSTS(2,1)
```

```
      XD=1.0-XM
      CALC=XM*U(2)+XD*U(3)
   36 CONTINUE
      IF(IMETH.NE.-1)GO TO 35
      RETURN
   35 CONTINUE
      RESID=CALC-XX(2)
      RETURN
    3 CONTINUE
      RETURN
    4 CONTINUE
      RETURN
    5 CONTINUE
      IF(IMETH.NE.-1)GO TO 20
      RETURN
   20 CONTINUE
      RETURN
    9 CONTINUE
      RETURN
   10 CONTINUE
      RETURN
   11 CONTINUE
      RETURN
   12 CONTINUE
      RETURN
   13 CONTINUE
      RETURN
      END
```

```
      SUBROUTINE EQN
C     ************************************************************
C     KINFIT
C     T.V. Atkinson
C     Department of Chemistry
C     Michigan State University
C     E. Lansing, MI 48824
C     Date 19-NOV-1985
C     ************************************************************
C
      IMPLICIT REAL*16(A-H,O-Z)
      IMPLICIT INTERGHER *4(I-N)
C
      INCLUDE 'KINFIT:KINFITCOM.FOR/LIST'
      INCLUDE 'KINFIT:KINEQNCOM:FOR/LIST'
C
      GOTO (2,3,4,5,1,7,8,9,10,11,12,13) ITYPE
    1 CONTINUE
      RETURN
    7 CONTINUE
      NOUNK=7
      NOVAR=2
      RETURN
    8 CONTINUE
      RETURN
    2 CONTINUE
C     ****************************************************
C     1:1 AND 2:1 COMPLEXATION IN BASIC MELT
C     CORRECTION FOR DIMERIZATION OF LICl2-
C     LARIAT ETHER COMPLEXATION
C     ****************************************************
C     XX(1)=LIGAND CONCENTRATION-MOLE FRACTION
C     XX(2)=LITHIUM-7 CHEMICAL SHIFTS-PPM
C     ****************************************************
C     CONSTS(2,1)=LICL CONCENTRATION-MOLE FRACTION
C     ****************************************************
C     U(1)=FIRST COMPLEXATION CONSTANT-(MOLE FRACTION)-1
C     U(2)=SECOND COMPLEXATION CONSTANT-(MOLE FRACTION)-1
C     U(3)=CHEMICAL SHIFT OF COMPLEX 1-PPM
C     U(4)=CHEMICAL SHIFT OF COMPLEX 2-PPM
C     U(5)=DIMERIZATION CONSTANT-(MOLE FRACTION)-1
C     U(6)=CHEMICAL SHIFT OF MONOMER-PPM
C     U(7)=CHEMICAL SHIFT OF DIMER-PPM
C     ****************************************************
C      CM, FREEM = CONCENTRATION OF LiCl2-
C      CD, CD1, FCHANGE = CONCENTRATION OF Li2Cl4 2-
C      XC1, DIFF = CONCENTRATION OF COMPLEX 1
C      XC2, XC22, DF = CONCENTRATION OF COMPLEX 2
```

```
C      FREEL = CONCENTRATION OF UNCOMPLEXED LIGAND
C      ***************************************************
       U(1)=ABS(U(1))
       U(2)=ABS(U(2))
       U(5)=ABS(U(5))
       IF(U(1).LT.U(2))U(1)=U(2)
       IF(U(4).GT.U(3))U(4)=U(3)
       GO TO (1501,1502)JDAT
 1501  CONTINUE
       CA=4.0*U(5)*XX(1)+1.0
       CB=16.0*(U(5)**2)*(XX(1)**2)
       CC=CA-SQRT((CA**2)-CB)
       CD=CC/(8.0*U(5))
       CM=XX(1)-(2.0*CD)
       IF(CM.LT.0.0)CM=0.0
       XM=CM/XX(1)
       XD=1.0-XM
       CALC=XM*U(6)+XD*U(7)
       IF(IMETH.NE.-1)GO TO 35
       RETURN
 1502  CONTINUE
       CA=4.0*U(5)*CONSTS(2,1)+1.0
       CB=16.0*(U(5)**2)*(CONSTS(2,1)**2)
       CC=CA-SQRT((CA**2)-CB)
       CD=CC/(8.0*U(5))
       CM=CONSTS(2,1)-(2.0*CD)
       IF(CM.LT.0.0)CM=0.0
       IF(XX(1).EQ.0.00)GO TO 1500
       A1=-U(1)*CM-U(1)*XX(1)-1.0
       A2=4.0*(U(1)**2)*XX(1)*CM
       XC1=(-A1-SQRT((A1**2)-A2))/(2.0*U(1))
       FREEM=CM-XC1
       FREEL=XX(1)-XC1
       IF(FREEL.LT.0.0)FREEL=0.0
       IF(FREEM.LT.0.0)FREEM=0.0
       A3=-U(2)*XC1-U(2)*FREEL-1.0
       A4=4.0*(U(2)**2)*XC1*FREEL
       XC2=(-A3-SQRT((A3**2)-A4)/(2.0*U(2))
       XC1=XC1-XC2
       FREEL=FREEL-XC2
       IF(FREEL.LT.0.0)FREEL=0.0
       IF(XC1.LT.0.0)XC1=0.0
  500  CONTINUE
       A5=-U(1)*FREEM-U(1)*FREEL-1.0
       A6=4.0*(U(1))*(U(1)*FREEM*FREEL-XC1)
       DIFF=(-A5-SQRT(A5**2)-A6)/(2.0*U(1))
       XC1 =XC1+DIFF
       FREEM=FREEM-DIFF
       FREEL=FREEL-DIFF
       IF(FREEL.LT.0.0)FREEL=0.0
```

```
      IF(FREEM.LT.0.0)FREEM=0.0
      A7=-U(2)*XC1-U(2)*FREEL-1.0
      A8=4.0*(U(2))*((U(2)*XC11*FREEL)-XC2)
      DF=(-A7-SQRT((A7**2)-A8)/(2.0*U(2))
      XC22=XC2+DF
      XC1=XC1-DF
      FREEL=FREEL-DF
      IF(FREEL.LT.0.0)FREEL=0.0
      IF(XC1.LT.0.0)FREEM=0.0
      RAT=ABS((XC22-XC2)/XC22)
      XC2=XC22
      IF(RAT.GT.0.0000001)GO TO 500
      CC=-4.0*FREEM*U(5)-1.0
      CF=16.0*(U(5))*(U(5)*(FREEM**2)-CD)
      FCHANGE=(-CC-SQRT((CC**2)-CF)/(8.0*U(5))
      CD1=CD+FCHANGE
      FREEM=FREEM-(2.0*FCHANGE)
      IF(FREEM.LT.0.0)FREEM=0.0
      RAT=ABS((CD-CD1)/CD1)
      CD=1
      IF(RAT.GT.0.0000001)GO TO 500
      XM=FREEM/CONSTS(2,1)
      XD=(2.0*CD)/CONSTS(2,1)
      XCC1=XC1/CONSTS(2,1)
      XCC2=1.0-XM-XD-XCC1
      CALC=XM*U(6)+XD*U(7)+XCC1*U(3)*XCC2*U(4)
      GO TO 36
1500  XM=CM/CONSTS(2,1)
      XD=1.0-XM
      CALC=XM*U(6)+XD*U(7)
   36 CONTINUE
      IF(IMETH.NE.-1)GO TO 35
      RETURN
   35 CONTINUE
      RESID=CALC-XX(2)
      RETURN
    3 CONTINUE
      RETURN
    4 CONTINUE
      RETURN
    5 CONTINUE
      IF(IMETH.NE.-1)GO TO 20
      RETURN
   20 CONTINUE
      RETURN
    9 CONTINUE
      RETURN
   10 CONTINUE
      RETURN
```

```
11 CONTINUE
   RETURN
12 CONTINUE
   RETURN
13 CONTINUE
   RETURN
   END
```

C. Determination of Ion Pairing Constants from Electrical Conductance Measurements

The two conductance equations used to obtain ion pairing constants from electrical conductance measurements were the Justice and Fuoss-Kraus equations. The EQN subroutine written for the fitting process requires that four data sets exist, one for the molar concentration and another for the conductance measurements. The conductance measurements are entered into the program as K/R, where R is the solution resistance and K is the cell constant. The other data sets contain the variances of the concentrations and the electrical conductance measurements. Before the program begins fitting the electrical conductance data to either equation, the K/R data set is transformed to equivalent conductances. When using the Fuoss-Kraus equation, the K/R's and concentrations are transformed to $\Lambda g(C)C^{1/2}$ and $(1 - \Lambda/\Lambda_o)C$, respectively. This process occurs in the EQN subroutine between 8 continue and 2 continue. The variances are also computed using equations derived from the propagation of errors.

The Justice equation is:

$$\Lambda = \Lambda_o - S(C\alpha)^{1/2} + EC\alpha \ln C\alpha + J_1 C\alpha - J_2(C\alpha)^{3/2} - K_a C\alpha f_{\pm}^2 \Lambda \qquad (C\text{-}1)$$

$$\text{where } \alpha = \frac{-1 + \sqrt{1 + 4K_a C_T f_{\pm}^2}}{2K_a C_T f_{\pm}^2} \qquad (C\text{-}2)$$

$$\text{and } f_{\pm} = \exp\left\{\frac{-4.20179 \times 10^6 |Z_+ Z_-| (\alpha C)^{1/2}}{(\epsilon T)^{3/2}(1 + 50.29a(\alpha C)^{1/2}/(\epsilon T)^{1/2})}\right\} \qquad (C\text{-}3)$$

This equation resembles the Fuoss-Hsia equation except that the interatomic distance in the J_1 term and the mean activity coefficient were set equal to the Bjerrum distance. The Bjerrum distance is defined as:

$$q = \frac{e^2}{2\epsilon kT} \tag{C-4}$$

where ϵ is the dielectric constant of the solvent and T is the absolute temperature.

The $E\alpha C \ln \alpha C$ term is set equal to the Chen correction term given by:

$$E\alpha C \ln \alpha C = \frac{(b\kappa a)^2 \Lambda_o \ln (\kappa a)}{12} + \frac{\beta C^{1/2} \kappa a b \ln (\kappa a)}{4} \tag{C-5}$$

The S term is the Onsager term and is given as:

$$S = \alpha\Lambda_o + \beta \tag{C-6}$$

$$\alpha = 0.8204 \times 10^6 Z^3/(\epsilon T)^{3/2}/(\text{mole}^{-1/2} l^{1/2}) \tag{C-7}$$

$$\beta = 82.486 Z^3/[\eta(\epsilon T)^{1/2}]/(\Omega^{-1} \text{cm}^2 \text{mole}^{-3/2} l^{1/2}) \tag{C-8}$$

In the above equations, the dielectric constant and the viscosity of the solution were assumed to be equal to those of the solvent (300).

The J_1 and J_2 terms are given by Fernandez-Prini (310) as:

$$E_1 = 2.94257 \times 10^{12} Z^6/(\epsilon T)^3/(\text{mole})^{-1} l) \tag{C-9}$$

$$E_2 = 4.33244 \times 10^7 Z^5/(\epsilon T)^2 \eta/(\Omega^{-1}cm^2mol.^{-2}l) \quad (C\text{-}10)$$

$$\beta = 82.487 Z^3/\eta\ (\epsilon T)^{1/2}/\ \Omega^{-1}cm^2mol.^{-3/2}l^* \quad (C\text{-}11)$$

$$\kappa = 50.2916 Z \sqrt{C}/(\epsilon T)^{1/2}/(\text{Å}^{-1}) \quad (C\text{-}12)$$

$$\Delta_1 = 1/b^3(2b^2 + 2b - 1) + 0.90735 \quad (C\text{-}13)$$

$$\Delta_2 = 22/3b + 0.01420 \quad (C\text{-}14)$$

$$\Delta_3 = 0.9571/b^3 + 1.1187/b^2 + 0.1523/b \quad (C\text{-}15)$$

$$\Delta_4 = 1/b^3(0.5738b^2 + 7.0572b - 2/3) - 0.6461 \quad (C\text{-}16)$$

$$\Delta 5 = \frac{E_2\beta}{\Lambda_o}\ (4/3b - 2.2194) \quad (C\text{-}17)$$

$$J_1 = 2E_1\Lambda_o\ [\ln(\kappa a/C^{1/2}) + \Delta_1] + 2E_2\ [\Delta_2 - \ln(\kappa a/C^{1/2})] \quad (C\text{-}18)$$

$$J_2 = \frac{\kappa ab(4E_1\Lambda_o\Delta_3 + 2E_2\Delta_4)}{C^{1/2}} - \Delta_5 \quad (C\text{-}19)$$

The interatomic distance parameters in the J_2 and the $E\alpha C \ln \alpha C$ terms are obtained from fitting the equivalent conductances. The Λ_o and K_a are also obtained from the fit. When $K_a \gtrsim 10^5$, the Λ_o value is set to a constant value in the program. The Λ_o value is calculated using the Walden product and/or the Kohlrausch law.

$$\Lambda^a_o\ \eta^a = \Lambda^b_o\ \eta^b \quad (C\text{-}20)$$

$$\Lambda^a_o = \nu_+\lambda^a_+ + \nu_-\lambda^a_- \quad (C\text{-}21)$$

Use of the Walden product, represented by equation (C-20), requires that the limiting equivalent conductance of the specific salt be available along with the viscosity in another solvent at the same

temperature. The Kohlrausch law, represented by equation (C-21), requires that the conductivity of the ions at infinite be known in that solvent at the same temperature.

When the Fuoss-Kraus equation was used, the limiting equivalent conductance is held constant so the data can be fitted to a straight line. The limiting equivalent conductances were obtained from fitting the equivalent conductances to the Justice equation or using the Walden product. From the fit of this equation:

$$\Lambda g(C)C^{1/2} = \frac{\Lambda_o}{K_a^{1/2}} + \frac{\Lambda^T{}_o K_T}{K_a^{1/2}} (1 - \Lambda/\Lambda_o)C \qquad \text{(C-22)}$$

$$g(c) = \frac{\exp\left(\frac{-2.303\beta'}{(\Lambda_o)^{1/2}} (\Lambda C)^{1/2} \right)}{(1 - S/\Lambda_o^{3/2} (\Lambda C)^{1/2})(1 - \Lambda/\Lambda_o)^{1/2}} \qquad \text{(C-23)}$$

one obtains from the intercept the ion pairing formation constant (K_a) and from the slope, the triple ion formation constant (K_T) assuming $\Lambda^T{}_o = 2/3\Lambda_o$. The dielectric constant and the viscosity were assumed to be equal to those of the solvent (300).

```
      SUBROUTINE EQN
      COMMON KOUNT,ITAPE,JTAPE,IWT,LAP,XINCR,NOPT,NOVAR,NOUNK
     1,X,U,ITMAX,WTX,TEST,I,AV,RESID,IAR,EPS,ITYP,XX,RXTYP
     2,DX1I,FOP,FO,FU,P,ZL,TO,EIGVAL,XST,T,DT,L,M,JJJ,Y,DY
     3,VECT,NCST,CONST,NDAT,JDAT,MOPT,LOPT,YYY,CONSTS
      COMMON/FREDT/IMETH
      COMMON/POINT/KOPT,JOPT,XXX
      DIMENSION X(4,300),U(20),WTX(4,300),XX(4),FOP(300)
     1,FO(300),FU(300),P(20,21),VECT(20,21),ZL(300)
     2,TO(20),EIGVAL(20),XST(300),Y(10),DY(10),CONSTS(50,16)
     3,NCST(50),ISMIN(50),RXTYP(50),DX1I(50),IRX(50)
     4,MOPT(50),LOPT(50),YYY(50),CONST(16),XXX(15)
      GO TO (2,3,4,5,1,7,8,9,10,11,12)  ITYP
    1 CONTINUE
      ITAPE=60
      JTAPE=61
      RETURN
    7 CONTINUE
      NOUNK=2
      NOVAR=2
      RETURN
    8 CONTINUE
C     ************************************************************
C     ENTER DATA AS K/R WHERE K=CELL CONSTANT, R=RESISTANCE
C     CONVERSION TO EQUIVALENT CONDUCTANCE
C     ************************************************************
      DO 99 N=1,NOPT
      WRITE(JTAPE,500)X(1,N),WTX(1,N),X(2,N),WTX(2,N)
  500 FORMAT(5X,4E10.4)
   99 CONTINUE
      DO 88 N=1,NOPT
      EEE=(1000.0*X(2,N))/X(1,N)
      E=((1000.0/X(1,N))**2)*((WTX(2,N)))
      E1=(((1000.0*X(2,N))/(X(1,N)**2))**2)*WTX(1,N)
      WTX(2,N)=E+E1
      X(2,N)=EEE
      WRITE(JTAPE,501)X(1,N),WTX(1,N),X(2,N),WTX(2,N)
  501 FORMAT(5X,4E10.4)
C     ************************************************************
C     CONVERSION TO Λg(C)C^1/2 AND (1 - Λ/Λo)C AND THEIR VARIANCES
C     ************************************************************
   88 CONTINUE
      DO 100 N=1,NOPT
      A=(1.8247E+06)/((CONST(2)*CONST(3))**1.5)
      A1=(0.82047E+06)/((CONST(2)*CONST(3))**1.5)
      A2=A1*CONST(1)
      A3=(82.501)/(((CONST(2)*CONST(3))**0.5)*CONST(4))
      A4=A3+A2
      B=EXP(-2.303*(A/(CONST(1)**0.5))*((X(1,N)*X(2,N))**0.5))
```

```
      B1=1.0-(A4/(CONST(1)**1.5))*((X(1,N)*X(2,N))**0.5)
      B2=(1.0-(X(2,N)/CONST(1)))**0.5
      B3=(B/(B1*B2))*(X(1,N)**0.5)*X(2,N)
      B4=(1.0-(X(2,N)/CONST(1)))*X(1,N)
      C=((X(1,N)/CONST(1))**2.)*WTX(2,N)
      C1=((1.0-X(2,N)/CONST(1))**2.)*WTX(1,N)
      C2=C+C1
      D=(B*0.5*((-2.303*A)/(CONST(1)**0.5))
     1*((X(1,N)*X(2,N))**(-0.5)))
      D=D*X(2,N)
      DD=B1*B2
      D=D/DD
      D1=0.5*B*(A4/(CONST(1)**1.5))*X(2,N)
      D2=(B2*(B1**2.)*(X(1,N)*X(2,N))**0.5)
      D3=D1/D2
      D4=D+D3
      D5=(-0.5*(B/B1)*((1.-(X(2,N)/CONST(1)))
     1**(-1.5))*(-1./CONST(1)))
      D6=(D*(X(1,N)/X(2,N)))+(D3*(X(1,N)/X(2,N)))+D5
      FF=(X(2,N)*D4*(X(1,N)**0.5))
      F1=FF+(0.5*(X(1,N)**(-0.5))*X(2,N)*(B/(B1*B2)))
      F2=((B/(B1*B2))*(X(1,N)**0.5))+((X(1,N)**0.5)*X(2,N)*D6)
      F3=(F1**2.)*(WTX(1,N))+(F2**2.)*(WTX(2,N))
      X(1,N)=B4
      X(2,N)=B3
      WTX(1,N)=C2
      WTX(2,N)=F3
  100 CONTINUE
      RETURN
    2 CONTINUE
C     ***************************************************
C     FUOSS-KRAUS EQUATION
C     ***************************************************
C     XX(1)=(1 - Λ/Λo)C VALUES
C     XX(2)=Λg(C)C^1/2 VALUES
C     ***************************************************
C     CONST(1)=LIMITING CONDUCTANCE OF FREE IONS-CM^2/OHM MOLE
C     CONST(2)=DIELECTRIC CONSTANT
C     CONST(3)=TEMPERATURE-KELVIN
C     CONST(4)=VISCOSITY-POISE
C     CONST(5)=LIMITING CONDUCTANCE OF TRIPLE ION-CM^2/OHM MOLE
C     ***************************************************
C     U(1)=ION PAIRING CONSTANT-M^-1
C     U(2)=TRIPLE ION FORMATION CONSTANT-M^-1
C     ***************************************************
      U(1)=ABS(U(1))
      CALC=(CONST(1)/U(1)**0.5))+((CONST(5)*U(2))/(U(1)**0.5))*XX(1)
      IF(IMETH.NE.-1)GO TO 35
      RETURN
```

```
35 CONTINUE
   RESID=CALC-XX(2)
   RETURN
 3 CONTINUE
   RETURN
 4 CONTINUE
   RETURN
 5 CONTINUE
   IF(IMETH.NE.-1)GO TO 20
   RETURN
20 CONTINUE
   RETURN
 9 CONTINUE
   RETURN
10 CONTINUE
   RETURN
11 CONTINUE
   RETURN
12 CONTINUE
   RETURN
13 CONTINUE
   RETURN
   END
```

```
      SUBROUTINE EQN
      COMMON KOUNT,ITAPE,JTAPE,IWT,LAP,XINCR,NOPT,NOVAR,NOUNK
     1,X,U,ITMAX,WTX,TEST,I,AV,RESID,IAR,EPS,ITYP,XX,RXTYP
     2,DX1I,FOP,FO,FU,P,ZL,TO,EIGVAL,XST,T,DT,L,M,JJJ,Y,DY
     3,VECT,NCST,CONST,NDAT,JDAT,MOPT,LOPT,YYY,CONSTS
      COMMON/FREDT/IMETH
      COMMON/POINT/KOPT,JOPT,XXX
      DIMENSION X(4,300),U(20),WTX(4,300),XX(4),FOP(300)
     1,FO(300),FU(300),P(20,21),VECT(20,21),ZL(300)
     2,TO(20),EIGVAL(20),XST(300),Y(10),DY(10),CONSTS(50,16)
     3,NCST(50),ISMIN(50),RXTYP(50),DX1I(50),IRX(50)
     4,MOPT(50),LOPT(50),YYY(50),CONST(16),XXX(15)
      GO TO (2,3,4,5,1,7,8,9,10,11,12)  ITYP
    1 CONTINUE
      ITAPE=60
      JTAPE=61
      RETURN
    7 CONTINUE
      NOUNK=3
      NOVAR=2
      RETURN
    8 CONTINUE
C     ************************************************************
C     ENTER DATA AS K/R WHERE K=CELL CONSTANT, R=RESISTANCE
C     CONVERSION TO EQUIVALENT CONDUCTANCE
C     ************************************************************
      DO 99 N=1,NOPT
      WRITE(JTAPE,500)X(1,N),WTX(1,N),X(2,N),WTX(2,N)
  500 FORMAT(5X,4E10.4)
   99 CONTINUE
      DO 88 N=1,NOPT
      EEE=(1000.0*X(2,N))/X(1,N)
      E=((1000.0/X(1,N)**2.)*((WTX(2,N)))
      E1=(((1000.0*X(2,N))/(X(1,N))**2))**2)*WTX(1,N)
      WTX(2,N)=E+E1
      X(2,N)=EEE
      WRITE(JTAPE,501)X(1,N),WTX(1,N),X(2,N),WTX(2,N)
  501 FORMAT(5X,4E10.4)
   88 CONTINUE
      RETURN
    2 CONTINUE
      GAMA=1.0
C     ****************************************************
C     JUSTICE EQUATION
C     ****************************************************
C     XX(1)=SALT CONCENTRATION-MOLARITY
C     XX(2)=EQUIVALENT CONDUCTANCE-CM2/OHM MOLE
C     ****************************************************
C     CONST(1)=(DIELECTRIC CONSTANT*TEMPERATURE)**0.5
```

```
C      CONST(2)=VISCOSITY-POISE
C      CONST(3)=BJERRUM DISTANCE-CM
C      ***************************************************
C      U(1)=ION PAIRING CONSTANT-M^-1
C      U(2)=LIMITING CONDUCTANCE OF FREE IONS-CM^2/OHM MOLE
C      U(3)=INTERATOMIC DISTANCE-CM
C      ***************************************************
C      GAM ,GAMAN =ACTIVITY COEFFICIENTS
C      EKPA=DEBYE INVERSE DISTANCE
C      ALPHA,BETA=COEFFICIENTS OF LIMITING LAW
C      EJ1,EJ2=COEFFICIENTS IN CONDUCTANCE EQUATION
c      ***************************************************
       U(1)=ABS(U(1))
       U(2)=ABS(U(2))
       U(3)=ABS(U(3))
       GAM=GAMA**2
       SDT=CONST(1)
       SDT2=SDT**2
       SDT3=SDT**3
       ETA=CONST(2)
       EX=SQRT(XX(1))
       AA=CONST(3)
       A1=U(3)
       EKP=((50.29E+08)*EX)/SDT
       EKPA=EKP*AA
       EKPA1=EKP*A1
       EKPC=EKPA/EX
       EKPC1=EKPA1/EX
       EKPC2=EKPC**2
       EKPC21=EKPC1**2
       AB=(1.6710207E-03)/SDT2
       BB=AB/AA
       BB1=AB/A1
       BBB=(2.0*(BB*2))+(2.0*BB)-1.0
       ALPHA=(8.2045E+05)/SDT3
       BETA=82.486/(SDT*ETA)
       SS=(ALPHA*U(2))+BETA
       E1=(EKPC2*(BB**2))/24.0
       E11=(EKPC21+(BB1**2))/24.0
       E2=(EKPC*BB*BETA)/16.0
       E21=(EKPC1*BB1*BETA)/16.0
       EC=((EKPA1**2)*(BB1**2)*(ALOG(EKPA1))*(U(2)))/12.0
      1-(BETA*EX*EKPA1*BB1*ALOG(EKPA1))/4.0
       ZIG1=E1*(1.8147+(2.0*ALOG(EKPC))+((2.0/(BB**3))*BBB))
       ZIG2=E2*(0.0284+(44.0/(3.0*BB))-(2.0*ALOG(EKPC)))
       EJ1=(ZIG1*U(2))+ZIG2
       ZIG3=(((BB1**2)*(EKPA1**3))/(24.0*(XX(1)**1.5)))*(0.6094+
      1(4.4748/BB1)+(3.8284/(BB1**2)))
       ZIG41=(EKPC1*BB1)*(2.*E21)*((0.5738/BB1)+(7.0572/(BB1**2))
```

```
     1-(2.0/(3.0*(BB1**3)))-0.6467)
      ZIG42=((E21*BETA)/U(2))*((4.0/3.0*BB1)-2.2194)
      ZIG4=ZIG41-ZIG42
      EJ2=(ZIG3*U(2))+ZIG4
  101 CONTINUE
      FF=1.0+(4.0*U(1)*XX(1)*GAM)
      DD=(-1.0+SQRT(FF))/(2.0*U(1)*XX(1)*GAM)
      STREN=XX(1)*DD
      STR=SQRT(STREN)
      XL=(1.0+((50.29E+08*AA*STR)/SDT))*SDT3
      GAMAN=EXP(-4197640.0*STR/XL)
      RAT=ABS((GAMAN-GAMA)/GAMAN)
      GAMA=GAMAN
      GAM=GAMA**2
      IF(RAT.GT.1.0E-10)GO TO 101
      CALC=(U(2)-(SS*STR)+EC+(EJ1*
     1STREN)-(EJ2*(STR**3)))/(1.0+(U(1)*STREN*GAM))
      IF(IMETH.NE.-1)GO TO 35
      RETURN
   35 CONTINUE
      RESID=CALC-XX(2)
      IF(LAP.NE.3)GO TO 666
      WRITE(JTAPE,222)XX(1),EJ1,EJ2,SS,EC,GAMA
  222 FORMAT(5X,6E10.4)
  666 CONTINUE
      RETURN
    3 CONTINUE
      RETURN
    4 CONTINUE
      RETURN
    5 CONTINUE
      IF(IMETH.NE.-1)GO TO 20
      RETURN
   20 CONTINUE
      RETURN
    9 CONTINUE
      RETURN
   10 CONTINUE
      RETURN
   11 CONTINUE
      RETURN
   12 CONTINUE
      RETURN
   13 CONTINUE
      RETURN
      END
```

REFERENCES

(1) Devlin, J.P.; Consani, K. J. Phys. Chem. 1984, 88, 3269.

(2) Handy, P.R.; Popov, A.I. Spectrochim. Acta 1972, 28A, 1545.

(3) Bjerrum, N. Kgl. Danske Vidensk. Selskab 1926, 7, 9.

(4) O'M Bockris, J.; Reddy, A.K.N. "Modern Electrochemistry"; Plenum Rosetta: New York, 1977; Vol. 1, Chapter 3.

(5) Fuoss, R.M.; Kraus, C.A. J. Am. Chem. Soc. 1933, 55, 1019.

(6) Fuoss, R.M. Trans. Faraday Soc. 1934, 30, 967.

(7) Fuoss, R.M. J. Am. Chem. Soc. 1958, 80, 5059.

(8) Petrucci, S. "Ionic Interactions from Dilute Solutions to Fused Salts"; Petrucci, S., Ed.; Academic Press: New York, 1971; Vol. 1, Chapter 3.

(9) Jagodzinski, P.; Petrucci S. J. Phys. Chem. 1974, 78, 917.

(10) Fuoss, R.M. Proc. Natl. Acad. Sci. U.S.A. 1978, 75, 16.

(11) Denison, J.T.; Ramsey, J.B. J. Am. Chem. Soc. 1955, 77, 2615.

(12) D'Aprano, A.; Fuoss, R.M. J. Phys. Chem. 1963, 67, 1871.

(13) D'Aprano, A.; Fuoss, R.M. J. Phys. Chem. 1969, 73, 400.

(14) D'Aprano, A.; Komiyama, J.; Fuoss, R.M. J. Solution Chem. 1975, 5, 279.

(15) D'Aprano, A.; Fuoss, R.M. J. Am. Chem. Soc. 1969, 91, 211.

(16) Gilkerson, W.R. J. Chem. Phys. 1956, 25, 1199.

(17) D'Aprano, A.; Donato, D.; Carrubba, A. J. Solution Chem. 1982, 11, 271.

(18) Evans, D.F.; Matesich, M.A. J. Solution Chem. 1973, 2, 193.

(19) D'Aprano, A.; Fuoss, R.M. J. Solution Chem. 1975, 4, 175.

(20) D'Aprano, A. J. Solution Chem. 1974, 3, 363.

(21) Krumgalz, S.B. J. Solution Chem. 1982, 11, 283.

(22) Petrella, G.; Petrella, M. Electrochim. Acta 1982, 27, 1733.

(23) D'Aprano, A., Komiyama, J.; Fuoss, R.M. J. Solution Chem. 1976, 5, 279.

(24) Gilkerson, W.R. J. Phys. Chem. 1970, 74, 746.

(25) Feng-chun, H.; Gilkerson, W.R. J. Solution Chem. 1983, 12, 161.

(26) Justice, J.C.; Justice, M.C. Faraday Discuss. Chem. Soc. 1977, 64, 265.

(27) Fuoss, R.M. J. Phys. Chem. 1978, 82, 2427.

(28) Fuoss, R.M.; Accascinia, F. "Electrolytic Conductance"; Interscience: New York, 1959.

(29) Fuoss, R.M.; Kraus, C.A. J. Am. Chem. Soc. 1933, 55, 2387.

(30) Delsignore, M.; Farber, H.; Petrucci, S. J. Phys. Chem. 1986, 90, 66.

(31) Chabanel, M.; Lucon, M.; Paoli, D. J. Phys. Chem. 1981, 85, 1058.

(32) Saar, D.; Brauner, J.; Farber, H.; Petrucci, S. J. Phys. Chem. 1980, 84, 341.

(33) Justice, J.C. Electrochim. Acta 1971, 16, 701.

(34) Justice, J.C. J. Chim. Phys. 1968, 65, 353.

(35) DeRossi, C.; Sesta, B.; Battistini, M.; Petrucci, S. J. Am. Chem. Soc. 1972, 94, 2961.

(36) Fuoss, R.M. J. Am. Chem. Soc. 1934, 56, 1027.

(37) Fuoss, R.M. J. Am. Chem. Soc. 1934, 56, 1031.

(38) Fuoss, R.M., J. Am. Chem. Soc. 1936, 58, 982.

(39) Fuoss, R.M.; Kraus, C.A. J. Am. Chem. Soc. 1935, 57, 1.

(40) Fuoss, R.M.; Kraus, C.A. J. Am. Chem. Soc. 1933, 55, 3614.

(41) Papovych, O.; Tomkins, R.P.T. "Nonaqueous Solution Chemistry"; Wiley-Interscience: New York, 1981; Chapter 7.

(42) Fuoss, R.M. J. Phys. Chem. 1975, 79, 525.

(43) Nicolas, M.; Reich, R. J. Phys. Chem. 1981, 85, 2843.

(44) Mattina, C.F.; Fuoss, R.M. J. Phys. Chem. 1975, 79, 1604.

(45) DeRossi, C.; Sesta, B.; Battistini, M.; Petrucci, S. J. Am. Chem. Soc. 1972, 94, 2961.

(46) Hanna, E.M.; Pethybridge, A.D.; Prue, J.E. J. Phys. Chem. 1971, 75, 291.

(47) Khazaeli, S., Ph.D. Thesis, Michigan State University, E. Lansing, MI, 1982.

(48) Fernandez-Prini, R. Trans. Faraday Soc. 1969, 65, 3311.

(49) Pitt, E. Proc. Roy. Soc. A 1953, 217, 43.

(50) Fuoss, R.M.; Hsia, K.L. Proc. Natl. Acad. Sci. U.S.A. 1967, 59, 1550.

(51) Justice, J.C. J. Chim. Phys. 1968, 65, 353.

(52) Justice, J.C. Electrochim. Acta 1971, 16, 701.

(53) Fuoss, R.M. J. Phys. Chem. 1974, 78, 1383.

(54) Fuoss, R.M. Proc. Natl. Acad. Sci. U.S.A. 1974, 71, 4491.

(55) Fuoss, R.M. J. Phys. Chem. 1975, 79, 525.

(56) Fuoss, R.M. J. Solution Chem. 1978, 7, 771.

(57) Delsignore, M.; Farber, H.; Petrucci, S. J. Phys. Chem. 1985, 89, 4968.

(58) Fuoss, R.M.; Kraus, C.A. J. Am. Chem. Soc. 1933, 55, 2387.

(59) Boileau, S.; Hemery, P. Electrochim. Acta 1976, 21, 647.

(60) Delsignore, M.; Maaser, H.E.; Petrucci, S. J. Phys. Chem. 1984, 88, 2405.

(61) Beronius, P.; Lindback, T. Acta Chem. Scand. A 1978, 32, 423.

(62) Sukhotin, M.; Timofeeva, Z.N. Zhur. Fiz. Khim. 1959, 33, 1602.

(63) Ebeling, W.; Grigo, M. J. Solution Chem. 1982, 11, 151.

(64) Cachet, H.; Cyrot, A.; Fekir, M.; Lestrade, J.C. J. Phys. Chem. 1979, 83, 2419.

(65) Badiali, J.P.; Cachet, H.; Cyrot, A.; Lestrade, J.C. J. Chem. Soc., Faraday Trans. 2 1973, 69, 1339.

(66) Farber, H.; Petrucci, S. J. Phys. Chem. 1976, 80, 327.

(67) Reger, A.; Peled, E.; Gileadi, E. J. Phys. Chem. 1979, 83, 869.

(68) Erlich, R.H.; Popov, A.I. J. Am. Chem. Soc. 1971, 93, 5620.

(69) Maciel, G.E.; Hancock, J.K.; Lafferty, L.F.; Mueller, P.A.; Musker, W.K. Inorg. Chem. 1966, 5, 554.

(70) Baum, R.G.; Popov, A.I. J. Solution Chem. 1975, 4, 441.

(71) Greenberg, M.S.; Bodner, R.L.; Popov, A.I. J. Phys. Chem. 1973, 77, 2449.

(72) Jameson, C.J.; Gutowsky, H.S. J. Chem. Phys 1964, 40, 1714.

(73) DeWitte, W.J.; Lulu, L.; Mei, E.; Dye, J.L.; Popov, A.I. J. Solution Chem. 1977, 6, 337.

(74) Popov, A.I. Pure Appl. Chem. 1979, 51, 101.

(75) Shih, J.S.; Popov, A.I. Inorg. Nucl. Chem. Lett. 1977, 13, 105.

(76) Greenberg, M.S., Ph.D. Thesis, Michigan State University, E. Lansing, MI, 1974.

(77) Gilkerson, W.R.; Kendrick, K.L. J. Phys. Chem. 1984, 88, 5352.

(78) Khazaell, S.; Popov, A.I.; Dye, J.L. J. Phys. Chem. 1982, 86, 4238.

(79) Deverell, C.; Richards, R.E. Mol. Phys. 1966, 10, 551.

(80) Tong, J.P.K.; Langford, C.H.; Stengle, T.R. Can. J. Chem. 1974, 52, 1721.

(81) Carrington, A.; Dravnicks, F.; Symons, M.C.R. Mol. Phys. 1960, 3, 174.

(82) Hirata, F.; Friedman, H.L.; Holz, M.; Hertz, H.G. J. Chem. Phys. 1980, 73, 6031.

(83) Holz, M.; Friedman, H.L.; Tembe, B.L. J. Magn. Res. 1982, 47, 454.

(84) Halliday, J.D.; Richards, R.E.; Sharp, R.R. Proc. Roy. Soc. Lond. 1969, A313, 45.

(85) Hall, C.; Richards, R.E.; Sharp, R.R. Proc. Roy. Soc. Lond. 1974, A337, 297.

(86) Berman, H.A.; Stengle, T.R. J. Phys. Chem. 1975, 79, 1001.

(87) Mishustin, A.I.; Kessler, Y.M. J. Solution Chem. 1975, 4, 779.

(88) Lindman B.; Forsen, S., "Chlorine, Bromine, and Iodine NMR. Physico-Chemical, and Biological Applications"; Diehl, P.; Fluck, E.; Kosfeld, R., Eds.; Springer-Verlag: Berlin, Germany, 1976; Vol. 12.

(89) Reimarsson, P.; Lindman, B. Inorg. Nucl. Chem. Lett. 1977, 13, 449.

(90) Yudasaka, M.; Sugawara, T.; Iwamura, H.; Fujiyama, T. Bull. Chem. Soc. Jpn. 1981, 54, 1933.

(91) Kintzinger, J.P.; Lehn, J.M. J. Am. Chem. Soc. 1974, 96, 3313.

(92) Dechter, J.J.; Henriksson, U.; Kowalewski, J.; Nilsson, A.C. J. Magn. Res. 1982, 48, 503.

(93) Gierer, A.; Wirtz, K. Z. Naturforsch. 1953, A8, 532.

(94) Hill, N.E. Proc. Phys. Soc. London, Sect. B 1954, 67, 149.

(95) Burke, T.; Chan, S.I. J. Magn. Res. 1970, 3, 55.

(96) Sugawara, T.; Yudasaka, M.; Yokoyama, Y.; Fujiyama, T.; Iwamura, H. J. Phys. Chem. 1982, 86, 2705.

(97) Miller, A.G.; Franz, J.A.; Macklin, J.W. J. Phys. Chem. 1985, 89, 1190.

(98) Kintzinger, J.P.; Lehn, J.M.; Kauffmann, E.; Dye, J.L.; Popov, A.I. J. Am. Chem. Soc. 1983, 105, 7549.

(99) Irish, D.E.; Chang, T.G.; Tang, S.Y.; Petrucci, S. J. Phys. Chem. 1981, 85, 1686.

(100) Findlay, T.J.V.; Symons, M.C.R. J. Chem. Soc., Faraday Trans. 2 1976, 72, 820.

(101) Moore, J.C.; Devlin, J.P. J. Chem. Phys. 1978, 68, 826.

(102) Irish, D.E.; Brooker, M.H., "Advances in Infrared and Raman Spectroscopy"; Clarke, R.J.H.; Hester, R.E., Eds.; Heyden: London, 1976; Volume 2.

(103) Irish, D.E.; Davis, A.R. Can. J. Chem. 1968, 46, 943.

(104) Lockwood, D.J. J. Chem. Soc., Faraday Trans. 2 1975, 71, 1440.

(105) Toth, J.P.; Thornton, C.; Devlin, J.P. J. Solution Chem. 1978, 7, 783.

(106) Chang, T.G.; Irish, D.E. J. Solution Chem. 1974, 3, 161.

(107) Chang, T.G.; Irish, D.E. J. Solution Chem. 1974, 3, 175.

(108) Mathieu, J.P.; Lounsbury, M. Discuss. Faraday Soc. 1950, 9, 196.

(109) Brooker, M.H.; DeYoung, B.S. J. Solution Chem. 1980, 3, 279.

(110) Frost, R.L.; James, D.W. J. Chem. Soc., Faraday Trans. 1 1982, 78, 3223, 3235.

(111) Frost, R.L.; James, D.W. J. Chem. Soc., Faraday Trans. 1 1982, 78, 3263.

(112) Hathaway, B.J.; Underhill, A.E. J. Chem. Soc. 1961, 3091.

(113) Ritzhaupt, G.; Devlin, J.P. J. Chem. Phys. 1975, 62, 1982.

(114) Draeger, J.; Ritzhaupt, G.; Devlin, J.P. Inorg. Chem. 1979, 18, 1808.

(115) Greenberg, M.S.; Popov, A.I. J. Solution Chem. 1976, 5, 653.

(116) Cahen, Y.M., Ph.D. Thesis, Michigan State University, E. Lansing, MI, 1975.

(117) Frost, R.L.; James, D.W.; Appleby, R.; Mayes, R.E. J. Phys. Chem. 1982, 86, 3840.

(118) Miller, A.G.; Franz, J.A.; Macklin, J.W. J. Phys. Chem. 1985, 89, 1193.

(119) James, D.W.; Mayes, R.E. Aust. J. Chem. 1982, 35, 1775, 1785.

(120) Jones, L.H. J. Chem. Phys. 1956, 25, 1069.

(121) Saar, D.; Petrucci S., J. Phys. Chem. in press.

(122) Chabanel, M.; Wang, Z. J. Phys. Chem. 1984, 88, 1441.

(123) Paoli, D.; Lucon, M.; Chabanel, M. Spectrochim. Acta 1979, 35A, 593.

(124) Evans, J.C.;Lo, G.Y-S. J. Phys. Chem. 1965, 69, 3223.

(125) Edgell, W.F.; Watts, A.T.; Lyford, J.; Risen, W.M. J. Am. Chem. Soc. 1966, 88, 1815.

(126) Edgell, W.F.; Lyford, J.; Wright, R.; Risen, W.; Watts, A. J. Am. Chem. Soc. 1970, 92, 2240.

(127) Maxey, B.W.; Popov, A.I. J. Am. Chem. Soc. 1967, 89, 2230.

(128) Maxey, B.W.; Popov, A.I. J. Am. Chem. Soc. 1969, 91, 20.

(129) Wuepper, J.L.; Popov, A.I. J. Am. Chem. Soc. 1970, 92, 1493.

(130) Popov, A.I. Pure Appl. Chem. 1975, 41, 275.

(131) Wong, M.K.; Popov, A.I. J. Inorg. Nucl. Chem. 1971, 33, 1203.

(132) Chang, S.; Severson, M.W.; Schmidt, P.P. J. Phys. Chem. 1985, 89, 2892.

(133) Wong, M.K.; McKinney, W.J.; Popov, A.I. J. Phys. Chem. 1971, 75, 56.

(134) Freiberg, M.; Ron, A.; Schnepp, O. J. Phys. Chem. 1968, 72, 3526.

(135) Baum, R.G.; Popov, A.I. J. Solution Chem. 1975, 4, 441.

(136) Cahen, Y.M.; Popov, A.I. J. Solution Chem. 1975, 4, 599.

(137) Blandamer, M.J.; Fox, M.F. Chem. Rev. 1970, 70, 59.

(138) Smith, M.; Symons, M.C.R. Trans. Faraday Soc. 1958, 54, 338.

(139) Smith, M.; Symons, M.C.R. Trans. Faraday Soc. 1958, 54, 346.

(140) Blandamer, M.J.; Fox, M.F.; Symons, M.C.R.; Wood, K.J.; Wootten, M.J. Trans. Faraday Soc. 1968, 64, 3210.

(141) Griffiths, T.R.; Symons, M.C.R. Trans. Faraday Soc. 1960, 56, 1125.

(142) Blandamer, M.J.; Fox, M.F.; Symons, M.C.R.; Wootten, M.J. Trans. Faraday Soc. 1970, 66, 1574.

(143) Blandamer, M.J.; Burdett, T.R. J. Chem. Soc., Faraday Trans. 2 1972, 68, 577.

(144) Blandamer, M.J.; Gough, T.E.; Symons, M.C.R. Trans. Faraday Soc. 1963, 59, 1748.

(145) Griffiths, T.R.; Wijayanayake, R.H. J. Chem. Soc., Faraday Trans. 1 1973, 69, 1899.

(146) Hogen-Esch, T.E.; Smid, J. J. Am. Chem. Soc. 1965, 87, 669.

(147) Burley, J.W.; Young, R.N. J. Chem. Soc. B 1971, 1018.

(148) Waack, R.; Doran, M.A.; Stevenson, P.E. J. Am. Chem. Soc. 1966, 88, 2109.

(149) Chan, L.L.; Smid, J. J. Am. Chem. Soc. 1968, 90, 4654.

(150) Waack, R.; Doran, M.A. J. Phys. Chem. 1963, 67, 148.

(151) Hogen-Esch, T.E.; Smid, J. J. Am. Chem. Soc. 1966, 88, 307.

(152) Smid, J. Angew. Chem. Int. Edit. Engl. 1972, 11, 112.

(153) Hogen-Esch, T.E.; Smid, J. J. Am. Chem. Soc. 1966, 88, 318.

(154) Griffiths, T.R.; Symons, M.C.R. Mol. Phys. 1960, 3, 90.

(155) Griffiths, T.R.; Wijayanayake, R.H. Trans. Faraday Soc. 1970, 66, 1563.

(156) Pedersen, C.J. J. Am. Chem. Soc. 1967, 89, 2495.

(157) Pedersen, C.J. J. Am. Chem. Soc. 1967, 89, 7017.

(158) Frensdorff, H.K. J. Am. Chem. Soc. 1971, 93, 600.

(159) Shamsipur, M.; Popov, A.I. Inorg. Chim. Acta 1980, 43, 243.

(160) Smetana, A.J.; Popov, A.I. J. Solution Chem. 1980, 9, 183.

(161) Khazaell, S.; Dye, J.L.; Popov, A.I. Spectrochim. Acta 1983, 39A, 19.

(162) Hoeiland, H.; Ringseth, J.A.; Brun, T.S. J. Solution Chem. 1979, 8, 779.

(163) Shamsipur, M.; Popov, A.I. J. Am. Chem. Soc. 1979, 101, 4051.

(164) Mei, E.; Dye, J.L.; Popov, A.I. J. Am. Chem. Soc. 1977, 99, 5308.

(165) Khazaell, S.; Popov, A.I.; Dye, J.L. J. Phys. Chem. 1982, 86, 5018.

(166) Rahimi, A.K.; Popov, A.I. Inorg. Nucl. Chem. Lett. 1976, 12, 703.

(167) Rounaghi, G.; Popov, A.I. J. Inorg. Nucl. Chem. 1981, 43, 911.

(168) Mei, E.; Popov, A.I.; Dye, J.L. J. Phys. Chem. 1977, 81, 1677.

(169) Shamsipur, M.; Rounaghi, G.; Popov, A.I. J. Solution Chem. 1980, 9, 701.

(170) DeJong, F.; Reinhoudt, D.N.; Smit, C.J. Tetrahedron Lett. 1976, 17, 1375.

(171) Mosier-Boss, P.A.; Popov, A.I. J. Am. Chem. Soc. 1985, 107, 6168.

(172) Christensen, J.J.; Hall, J.O.; Izatt, R.M. Science 1971, 174, 459.

(173) Lehn, J.M.; Sauvage, J.P. J. Am. Chem. Soc. 1975, 97, 6700.

(174) Dalley, N.K.; Smith, J.S.; Larson, S.B.; Matheson, K.L.; Christensen, J.J.; Izatt, R.M. J. Chem. Soc., Chem. Comm. 1975, 84.

(175) Cram, D.J.; Helgeson, R.C.; Sousa, L.R.; Timko, J.M.; Newcomb, M.; Moreau, P.; DeJong, F.; Gokel, G.W.; Hoffman, D.H.; Domeier, L.A.; Peacock, S.C.; Madan, K.M.; Kaplan, I. Pure Appl. Chem. 1975, 43, 327.

(176) Ungaro, R.; El Haj, B.; Smid, J. J. Am. Chem. Soc. 1976, 98, 5198.

(177) Shah, S.C.; Kopolow, S.L.; Smid, J. J. Polym. Sci. 1976, 14, 2023.

(178) Steinmann, W.; Kaden, T.A. Helv. Chim. Acta 1975, 58, 1358.

(179) Jepson, B.E.; DeWitt, R. J. Inorg. Nucl. Chem. 1976, 38, 1175.

(180) Matsuura, N.; Umemoto, K.; Takeda, Y.; Sasaki, A. Bull. Chem. Soc. Jpn. 1976, 49, 1246.

(181) Arnett, E.M.; Moriarity, T.C. J. Am. Chem. Soc. 1971, 93, 4908.

(182) Ryan, T.H.; Koryta, J.; Hofmanova-Matejkova, A.; Brezina, M. Anal. Lett. 1974, 7, 335.

(183) Pedersen, C.J.; Frensdorff, H.K. Angew. Chem. Int. Edit. Engl. 1972, 11, 16.

(184) Dunitz, J.D.; Dobler, M.; Seiler, P.; Phizackerley, R.P. Acta Cryst. Sect. B 1974, B30, 2733.

(185) Live, D.; Chan, S.I. J. Am. Chem. Soc. 1976, 98, 3769.

(186) Gokel, G.W.; Goli, D.M.; Minganti, C.; Echegoyen, L. J. Am. Chem. Soc. 1983, 105, 6786.

(187) Mallinson, P.R.; Truter, M.R. J. Chem. Soc., Perkins Trans. 2 1972, 1818.

(188) van Remoortere, F.P.; Boer, F.P. Inorg. Chem. 1974, 13, 2071.

(189) Boer, F.P.; Neuman, M.A.; van Remoortere, F.P.; Steiner, E.C. Inorg. Chem. 1974, 13, 2826.

(190) Pedersen, C.J., J. Am. Chem. Soc. 1970, 92, 386.

(191) Parsons, D.G.; Truter, M.R.; Wingfield, J.N. Inorg. Chim. Acta 1975, 14, 45.

(192) Owen, J.D.; Trutor, M.R. J. Chem. Soc. Dalton Trans. 1979, 1831.

(193) Sugimoto, M.; Nonoyama, M.; Ito, T.; Fujita, J. Inorg. Chem. 1983, 22, 950.

(194) Alcock, N.W.; Curzon, E.N.; Moore, P.; Pierpoint, G. J. Chem. Soc., Dalton Trans. 1984, 605.

(195) Drew, M.G.B.; Esho, F.S.; Lavery, A.; Nelson, S.M. J. Chem. Soc., Dalton Trans. 1984, 545.

(196) Suh, M.P.; Shin, W.; Kim, D.; Kim, S. Inorg. Chem. 1984, 23, 618.

(197) Chen, Y.D.; Bard, A.J. Inorg. Chem. 1984, 23, 2175.

(198) Walker, D.D.; Taube, H. Inorg. Chem. 1981, 20, 2828.

(199) Addison, A.W.; Rao, T.; Sinn, E. Inorg. Chem. 1984, 23, 1957.

(200) Dietrich, B.; Lehn, J.M.; Sauvage, J.P. Tetrahedron Lett. 1969, 34, 2885.

(201) Mei, E.; Lulu, L.; Dye, J.L.; Popov, A.I. J. Solution Chem. 1977, 6, 771.

(202) Mei, E.; Popov, A.I.; Dye, J.L. J. Am. Chem. Soc. 1977, 99, 6532.

(203) Kauffmann, E.; Dye, J.L.; Lehn, J.M.; Popov, A.I. J. Am. Chem. Soc. 1980, 102, 2274.

(204) Vogtle, F.; Weber, E. Angew. Chem. Int. Edit. Engl. 1979, 18, 753.

(205) Haymore, B.L.; Lamb, J.D.; Izatt, R.M.; Christensen, J.J. Inorg. Chem. 1982, 21, 1598.

(206) Buschmann, H.J. Polyhedron 1985, 4, 2039.

(207) Cabbiness, D.K.; Margerum, D.W. J. Am. Chem. Soc. 1969, 91, 6540.

(208) Gokel, G.W.; Dishong, D.M.; Diamond, C.J. J. Chem. Soc., Chem. Comm. 1980, 1053.

(209) Dishong, D.M.; Diamond, C.J.; Gokel, G.W. Tetrahedron Lett. 1981, 22, 1663.

(210) Schultz, R.; Dishong, D.M.; Gokel, G.W. Tetrahedron Lett. 1981, 22, 2623.

(211) Dishong, D.M.; Diamond, C.J.; Cinoman, M.I.; Gokel, G.W. J. Am. Chem. Soc. 1983, 105, 586.

(212) Goli, D.M.; Dishong, D.M.; Diamond, C.J.; Gokel, G.W. Tetrahedron Lett. 1982, 23, 5243.

(213) Nakatsuji, Y.; Nakamura, T.; Okahara, M. Chem. Lett. 1982, 1207.

(214) Kaifer, A.; Durst, H.D.; Echegoyen, L.; Dishong, D.M.; Schultz, R.A.; Gokel, G.W. J. Org. Chem. 1982, 47, 3195.

(215) Schultz, R.A.; Dishong, D.M.; Gokel, G.W. Tetrahedron Lett. 1981, 2623.

(216) Gokel, G.W.; Dishong, D.M.; Diamond, C.J. J. Chem. Soc., Chem. Comm. 1980, 1053.

(217) Mamantov, G.; Osteryoung R.A., in "Characterization of Solutes in Nonaqueous Solvents"; Mamantov, G., Ed.; Plenum Press: New York, 1978.

(218) Holleck, G.L.; Gimer, J. J. Electrochem. Soc. 1972, 119, 1161.

(219) Robinson, J.; Osteryoung, R.A. J. Am. Chem. Soc. 1979, 101, 323.

(220) Gale, R.J.; Gilbert, B.; Osteryoung, R.A. Inorg. Chem. 1978, 17, 2728.

(221) Hussey, C.L. in "Advances in Molten Salt Chemistry"; Mamantov, G., Ed.; Elsevier: New York, 1983; Vol. 5.

(222) Gale, R.J.; Osteryoung, R.A. Inorg. Chem. 1979, 18, 1603.

(223) Wilkes, J.S.; Levisky, J.A.; Wilson, R.A.; Hussey, C.L. Inorg. Chem. 1982, 21, 1263.

(224) Robinson, J.; Bugle, R.C.; Chum, H.L.; Koran, D.; Osteryoung, R.A. J. Am. Chem. Soc. 1979, 101, 3776.

(225) Robinson, J.; Osteryoung, R.A. J. Electrochem. Soc. 1980, 127, 122.

(226) Fung, K.W.; Mamantov, G.; Young, J.P. Inorg. Nucl. Chem. Lett. 1972, 8, 219.

(227) Gale, R.J.; Osteryoung, R.A. J. Electrochem. Soc. 1980, 127, 2167.

(228) Cheek, C.T.; Osteryoung, R.A. Inorg. Chem. 1982, 21, 3581.

(229) Corbett, J.D. in "Preparative Inorganic Reactions"; Jolly, W.L., Ed.; Interscience Publishers: New York, 1966; Volume 3.

(230) Marassi, R.; Mamantov, G.; Chambers, J.Q. Inorg. Nucl. Chem. Lett. 1975, 11, 245.

(231) Fehrmann, R.; Bjerrum, N.J.; Andreasen, H.A. Inorg. Chem. 1976, 15, 2187.

(232) Potts, R.A.; Barnes, R.D.; Corbett, J.D. Inorg. Chem. 1968, 7, 2558.

(233) Fehrmann, R.; Bjerrum, N.J.; Andreasen, H.A. Inorg. Chem. 1975, 14, 2259.

(234) Fehrmann, R.; Bjerrum, N.J. Inorg. Chem. 1977, 16, 2089.

(235) Torsi, G.; Fung, K.W.; Begun, G.M.; Mamantov, G. Inorg. Chem. 1971, 10, 2285.

(236) Bjerrum, N.J. Inorg. Chem. 1972, 11, 2648.

(237) Jones, H.L.; Boxall, L.G.; Osteryoung, R.A. J. Electroanal. Chem. 1972, 38, 476.

(238) Jones, H.L.; Osteryoung, R.A. J. Electroanal. Chem. 1974, 49, 281.

(239) Fung, F.W.; Chambers, J.Q.; Mamantov, G. J. Electroanal. Chem. 1973, 47, 81.

(240) Fehrmann, R.; von Winbush, S.; Papatheodorou, G.N.; Berg, R.W.; Bjerrum, N.J. Inorg. Chem. 1982, 21, 3396.

(241) Boxall, L.G.; Jones, H.L.; Osteryoung, R.A. J. Electrochem. Soc. 1974, 121, 212.

(242) von Barner, J.H.; Brekke, P.B.; Bjerrum, N.J. Inorg. Chem. 1985, 24, 2162.

(243) Laher, T.M.; Hussey, C.L. Inorg. Chem. 1982, 21, 4079.

(244) Laher, T.M.; Hussey, C.L. Inorg. Chem. 1983, 22, 3247.

(245) Taulelle, F.; Popov, A.I. Polyhedron 1983, 2, 889.

(246) Lipsztajn, M.; Osteryoung, R.A. Inorg. Chem. 1985, 24, 3492.

(247) DeWaele, R.; Heerman, L.; D'Olieslager, W. J. Electroanal. Chem. 1982, 142, 137.

(248) Gale, R.J.; Gilbert, B.; Osteryoung, R.A. Inorg. Chem. 1979, 18, 2723.

(249) von Barner, J.H.; Bjerrum, N.J.; Kiens, K. Inorg. Chem. 1974, 13, 1708.

(250) von Barner, J.H.; Bjerrum, N.J.; Smith, G.P. Acta Chem. Scand. 1978, 32A, 837.

(251) von Barner, J.H.; Bjerrum, N.J. Inorg. Chem. 1973, 12, 1891.

(252) Nanjundiah, C.; Shimizu, K.; Osteryoung, R.A. J. Electrochem. Soc. 1982, 129, 2474.

(253) Schoebrechts, J.P.; Gilbert, B.P.; Duyckaerts, G. J. Electroanal. Chem. 1983, 145, 127.

(254) Schoebrechts, J.P.; Gilbert, B. Inorg. Chem. 1985, 24, 2105.

(255) Laher, T.M.; Hussey, C.L. Inorg. Chem. 1982, 21, 4079.

(256) Hugler, R.; Mamantov, G.; Smith, G.P.; Begun, G.M. J. Raman Spectros. 1979, 11, 326.

(257) Laher, T.M.; Hussey, C.L. Inorg. Chem. 1983, 22, 1279.

(258) Bartak, D.E.; Osteryoung, R.A. J. Electroanal. Chem. 1976, 74, 69.

(259) Bartak, D.E.; Osteryoung, R.A. J. Electrochem. Soc. 1975, 122, 600.

(260) Fung, K.W.; Mamantov, G. J. Electroanal. Chem. 1972, 35, 27.

(261) Robinson, J.; Osteryoung, R.A. J. Electrochem. Soc. 1978, 125, 1454.

(262) Hussey, C.L.; Laher, T.M. Inorg. Chem. 1981, 20, 4201.

(263) Berg, R.W.; von Winbush, S.; Bjerrum, N.J. Inorg. Chem. 1980, 19, 2688.

(264) Gilbert, B.P.; Osteryoung, R.A. J. Am. Chem. Soc. 1978, 100, 2725.

(265) Robinson, J.; Gilbert, B.; Osteryoung, R.A. Inorg. Chem. 1977, 16, 3040.

(266) Taulelle, F.; Piolet, C.; Tremillon, B. J. Electroanal. Chem. 1982, 134, 131.

(267) Tremillon, B.; Bermond, A.; Molina, R. J. Electroanal. Chem. 1976, 74, 53.

(268) Taulelle, F.; Tremillon, B.; Gilbert, B. J. Electroanal. Chem. 1982, 134, 141.

(269) Fung, F.W.; Aikens, D.A. Inorg. Nucl. Chem. Lett. 1975, 11, 669.

(270) Fannin, A.A., Jr.; King, L.A.; Seegmiller, D.W. J. Electrochem. Soc. 1972, 119, 801.

(271) Boxall, L.G.; Jones, H.L.; Osteryoung, R.A. J. Electrochem. Soc. 1973, 120, 223.

(272) Torsi, G.; Mamantov, G.; Begun, G.M. Inorg. Nucl. Chem. Lett. 1970, 6, 553.

(273) Begun, G.M.; Boston, C.R.; Torsi, G.; Mamantov, G. Inorg. Chem. 1971, 10, 886.

(274) Poulsen, F.W. J. Raman Spectros. 1981, 11, 302.

(275) Brekke, P.B.; von Barner, J.H.; Bjerrum, N.J. Inorg. Chem. 1979, 18, 1372.

(276) Hjuler, H.A.; Mahan, A.; von Barner, J.H.; Bjerrum, N.J. Inorg. Chem. 1982, 21, 402.

(277) Heerman, L.; D'Olieslager, W. Inorg. Chem. 1985, 24, 4704.

(278) Dymek, C.J., Jr.; Hussey, C.L.; Wilkes, J.S.; Oye, H.A. in "Proceedings of the International Symposium on Molten Salts"; Honolulu, HA, 1987.

(279) Einarsrud, M.A.; Wilkes, J.S.; Øye, H.A., in press.

(280) Torsi, G.; Mamantov, G. Inorg. Chem. 1972, 11, 1439.

(281) Rytter, E.; Oye, H.A.; Cyvin, S.J.; Cyvin, B.N.; Klaeboe, P. Inorg. Nucl. Chem. 1973, 35, 1185.

(282) Gale, R.J.; Osteryoung, R.A. Inorg. Chem. 1980, 19, 2240.

(283) Fannin, A.A., Jr.; King, L.A.; Levisky, J.A.; Wilkes, J.S. J. Phys. Chem. 1984, 88, 2609.

(284) Ackerman, B.L.; Tsarbopoulos, A.; Allison, J. Anal. Chem. 1985, 57, 1766.

(285) Wilkes, J.S.; Reynolds, G.F.; Frye, J.S. Inorg. Chem. 1983, 22, 3870.

(286) Tait, S.; Osteryoung, R.A. Inorg. Chem. 1984, 23, 4352.

(287) Irish, D.E.; Tang, S.Y.; Talts, H.; Petrucci, S. J. Phys. Chem. 1979, 83, 3268.

(288) Bhattacharyya, D.N.; Lee, C.L.; Smid, J.; Szwarc, M. J. Phys. Chem. 1965, 69, 608.

(289) Vogel, A.I. "Textbook of Macro and Semimicro Qualitative Inorganic Analysis"; 5th ed., Longman: New York, 1979.

(290) Crisp, S.; Hughes, S.R.C.; Price, D.H. J. Chem. Soc. A 1968, 603.

(291) Jackson, M.D.; Gilkerson, W.R. J. Am. Chem. Soc. 1979, 101, 328.

(292) Mei, E. Ph.D. Thesis, Michigan State University, E. Lansing, MI, 1977.

(293) Perrin, D.D.; Armarego, W.L.F.; Perrin, D.R. "Purification of Laboratory Chemicals", 2nd ed., Pergamon Press: New York, 1980.

(294) Gokel, G.W.; Cram, D.J.; Liotta, C.L.; Harris, H.P.; Cook, F.L. J. Org. Chem. 1974, 39, 2445.

(295) Haymore, B.L.; Lamb, J.D.; Izatt, R.M.; Christensen, J.J. Inorg. Chem. 1982, 21, 1598.

(296) Mosier-Boss, P. Ph.D. Thesis, Michigan State University, E. Lansing, MI, 1985.

(297) Eubanks, D.; Abbott, F.J. Anal. Chem. 1969, 41, 1708.

(298) Desnoyers, J.E.; Perron, G. J. Solution Chem. 1972, 1, 199.

(299) Dye, J.L.; Nicely, V.A. J. Chem. Ed. 1971, 48, 443.

(300) Riddick, J.A.; Bunger, W.B. "Organic Solvents, Physical Properties and Methods of Purification," Wiley-Interscience: New York, 1970.

(301) Martin, M.L.; Delpuech, J.J.; Martin, G.J. "Practical NMR Spectroscopy"; Heyden and Sons, Ltd.: Philadelphia, PA 1980.

(302) "CRC Handbook of Chemistry and Physics," 62nd ed.; Weast, R.C. Ed.; The Chemical Rubber Company: Boca Raton, FL, 1981.

(303) Davis, A.R.; Irish, D.E.; Roden, R.B.; Weerheim, A.J. Appl. Spectrosc. 1972, 26, 384.

(304) Thompson, H.B.; Rogers, M.T. Rev. Sci. Instrum. 1956, 27, 1079.

(305) Smith, G.E. Ph.D. Thesis, Michigan State University, E. Lansing, MI, 1963.

(306) Barthel, J.; Feuerlein, F.; Neueder, R.; Wachter, R. J. Solution Chem. 1980, 9, 209.

(307) Jansen, M.L.; Yeager, H.L. J. Phys. Chem. 1974, 78, 1380.

(308) Savedoff, L.G. J. Am. Chem. Soc. 1966, 88, 664.

(309) Harada, Y.; Salomon, M.; Petrucci, S. J. Phys. Chem. 1985, 89, 2006.

(310) Fernandez-Prini, R. in "Physical Chemistry of Organic Solvents Systems", Covington, A.K.; Dickinson, T., Eds.; Plenum Press: London, 1973; chapter 5.1.

(311) Chen, M.S. J. Phys. Chem. 1977, 81, 2022.

(312) Bjerrum, N. Mat.-Fys. Medd.-K. Dan. Vidensk. Selsk. 1926, 7.

(313) Janz, G.J.; Tait, M.J. Can. J. Chem. 1967, 45, 1101.

(314) Hughes, S.R.C. J. Chem. Soc. A 1957, 634.

(315) Kraus, C.A. J. Phys. Chem. 1956, 60, 129.

(316) Crisp, S.; Hughes, S.C.R.; Price, D.H. J. Chem. Soc. A 1968, 603.

(317) Rasaiah, J.C.; Friedman, H.L. J. Phys. Chem. 1968, 72, 3352.

(318) Justice, J.C.; Justice, M.C. Faraday Discuss. Chem. Soc. 1977, 64, 265.

(319) Farber, H.; Irish, D.E.; Petrucci, S. J. Phys. Chem. 1983, 87, 3515.

(320) Delsignore, M.; Farber, H.; Petrucci, S. J. Phys. Chem. 1985, 89, 4968.

(321) Saar, D.; Brauner, J.; Farber, H.; Petrucci, S. J. Phys. Chem. 1978, 82, 545.

(322) Delsignore, M.; Maaser, H.E.; Petrucci, S. J. Phys. Chem. 1984, 88, 2405.

(323) Cahen, Y.M.; Handy, P.R.; Roach, E.T.; Popov, A.I. J. Phys. Chem. 1975, 79, 80.

(324) Menard, M.C.; Wojtkowiak, B.; Chabanel, M. Bull. Soc. Chim. Belges. 1972, 81, 24.

(325) Nakamota, K. "Infrared Spectra of Inorganic and Coordination Compounds," 3rd ed; Wiley-Interscience: New York, 1978; Part III-15.

(326) Bailey, R.A.; Kozak, S.I.; Michelsen, T.W.; Mills, W.N. Coord. Chem. Rev. 1971, 6, 407.

(327) Irish, D.E. in "Physical Chemistry of Organic Solvents Systems," Covington A.K.; Dickinson, T., Eds.; Plenum Press, London, 1973; Chapter 4.2.

(328) Toth, J.P.; Thornton, C.; Devlin, J.P. J. Solution Chem. 1978, 7, 783.

(329) Perelygin, I.S.; Klimchuk, M.A.; Belaboradova, N.W. Russ. J. Phys. Chem. 1980, 54, 605.

(330) Bacelon, P.; Corset, J.; de Loze, C. J. Solution Chem. 1980, 9, 129.

(331) Begun, G.M.; Rutenberg, A.C. Inorg. Chem. 1967, 6, 2212.

(332) Habboush, D.A.; Osteryoung, R.A. Inorg. Chem. 1984, 23, 1726.

(333) Angell, C.A.; Bennett, P.D. J. Am. Chem. Soc. 1982, 104, 6304.

(334) Nanjundiah, C.; Osteryoung, R.A. J. Electrochem. Soc. 1983, 130, 1312.

(335) Schoebrechts, J.P.; Gilbert, B.P.; Duychaerts, G. J. Electroanal. Chem. 1983, 145, 139.

(336) Akitt, J.W.; Downs, A.J. in "The Alkali Metal Symposium," The Chemical Society: London, 1967, p. 199.

(337) Rhinebarger, R. Ph.D. Thesis, Michigan State University, E. Lansing, MI, 1985.

(338) Scheffler, T.B.; Hussey, C.L. Inorg. Chem. 1984, 23, 1926.

(339) Hvistendahl, J.; Klaeboe, P.; Rytter, R.; Øye, H. Inorg. Chem. 1984, 23, 706.

(340) Gray, J.L.; Maciel, G.E. J. Am. Chem. Soc. 1981, 103, 7147.

(341) Abragam, R. "The Principles of Nuclear Magnetism," Oxford University Press: London, 1961.

(342) Brevard, C.; Granger, P. "Handbook of High Resolution Multinuclear NMR," John Wiley and Sons: New York, 1981.

(343) Linga, H.; Stojek, Z.; Osteryoung, R.A. J. Am. Chem. Soc. 1981, 103, 3754.

(344) Rovang, J.W.; Wilkes, J.W. personal communication.

(345) Cahen, Y.M.; Dye, J.L.; Popov, A.I. J. Phys. Chem. 1975, 79, 1289.

(346) Skoog, D.A.; West, D.M. "Fundamentals of Analytical Chemistry," Holt, Rhinhart, and Winston: New York, 1976.

(347) Takeda, Y. Bull. Chem. Soc. Jpn. 1982, 55, 2040.

(348) Takeda, Y.; Yamo, H.; Ishibashi, M.; Isozumi, H. Bull. Chem. Soc. Jpn. 1980, 53, 72.

(349) Morris, F.C. Struct. Bond. 1968, 4, 63.

(350) Pedersen, C.J. J. Am. Chem. Soc. 1970, 92, 386.

(351) Cahen, Y.M.; Dye, J.L.; Popov, A.I. J. Phys. Chem. 1975, 79, 1292.

(352) Dale, J. Isr. J. Chem. 1980, 20, 3.

(353) Dale, J. Tetrahedron 1974, 30, 1683.

(354) Wehrli, F.W.; Wirthlin, T. "Interpretation of Carbon-13 NMR Spectra", Heyden: London, 1978.

(355) Maciel, G.E.; Natterstad, J.J. J. Chem. Phys., 1965, 42, 2427.

(356) Spiesecke, H.; Schneider, W.G. J. Chem. Phys. 1961, 35, 731.

(357) Pedersen, C.J. J. Am. Chem. Soc. 1967, 89, 2495.

(358) Chan, L.L.; Wang, F.W.; Smid, J. J. Am. Chem. Soc. 1970, 92, 1955.

(359) Echegoyen, L.; Gokel, G.W.; Kim, M.S.; Eyring, E.M.; Petrucci, S. J. Phys. Chem. 1987, 91, 3854.

(360) Delibart, M.; Derouault, J.; Granger, R.; Chapelle, S. Inorg. Chem. 1982, 21, 1040.

(361) Evans, G.G.; Gibb, T.P.R.; Kennedy, J.K.; Del Greco, F.P. J. Am. Chem. Soc. 1954, 76, 4861.

(362) O'Malley, P.; Babcock, G.T.; Prince, R.C. Biochimica et Biophysica Acta 1984, 766, 283.